UNIVERSITY OF NAPLES FEDERICO II

Doctorate School in Molecular Medicine

Doctorate Program in
Genetics and Molecular Medicine
Coordinator: Prof. Lucio Nitsch
XXV Cycle

Bariatric surgery improves blood metabolic profile and miRNA based regulation of gene expression in subcutaneous adipose tissue from morbid obese patients

GIUSEPPE LABRUNA

Napoli 2013

Bariatric surgery improves blood metabolic profile and miRNA based regulation of gene expression in subcutaneous adipose tissue from morbid obese patients

Table of Contents

List of Publications

1. G Labruna, F Pasanisi, C Nardelli, G Tarantino, DF Vitale, R Bracale, C Finelli, MP Genua, F Contaldo, L Sacchetti. UCP1 –3826 AG+GG genotypes and serum adiponectin levels in complicated severe obesity. J Endocrinol Invest 2009;32(6):525-529. ISSN 0391-4097.

2. Labruna G, Pasanisi F, Nardelli C, Caso R, Vitale DF, Contaldo F, Sacchetti L. High Leptin/Adiponectin Ratio and Serum Triglycerides Are Associated With an "At-Risk" Phenotype in Young Severely Obese Patients. Obesity (Silver Spring). 2011;19(7):1492-6. doi: 10.1038/oby.2010.309. ISSN 1930-7381.

3. G Labruna, F Pasanisi, G Fortunato, C Nardelli, C Finelli, E Farinaro, F Contaldo, L Sacchetti. Sequence analysis of the UCP1 gene in a severe obese population from Southern Italy. J Obes 2011, article ID 269043, doi:10.1155/2011/269043. ISSN 2090-0716.

4. CV Musa, A Mancini, A Alfieri, G Labruna, G Valerio, A Franzese, F Pasanisi, MR Licenziati, L Sacchetti and P Buono. Four novel UCP3 gene variants associated to childhood obesity: effect on fatty acid oxidation and on prevention of triglyceride storage. Int J Obes (Lond). 2012;36(2):207-17. ISSN 0307-0565.

5. R. Bracale, G. Labruna, C. Finelli, A. Daniele, L. Sacchetti, G. Oriani, F. Contaldo, F. Pasanisi. The absence of polymorphisms in ADRB3, UCP1, PPARγ and ADIPOQ genes protects morbid obese patients toward insulin resistance. J Endocrinol Invest. 2012;35(1):2-4. ISSN 0391-4097.

6. L Iaffaldano, C Nardelli, M Raia, E Mariotti, M Ferrigno, F Quaglia, G Labruna, V Capobianco, A Capone, GM Maruotti, L Pastore, R Di Noto, P Martinelli, L Sacchetti, L Del Vecchio. High Aminopeptidase N/CD13 Levels Characterize Human Amniotic Mesenchymal Stem Cells and Drive Their Increased Adipogenic Potential in Obese Women. Stem Cells and Dev. 2013 in press. ISSN 1547-3287.

7. E. Leggiero, D. Astone, V. Cerullo, P. Wonganan, C. Mazzaccara, G. Labruna, L. Sacchetti, F. Salvatore, M. Croyle and L. Pastore. A PEGylated helper/dependent adenoviral vector expressing human apo A/I reduces atherosclerosis in LDLR deficient mice. Submitted to “Gene Therapy”. ISSN 0969-7128.

8. F Pasanisi, R Liguori, G Labruna, A Alfieri, D Martone, E Farinaro, F Contaldo, L Sacchetti, P Buono. MC4R, SIRT1 and FTO gene polymorphisms and metabolic syndrome in severely obese subjects from southern Italy. Submitted to “Nutrition, Metabolism & Cardiovascular Diseases”. ISSN 0939-4753

Abstract

Obesity is a multifactorial disorder influenced by the interaction of genetic, behavioral and environmental factors, control of appetite and energy expenditure, and the availability of high-calorie food.

Adipocyte and adipose tissue dysfunctions are the primary defects in obesity and may link obesity to such disorders as increased insulin resistance, type 2 diabetes, fatty liver disease, hypertension, dyslipidemia, atherosclerosis and cancer.

Bariatric procedures have been shown to be more effective in the management of morbid obesity than lifestyle interventions and pharmacotherapy. The aim of this study was to investigate if the significant and sustained weight loss after laparoscopic adjustable gastric banding (LAGB) resulted in an improvement in the metabolism of obese subjects in terms of serum biochemical parameters and phenotypic characteristics (cell size and number) of subcutaneous adipose tissue (SAT). Moreover, we investigated if miRNA based regulation of gene expression could be involved in the mechanisms underlying the weight loss.

We evaluated 20 severely obese subjects before LAGB (T0, mean body mass index [BMI] 44.9 kg/m^2) and after the loss of >30% excess weight (T1, mean BMI 31.5 kg/m^2). We also evaluated 10 normal weight subjects. We collected SAT and serum samples from all subjects. Conventional biochemical parameters were measured by routine laboratory procedures, and leptin and adiponectin by Luminex xMAP technology. Five-micron sections were prepared from all paraffin-embedded SAT blocks. Slides were then stained with hematoxylin & eosin. Macrophagic infiltration were evaluated by CD68 immunohistochemical analysis.

Levels of insulin, homeostasis model assessment-insulin resistance, triglycerides and liver markers as well as the leptin/adiponectin ratio were significantly lower at T1 vs T0 ($p<0.05$). The number of SAT adipocytes was greater and their size smaller at T1 than at T0 ($p<0.05$). Moreover, the morphological characteristics of SAT adipocytes at T1 did not differ from those of control adipocytes ($p=0.89$). Weight loss induced by bariatric surgery resulted in a significant reduction in the inflammation level, as measured by CD68 score. We found that 4% of miRNAs was differently expressed in T1 vs T0, of these 3% was up-expressed and 1% was down-expressed. Bioinformatic analysis of deregulated miRNAs showed several target genes which were involved in relevant pathways among which: pathways in cancer, regulation of endocytosis, MAPK signaling, TGF-beta signaling.

LAGB induces an improvement in the obese metabolic status, which could result in a decreased risk of obese-associated diseases. Moreover, the normalization of adipocyte features at T1 vs T0 suggests a regression of SAT inflammation. Furthermore, our data support that the improvement of the metabolic status induced by bariatric surgery in our obese patients could be obtained also by miRNA-based regulation of gene expression.

1. Background

In the last decades, the rate of obesity in industrialized countries is constantly raised. Obesity prevalence has increased from 15% to 34% among adults and from 5% to 17% among children and adolescents (Freedman 2011). In European Union, close to 14% population is obese (Mooney 2010). In particular, 10.3% of adult Italian population resulted to be obese (OECD obesity update, 2012). This epidemic growth of obesity is mainly due to changes in dietary habits, particularly in the high availability of high-calorie palatable foods. Moreover, in the last years the consumption of snacks and caloric beverages has also increased (St-Onge *et al* 2003). Changes in diet are often also accompanied by a reduction in physical activity. In fact, Only 22% of American children follow the recommendations on baseline levels for physical activity and 25% are classified as completely sedentary (Burgeson *et al* 2001). The environmental / behavioral component is believed to affect the etiopathogenesis of obesity for the 60-70%, while the remaining 30-40% is due to alteration in the genetic counterpart (Clement and Ferré 2003). With few exceptions, obesity is a complex multifactorial disease, and interindividual variations of this phenotype are due to the action of multiple genes and environmental factors. Studies of families, twins and adopted children, indicate that obesity is in part heritable (Miller *et al* 2004, Damcott *et al* 2006). Individual factors, both genetic and psychological, interact with environmental factors in the genesis of obesity. In evolutionary terms, the genetic predisposition to fat accumulation is a mechanism implemented in conditions of food's abundance to ensure survival during times of food shortage (Schwartz *et al* 2000, Bellisari *et al* 2008).

The severity of obesity is evaluated calculating the Body Mass Index (BMI), which is obtained dividing the weight in kilograms by the square of the height in meters of the subject under consideration: a BMI greater than 30 is indicative of moderate obesity, values greater than 40 are instead indicative of severe obesity. Being overweight or obese increases the risk of morbidity and mortality caused by the onset of other diseases such as type 2 diabetes mellitus, hypertension, heart disease and neoplasias (Chen *et al* 1999).

A complex physiological system balances energy intake and energy expenditure, including afferent and efferent signals to the central nervous system (Woods and D'Alessio 2008). The signals coming from the periphery are constituted by gastrointestinal hormones (ghrelin, GLP-1, Peptide Y, cholecystokinin, pancreatic polypeptide, etc..), adipokines released from adipose tissue and hormones, such as insulin, produced by other tissues.

Studies on genetically obese mice (*ob/ob*) led in 1994 to the identification of leptin, a major player in body weight regulation. This protein was the first to be identified among a long series of peptidic products secreted by adipose tissue that today is considered a true endocrine organ. The molecules synthesized and secreted by adipose tissue are collectively called "adipokines". Different cell types contribute to the secretion of these

molecules; for example, a considerable number of adipokines related to inflammation was found in the vasculo-stromal fraction and in the matrix of adipose tissue, which is rich in cells of the immune system.

One of the major peripheral signals is represented by leptin, produced by adipose tissue and regulating the sense of satiety by acting on the melanocortin circuit. Leptin acts through its receptors (ObRb) in two different subpopulations of neurons in the arcuate nucleus. One of this expresses both orexigenic neuropeptides: Neuripeptide Y (NPY) and Agouti Related Protein (AgRP), whose expression is reduced by leptin (Schwartz *et al* 2000); the other population expresses both anorexigenic neuropeptides: Cocaine and Amphetamine Related Transcript (CART) and α-MSH peptide, derived from the proteolytic processing of the POMC gene (proopiomelanocortin), operated by enzymes proconvertasi (PC1 and PC2). The expression of POMC is induced by leptin (Schwartz *et al* 2000). AgRP and α-MSH compete, at hypothalamic level, for binding to melanocortin receptors (MC-Rs), in particular for subtype 4 (MC4R). The interaction between the central circuits and peripheral signals produces, under normal conditions, a coordinated response to any change in nutritional status (Figure 1).

Figure 1. Melanocortin circuit.

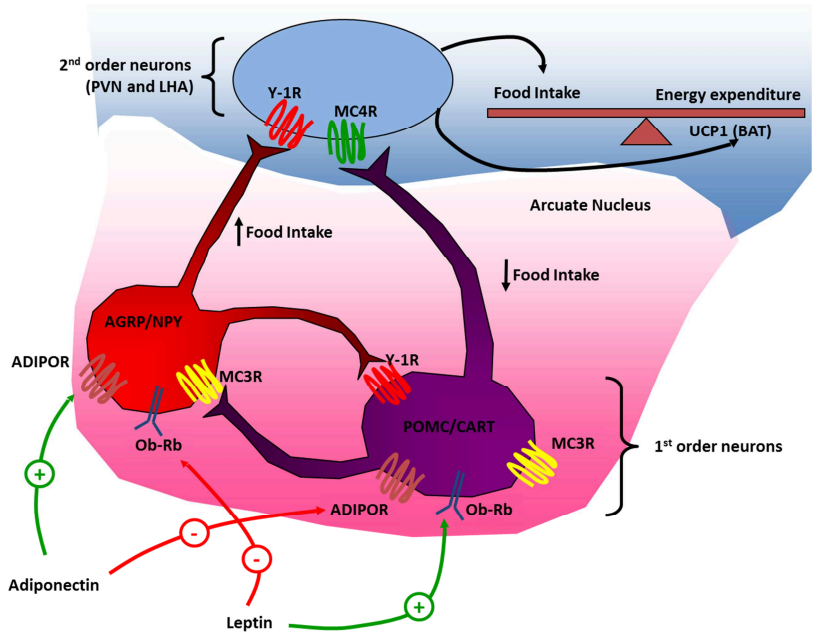

At level of arcuate nucleus, a complex neuronal network decodes the afferent signals from the periphery of the body. In particular, leptin produced by adipose tissue activate the transcription of the anorexigenic peptides POMC/CART, causing a reduction of food intake and an increase of energy expenditure. On the other hand, leptin suppress the transcription of orexigenic AGRP/NPY peptides. At central level, adiponectin has opposite effects than leptin on peptides regulating appetite and energy expenditure.

Severe monogenic obesity in humans is associated with mutations in POMC, PC1, PC2, and MC4R genes (Bellisari *et al* 2008, Chen *et al* 1999,

Farooqi *et al* 2000, Krude *et al* 1998, Raffin-Sanson *et al* 2003, Echwald *et al* 1999, Challis *et al* 2002, Miraglia del Giudice *et al* 2001). These observations suggest that this pathway is important for energy homeostasis and that it is strictly regulated. In parallel, leptin also acts on the CNS inducing release of noradrenaline. Noradrenaline exerts its action on adipose tissue by binding to β3-adrenergic receptors, so activating lipolysis in white adipose tissue (WAT) and thermogenesis in the brown adipose tissue (BAT). The latter mechanism is responsible for the increase in energy expenditure.

Concerning leptin, its serum concentration and its expression in adipose tissue are directly proportional to the levels of adiposity and changes in body weight, making the hormone a good indicator of the deposits of fat in the body. The absence of both leptin or its receptor causes hyperphagia and obesity in animal models and in humans; however, such mutations are rare in obese patients. The serum leptin levels show a circadian rhythm with a peak between 11:00 p.m. to 1:00 a.m., after which the circulating leptin decreases until late afternoon. The pulsatile secretion nature of leptin may be due to the capacity of the adipocytes to store significant amounts of the hormone in subcellular compartments, such as the endoplasmic reticulum. The secretion also shows a clear sexual dimorphism with higher values in females than in males (Vázquez-Vela *et al* 2008).

There are 5 different isoforms of the leptin receptor (Ob-Ra, b, c, d, e). Ob-Rb, the long isoform and metabolically active receptor, is characterized by the presence of a long intracytoplasmic region containing several domains responsible for signal transduction. It is present in high concentrations in the brain (30-40% of all receptors), and in particular in the areas responsible for regulating energy intake, such as the arcuate, dorsal and ventromedial hypothalamic nuclei (Galic *et al* 2010). At low concentrations (approximately 5-8% of the total), Ob-Rb is found also at level of peripheral tissues, such as adipose tissue, ovary, testes, placenta, peripheral blood mononuclear cells, chondrocytes and in skeletal muscle and heart. Like other cytokine receptors of class I, Ob-Rb lacks intrinsic tyrosine kinase activity and therefore requires the recruitment of kinase belonging to the Janus family (Jaks). These kinases phosphorylate the signal transducer and activator of transcription STAT, inducing dimerization and translocation to the nucleus, so causing in the hypothalamus transcriptional suppression of orexigenic genes (Galic *et al* 2010). Moreover, leptin activates also the IRS-PI3K (insulin receptor substrate-phosphoinositide-3-kinase) pathway, which seems to act at the level of adipose tissue in suppressing lipogenesis. The block of leptin signaling is mediated by the activation of the phosphatase PTP-1B (Protein Tyrosine Phosphatase 1B) and SOCS-3 (Suppressors of cytokine signaling 3) that interferes with the phosphorylation of Jak2. A fat-rich diet increases the expression of these two proteins thus decreasing the action of leptin in target tissues (leptin-resistance); this alteration is often observed in obesity (Galic *et al* 2010). In particular, in liver, leptin causes an increased expression of PPARα, a protein that affects lipid metabolism. Leptin-resistance is often associated with hyperleptinemia,

which favors the accumulation of ectopic fat in the liver, skeletal muscle, heart and pancreas. Leptin-resistance was therefore proposed as an important cause of adipocyte dysfunction and deposition of lipids in not-adipose tissue (Galic *et al* 2010).

Adiponectin is another protein secreted from adipose tissue. It is a protein of 30 kDa secreted by adipocytes whose circulating levels are decreased in presence of obesity and insulin resistance. Adiponectin is present in the blood in different isoforms: trimeric (low-molecular weight LMW), hexameric (two homotrimers) and multimeric (from 12 to 18 monomers, high molecular weight-HMW) which have different biological functions. The HMW form has an insulin-sensitizing effect, while the LMW form exerts its effects centrally. The monomer is composed of three functional domains: an N-terminal variable region, an α helix collagen-like region characterized by repetitions of the sequence GXX necessary for polymerization, and a C-terminal globular domain of about 140 amino acids. After the synthesis, it undergoes extensive post-translational modifications, such as hydroxylation and glycosylation, in particular at level of the collagenous domain (Galic *et al* 2010).

Adiponectin binds to its receptors ubiquitously expressed, AdipoR1 and AdipoR2, so activating AMP dependent kinase. The first receptor is expressed primarily in skeletal muscle, the second is more expressed in the liver, both are also present in the hypothalamus where colocalize with the leptin receptor. In hypothalamus, adiponectin has opposite effects to leptin, through the activation of orexigenoic genes and the silencing of anorexigenic ones. At peripheral level, the adiponectin is involved in the phosphorylation of the insulin receptor and its substrate, a necessary mechanism for the translocation of GLUT4 transporter to the cell membrane of muscle and liver (Vázquez-Vela *et al* 2008). A third adiponectin receptor, T-cadherin (also known as cadherin13-CDH13) has been recently identified (Hug *et al* 2004). This receptor can bind the MMW and HMW forms of adiponectin but not the trimeric or globular species.

In humans, adiponectin levels inversely correlate with insulin resistance and the metabolic syndrome and are also decreased in the presence of obesity, type 2 diabetes and atherosclerosis. Adiponectin also counteracts the effects of TNF-α, a pro-inflammatory molecule, inhibiting the expression of adhesion molecules in endothelial cells, thereby diminishing the atherogenic risk. Adiponectin exerts its vasoprotective effects also through the increased production of nitric oxide, or by modulating the expression of scavenger receptors (Galic *et al* 2010).

In mammals, it is possible to recognize two distinct populations of adipocytes. The one forms the so-called white adipose tissue (White Adipose Tissue, WAT) and is characterized by the presence within the cell cytoplasm a single large vacuole containing lipids which occupies about 80% of the cell volume, confining the nucleus and the other organelles to the periphery of the cell. The other population form the brown adipose tissue (Brown Adipose

Tissue, BAT), and is instead characterized by the presence within cells of numerous lipid droplets of small size and several mitochondria. Moreover, based on the localization of WAT, it is possible to identify a subcutaneous adipose tissue (SAT) and a visceral adipose tissue (VAT).

SAT deposits covers the whole body surface: in women they are particularly developed in gluteal-femoral region and breast, while in men they are present mainly in the abdomen and around the muscles of the limbs. VAT is largely localized in the mesenteric and omental regions, while smaller deposits are also present in the epicardial region and in the mediastinum. WAT contains in addition to mature adipocytes, several multipotent mesenchymal stem cells (MSCs) and pre-adipocytes. The increase of the deposits of TG, in conditions of positive caloric balance, produces a hypertrophy of the adipose cell. When these cells reach a critical volume, the differentiation of mesenchymal cells is subsequently stimulated (adipogenesis). Adipocyte differentiation is an important component of hyperplasia of adipose tissue.

Adipocytes are the main cellular component of adipose tissue, and they are crucial for both energy storage and endocrine activity. The other cell types that are present are precursor cells (including pre-adipocytes), fibroblasts, vascular cells and immune cells, constituting the stromal vascular fraction of adipose tissue. Vascular cells include both endothelial and vascular smooth muscle cells, which are associated with the major blood vessels. The blood vessels in adipose tissue are required for the proper flow of nutrients and oxygen to adipocytes, and they are the conduits that allow for the distribution of adipokines. Other active adipose tissue components include macrophages and T cells, which have major roles in determining the immune status of adipose tissue.

Factors that are secreted by these different cellular components are critical for maintaining homeostasis in adipose tissue and throughout the body (Vázquez-Vela *et al* 2008).

Examples of intercellular communication between different adipose tissue cell types include the counter-regulation between adiponectin and tumour necrosis factor (TNF), and between secreted frizzled-related protein 5 (SFRP5) and WNT5a. Under conditions of obesity, the pro-inflammatory factors (TNF and WNT5a) predominate (Vázquez-Vela *et al* 2008).

With limited obesity, it is likely that the tissue retains relatively normal metabolic function and has low levels of immune cell activation and sufficient vascular function. However, qualitative changes in the expanding adipose tissue can promote the transition to a metabolically dysfunctional phenotype. Macrophages in lean adipose tissue express markers of an M2 or alternatively activated state, whereas obesity leads to the recruitment and accumulation of M1 or classically activated macrophages, as well as T cells, in adipose tissue (Ouchi *et al* 2011).

Anti-inflammatory adipokines, including adiponectin, are preferentially produced by lean adipose tissue. During obesity, adipose tissue

generates large amounts of pro-inflammatory factors, including leptin, resistin, retinol-binding protein 4 (RBP4), lipocalin 2, angiopoietin-like protein 2 (ANGPTL2), tumour necrosis factor α (TNF-α), interleukin-6 (IL-6), IL-18, CC-chemokine ligand 2 (CCL2), CXC-chemokine ligand 5 (CXCL5) and nicotinamide phosphoribosyltransferase (NAMPT, visfatin). Obese individuals with adipose tissue in a metabolically intermediate state have improved metabolic parameters, diminished inflammatory marker expression and better vascular function compared with individuals that have metabolically dysfunctional adipose tissue. Metabolically dysfunctional adipose tissue can be associated with higher levels of adipocyte necrosis, and M1 macrophages are arranged around these dead cells in crown-like structures (Romeo *et al* 2012, Gil *et al* 2011, Ouchi *et al* 2011).

Beside the rare monogenic forms of obesity, accounting in humans for 0.5-6% of all obesity forms (Ramachandrappa and Farooqi 2011), several sequence variations in DNA of obese patients have been described in different genes, causing alterations in central regulation of food intake – energy expenditure balance (Yang *et al* 2007). In the last years, a growing number of publications on the role of epigenetic modifications on obesity insurgence have been produced. Among epigenetic mechanisms in regulating gene expression, microRNAs have recently emerged as an important class of mRNA expression regulators. MiRNAs are found in all multicellular organisms, from plants to humans, and in many instances are highly conserved through evolution. For this reason they are likely to be important for normal cellular function.

MiRNA biogenesis can be briefly summarized as follows (Figure 2). A primary miRNA, which may be several thousands of bases long, is cleaved in the nucleus by a protein complex containing the enzyme Drosha to give a precursor miRNA of around 70 nucleotides in a stem-loop structure. This is then transported out of the nucleus into the cytoplasm and further processed by the enzyme Dicer to give a short double-stranded miRNA complex, which contains the mature miRNA strand and a passenger strand (miRNA*), which is normally degraded. The mature miRNA is incorporated with the Argonaute subfamily of proteins into the RNA-induced silencing complex (miRISC). In this complex, the mature miRNA is able to regulate gene expression, binding through partial complementary generally, for the most part to the 3'-untranslated region (3'-UTR) of target mRNAs, and leading at the same time to some degree of mRNA degradation and translation inhibition. The most stringent requirement for this interaction is a contiguous and perfect Watson-Crick basepairing of the miRNA 5'nucleotides 2-8, representing the "seed region" nucleating the interaction (Rottiers and Naar 2012).

Figure 2. MiRNAs biogenesis.

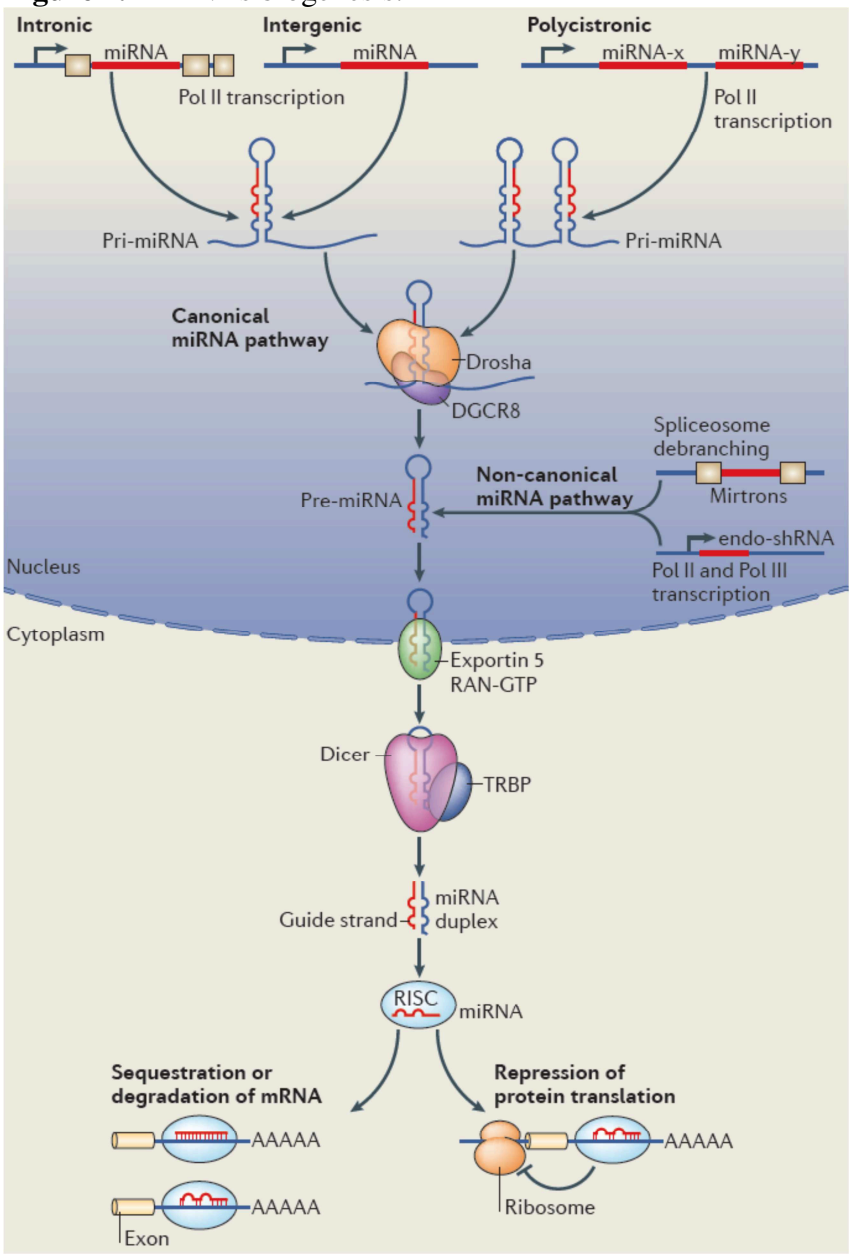

MicroRNAs (miRNAs) are transcribed as precursor RNAs from intergenic, intronic or polycistronic genomic loci by RNA polymerase II (Pol II). The primary miRNA (pri-miRNA) transcript forms a stem–loop structure that is recognized and processed by the Drosha/DGCR8 complex or the spliceosome in the nucleus. The precursor (pre-miRNA) hairpins from both canonical and non-canonical miRNA pathways are then transported by an exportin 5 and RAN-GTP-dependent process to the cytosol, where they are processed by the Dicer/TRBP RNase III enzyme complex to form the mature double-stranded ~22-nucleotide miRNA. Argonaute proteins unwind the miRNA duplex and facilitate incorporation of the miRNA-targeting strand into the AGO-containing RNA-induced silencing complex (RISC). The RISC–miRNA assembly is then guided to specific target sequences in mRNAs. Image from Mol Cell Biol 2012.

MiRNAs are likely to be predominantly fine tuners of gene expression, but there is some evidence that on reaching a critical threshold, they may highly repress protein production and in so doing act as 'switches'.

Each miRNA may fine tune the expression of hundreds or even thousands of proteins, and it is estimated that over 60% of mammalian mRNAs are conserved targets for miRNAs. Additionally, each mRNA may be targeted by many miRNAs. This system therefore potentially has enormous regulatory capacity, but also possesses a complexity that can make it difficult to clarify.

Treatment of obesity is principally based on diet and physical exercise; however, in case of pathological obesity, in which repeated dietetic-pharmacological and behavioral attempts failed, bariatric surgery represents the best approach aimed to the largest excess weight loss (EWL), resulting in improved longevity.

In particular, laparoscopic adjustable gastric banding (LAGB) is among the widespread possibilities for volumetrically reducing the stomach, to induce rapid and early satiety. Moreover, this procedure allows for controlled weight loss without major alterations to the structure and function of the gastrointestinal tract. Compared to other more invasive surgical procedure, such as Roux-en-Y gastric bypass and biliopancreatic diversion, LAGB has proved to be effective with less perioperative morbidity and mortality. This procedure, in more than 95% of cases in literature is performed by laparoscopy (Kral *et al* 2007). The average %EWL at 1 year and 5 years is 41% and 55.4%, respectively, with a large variability in literature related to selection of patients (Kral *et al* 2007).

2. Aims

Therapeutic options for obesity treatment, including lifestyle interventions and pharmacotherapy, are limited, because long-term maintenance of weight loss often fails. Instead, a significant and durable weight loss is obtained by bariatric surgery, that is the most successful clinical intervention leading to an improvement in obesity-related comorbidities (insulin resistance, glucose metabolism, hyperlipidemia and inflammatory profile).

The aim of the present study is to test if the sustained weight loss, following the LAGB, could ameliorate the obese metabolism in term of:

- Improvement of the lipid and glucose metabolism, and/or the liver function evaluated by hepatic markers.
- Normalization of serum levels of main adipocytokines and leptin/adiponectin ratio before (T0) and after (T1) LAGB.
- Normalization of Adiponectin and adiponectin receptors (AdipoR1 and AdipoR2) gene expression in SAT at T1 (after LAGB) compared with T0 (before LAGB).
- Normalization of the SAT phenotype (number and size of adipocytes and inflammatory cell presence) at T1 (after LAGB) compared with T0 (before LAGB).
- Normalization of the SAT miRNAs expression profiling and of miRNAs-deregulated pathways after LAGB respect to before LAGB, also compared with controls.

3. Patients and Methods

Patients and controls

We evaluated 20 severely obese subjects before LAGB (T0, mean body mass index [BMI] 45 kg/m^2) and after the loss of ≥30% excess weight (T1, mean BMI 32 kg/m^2). We also evaluated 10 normal weight subjects. We collected perioperatively SAT and serum samples from all subjects.

The families of all subjects had lived in Southern Italy for at least three generations and all subjects gave their informed consent to the study. The research was approved by the Ethics Committee of the Faculty of Medicine, University of Naples Federico II, and was carried out according to the Helsinki II Declaration.

Main electrolytes, serum glucose, total cholesterol, triglycerides, aspartate aminotransferase (AST), alanine aminotransferase (ALT), alkaline phosphatase (ALP), γ-glutamyl transferase (GGT), lactate dehydrogenase (LDH), cholinesterase (CHE), creatine kinase (CK), amylase (AMS), urea, creatinine, uric acid (UA), total bilirubin (T-bil), total protein (TP), albumin, C reactive protein (CRP) and insulin were measured by routine laboratory methods. Insulin resistance was estimated according to the homeostasis model assessment (HOMA) and the formula: fasting insulin (mIU/l) × fasting glucose (mmol/l)/22.5. A HOMA lower or greater than 1.95 defined insulin sensitivity or resistance, respectively (Messier *et al* 2010, Bonora *et al* 1998, Labruna *et al* 2011).

Serum leptin and adiponectin were measured by Luminex xMAP Technology on a BioRad Multiplex Suspension Array System (BioRad, Hemel Hempstead, Herts), according to the manufacturer's instructions. We also calculated the leptin/adiponectin (L/A) ratio.

Serum protein electrophoresis was performed by capillary electrophoresis.

Hematoxylin & eosin staining

The hematoxylin and eosin (H&E) stain uses two separate dyes, one staining the nucleus and the other staining the cytoplasm and connective tissue. Hematoxylin is a dark purplish dye that will stain the chromatin (nuclear material) within the nucleus, leaving it a deep purplish-blue color. Eosin is an orangish-pink to red dye that stains the cytoplasmic material including connective tissue and collagen, and leaves an orange-pink counterstain. This counterstain acts as a sharp contrast to the purplish-blue nuclear stain of the nucleus, and helps identify other entities in the tissues such as cell membrane (border), red blood cells, and fluid.

The process of performing the H&E stain is relatively simple. After the tissue has been paraffin embedded, sectioned (five-micron sections), placed

on a slide and the slide dried in an oven, the slide is taken through brief changes of xylene, alcohol and water to 'hydrate' the tissue. This process is called 'running the slides down to water' and must be done to give the cells an affinity for the dyes. The slides are then stained with the nuclear dye (hematoxylin) and rinsed, then stained in the counterstain (eosin). They are then rinsed, run in the reverse manner from the run down (taken back through water, alcohol, and xylene), then cover slipped.

For each samples three different fields were evaluated from two different operators. Adipocytes were counted in the same area and the average of the three different fields was calculated.

CD68 evaluation by immunohistochemistry

The CD68 protein was identified by immunohistochemical analysis on formalin-fixed paraffin-embedded adipose tissue blocks. Sections 5-μm thick were cut from the formalin-fixed tissue blocks, dewaxed in xylene analogs (Bio-Clear Bio-Optica, Milan, Italy) and rehydrated with graded ethanol concentrations.

The sections were incubated for 45 min at 97°C in citrate buffer pH 6 (DAKO, S2369) in order to retrieve immunogenicity. Endogenous peroxidase activity was blocked by immersing slides in 3% hydrogen peroxide methanol for 10'. Aspecific antigen sites were blocked by incubating at room temperature for 30' with background reducing components (DAKO).

The primary antibodies used in the immunohistochemical staining was anti-CD68 mouse monoclonal antibody (1:500 Abcam). Tissue sections were incubated at room temperature for 1 h with primary antibodies. Staining was carried out with LSAB+System-HRP (DAKO); the signal was developed using diaminobenzidine (DAB) chromogen as substrate (DAKO). The tissue sections were then lightly counterstained with Mayer's hematoxylin and cover-slipped.

The following scoring system was used: score 0, no staining; 1+, incomplete staining; 2+, strong and complete staining (Barros-Silva *et al* 2009). Two independent observers evaluated the immunohistochemical slides and manually counted the number of macrophages stained in each tissue.

MiRNA expression profile in SAT

Total RNA (including miRNAs) was purified from SAT using the mirVana^{TM} miRNA isolation kit (Ambion) and its concentration was evaluated by NanoDrop® ND-1000 UV-Vis spectrophotometer (NanoDrop Technologies, Wilmington, DE, USA).

TaqMan low density arrays (TLDA), micro fluidic cards were used to detect and quantify mature miRNAs according to manufacturer's

instructions. Each TLDA Human MicroRNA Panel v1.0 card contained 365 preloaded human miRNA targets and two endogenous controls (small nucleolar RNAs: RNU48 and RNU44). TLDAs were prepared in two-steps. In the first step, 640 ng of total RNA were reverse transcribed in eight multiplex reverse transcriptase (RT) reaction pools using stem loop RT primers specific for mature miRNA species. Then, each of the resulting eight cDNA pools was diluted, mixed with TaqMan Universal PCR master mix, and loaded into one of the eight fill ports on the TLDA microfluidic card. The card was centrifuged for 2 min at 1200 rpm to distribute samples to the multiple wells of the fill ports and sealed to prevent well-to-well contamination. Finally, the cards were processed on an 7900 HT Real-Time PCR System (Applied Biosystems). The miRNA expression values were normalized to RNU48 (endogenous control), and relative expression values were obtained using the ΔΔCT method (Relative Quantification, $RQ=2^{-\Delta\Delta CT}$) with Sequence Detection System (SDS) v2.3 and RQ Manager 1.2 software (Applied Biosystems).

Analysis of miRNA targets

After miRNA expression profiling, we predicted the pathways that were likely to be differently regulated in obese patients before and after bariatric surgery by TargetScan Release 5.0 (http://www.targetscan.org) algorithm (Grimson, 2007- Friedman, 2009). This algorithm assigns a "total context score" for each predicted target. Predicted target genes with a "total context score" <-0.30 were then combined and analyzed using the KEGG database (http://www.genome.ad.jp/kegg/) so identifying the biological pathways involving the target genes of our selected miRNAs. By this latter program we selected the biological pathways that contained at least two predicted genes to be miRNA-altered in obese samples with a statistically significant probability $p<0.05$.

Western blot analysis

Protein evaluation by Western blot was performed in 3/20 obese patients before and after bariatric surgery with 35 μg of total proteins separated by SDS-PAGE (13% polyacrylamide gel) and electroblotted onto hydrophobic polyvinylidene difluoride (PVDF) membranes (Amersham) for 19 h at 33 V. Blots were blocked with 5% BSA in TBS buffer with 0.1% Tween 20 for 2 h at room temperature. Immunoblotting was performed with the specific polyclonal antibody: rabbit anti-PPARα (dilution 1:800), and rabbit anti-actin (dilution 1:800) (Abcam, Cambridge, UK) for 4 h. For the following incubation with primary antibody, membrane was washed in TBS buffer with 0.1% Tween 20 and incubated for 45 min IgG-HRP-conjugated secondary antibody (dilution 1:10000). Immunoreactive bands were visualized with the chemiluminescence

reagent kit (ECL Western blotting detection reagents, GE Healthcare). We used the same membrane for each immunoblot, washing it in TBS buffer with 0.1% Tween 20 for 10 min after each experiment. After each immunoblot, the membrane was exposed to X-ray film (Amersham) for different times. The images of three different exposures were captured by Gel Doc XR (Bio-Rad) and quantitated with the Quantity One software (Bio-Rad).

Each protein band was contained within a rectangular area, identical for each sample, and background values were subtracted from each band. The triplicate sample values were normalized to the corresponding triplicate actin values. Then, the mean values from the different ratio calculations were calculated for each sample. The data were expressed as percent relative expression, the sample with the highest expression of PPARα having been set as 100%. The obtained data were used to obtain the corresponding box plots and p-values (Student's t test) in the Microsoft Excel software.

Statistics

Data are reported as mean ± SD, unless differently stated. Between groups comparison were performed by unpaired or paired Student's t test, as appropriate. Multiple groups comparisons were performed by ANOVA or χ^2 test; multiple comparisons were corrected by Bonferroni test. Differences were considered statistically significant at a p level <0.05.

4. Results

Improvements of clinical, biochemical and metabolic parameters

All the investigated parameters are shown in Table 1, and are reported as mean ± SD. After the achievement of the therapeutic goal (EWL≥30%), we observed a significant weight loss ranging from 16.0 to 67.0 kg, corresponding to a mean weight loss of 38.7 ± 13.7 kg in study patients (n=20), with a significant change in weight ($p<0.0001$) (mean ± SD: 128.2 ± 28.1, and 89.7 ± 24.7 Kg, at T0 and at T1, respectively). Also BMI changed significantly ($p<0.0001$), from 44.9 ± 7.8 to 31.5 ± 7.7, at T0 and at T1 respectively.

Based on the HOMA index >1.95, 15/20 patients at T0 were classified as insulin resistant subjects (mean/SD: HOMA 3.3 ± 1.3), whereas at T1, the number of insulin resistant obeses reduced significantly ($p=0.004$), in fact only 5/20 patients still presented HOMA index > 1.95 (mean/SD: HOMA 1.7 ± 0.8). To HOMA values contribute both glucose and insulin concentrations, indeed, we observed a significant reduction both of glucose levels (mean/SD: from 86.3 ± 12.9 mg/dL at T0 to 79.6 ± 11.7 mg/dL at T1 ($p=0.03$), and of insulin levels (mean/SD: from 17.1 ± 11.3 at T0 to 8.6 ± 4.1 at T1) ($p= 0.007$).

Also lipid metabolism, as evaluated by serum cholesterol and triglycerides levels, showed an improvement at T1. In particular, we observed a statistically significant reduction of triglycerides (mean/SD: from 119.5 ± 75.4 to 70.6 ± 22.7 mg/dL at T0 and T1, respectively) ($p=0.004$), while only a very slight reduction in cholesterol levels (mean: 188.8 mg/dL at T0 vs 183.0 mg/dL at T1, p=n.s.).

Surgery-induced weight loss resulted in a significant improvement of liver function as evaluated by AST, ALT, ALP and GGT serum concentrations. In fact, we observed a significant reduction (~30%) of AST (mean/SD: 24.4 ± 13.8 U/L vs 17.2 ± 3.9 U/L at T0 and T1, respectively; $p=0.025$), (~40%) of ALT (mean/SD: 23.5 ± 14.8 U/L vs 14.2 ± 6.8 U/L at T0 and T1, respectively; $p=0.041$), and (~40%) of GGT (mean/SD: 23.2 ± 16.6 U/L vs 14.1 ± 6.5 U/L at T0 and T1, respectively; $p=0.007$).

Total protein and albumin levels did not change after the bariatric surgery intervention, indicating that this surgical procedure did not cause a malnourishment state. But, by protein electrophoresis, we observed a reduction in α1 globulins (mean/SD: 5.1 ± 0.8 % vs 4.5 ± 0.6 %, at T0 and T1, respectively; $p=0.007$) and in β1 globulins (mean/SD: 8.4 ± 2.1 % vs 6.2 ± 0.6 %, at T0 and T1, respectively; $p<0.0001$), and an increase in β2 globulins (mean/SD: 4.1 ± 1.3 % vs 5.1 ± 1.3 %, at T0 and T1, respectively; $p<0.0001$). Median PCR values were a bit, but not statistically significant lower at T1 vs T0 (median values: 7.6 mg/L vs 3.4 mg/L, at T0 and T1, respectively).

Table 1. Clinical and biochemical parameters of the analysed patients (n=20) before (T0) and after (T1) laparoscopic gastric banding.

	T0		T1		T0 vs T1
	Mean	SD	Mean	SD	p°
Age (years)	37.00	13.17	38.67	12.78	**0.000**
Weight (kg)	128.21	28.16	89.69	24.76	**0.000**
EWL (%)			62.53	20.82	
BMI (kg/m^2)	44.91	7.85	31.56	7.79	**0.000**
Na^+ (mmol/L)	140.68	2.16	141.94	1.71	0.168
K^+ (mmol/L)	4.42	0.45	4.39	0.56	0.926
Ca^{++} (mg/dL)	9.63	0.55	9.26	2.40	0.565
Phosphorus (mg/dL)	3.58	0.75	3.44	0.45	0.642
Fe (µg/dL)	92.22	34.99	93.06	28.08	0.636
Glucose (mg/dL)	86.32	12.91	79.63	11.74	**0.031**
Insulin (mU/L)	17.10	11.53	8.67	4.17	**0.007**
HOMA	3.27	1.31	1.69	0.80	**0.004**
Cholesterol (mg/dL)	188.83	40.91	183.00	42.94	0.318
Triglycerides (mg/dL)	119.50	75.42	70.59	22.77	**0.004**
AST (U/L)	24.42	13.89	17.24	3.98	**0.025**
ALT (U/L)	23.56	14.83	14.24	6.85	**0.041**
ALP (U/L)	78.44	23.50	70.47	24.02	**0.013**
GGT (U/L)	23.28	16.67	14.13	6.58	**0.007**
LDH (U/L)	396.26	90.45	353.29	79.79	0.084
CHE (U/L)	9215.11	2270.51	8490.27	1475.32	0.087
CK (U/L)	149.26	101.04	115.40	91.62	0.368
AMS (U/L)	46.39	13.75	58.88	21.06	**0.001**
Urea (mg/dL)	32.05	11.83	30.35	8.64	0.502
Creatinine (mg/dL)	0.76	0.12	0.78	0.11	0.805
UA (mg/dL)	5.58	1.65	4.59	1.20	**0.001**
T-bil (mg/dL)	0.75	0.47	0.90	0.87	0.224
TP (g/dL)	7.56	0.32	7.47	0.58	0.489
Albumin (g/dL)	4.41	0.33	4.53	0.23	0.056
Albumin (%)	55.63	3.72	56.93	3.68	0.050
alfa1 (%)	5.06	0.81	4.49	0.64	**0.007**
alfa2 (%)	10.22	1.96	10.18	1.62	0.923
beta1 (%)	8.38	2.10	6.24	0.65	**0.000**
beta2 (%)	4.11	1.38	5.21	1.39	**0.000**
gamma (%)	16.60	2.51	16.92	2.68	0.405
A/G	1.27	0.20	1.34	0.23	**0.043**
CRP (mg/L)*	7.6	12.0	3.4	7.5	0.108
Adiponectin (µg/mL)	11.17	5.67	25.68	12.91	**0.002**
Leptin (ng/mL)	31.47	19.70	8.91	6.65	**0.011**
L/A	3.82	1.50	0.28	0.25	**0.003**

Abbreviations: EWL: excess weight loss; BMI: body mass index; HOMA: homeostasis model assessment; AST: aspartate aminotransferase; ALT: alanine aminotransferase; ALP: alkaline phosphatase; GGT: γ-glutamyl transferase; LDH: lactate dehydrogenase; CHE: cholinesterase; CK: creatine kinase; AMS: amylase; UA: uric acid; T-bil: total bilirubin; TP: total protein; CRP: C reactive protein; A/G: albumin/gamma globulin ratio; L/A: leptin/adiponectin ratio;
°: statistically significant difference at paired Student's t test are in bold;
*: data reported as median value and interquartile range.

Adiponectin and leptin before and after LAGB

LAGB surgery was accompanied by a significant increase in adiponectin serum levels after the therapeutic goal achievement (mean/SD: 11.1 ± 5.6 µg/mL at T0 vs 25.7 ± 12.9 µg/mL at T1, p=0.002.) (Table 1, Figure 4). SAT adiponectin (ADIPOQ), adiponectin receptor (ADIPOR) 1 and ADIPOR2 mRNA expression were about doubled at T1 respect to T0 (Figure 3). In particular, ADIPOQ/GAPDH cDNA ratio increased at T1 1.8 fold than T0 (T0 value set equal to 1), while ADIPOR1/GAPDH and ADIPOR2/GAPDH cDNA ratios increased 1.7 and 2.2 fold, respectively.

Figure 3. ADIPOQ, ADIPO-R1 and 2 mRNAs expression levels in SAT from obese patients at T1 (T0 mRNA value set equal to 1).

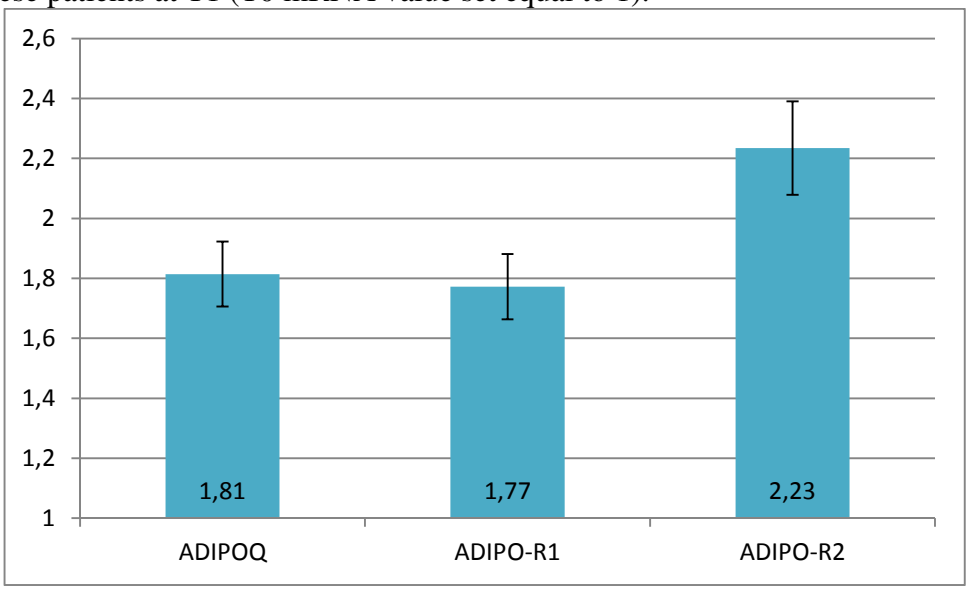

Data are reported as mean RQ ADIPOQ or ADIPO-R1 or ADIPO-R2/GAPDH cDNA ratio. Error bars represent SEM.

Concerning leptin, in the present study, weight loss resulted in a significant decrease in serum leptin levels (mean/SD: 31.4 ± 19.7 ng/mL at T0 vs 8.9 ± 6.6 µg/mL at T1; p=0.011) (Table 1, Figure 4).

In parallel to variations observed in adiponectin and leptin concentrations, we found a decrease in the L/A ratio whose values significantly changed (mean/SD: 3.8 ± 1.5 at T0 vs 0.3 ± 0.2 at T1, (p=0.003) (Table 1, Figure 4).

Figure 4. Adiponectin, leptin and L/A ratio in obese patients before and after surgery.

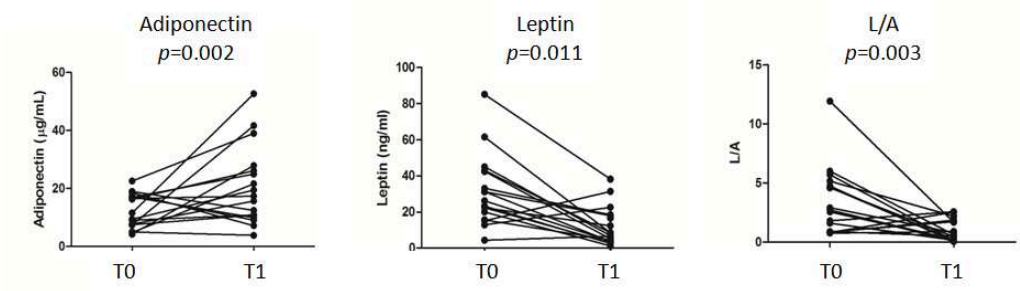

miRNA expression profile

We explored miRNA expression profile in 5/20 of our patients. Results were normalized toward miRNA expression profile obtained in 2 normal weight control subjects. Of the investigated miRNAs, 151/377 (40%) resulted to be not expressed, 22% was not differently expressed between obese and control subjects, while 31% resulted to be higher and 7% lower in the obese patients than in controls (Figure 5). The expression profile of 96% of the tested miRNA was unchanged between T0 and T1; for the remaining miRNAs (8/206), in respect to control subjects, we found the following differences (Figure 6):

- 1/8 becomes down-expressed;
- 7/8 become up-expressed.

Figure 5. Differently expressed miRNAs in SAT from obese patients before bariatric surgery (T0) in comparison to baseline levels evaluated in controls.

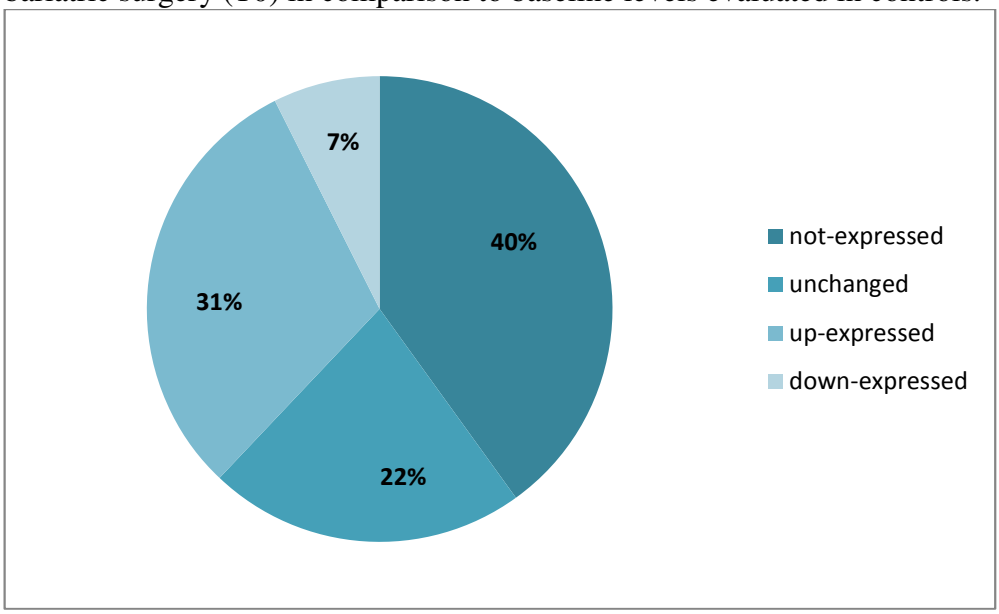

Figure 6. Differently expressed miRNAs in SAT from obese patients after bariatric surgery (T1) in comparison to baseline levels evaluated at T0.

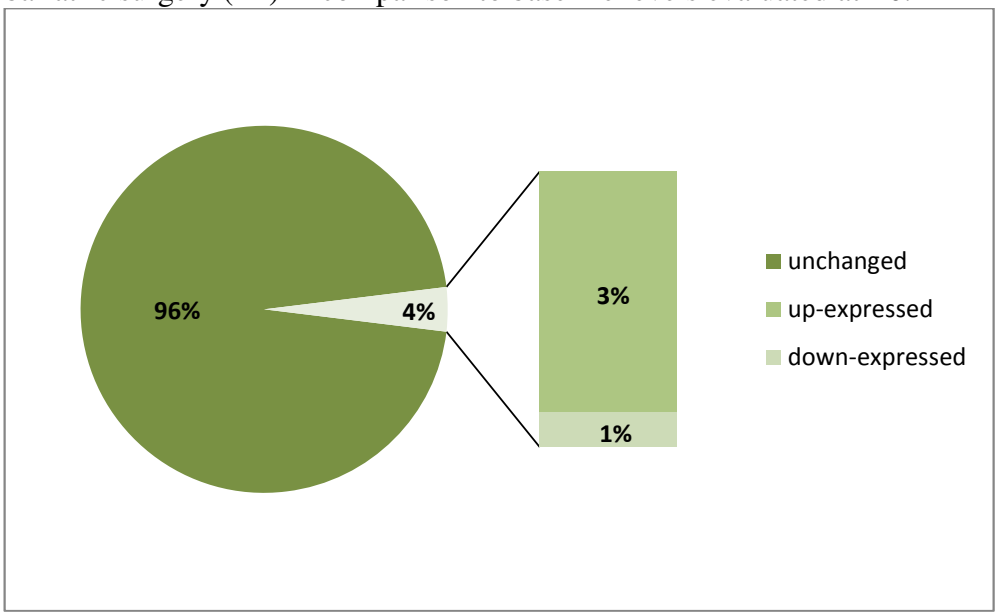

Figure 7. MiRNA whose expression changed after LAGB.

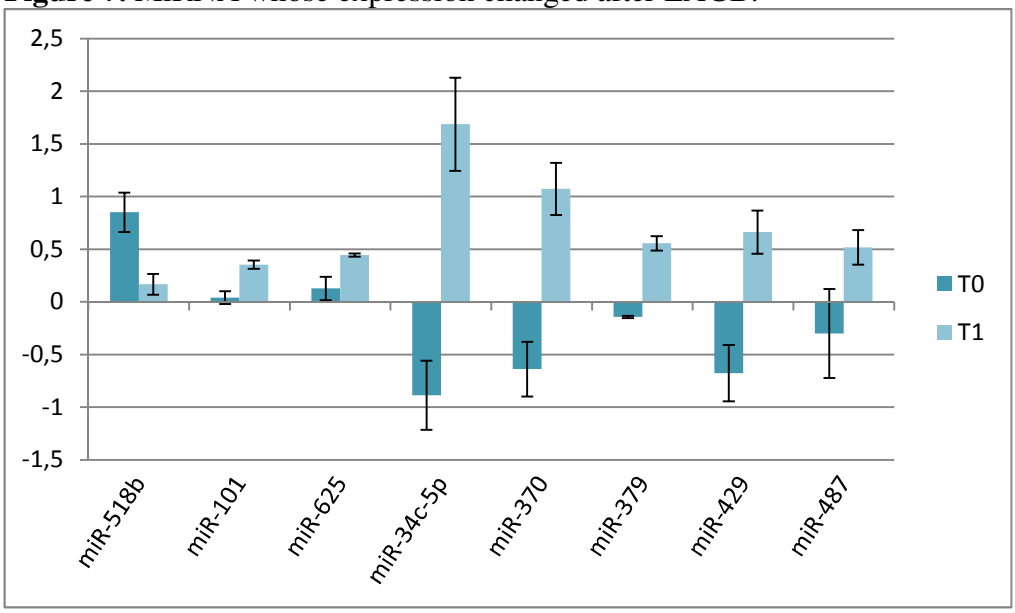

Data are reported an mean logRQ values. Error bars represent SEM.

Among the up-expressed miRNAs, we observed that the expression of some of those resulted to be reduced, even if not at a statistically significant levels, after surgery. In particular, we focused our attention on miR-519d, that was previously studied by our group. MiR-519d expression resulted to be reduced by half after weight loss (mean/SD logRQ: 2.0 ± 1.5 vs 1.6 ± 1.1 at T0 and T1, respectively).

Pathways

By bioinformatics analysis, we found that up-expressed miRNAs at T1 regulate biological pathways reported in Table 2. The most represented pathway is composed by genes involved in cancer regulation (including 25 genes regulated by miRNA up-expressed), followed by endocytosis (16 genes) and MAPK signaling (12 genes) pathways. Moreover, there are many miRNA-regulated genes involved in different pathways related to cell-cell interaction and cell structure maintenance.

Table 2. Pathways predicted by TargetScan analysis as potentially regulated by up-expressed miRNAs after LAGB.

KEGG pathway	Gene Symbol	Gene description
Cancer regulation	WNT10B	wingless-type MMTV integration site family, member 10B
	LAMC1	laminin, gamma 1 (formerly LAMB2)
	FOXO1	forkhead box O1
	FZD4	frizzled family receptor 4
	TGFA	transforming growth factor, alpha
	WNT7A	wingless-type MMTV integration site family, member 7A
	E2F3	E2F transcription factor 3
	PTCH1	patched 1
	TGFBR1	transforming growth factor, beta receptor 1
	TCEB1	transcription elongation factor B (SIII), polypeptide 1 (15kDa, elongin C)
	FOS	FBJ murine osteosarcoma viral oncogene homolog
	TGFBR2	transforming growth factor, beta receptor II (70/80kDa)
	FZD6	frizzled family receptor 6
	MITF	microphthalmia-associated transcription factor
	IGF1	insulin-like growth factor 1 (somatomedin C)
	SMO	smoothened, frizzled family receptor
	KITLG	KIT ligand
	GSK3B	glycogen synthase kinase 3 beta
	MET	met proto-oncogene (hepatocyte growth factor receptor)
	ZMAT3	zinc finger, matrin-type 3
	PMAIP1	phorbol-12-myristate-13-acetate-induced protein 1
	SESN1	sestrin 1
	RAP1B	RAP1B, member of RAS oncogene family
	RAPGEF1	Rap guanine nucleotide exchange factor (GEF) 1
	CALM1	calmodulin 1 (phosphorylase kinase, delta)

Endocytosis	ARAP2	ArfGAP with RhoGAP domain, ankyrin repeat and PH domain 2
	RAB11FIP4	RAB11 family interacting protein 4 (class II)
	STAMBP	STAM binding protein
	TGFBR1	transforming growth factor, beta receptor 1
	RAB5A	RAB5A, member RAS oncogene family
	CAV3	caveolin 3
	TGFBR2	transforming growth factor, beta receptor II (70/80kDa)
	RAB11A	RAB11A, member RAS oncogene family
	GIT2	G protein-coupled receptor kinase interacting ArfGAP 2
	ASAP2	ArfGAP with SH3 domain, ankyrin repeat and PH domain 2
	VPS37D	vacuolar protein sorting 37 homolog D (S. cerevisiae)
	ASAP1	ArfGAP with SH3 domain, ankyrin repeat and PH domain 1
	FLT1	fms-related tyrosine kinase 1 (vascular endothelial growth factor/vascular permeability factor receptor)
	ADRB1	adrenoceptor beta 1
	MET	met proto-oncogene (hepatocyte growth factor receptor)
	SMURF1	SMAD specific E3 ubiquitin protein ligase 1
MAPK signaling pathway	NF1	neurofibromin 1
	CACNA1E	calcium channel, voltage-dependent, R type, alpha 1E subunit
	CACNB2	calcium channel, voltage-dependent, beta 2 subunit
	RAP1B	RAP1B, member of RAS oncogene family
	NLK	nemo-like kinase
	DUSP9	dual specificity phosphatase 9
	TGFBR1	transforming growth factor, beta receptor 1
	FOS	FBJ murine osteosarcoma viral oncogene homolog
	TGFBR2	transforming growth factor, beta receptor II (70/80kDa)
	STMN1	stathmin 1
	PPM1B	protein phosphatase, Mg2+/Mn2+ dependent, 1B
	DUSP1	dual specificity phosphatase 1
Ubiquitin mediated proteolysis	UBE2D2	ubiquitin-conjugating enzyme E2D 2
	UBE2A	ubiquitin-conjugating enzyme E2A
	TCEB1	transcription elongation factor B (SIII), polypeptide 1 (15kDa, elongin C)
	UBE2E3	ubiquitin-conjugating enzyme E2E 3
	UBE2D1	ubiquitin-conjugating enzyme E2D 1
	UBE2R2	ubiquitin-conjugating enzyme E2R 2
	SMURF1	SMAD specific E3 ubiquitin protein ligase 1

	UBE2K	ubiquitin-conjugating enzyme E2K
Axon guidance	GSK3B	glycogen synthase kinase 3 beta
	UNC5C	unc-5 homolog C (C. elegans)
	SEMA3C	sema domain, immunoglobulin domain (Ig), short basic domain, secreted, (semaphorin) 3C
	SEMA4C	sema domain, immunoglobulin domain (Ig), transmembrane domain (TM) and short cytoplasmic domain, (semaphorin) 4C
	MET	met proto-oncogene (hepatocyte growth factor receptor)
	EFNB1	ephrin-B1
	SEMA6C	sema domain, transmembrane domain (TM), and cytoplasmic domain, (semaphorin) 6C
	SRGAP1	SLIT-ROBO Rho GTPase activating protein 1
Cytokine-cytokine receptor interaction	FLT1	fms-related tyrosine kinase 1 (vascular endothelial growth factor/vascular permeability factor receptor)
	KITLG	KIT ligand
	CCL21	chemokine (C-C motif) ligand 21
	IL25	interleukin 25
	TGFBR1	transforming growth factor, beta receptor 1
	ACVR2B	activin A receptor, type IIB
	MET	met proto-oncogene (hepatocyte growth factor receptor)
	TGFBR2	transforming growth factor, beta receptor II (70/80kDa)
Wnt signaling pathway	GSK3B	glycogen synthase kinase 3 beta
	NLK	nemo-like kinase
	WNT10B	wingless-type MMTV integration site family, member 10B
	FZD4	frizzled family receptor 4
	PPP2R5D	protein phosphatase 2, regulatory subunit B', delta
	FZD6	frizzled family receptor 6
	WNT7A	wingless-type MMTV integration site family, member 7A
Neurotrophin signaling pathway	SH2B3	SH2B adaptor protein 3
	GSK3B	glycogen synthase kinase 3 beta
	NTRK3	neurotrophic tyrosine kinase, receptor, type 3
	RAPGEF1	Rap guanine nucleotide exchange factor (GEF) 1
	CALM1	calmodulin 1 (phosphorylase kinase, delta)
	RAP1B	RAP1B, member of RAS oncogene family
Cell adhesion molecules	NLGN4X	neuroligin 4, X-linked
	NFASC	neurofascin
	MPZ	myelin protein zero

	NCAM2	neural cell adhesion molecule 2
	NRCAM	neuronal cell adhesion molecule
	CDH5	cadherin 5, type 2 (vascular endothelium)
Adherens junction	NLK	nemo-like kinase
	TGFBR1	transforming growth factor, beta receptor 1
	MET	met proto-oncogene (hepatocyte growth factor receptor)
	TGFBR2	transforming growth factor, beta receptor II (70/80kDa)
	SSX2IP	synovial sarcoma, X breakpoint 2 interacting protein
TGF-beta signaling pathway	TGFBR1	transforming growth factor, beta receptor 1
	FST	follistatin
	ACVR2B	activin A receptor, type IIB
	SMURF1	SMAD specific E3 ubiquitin protein ligase 1
	TGFBR2	transforming growth factor, beta receptor II (70/80kDa)
Type II diabetes mellitus	PRKCE	protein kinase C, epsilon
	KCNJ11	potassium inwardly-rectifying channel, subfamily J, member 11
	CACNA1E	calcium channel, voltage-dependent, R type, alpha 1E subunit

Western blot

On the basis of previous results obtained by our group regarding the role of up-expressed miR-519d in the down-regulation of PPARα expression, we studied if the expression of this protein normalized after surgery. We performed a western blot analysis of PPARα in 3/10 patients previously screened for miRNAs and found the PPARα/actinin ratio more than doubled (mean/SD: 0.72 ± 0.4 vs 1.84 ± 0.3, respectively; p=0.01) paralleling the miR-519d reduction from T0 to T1 (Figure 8).

Figure 8. Western blot analysis of PPARα from SAT of obese patients at T0 and T1.

A.

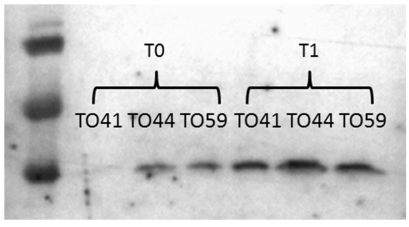

B.

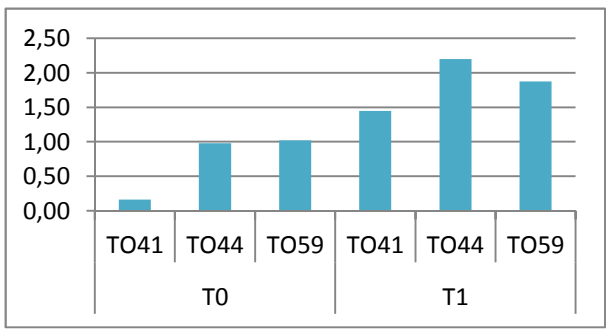

Panel A: western blot image; panel B: relative quantitation of PPARα/actinin ratio at T0 and T1, p=0.01.

Improvement in SAT histology

Paired SAT biopsies were available from 10/20 patients before bariatric surgery and after the achievement of the therapeutic goal. Weight loss induced by bariatric surgery resulted in a significant reduction in the inflammation level, as measured by CD68 score (Figure 9).

Figure 9. CD68 score measured in SAT samples from controls (CO) and obese patients (at T0 before and at T1 after LAGB).

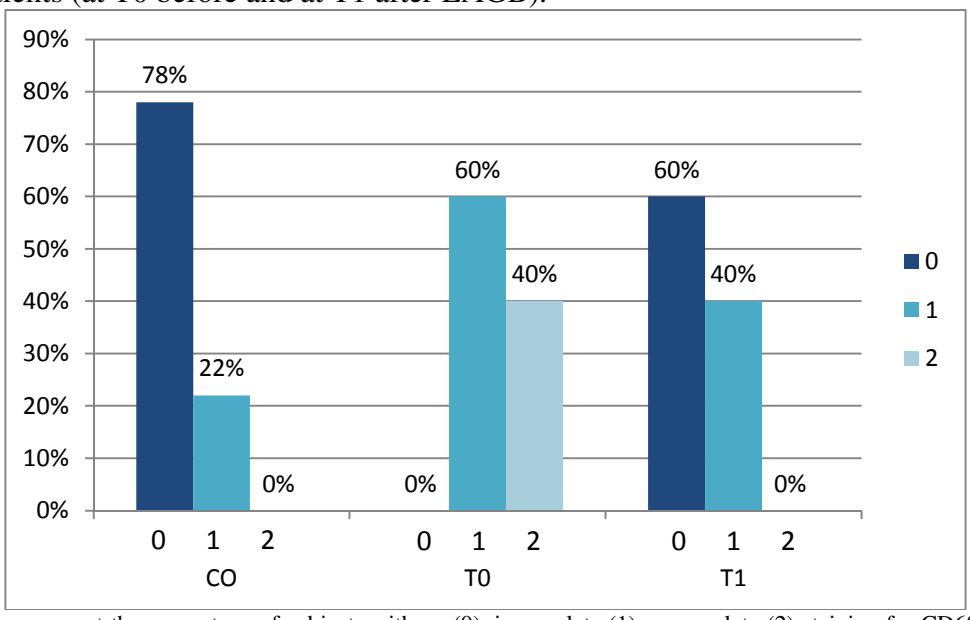

Bars represent the percentage of subjects with no (0), incomplete (1) or complete (2) staining for CD68. Differences in score distribution between the three groups of subjects resulted to be statistically significant at χ^2 test (p=0.003).

We also observed an increase in adipocytes number and a reduction of the cell size at T1 compared to T0 (Figure 10). In particular, cells number significantly increased (mean/SD: 31.6 ± 6.1 at T0 vs 57.7 ± 2.4 at T1, p<0.0001), while cell diameter significantly reduced (mean/SD: 14.6 ± 0.8 µm at T0 vs 7.6 ± 0.3 µm at T1, p<0.0001) (Figure 11). At T1, we did not observed any statistically significant difference in cells number and cell diameter in SAT between obese and control subjects.

Figure 10. SAT biopsies from controls (CO) and obese patients (T0 and T1).

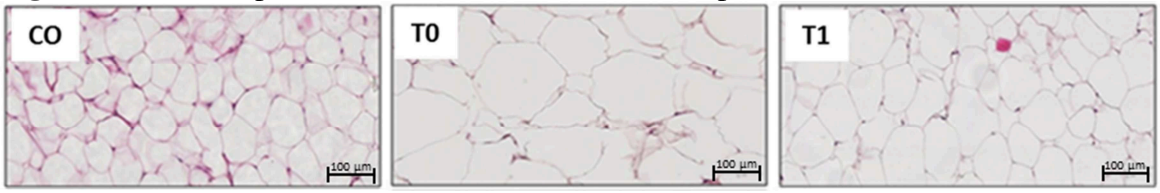

Bars correspond to 100 µm.

Figure 11. Comparison of cells number and cell diameters between controls (CO) and obese patients (T0 and T1).

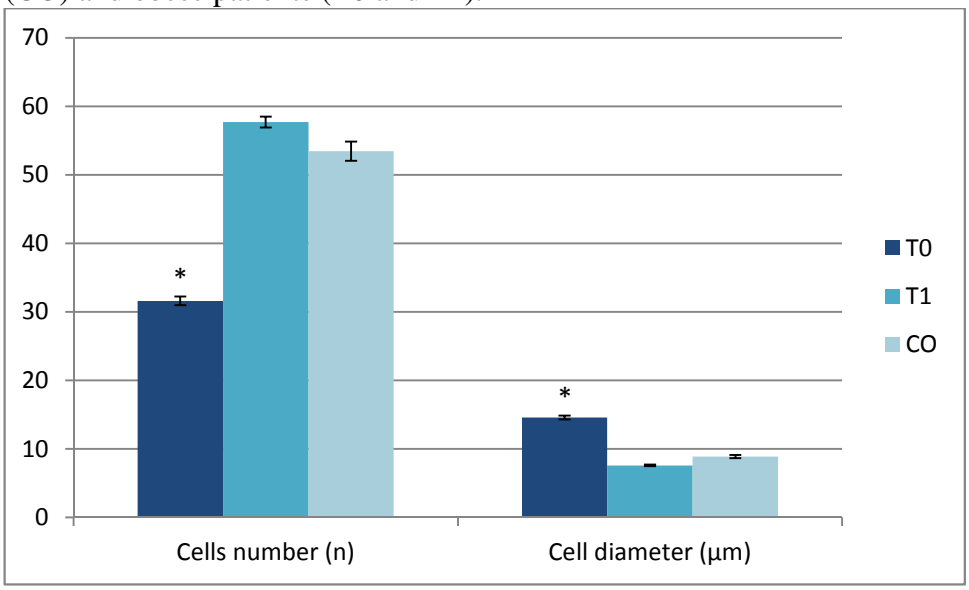

*statistically significant difference between T0 and T1 and between T0 and CO; $p<0.0001$.

5. Discussion

In this study, we found that LAGB-induced weight loss caused in obese patients an improvement in biochemical, hormonal, and histological markers. Moreover, we found that this bariatric surgery procedure induced a modification in SAT miRNA expression profile in the analyzed patients.

Many studies have shown that resolution of obesity related comorbidities depends on significant and sustained weight loss and excess weight loss (Dixon *et al* 2008; Dixon *et al* 2013; Schauer *et al* 2003, Cobourn *et al* 2013). Results of a controlled study found that, among individuals who have had diabetes for less than 2 years, the disease remits in most patients who lose at least 10 % of their body weight following LAGB (Dixon *et al* 2003). None of our patients was diabetic at T0; however, on the basis of HOMA index, 15/20 patients at T0 were classified as insulin resistant. After weight loss, only 5/20 patients had a HOMA > 1.95; therefore, we observed a resolution of insulin resistance in 66% of our patients.

In agreement with our results, two recent prospective studies exploring mechanisms of type 2 diabetes remission have demonstrated that early improvements of insulin sensitivity and intracellular glucose disposition were secondary to caloric restriction shortly after surgery and from the amount of weight lost over time (Camastra *et al* 2011, Nannipieri *et al* 2011).

The importance of insulin resistance is well known as it relates to the metabolic syndrome (Razani *et al* 2008), and insulin resistance is even implicated in the pathogenesis of nonalcoholic fatty liver disease (Duseja *et al* 2007, Jaskiewicz *et al* 2008).

In a study by Nadler et al, it was demonstrated that LAGB improves glucose metabolism in morbidly obese adolescents as well, reducing the risk of developing the consequences of insulin resistance (Nadler *et al* 2009). Patients may expect improved metabolic function, as demonstrated by improvement in liver function enzymes, serum lipid levels, and measures of glucose homeostasis, without significant nutritional deficiencies. Based on these results, several authors proposed LAGB as a therapy for type 2 diabetes and for preventing insulin resistance complications (Moo and Rubino 2008, Inge *et al* 2009).

Concerning inflammatory markers, we found that LAGB induced an improvement in CRP circulating levels and a reduction of the α1 fraction percentage, as measured by protein capillary electrophoresis. This result is in agreement with those obtained by other authors (Widhalm *et al* 2004, Conroy *et al* 2011), that reported a reduction of CRP after bariatric surgery both in adults and adolescent obese patients. This result is really impressive, as CRP is an inflammatory biomarker that independently predicts future vascular events (Al-Qahtani 2007), and its decrease has been associated with reductions in the occurrence of adverse cardiovascular outcomes (Ridker *et al* 2008). LAGB-induced weight loss appears to eliminate some risk factors associated to obesity, in addition to reducing CRP levels, all of which may lead to improved

cardiovascular health in patients underwent bariatric surgery (Moschen *et al* 2010, O'Brien *et al* 2013).

In previous studies of our group (Labruna *et al* 2009, Labruna *et al* 2011) we demonstrated that a high serum L/A ratio was a marker of "at risk" obesity, i.e. a type of obesity associated with metabolic impairment, and a good predictor of metabolic syndrome and non-alcoholic fatty liver disease insurgence in morbid obese patients. Moreover, L/A ratio has also been reported as a useful index to evaluate insulin resistance in the absence of hyperglycemia (Inoue *et al* 2006) and as a predictor for carotid atherosclerosis in healthy males (Norata *et al* 2007).

In the present study, we found that leptin levels significantly decrease in T1 compared to T0. This result is in agreement with those previously reported in several papers, in which leptin serum level was reduced after bariatric surgery (van Dielen *et al* 2002, Faraj *et al* 2003), even if with greater reduction following a RYGB versus gastric banding (Trakhtenbroit *et al* 2009). It has been proposed that after bariatric surgery, the changes in cytokines and hormones derived from adipose tissue and the GI tract appear to impart a significantly greater physiological effect than the restrictive and malabsorptive effects alone would predict (Edwards *et al* 2011). Reduction in circulating levels of leptin has been associated in a decreased expression of *ob* gene in adipose tissue of patients undergoing bariatric surgery (Greco *et al* 2002, Knerr *et al* 2006). Unluckily, we do not have data on leptin expression at level of adipose tissue, but it is possible to argue such described mechanism acting also in our patients.

In parallel with leptin reduction, we observed an increase in adiponectin concentration in our patients after bariatric surgery. Adiponectin is a well described anti-inflammatory and anti-atherogenic factor. We evaluated the response of the adiponectin and adiponectin receptors, AdipoR1 and AdipoR2, to metabolic changes induced by LAGB. We found an increase not only in adiponectin serum levels, but also in adiponectin gene expression in SAT from obese patients at T1. However, the link between circulating level of this protein and SAT adiponectin mRNA expression appears to be controversial (Savu *et al* 2009, Garaulet *et al* 2004, Osei *et al* 2005). Also studies of changes in the gene expression of AdipoRs have been controversial. AdipoRs have been reported to be both positively and negatively associated with obesity and insulin resistance (Wang *et al* 2002, Bluher *et al* 2006, Civitarese *et al* 2004). However, in the present study we found that, independently from the receptor's isoform, adiponectin receptors mRNA expression increased in SAT samples from obese patients after bariatric surgery. Two different function and regulation were described for ADIPOR1 and 2: ADIPOR1 is likely involved in the insulin-sensitization function of adiponectin, and ADIPOR2 might be more involved in the pathways involved in energy homeostasis (Yamauchi *et al* 2007, Rasmussen *et al* 2006, Bjursell *et al* 2007). This could reflect the improvement that we observed in our patients both in insulin-resistance and in lipid metabolism.

In the present study, we observed a different miRNA expression profile in SAT from patients before and after bariatric surgery. In particular, 3% of the expressed miRNA appear to be up regulated after LAGB, while 1% are down regulated after weight loss. MiR101 was described to be a regulator of innate immune response to microbial infection (Zhu *et al* 2010). Zhu et al demonstrated that miR101 directly targets mkp-1 to regulate the activation of MKP phosphatese and subsequent production of cytokines in response to LPS stimulation (Zhu *et al* 2010). Moreover, it was proposed as an important protective factor against liver damage induced by COX2 activator in mice (Yoshioka *et al* 2011). All together, these results could suggest that in our patients LAGB could be responsible of a liver-protective effect and of a restoration of innate immune system regulation by inducing an up-regulation of miR-101.

Mir-625 is another miRNA we found up-regulated in our patient at T1. It resulted down-regulated in chronic liver disease (Katayama *et al* 2012) and it was suggested to have a protective influence on the development of non-small cell lung cancer (Roth *et al* 2012). We could argue that this miRNA could exert a protective liver function also in our tested patients after weight loss.

Interestingly, among the target genes of miR-34c-5p, MAPT is a microtubule-associated protein which promotes the assembly of tubulin into microtubules, indicating a possible role for this miRNA in cytoskeleton assembly and regulation (Wu *et al* 2013).

Two of the differently expressed miRNA between T0 and T1 comparison, miR-370 and mR-379, were described to have a role in lipid metabolism. In particular, miR-370 targets carnitine palmitoyl transferase (Cpt1a), a mitochondrial enzyme that mediates the transport of long-chain fatty acids across the membrane by binding them to carnitine, thereby reducing fatty acid oxidation (Iliopoulos *et al* 2010). Notably, transfection of the human hepatic cell line HepG2 with miR-370, upregulates the expression of miR-122 leading to an increased expression of lipogenic genes including SREBP1c and DGAT2, suggesting that miR-370 provides an additional point of regulation of this pathway (Iliopoulos *et al* 2010). Gao et al showed that plasma levels of miR-122 and miR-370 are increased in patients with hyperlipidemia and positively correlated with total cholesterol, triglycerides and LDL-cholesterol levels (Gao *et al* 2012). Furthermore, the increased levels of miR-122 and miR-370 were associated with CAD presence. These results appear to be in contrast with our ones, even if it must be noted that we performed a gene expression study at level of adipose tissue and what we observed could not reflect what Gao et al observed at level of blood streaming.

Concerning miR-379, Chartoumpekis *et al* observed an up-regulation of this miRNA in adipose tissue from mice during obesity development. This contrasting data could be due to the different examined species (Chartoumpekis *et al* 2012).

Interestingly, we found that LAGB induced weight loss caused a decrease in miR-519d expression in SAT from studied patients.

By a previous study of our group (Martinelli *et al* 2010), we know that miR-519d was overexpressed and protein levels of PPARα, one of the predicted miR-519d targets, were reduced in SAT from obese vs nonobese subjects. MiR-519d was found to suppress PPARα translation and increased lipid accumulation during adipocyte differentiation. Moreover, PPARα is highly expressed in tissues that rely on fatty acid oxidation as their primary energy substrate, namely, heart, liver, and skeletal muscle (Braissant *et al* 1996), where, under stress conditions, it appears to mediate the balance between cellular fatty acid metabolism and glucose homeostasis (Leone *et al* 1999). In vitro, the effect of miR-519d on adipogenesis was similar to that of miR-143, a well-known marker of adipogenesis (Esau *et al* 2004). Our previous findings suggested that miR-519d overexpression and alteration of PPARα protein expression could be associated with obesity, so the reduction we observed in miR-519d after bariatric surgery, and the subsequent PPARα increment, could reflect an improvement in lipid metabolism and adipose tissue functionality.

In the presence of its endogenous ligands, i.e. fatty acids, PPARα form heterodimers with the retinoid X receptor-α, and binds to the peroxisome proliferator–response elements in the promoter regions of target genes so increasing their transcriptional activation (Cho *et al* 2008, Cresci 2007). The target genes of PPARα are primarily those involved in energy metabolism and substrate utilization, namely, genes involved in fatty acid uptake, fatty acid esterification, fatty acid β-oxidation, glucose oxidation, mitochondrial transport, and energy uncoupling (Cresci 2007).

Furthermore, PPARα was found to prevent adipocytes hypertrophy and to reduce inflammation in white adipose tissue (Tsuchida *et al* 2005).

MiR-519d was also reported to be a part of a microRNA signature of pluripotency in human embryonic stem cell cultures (Bar *et al* 2008). So, the higher miR-519d expression in SAT from obese vs nonobese subjects and the miR-519d's role in preadipocyte differentiation are in line with an altered microRNA-based adipocyte differentiation mechanism in obesity.

Obesity is characterized by increased fat mass and energy storage in adipose tissue. Increased fat mass can be due to increases in the size of adipocytes (adipocyte hypertrophy), or expanding the numbers of adipocytes (adipocyte hyperplasia) (Rosen and MacDougald 2006). In addition, obesity is strongly associated with inflammation and insulin resistance. Larger fat cells are closely linked to greater fat mass and the production of inflammatory cytokines (Rosen and MacDougald 2006); moreover, they attract macrophages leading to adipocyte necrosis and release of fatty acids into circulation so contributing to excess fat deposition in the liver (Rosen and MacDougald 2006). Nevertheless, alterations in adipocyte turnover rate, differentiation and apoptosis could all contribute to changes in fat mass underlying obesity. However, recent findings suggest the turnover rate of pre-adipocytes in humans

is very low, amounting to 10% self-renewal every year (Arner *et al* 2010), and several studies have suggested pre-adipocyte differentiation may be impaired in obese humans (Gustafson *et al* 2009, Permana *et al* 2004, Isakson *et al* 2009). Our results demonstrate that excess weight loss induced by LAGB caused not only a reduction in fat cells dimension, but also a reduction of macrophage infiltration in subcutaneous adipose tissue, so reducing the inflammatory level. Interestingly, a number of miRNAs have been described to have a role in adipocytes differentiation and morphology of adipose tissue (McGregor and Choi 2011, Kloting *et al* 2009). In particular, miR-95 expression was described to be negatively associated with mean adipocyte volume both in SAT and in VAT (Kloting *et al* 2009). In our study, we found that miR-95 expression increased from T0 to T1 even if not at a statistically significant level. This is in line with what we observe histologically by H&E staining.

Several pathways that we identified as potentially deregulated by differently expressed miRNAs, have been described as associated to obesity insurgence and maintenance. Several genes involved in endocytosis have been studied in the last years during obesity. RAB7 was described to have a role in early and late endocytic processes in the regulation of fat storage and as a target of *tubby*, an important locus for the regulation of fat storage in humans (Mukhopadhyay *et al* 2007). We found other members of RAB family deregulated by up-expressed miRNAs. In particular, RAB11A protein may lead to increased glucose uptake and to increased triglyceride synthesis, as described in a previous study by our group (Capobianco *et al* 2012). Moreover, Arf6 is a novel regulator of adrenergic-stimulated and basal lipolysis via its influence on receptor trafficking that was proposed as an important regulator of lipolysis in vivo (Liu *et al* 2010). We found that both adrenergic receptor beta 1 and two Arf6 interactors (ASAP1 and ASAP2) could be potentially regulated by up-expressed miRNAs as predicted by TargetScan analysis.

Also the MAPK pathway was previously associate to obesity, being MAPKs able to regulate adipogenesis at each steps of the process, from stem cells to adipocytes (Bost *et al* 2005), together with the ubiquitin mediated proteolysis pathway, that resulted deregulated during obesity (Das *et al* 2007). Among genes included in the axon guidance pathway, SRGAP1 is a protein interactor of ROBO1, a gene previously reported as associated to BMI (Vehof *et al* 2011).

Concerning neurotrophin signaling pathway, it includes several genes involved in the transmission of molecular signaling activates by neurotrophins. These latter are known to have a wide range of roles in development and function of the nervous system. One of these, BDNF, plays a part in the control of energy balance by the central nervous system (Schwartz and Mobbs 2012). Beside the direct involvement of BDNF in obesity, our results indicate that miRNAs could have a role in mediate the association between neurotrophins and obesity in humans.

Cell adhesion molecules have been described to be associated with measures of obesity (Miller and Cappuccio 2006). We found that several genes coding for cells adhesion molecules expressed in CNS or in vascular endothelium are potentially target of up-expressed miRNAs after LAGB.

It was described that TGF-β signaling regulates glucose tolerance and energy homeostasis. In particular, Smad3 (a target of TGF-β) KO mice were protected from diet induced obesity and diabetes (Yadav *et al* 2011). We found that both TGFBR1 and 2 (TGF-β receptors) are target genes of up-expressed miRNA, their expression possibly being down-regulated. This could cause a damping of signaling transduction so exerting a protective role against obesity.

All together, our results highlight the complex web of interacting genetic and epigenetic factors concurring to human obesity.

6. Conclusions

In this study we characterized from a biochemical, genetic and histological point of view a group of severe obese patients before and after bariatric surgery.

We found that excess weight loss induced by LAGB caused an improvement in metabolic pathways in all patients, as supported by significant decreased serum levels in T1 vs T0 samples of insulin, HOMA, triglycerides, hepatic markers and leptin/adiponectin ratio. Moreover, we found a significant increase in mRNA expression of adiponectin, ADIPOR1 and ADIPOR2 in SAT at T1 compared to T0. This suggest that bariatric surgery could exert an anti-inflammatory and vascular protective function partially mediated by adiponectin. The improvements of the inflammatory profile is also highlighted by the reduction of macrophage infiltration at level of SAT, as shown by the reduction in CD68 signals in biopsies from patients after weight loss. Furthermore, surgery have a role in phenotypic modulation of SAT causing a reduction of cell diameters and an increase of cells number.

Concerning miRNAs, we found a subgroup of miRNAs whose expression profile is influenced by surgery. These dysregulated miRNAs in SAT are possibly involved in the pathogenesis of obesity. Pharmacologically targeting of such miRNAs could address to specific therapeutic interventions aimed to silence (in the case of overexpressed miRNA) or to overexpress (in the case of downregulated miRNA) these small regulatory molecules and so to prevent the insurgence of obesity-related diseases.

7. References

Al-Qahtani AR. Laparoscopic adjustable gastric banding in adolescent: safety and efficacy. J Pediatr Surg 2007;42(5):894–897.

Arner E, Westermark PO, Spalding KL, Britton T, Rydén M, Frisén J, Bernard S, Arner P. Adipocyte turnover: relevance to human adipose tissue morphology. Diabetes. 2010;59(1):105-9.

Bar M, Wyman SK, Fritz BR, Qi J, Garg KS, Parkin RK, Kroh EM, Bendoraite A, Mitchell PS, Nelson AM, Ruzzo WL, Ware C, Radich JP, Gentleman R, Ruohola-Baker H, Tewari M.. MicroRNA discovery and profiling in human embryonic stem cells by deep sequencing of small RNA libraries. Stem Cells 2008;26:2496–2505.

Barros-Silva JD, Leitão D, Afonso L, Vieira J, Dinis-Ribeiro M, Fragoso M, Bento MJ, Santos L, Ferreira P, Rêgo S, Brandão C, Carneiro F, Lopes C, Schmitt F, Teixeira MR. Association of ERBB2 gene status with histopathological parameters and disease-specific survival in gastric carcinoma patients. Br J Cancer. 2009;100(3):487-93.

Bellisari A. Evolutionary origins of obesity. Obes Rev. 2008;9(2):165-80.

Bjursell M, Ahnmark A, Bohlooly-Y M, William-Olsson L, Rhedin M, Peng XR, Ploj K, Gerdin AK, Arnerup G, Elmgren A, Berg AL, Oscarsson J, Lindén D. Opposing effects of adiponectin receptors 1 and 2 on energy metabolism. Diabetes 2007;56:583–93.

Blüher M, Bullen JW Jr, Lee JH, Kralisch S, Fasshauer M, Klöting N, Niebauer J, Schön MR, Williams CJ, Mantzoros CS. Circulating adiponectin and expression of adiponectin receptors in human skeletal muscle: associations with metabolic parameters and insulin resistance and regulation by physical training. J Clin Endocrinol Metab 2006;91:2310–6.

Bonora E, Kiechl S, Willeit J, Oberhollenzer F, Egger G, Targher G, Alberiche M, Bonadonna RC, Muggeo M. Prevalence of insulin resistance in metabolic disorders: the Bruneck Study. Diabetes 1998;47:1643–1649.

Bost F, Aouadi M, Caron L, Binétruy B. The role of MAPKs in adipocyte differentiation and obesity. Biochimie. 2005;87(1):51-6

Braissant O, Foufelle F, Scotto C, Dauça M, Wahli W. Differential expression of peroxisome proliferator-activated receptors (PPARs): tissue distribution of PPAR-alpha, -beta, and -gamma in the adult rat. Endocrinology 1996;137:354–366.

Burgeson CR, Wechsler H, Brener ND, Young JC, Spain CG. Physical education and activity: results from the School Health Policies and Programs Study 2000. J Sch Health. 2001;71(7):279-93

Camastra S, Gastaldelli A, Mari A, Bonuccelli S, Scartabelli G, Frascerra S, Baldi S, Nannipieri M, Rebelos E, Anselmino M, Muscelli E, Ferrannini E. Early and longer term effects of gastric bypass surgery on tissue-specific insulin sensitivity and beta cell function in morbidly obese patients with and without type 2 diabetes. Diabetologia. 2011;54:2093–102.

Capobianco V, Nardelli C, Ferrigno M, Iaffaldano L, Pilone V, Forestieri P, Zambrano N, Sacchetti L. miRNA and Protein Expression Profiles of Visceral Adipose Tissue Reveal miR-141/YWHAG and miR-520e/RAB11A as Two Potential miRNA/Protein Target Pairs Associated with Severe Obesity. J Proteome Res. 2012. [Epub ahead of print]

Challis BG, Pritchard LE, Creemers JW, Delplanque J, Keogh JM, Luan J, Wareham NJ, Yeo GS, Bhattacharyya S, Froguel P, White A, Farooqi IS, O'Rahilly S. A missense mutation disrupting a dibasic prohormone processing site in pro-opiomelanocortin (POMC) increases susceptibility to early-onset obesity through a novel molecular mechanism. Hum Mol Genet 2002;11:1997-2004.

Chartoumpekis DV, Zaravinos A, Ziros PG, Iskrenova RP, Psyrogiannis AI, Kyriazopoulou VE, Habeos IG. Differential Expression of MicroRNAs in Adipose Tissue after Long-Term High-Fat Diet-Induced Obesity in Mice. PLoS One. 2012;7(4):e34872.

Chen D, Garg A. Monogenic disorders of obesity and body fat distribution. J Lipid Res 1999;40:1735-1746.

Cho MC, Lee K, Paik SG, Yoon DY. Peroxisome proliferators-activated receptor (PPAR) modulators and metabolic disorders. PPAR Res 2008;2008:679137.

Civitarese AE, Jenkinson CP, Richardson D, Bajaj M, Cusi K, Kashyap S, Berria R, Belfort R, DeFronzo RA, Mandarino LJ, Ravussin E. Adiponectin receptors gene expression and insulin sensitivity in non-diabetic Mexican Americans with or without a family history of type 2 diabetes. Diabetologia 2004;47:816 –20.

Clement K and Ferré P. Genetics and pathophysiology of obesity. Pediatr Res 2003;53:721-5.

Cobourn C, Chapman MA, Ali A, Amrhein J. Five-Year Weight Loss Experience of Outpatients Receiving Laparoscopic Adjustable Gastric Band Surgery. Obes Surg. 2013. [Epub ahead of print]

Conroy R, Lee EJ, Jean A, Oberfield SE, Sopher A, Kiefer K, Raker C, McMahon DJ, Zitsman JL, Fennoy I. Effect of laparoscopic adjustable gastric banding on metabolic syndrome and its risk factors in morbidly obese adolescents.J Obes. 2011;2011:906384.

Cresci S. Pharmacogenetics of the PPAR genes and cardiovascular disease. Pharmacogenomics 2007;8:1581–1595.

Damcott CM, Sack P, Shuldiner AR. The genetics of obesity. Endocrinol Metab Clin North Am. 2003;32(4):761-86.

Das UN, Rao AA. Gene expression profile in obesity and type 2 diabetes mellitus. Lipids Health Dis. 2007;6:35.

Dixon JB, Chuang LM, Chong K, Chen SC, Lambert GW, Straznicky NE, Lambert EA, Lee WJ. Predicting the glycemic response to gastric bypass surgery in patients with type 2 diabetes. Diabetes Care 2013;36(1):20-6.

Dixon JB, Dixon AF, O'Brien PE. Improvements in insulin sensitivity and beta-cell function (HOMA) with weight loss in the severely obese. Homeostatic model assessment. Diabet Med. 2003;20:127–34.

Dixon JB, O'Brien PE, Playfair J, Chapman L, Schachter LM, Skinner S, Proietto J, Bailey M, Anderson M. Adjustable gastric banding and conventional therapy for type 2 diabetes: a randomized controlled trial. JAMA. 2008;299:316–23.

Duseja A, Das A, Dhiman RK, Chawla YK, Thumburu KT, Bhadada S, Bhansali A. Metformin is effective in achieving biochemical response in patients with nonalcoholic fatty liver disease (NAFLD) not responding to lifestyle interventions. Ann Hepatol 2007;6:222–226.

Echwald SM, Sørensen TIA, Andersen T, Tybjaerg-Hansen A, Clausen JO, Pedersen O. Mutational analysis of the proopiomelanocortin gene in Caucasians with early onset obesity. Int J Obes Relat Metab Disord 1999;23:293-8.

Edwards C, Hindle AK, Fu S, Brody F. Downregulation of leptin and resistin expression in blood following bariatric surgery. Surg Endosc. 2011;25(6):1962-8.

Esau C, Kang X, Peralta E, Hanson E, Marcusson EG, Ravichandran LV, Sun Y, Koo S, Perera RJ, Jain R, Dean NM, Freier SM, Bennett CF, Lollo B, Griffey R. MicroRNA-143 regulates adipocyte differentiation. J Biol Chem 2004;279:52361–52365.

Faraj M, Havel PJ, Phelis S, Blank D, Sniderman AD, Cianflone K. Plasma acylation-stimulating protein, adiponectin, leptin, and ghrelin before and after

weight loss induced by gastric bypass surgery in morbidly obese subjects. J Clin Endocrinol Metab 2003;88:1594–1602

Farooqi IS, Yeo GS, Keogh JM. Dominant recessive and inheritance of morbid obesity associated with melanocotin 4 deficiencies. J Clin Invest 2000;106:271-279.

Freedman DS. Obesity – United States, 1988–2008. MMWR Surveill Summ 2011; 60(Suppl.): 73–77.

Galic S, Oakhill JS, Steinberg GR. Adipose tissue as an endocrine organ. Mol Cell Endocrinol. 2010;316(2):129-39.

Gao W, He HW, Wang ZM, Zhao H, Lian XQ, Wang YS, Zhu J, Yan JJ, Zhang DG, Yang ZJ, Wang LS. Plasma levels of lipometabolism-related miR-122 and miR-370 are increased in patients with hyperlipidemia and associated with coronary artery disease. Lipids Health Dis. 2012;11:55.

Garaulet M, Viguerie N, Porubsky S, Klimcakova E, Clement K, Langin D, Stich V. Adiponectin gene expression and plasma values in obese women during very-low-calorie diet: relationship with cardiovascular risk factors and insulin resistance. J Clin Endocrinol Metab 2004;89:756–60.

Gil A, Olza J, Gil-Campos M, Gomez-Llorente C, Aguilera CM. Is adipose tissue metabolically different at different sites? Int J Pediatr Obes. 2011;6 Suppl 1:13-20.

Greco AV, Mingrone G, Vettor R, Manco M, Rosa G, Capristo E, Federspil G, Castagneto M, Gasbarrini G. Lowering of circulating free-fatty acids levels and reduced expression of leptin in white adipose tissue in post-obesity status. J Invest Med 2002;50:207–13.

Gustafson B, Gogg S, Hedjazifar S, Jenndahl L, Hammarstedt A, Smith U. Inflammation and impaired adipogenesis in hypertrophic obesity in man. Am J Physiol Endocrinol Metab. 2009;297(5):E999-E1003.

Hug C, Wang J, Ahmad NS, Bogan JS, Tsao TS, Lodish HF. T-cadherin is a receptor for hexameric and high-molecular-weight forms of Acrp30/adiponectin. Proc Natl Acad Sci U S A. 2004;101(28):10308-13.

Iliopoulos D, Drosatos K, Hiyama Y, Goldberg IJ, Zannis VI. MicroRNA-370 controls the expression of microRNA-122 and Cpt1alpha and affects lipid metabolism. J Lipid Res 2010;51(6):1513–1523.

Inge TH, Miyano G, Bean J, Helmrath M, Courcoulas A, Harmon CM, Chen MK, Wilson K, Daniels SR, Garcia VF, Brandt ML, Dolan LM. Reversal of type 2 diabetes mellitus and improvements in cardiovascular risk factors after surgical weight loss in adolescents. Pediatrics 2009;123:214–222.

Inoue M, Yano M, Yamakado M, Maehata E, Suzuki S. Relationship between the adiponectin-leptin ratio and parameters of insulin resistance in subjects without hyperglycemia. Metabolism 2006;55:1248-54.

Isakson P, Hammarstedt A, Gustafson B, Smith U. Impaired preadipocyte differentiation in human abdominal obesity: role of Wnt, tumor necrosis factor-alpha, and inflammation. Diabetes 2009; 58: 1550-7.

Jaskiewicz K, Rzepko R, Sledzinski Z. Fibrogenesis in fatty liver associated with obesity and diabetes mellitus type 2. Dig Dis Sci 2008;53:785–788.

Katayama Y, Maeda M, Miyaguchi K, Nemoto S, Yasen M, Tanaka S, Mizushima H, Fukuoka Y, Arii S, Tanaka H. Identification of pathogenesis-related microRNAs in hepatocellular carcinoma by expression profiling. Oncol Lett. 2012;4(4):817-823.

Klöting N, Berthold S, Kovacs P, Schön MR, Fasshauer M, Ruschke K, Stumvoll M, Blüher M. MicroRNA Expression in Human Omental and Subcutaneous Adipose Tissue. PLoS One. 2009;4(3):e4699.

Knerr I, Herzog D, Rauh M, Rascher W, Horbach T. Leptin and ghrelin expression in adipose tissues and serum levels in gastric banding patients. Eur J Clin Invest. 2006;36(6):389-94.

Kral JG, Näslund E. Surgical treatment of obesity. Nat Clin Pract Endocrinol Metab. 2007;3(8):574-83.

Krude H, Biebermann H, Werner L, Rudiger H, Brabant G, Gruters Á. Severe early-onset obesity, adrenal insufficiency and red hair pigmentation caused by POMC mutations in humans. Nat Genet 1998;19(2):155-7.

Labruna G, Pasanisi F, Nardelli C, Tarantino G, Vitale DF, Bracale R, Finelli C, Genua MP, Contaldo F, Sacchetti L. UCP1 -3826 AG+GG genotypes, adiponectin, and leptin/adiponectin ratio in severe obesity. J Endocrinol Invest. 2009;32(6):525-9.

Labruna G, Pasanisi F, Nardelli C, Caso R, Vitale DF, Contaldo F, Sacchetti L. High leptin/adiponectin ratio and serum triglycerides are associated with an "at-risk" phenotype in young severely obese patients. Obesity (Silver Spring). 2011;19(7):1492-6

Leone TC, Weinheimer CJ, Kelly DP. A critical role for the peroxisome proliferator-activated receptor alpha (PPARalpha) in the cellular fasting response: the PPARalpha-null mouse as a model of fatty acid oxidation disorders. Proc Natl Acad Sci USA 1999;96:7473–7478.

Liu Y, Zhou D, Abumrad NA, Su X. ADP-ribosylation factor 6 modulates adrenergic stimulated lipolysis in adipocytes. Am J Physiol Cell Physiol. 2010;298(4):C921-8.

Martinelli R, Nardelli C, Pilone V, Buonomo T, Liguori R, Castanò I, Buono P, Masone S, Persico G, Forestieri P, Pastore L, Sacchetti L. miR-519d Overexpression Is Associated With Human Obesity. Obesity (Silver Spring). 2010;18(11):2170-6.

McGregor RA, Choi MS. microRNAs in the regulation of adipogenesis and obesity. Curr Mol Med. 2011 Jun;11(4):304-16.

Messier V, Karelis AD, Prud'homme D, Primeau V, Brochu M, Rabasa-Lhoret R. Identifying metabolically healthy but obese individuals in sedentary postmenopausal women. Obesity (Silver Spring) 2010;18:911–917.

Miller J, Rosenbloom A, Silverstein J.Childhood obesity. J Clin Endocrinol Metab. 2004;89(9):4211-8.

Miller MA, Cappuccio FP. Cellular adhesion molecules and their relationship with measures of obesity and metabolic syndrome in a multiethnic population. Int J Obes (Lond). 2006 Aug;30(8):1176-82.

Miraglia del Giudice E, Cirillo G, Santoro N, D'Urso L, Carbone MT, Di Toro R, Perrone L. Molecular screening of the proopiomelanocortin (POMC) gene in Italian obese children: report of three new mutations. Int J Obes Relat Metab Disord 2001;25:61-7.

Moo TA, Rubino F. Gastrointestinal surgery as treatment for type 2 diabetes. Curr Opin Endocrinol Diabetes Obes 2008;15:153–158.

Mooney H. British are the most overweight in Europe, new study shows. BMJ 2010; 341: c7225.

Moschen AR, Molnar C, Geiger S, Graziadei I, Ebenbichler CF, Weiss H, Kaser S, Kaser A, Tilg H. Anti-inflammatory effects of excessive weight loss: potent suppression of adipose interleukin 6 and tumour necrosis factor α expression. Gut 2010;59:1259e1264.

Mukhopadhyay A, Pan X, Lambright DG, Tissenbaum HA. An endocytic pathway as a target of tubby for regulation of fat storage. EMBO Rep. 2007 Oct;8(10):931-8.

Nadler EP, Reddy S, Isenalumhe A, Youn HA, Peck V, Ren CJ, Fielding GA. Laparoscopic adjustable gastric banding for morbidly obese adolescents affects android fat loss, resolution of comorbidities, and improved metabolic status. J Am Coll Surg. 2009;209(5):638-44.

Nannipieri M, Mari A, Anselmino M, Baldi S, Barsotti E, Guarino D, Camastra S, Bellini R, Berta RD, Ferrannini E.The role of beta-cell function and insulin sensitivity in the remission of type 2 diabetes after gastric bypass surgery. J Clin Endocrinol Metab. 2011;96: E1372–9.

Norata GD, Raselli S, Grigore L, Garlaschelli K, Dozio E, Magni P, Catapano AL. Leptin:adiponectin ratio is an independent predictor of intima media thickness of the common carotid artery. Stroke 2007;38:2844-6.

O'Brien PE, MacDonald L, Anderson M, Brennan L, Brown WA. Long-term outcomes after bariatric surgery: fifteen-year follow-up of adjustable gastric banding and a systematic review of the bariatric surgical literature. Ann Surg. 2013;257(1):87-94.

OECD (Organisation for Economic Co-operation and Development) Obesity update 2012; www.oecd.org/health/49716427.pdf .

Osei K, Gaillard T, Cook C, Kaplow J, Bullock M, Schuster D. Discrepancies in the regulation of plasma adiponectin and TNF-alpha levels and adipose tissue gene expression in obese African Americans with glucose intolerance: a pilot study using rosiglitazone. Ethn Dis 2005;15:641–8.

Ouchi N, Parker JL, Lugus JJ, Walsh K. Adipokines in inflammation and metabolic disease. Nat Rev Immunol. 2011;11(2):85-97.

Permana PA, Nair S, Lee YH, Luczy-Bachman G, Vozarova De Courten B, Tataranni PA. Subcutaneous abdominal preadipocyte differentiation in vitro inversely correlates with central obesity. Am J Physiol Endocrinol Metab. 2004;286(6):E958-62.

Raffin-Sanson ML, de Keyzer Y, Bertagna X. Proopiomelanocortin, a polypeptide precursor with multiple functions: from physiology to pathological conditions. Eur J Endocrinol 2003;149:79- 90.

Ramachandrappa S, Farooqi IS. Genetic approaches to understanding human obesity. J Clin Invest. 2011;121(6):2080-6.

Rasmussen MS, Lihn AS, Pedersen SB, Bruun JM, Rasmussen M, Richelsen B. Adiponectin receptors in human adipose tissue: effects of obesity, weight loss, and fat depots. Obesity 2006 (Silver Spring) 14:28 –35.

Razani B, Chakravarthy MV, Semenkovich CF. Insulin resistance and atherosclerosis. Endocrinol Metab Clin North Am 2008;37:603–621.

Ridker PM, Danielson E, Fonseca FA, Genest J, Gotto AM Jr, Kastelein JJ, Koenig W, Libby P, Lorenzatti AJ, MacFadyen JG, Nordestgaard BG, Shepherd J, Willerson JT, Glynn RJ; JUPITER Study Group. Rosuvastatin to

prevent vascular events in men and women with elevated C-reactive protein. N Engl J Med 2008;359(21):2195–2207.

Romeo GR, Lee J, Shoelson SE. Metabolic syndrome, insulin resistance, and roles of inflammation mechanisms and therapeutic targets. Arterioscler Thromb Vasc Biol. 2012;32(8):1771-6.

Rosen ED, MacDougald OA. Adipocyte differentiation from the inside out. Nat Rev Mol Cell Biol 2006;7:885-96.

Roth C, Stückrath I, Pantel K, Izbicki JR, Tachezy M, Schwarzenbach H. Low Levels of Cell-Free Circulating miR-361-3p and miR-625* as Blood-Based Markers for Discriminating Malignant from Benign Lung Tumors. PLoS One. 2012;7(6):e38248.

Rottiers V, Näär AM. MicroRNAs in metabolism and metabolic disorders. Nat Rev Mol Cell Biol. 2012;13(4):239-50.

Savu MK, Phillips SA, Oh DK, Park K, Gerlan C, Ciaraldi TP, Henry RR. Response of adiponectin and its receptors to changes in metabolic state after gastric bypass surgery: dissociation between adipose tissue expression and circulating levels. Surg Obes Relat Dis. 2009;5(2):172-80.

Schauer PR, Burguera B, Ikramuddin S, Cottam D, Gourash W, Hamad G, Eid GM, Mattar S, Ramanathan R, Barinas-Mitchel E, Rao RH, Kuller L, Kelley D. Effect of laparoscopic Roux-en Y gastric bypass on type 2 diabetes mellitus. Ann Surg. 2003;238:467–84.

Schwartz E, Mobbs CV. Hypothalamic BDNF and obesity: found in translation. Nat Med. 2012;18(4):496-7.

Schwartz MW, Woods SC, Porte D Jr, Seeley RJ, Baskin DG. Central nervous system control of food intake. Nature. 2000;404(6778):661-71.

St-Onge MP, Keller KL, Heymsfield SB. Changes in childhood food consumption patterns: a cause for concern in light of increasing body weights. Am J Clin Nutr. 2003;78(6):1068-73.

Trakhtenbroit MA, Leichman JG, Algahim MF, Miller CC III, Moody FG, Lux TR, Taegtmeyer H. Body weight, insulin resistance, and serum adipokine levels 2 years after 2 types of bariatric surgery. Am J Med 2009;122:435–442

Tsuchida A, Yamauchi T, Takekawa S, Hada Y, Ito Y, Maki T, Kadowaki T. Peroxisome proliferator-activated receptor (PPAR)alpha activation increases adiponectin receptors and reduces obesity-related inflammation in adipose tissue: comparison of activation of PPARalpha, PPARgamma, and their combination. Diabetes 2005;54:3358–3370.

van Dielen FMH, van ‘t Veer C, Buurman WA, Greve JWM. Leptin and soluble leptin receptor levels in obese and weight-losing individuals. J Clin Endocrinol Metab. 2002;87:1708–1716

Vázquez-Vela ME, Torres N, Tovar AR. White adipose tissue as endocrine organ and its role in obesity. Arch Med Res. 2008;39(8):715-28.

Vehof J, Al Hadithy AF, Burger H, Snieder H, Risselada AJ, Wilffert B, Cohen D, Arends J, Wiersma D, Mulder H, Bruggeman R. Association between the ROBO1 gene and body mass index in patients using antipsychotics. Psychiatr Genet. 2011;21(4):202-7.

Wang Y, Xu A, Knight C, Xu LY, Cooper GJ. Hydroxylation and glycosylation of the four conserved lysine residues in the collagenous domain of adiponectin: potential role in the modulation of its insulinsensitizing activity. J Biol Chem 2002;277:19521–9.

Widhalm K, Dietrich S, and Prager G. Adjustable gastric banding surgery in morbidly obese adolescents: experiences with eight patients. Int J Obes 2004;28(s 3):S42–S45.

Woods SC, D'Alessio DA. Central control of body weight and appetite. J Clin Endocrinol Metab. 2008;93(11 s 1):S37-50.

Wu H, Huang M, Lu M, Zhu W, Shu Y, Cao P, Liu P. Regulation of microtubule-associated protein tau (MAPT) by miR-34c-5p determines the chemosensitivity of gastric cancer to paclitaxel. Cancer Chemother Pharmacol. 2013. [Epub ahead of print]

Yadav H, Quijano C, Kamaraju AK, Gavrilova O, Malek R, Chen W, Zerfas P, Zhigang D, Wright EC, Stuelten C, Sun P, Lonning S, Skarulis M, Sumner AE, Finkel T, Rane SG. Protection from Obesity and Diabetes by Blockade of TGF-b/Smad3 Signaling. Cell Metab. 2011;14(1):67-79.

Yamauchi T, Nio Y, Maki T, Kobayashi M, Takazawa T, Iwabu M, Okada-Iwabu M, Kawamoto S, Kubota N, Kubota T, Ito Y, Kamon J, Tsuchida A, Kumagai K, Kozono H, Hada Y, Ogata H, Tokuyama K, Tsunoda M, Ide T, Murakami K, Awazawa M, Takamoto I, Froguel P, Hara K, Tobe K, Nagai R, Ueki K, Kadowaki T. Targeted disruption of AdipoR1 and AdipoR2 causes abrogation of adiponectin binding and metabolic actions. Nat Med 2007;13:332–9.

Yang W, Kelly T, He J. Genetic epidemiology of obesity. Epidemiol Rev. 2007;29:49-61.

Yoshioka W, Higashiyama W, Tohyama C. Involvement of MicroRNAs in Dioxin-Induced Liver Damage in the Mouse. Toxicol Sci. 2011;122(2):457-65.

Zhu QY, Liu Q, Chen JX, Lan K, Ge BX. MicroRNA-101 Targets MAPK Phosphatase-1 To Regulate the Activation of MAPKs in Macrophages. J Immunol. 2010;185(12):7435-42.

J. Endocrinol. Invest. 32: 525-529, 2009
DOI: 10.3275/6108

UCP1 –3826 AG+GG genotypes, adiponectin, and leptin/adiponectin ratio in severe obesity

G. Labruna[1,2], F. Pasanisi[3]*, C. Nardelli[1,2], G. Tarantino[3], D.F. Vitale[4], R. Bracale[1,5], C. Finelli[3], M.P. Genua[3], F. Contaldo[3], and L. Sacchetti[1,2]

[1]CEINGE Biotecnologie Avanzate S.C. a R.L.; [2]Department of Biochemistry and Medical Biotechnologies; [3]Centro Interuniversitario di Studi e Ricerche sull'Obesità, Department of Clinical and Experimental Medicine, University of Naples "Federico II", Naples; [4]Fondazione Salvatore Maugeri, Istituto IRCCS, Benevento; [5]S.Pe.S. Department, University of Molise, Campobasso, Italy

ABSTRACT. ***Background and aims:*** **Non-alcoholic fatty liver disease (NAFLD) and metabolic syndrome (MS) are well-recognized complications of obesity. This study was designed to evaluate the role of the UCP1 –3826 A>G polymorphism, adiponectin levels, leptin/adiponectin ratio (L/A), and main biochemical parameters in 102 unrelated severely obese adults [61 females and 41 males, median body mass index (BMI) = 47.8 kg/m^2] with NAFLD, with (MS+) or without MS (MS–) from Southern Italy.** ***Subject and methods:*** **The UCP1 polymorphism was tested by the TaqMan method, main biochemical parameters by routinary methods, adiponectin, and leptin serum levels by enzyme-linked immunosorbent assay. MS was diagnosed according to the American Heart Association criteria, liver steatosis was detected by ultrasound.** ***Results:*** **MS was present in 53% male and 66% female obese patients. Only total cholesterol (*p*=0.04 males and *p*=0.002 females) and L/A ratio (*p*=0.03 males) differed between MS+ and MS– obese patients. At multivariate analysis, severe liver steatosis was significantly associated with: UCP1 (AG+GG) genotypes [odds ratio-confidence interval (OR-CI): 4.25; 1.12-16.13], MS (OR-CI: 8.47; 1.78-40.25), low adiponectin levels (OR-CI: 0.92; 0.87-0.98), high alanine aminotransferase levels (OR-CI: 1.03; 1.00-1.06), age (OR-CI: 1.08; 1.00-1.15), and male gender (OR-CI: 10.78; 1.61-71.96).** ***Conclusion:*** **In addition to traditional factors, total cholesterol and L/A ratio appear to contribute to MS characterization in severe obesity. Furthermore, the UCP1 (AG+GG) genotypes and low adiponectin levels could predispose to a more severe liver steatosis independently of MS presence. Based on our data, polymorphic UCP1 (AG+GG) obese patients with low adiponectin levels appear to be high-risk subjects for worsening of liver steatosis, a NAFLD, possibly requiring a second-step evaluation by liver biopsy.**

(J. Endocrinol. Invest. 32: 525-529, 2009)

INTRODUCTION

The prevalence of obesity [body mass index (BMI) ≥30 kg/m^2] is increasing worldwide and it is estimated that up to 9% and 30% of adults in Italy and in the United States respectively are obese (1-3). Severe obesity (i.e. BMI>40 kg/m^2) has also reached a dramatically high level and now affects about 1-2% of the adult European and 4% of the US population (2). Obesity, and in particular severe obesity, is associated with an increased risk of cardiovascular disease (CVD), sudden death, Type 2 diabetes, hypertension, liver steatohepatitis, and dysfunctions involving the endocrine and reproductive systems, bone metabolism, inflammation, immunity, and some types of cancer (4, 5). In 1998, the World Health Organization described the "metabolic syndrome" (MS) as a cluster of metabolic risk factors, namely, abdominal obesity, dyslipidemia (hypertriglyceridemia and low HDL-cholesterol concentrations), elevated blood pressure and hyperglycemia, to identify subjects at a higher risk of CVD (6). These criteria have been updated by the American Heart Association (AHA) (7).

Recently, leptin/adiponectin (L/A) ratio has also been reported as a useful index to evaluate insulin resistance in the absence of hyperglycemia (8) and as a predictor for carotid atherosclerosis in healthy males (9).

Non-alcoholic fatty liver disease (NAFLD) is a well-recognized complication of obesity, which is associated with MS, and with a risk of cirrhosis and liver cancer (10, 11). Liver biopsy is the only diagnostic test that can, within the NAFLD spectrum, reliably distinguish simple steatosis from steatosis with necroinflammatory changes and hepatocellular injury [i.e., non-alcoholic steatohepatitis (NASH)]. However, because this differentiation does not affect the management of obese patients, liver biopsy is not routinely performed, and the first-step evaluation of the liver is based on biochemical and imaging studies (11). The prevalence of NAFLD and MS is expected to increase with increasing excess body fat (10, 12). NAFLD is associated with decreased levels of adiponectin, a protective adipokine that inhibits such pro-inflammatory cytokines as tumor necrosis factor α and nuclear factor κβ (11). Furthermore, low adiponectin expression in intra-abdominal adipose tissue of morbidly obese patients may predispose to the progressive form of NAFLD, namely NASH (13).

A number of genes have been associated with human obesity phenotypes, including those encoding the thermogenic uncoupling proteins (UCP) (3). The reduced

Key-words: Adiponectin, liver disease, metabolic syndrome, severe obesity, uncoupling protein.

Correspondence: F. Pasanisi, Dipartimento di Medicina Clinica e Sperimentale, Università di Napoli "Federico II", Via S. Pansini, 5 – 80131 Naples, Italy.

E-mail: pasanisi@unina.it

Accepted December 29, 2009.

First published online March 26, 2009.

thermogenesis caused by UCP1 genetic variants has been implicated in increased susceptibility to obesity particularly when associated with aging and a high fat diet (14, 15). UCP1 is expressed only in mitochondria from brown adipose tissue where it uncouples respiration from ATP synthesis and dissipates energy as heat (14). The human UCP1 gene has been mapped to the long arm of chromosome 4 (16). An A>G point mutation at –3826 bp upstream from the UCP1 TATA box promoter has been related to changes in mRNA expression in intraperitoneal fat (16). Although the association between this UCP1 polymorphism and human obesity is controversial, it is clear that the minor variant allele is related to an increased propensity to gain weight over time (16).
The aim of this study was to evaluate, in a large population of severely obese adults from Southern Italy, the role of the UCP1 –3826 A>G gene polymorphism, adiponectin, and L/A ratio as risk factors in the onset of the obesity-associated complications, namely MS and liver steatosis.

MATERIALS AND METHODS

Study population

We studied 102 unrelated Caucasian adult patients [61 females (F) and 41 males (M), aged ≥18 yr] with severe obesity (median BMI =47.9 kg/m^2 males and 47.7 kg/m^2 females) from Southern Italy. The population was recruited at the obesity outpatient clinic of the Department of Clinical and Experimental Medicine, University of Naples "Federico II", Italy, from 2005 to 2006. Clinical and biochemical data were obtained from each patient at the first admission. All patients underwent screening for known obesity-related complications and CVD in a Day Hospital. Patients with previous CVD or cerebrovascular events, and alcohol abusers (i.e. alcohol consumption >20 g/day) were excluded from the study. Over 90% of patients had a family history of: obesity plus hypertension plus diabetes (52%), obesity (20%), hypertension (11%), diabetes (6%), hyperlipidemia (1%) or neoplasia (1%). We measured the following parameters in each individual: BMI [weight/height^2 (kg/m^2)], blood pressure and heart rate (following 5-min sitting). The general and biochemical characteristics of the population studied are reported in Table 1. As liver steatosis is 5-fold more frequent in obese patients than in lean individuals (17), we performed ultrasound liver examination in all patients. An Esaote Biomedica Apparatus (Firenze, Italy) equipped with a convex 3-5 MHz probe was used and the test imaging was read by two operators unaware of the laboratory data of the patients. Liver steatosis was also graded semiquantitatively on a scale of 0-3 (0= absent; 1= mild; 2= moderate; 3= severe) according to Saverymuttu et al. (18) on the basis of abnormally intense, high-level echoes arising from the hepatic parenchyma, liver-kidney difference in echo amplitude, echo penetration into the deep portion of the liver and clarity of liver blood vessel structure (19, 20). Healthy Caucasian normal-weight controls (M=29, F=66, BMI>20 and <25 kg/m^2) from the same geographic area were also recruited at the Ambulatory Medicine Service of the "Federico II" University Hospital. A venous blood sample was collected from each patient and control subject in the morning at 8.00 h after an overnight fast.

Laboratory investigations

Main biochemical and hormonal parameters [total cholesterol, HDL-cholesterol, triacylglycerols, aspartate aminotransferase (AST), alanine aminotransferase (ALT), γ-glutamyl-transferase (GGT), glucose, total proteins and insulin] were measured by routine laboratory methods. Insulin resistance was estimated according to the homeostasis model assessment (HOMA) and the formula: fasting insulin (mIU/l)/[22.5 × $e^{-\ln(\text{mmol/l glucose})}$].

Table 1 - *Main general and biochemical characteristics (median value and 2.5th-97.5th percentiles) of 102 severely adult obese patients (males=41; females=61).*

	Males		Females	
Age (yr)	34.5	18.0-57.0	31.0	18.4-67.0
BMI (kg/m^2)	47.9	38.7-93.4	47.7	40.0-76.0
Systolic blood pressure (mmHg)[a]	130.0	105.2-179.5	120.0	94.0-160.0
Diastolic blood pressure (mmHg)[b]	85.0	55.6-110.0	80.0	60.0-100.0
Heart rate (b/min)	80.0	56.4-108.0	76.0	57.9-100.0
Adiponectin (μg/ml)	17.2	3.3-57.1	20.2	3.3-48.3
Leptin (ng/ml)[c]	56.8	3.7-212.8	138.9	40.4-240.2
L/A ratio	3.3	0.02-50.0	5.8	0.9-50.0
Glucose (mmol/l)	5.2	3.2-10.6	4.9	3.6-7.7
Insulin (mIU/l)[a]	27.9	9.3-75.0	19.2	7.1-55.5
HOMA[d]	6.3	1.6-18.6	4.2	1.4-12.7
Total cholesterol (mmol/l)[e]	4.5	3.1-6.1	4.8	2.9-6.7
HDL cholesterol (mmol/l)[c]	1.0	0.6-1.5	1.2	0.9-1.9
Triacylglycerols (mmol/l)	1.3	0.4-3.5	1.4	0.6-3.2
AST (U/l)[a]	28.0	13.0-93.8	20.0	11.0-67.5
ALT (U/l)[c]	44.0	17.2-176.2	24.0	9.1-111.0
GGT (U/l)[c]	38.0	16.0-333.0	22.0	7.3-154.3
Total proteins (g/dl)	7.5	6.9-8.3	7.4	6.7-8.3

Statistically significant differences at Mann-Whitney test: [a]p=0.001; [b]p=0.004; [c]p<0.0001; [d]p=0.002; [e]p=0.011. BMI: body mass index; L/A: leptin/adiponectin; HOMA: homeostasis model assessement; AST: aspartate aminotransferase; ALT: alanine aminotransferase; GGT: γ-glutamyl transferase.

Total serum adiponectin and leptin concentrations were measured in duplicate in obese and control subjects by an enzyme-linked immunosorbent assay (LINCO Research, Mo, USA), using monoclonal anti-human adiponectin and leptin antibodies. We also calculated the L/A ratio.

Genomic DNA was extracted from whole blood (Nucleon BACC-II; Amersham Science Europe). The UCP1 –3826 A>G gene polymorphism was assayed with the Real Time TaqMan method. We used two fluorescent probes: one specific for the wild-type allele (VIC-CAGTTTGATCAAGTGCAT-Q-MGB, where VIC is the fluorescent reporter dye, Q the quencher molecule and MGB an enhancer of stabilization of the DNA-probe duplex), and one specific for the mutant allele (FAM-CAGTTTGATCGAGTGCAT-Q-MGB, where FAM is the fluorescent marker). We used the Primer Express software (Applied Biosystems, Foster City, CA) to design the PCR primers (forward: 5'-CTTGGGTAGTGACAAAGTAT-3'; reverse: 5'-CTTAAGGGTCAGATTTCTAC-3'). Reaction mixtures were assembled in a 384-well plate using a Biomek 2000 Workstation (Beckman Instruments, Fullerton, CA). Each well contained 40 ng genomic DNA, 36 nM primers, 8 nM probes, and 2.5 µl TaqMan Universal Master Mix (Applied Biosystems, Foster City, CA) in a total reaction volume of 5 µl. We also tested negative and positive controls (i.e. no DNA sample and homozygote and heterozygote samples for the UCP1 –3826 A>G polymorphism previously typed by sequence analysis on an ABI Prism 3100 Genetic Analyzer, Applied Biosystems, Foster City, CA). Real Time PCR was run on an ABI Prism 7900HT instrument and data were analyzed with the Sequence Detection System (SDS 2.1) and the SDS Enterprise Database (Applied Biosystems). The amplification protocol consisted of: 50 C for 2 min; 95 C for 10 min; 92 C for 15 sec and 60 C for 1 min for 40 cycles; final extension at 60 C for 1 min; final soak at 25 C.

MS was diagnosed according to the recently defined AHA criteria. Namely, the syndrome was diagnosed if 3 out of 5 criteria were present (7). All patients and controls gave their informed consent to the study, which was carried out according to the Helsinki II Declaration.

Statistics

For each investigated parameter we calculated the median value and the percentile (2.5^{th}-97.5^{th}) range. The Mann-Whitney test and/or χ^2, when necessary, were used for between-group comparison. Differences were considered significant at p level <0.05. Binomial logistic analysis was used to investigate the association between MS or liver steatosis severity (severe *vs* moderate steatosis) and the UCP1 –3826 A>G polymorphism, and in relation to biochemical and clinical characteristics. Allele frequencies were estimated by gene counting. Agreement with Hardy-Weinberg equilibrium was tested with a χ^2 goodness-of-fit test. Statistical analyses were carried out with the SPSS package for Windows (Ver.15; SPSS Inc. Headquarters, Chicago, Ill).

RESULTS

The main biochemical values obtained in male and female obese patients are reported in Table 1. MS was more prevalent in severely obese females (66%) than in males (53%) and a sex-dependent contribution was observed for hypertension (73% M and 31% F, p<0.001), dyslipidemia (54% M and 69% F, p=0.01) and hyperglycemia (34% M and 23% F, p=0.04), apart from waist circumference, which was well above normal limits in all subjects.

Table 2 - *Genotypes and allele frequencies of UCP1 –3826 A>G in obese patients (no.=102) and controls (no.=95).*

UCP1 genotypes	no. (%)		UCP1 allele	(%)	
	Obese	Controls		Obese	Controls
AA	51 (50.0)	52 (54.8)	A	0.71	0.72
AG	42 (41.2)	33 (34.7)	G	0.29	0.28
GG	9 (8.8)	10 (10.5)			

Further, among other tested biochemical parameters, only total cholesterol and L/A levels differed significantly between patients MS+ and MS– [respectively, median total cholesterol: (M), 4.4 mmol/l *vs* 4.6 mmol/l, p=0.04; (F), 4.7 mmol/l *vs* 5.1 mmol/l, p=0.002; median L/A ratio: (M) 3.7 *vs* 1.5, p=0.03; (F), 5.5 *vs* 6.6, p=ns). Among MS– obese patients 68% were insulin resistant (HOMA>4).

Liver steatosis was investigated by ultrasound and was present in all obese patients, it was severe in a higher percentage of MS+ *vs* MS– subjects (39% *vs* 20%, p=0.005) and more frequent in males than in females (57% *vs* 29%, p=0.0001). In obese with severe liver steatosis at univariate analysis we observed significantly higher median concentrations of AST, ALT, GGT, insulin, glucose, L/A ratio, and significantly lower HDL-cholesterol, adiponectin concentrations and AST/ALT ratio than in obese with mild/moderate liver steatosis (respectively, 28.0 U/l *vs* 21.0 U/l, p<0.0001; 42.5 U/l *vs* 27.0 U/l, p=0.001; 35.0 U/l *vs* 24.0 U/l, p=0.004; 28.4 mmol/l *vs* 19.2 mmol/l, p<0.0001; 5.2 mmol/l *vs* 5.0 mmol/l, p=0.03; 7.7 *vs* 4.0, p=0.007; 1.06 mmol/l *vs* 1.13 mmol/l, p=0.006; 12.7 µg/ml *vs* 24.2 µg/ml, p=0.001; 0.7 *vs* 0.8, p=0.03).

Table 2 shows the genotype and allele frequencies of the UCP1 –3826 A>G polymorphism in our obese patients and control subjects; genotype frequencies were in Hardy-Weinberg equilibrium (p=0.9). UCP1 (AG+GG) genotypes were more frequent in patients with severe liver steatosis than in those with mild/moderate liver steatosis (21/31; 65% *vs* 30/70; 43%, p=0.0003). UCP1 (AG+GG) genotypes did not differ among MS+ and MS– obese patients (46% *vs* 56%; ns). Binomial logistic regression showed that severe liver steatosis in obese patients was associated with the UCP1 (AG+GG) genotypes, low adiponectin levels, high ALT levels, age, MS, and male sex (Table 3).

DISCUSSION

The prevalence of MS in our severely obese subjects (M: 53% and F: 66%) was comparable to those reported in the QUOVADIS (Quality of Life in Obesity: Evaluation and Disease Surveillance) study (53%), a multicenter evaluation carried out in Italy (21) and slightly higher than in the general populations of European and US Caucasians of a similar age range (22).

We detected higher L/A ratio in obese male MS+ than in obese male MS– patients (3.7 *vs* 1.5) as previously reported for MS+ and MS– non-obese male patients (0.79

Table 3 - *Association between liver steatosis severity and clinical, biochemical variables in obese patients.*

Variable[a]	β	SE	*p*	Odds ratio	95% CI
UCP1[b]	1.45	0.68	0.033	4.25	1.12-16.13
Adiponectin	–0.08	0.03	0.012	0.92	0.87-0.98
MS	2.13	0.79	0.007	8.47	1.78-40.25
ALT	0.03	0.01	0.020	1.03	1.00-1.06
Male gender	2.38	0.97	0.014	10.78	1.61-71.96
Age	0.07	0.04	0.050	1.08	1.00-1.15

[a]Included variables at binomial logistic regression analysis were age, aspartate aminotransferase, alanine aminotransferase (ALT), g-glutamyl transferase, CHE, adiponectin, leptin/adiponectin ratio, gender, UCP1, metabolic syndrome (MS); [b]UCP1 genotypes were included as AA and AG+GG. CI: confidence interval.

vs 0.52) (9). Increased fat content is associated with insulin resistance in Type 2 diabetic patients (23). In our severe obese group 68% of MS– patients had HOMA>4. These data agree with the lipotoxicity theory, namely that increased and prolonged exposure to excessive free fatty acids results in decreased insulin secretion (22). In a chronic context such as severe obesity, lipids accumulate in muscle, liver, and pancreatic islet cells, and this event has been implicated in impaired insulin signaling and insulin secretion (24). In fact, in Zucker diabetic fatty rats, islet lipid accumulation precedes the development of diabetes (24). Further, insulin resistance and systemic hypertension features of the MS are also independently associated with advanced forms of NAFLD (25, 26).

Steatosis is frequent in obesity (27), particularly in severe obesity (12). Ultrasound studies showed that all our patients were affected by NAFLD, which was more severe in MS+ than in MS– obese patients. As a rule, imaging studies cannot predict the severity of NAFLD, which ranges from simple steatosis to steatohepatitis. However, no guidelines recommend liver biopsy in obese patients, except in the setting of persistent hypertransaminasemia or if it is necessary to rule out a cause of NAFLD other than MS or insulin resistance (11). In our obese population, the lack of risk factors other than MS, insulin resistance or persistent hypertransaminasemia did not justify liver biopsy.

There is compelling evidence that decreased adiponectin levels are involved in the development of NAFLD (28) in close association with insulin resistance, independently of obesity (29, 30). In our adult severely obese patients, serum adiponectin values were lower in patients with severe than in those with mild/moderate liver steatosis, and severe liver steatosis was also associated with older age and higher ALT transaminases. Recently, data obtained in an experimental model showed that adiponectin is a key regulator for the progression of hepatic fibrosis toward steatohepatitis (31).

The frequencies of the UCP1 AG and GG genotypes in our obese patients (respectively 41.2% and 8.8%) were similar to those reported for other Caucasians, namely between 29% and 42% for UCP1 AG and between 4% and 15% for UCP1 GG (16, 32-37), but lower than those reported in Japanese and Korean populations (respectively, 45-54% for AG and 23-27.5% for GG) (16, 38-40). An interesting finding of our study is that liver steatosis was more severe in obese patients bearing UCP1 (AG+GG) genotypes compared to those bearing the UCP1 AA genotype (odds ratio=4.25). This finding may suggest a genetic association between liver steatosis in obese subjects and the G allele. Interestingly, intraperitoneal fat UCP1 mRNA expression was found to be lower in obese subjects bearing the –3826 G polymorphism than in subjects with two wild-type alleles (16). Moreover, in a murine model, hepatic UCP1 overexpression reduced fat in the liver and adipose tissue, thereby improving insulin resistance in mice with high-fat-diet-inducing diabetes and obesity (41). Recently, the UCP1 gene was found to be expressed in the visceral adipose tissue of adult lean and obese patients in which brown adipocytes were dispersed among white adipocytes in a ratio of 1 to 100-200 (42). Interestingly, after dieting and a BMI reduction, UCP1 mRNA levels remained lower in obese than in lean subjects, which supports a genetic predisposition in obesity to a low energy dispersion (42).

In conclusion, in addition to traditional factors, total cholesterol and L/A ratio appear to contribute to MS characterization in severe obesity. Further, the UCP1 (AG+GG) genotypes and low adiponectin levels could predispose to a more severe liver steatosis independently of MS presence. Based on our data, polymorphic UCP1 (AG+GG) obese patients with low adiponectin levels appear to be high-risk subjects for worsening of liver steatosis or NAFLD, possibly requiring liver biopsy aimed to promote preventive interventions.

ACKNOWLEDGMENTS

We thank Jean Ann Gilder for text revision and editing. Work supported by grants from CEINGE – Regione Campania (Protocollo di intesa – Del. G.R. 29/12/2007), MIUR art. 5.2 and Regione Campania L.R. n° 5/2005.

REFERENCES

1. Daniels J. Obesity: America's epidemic. Am J Nurs 2006, 106: 40-9.
2. Caballero B. The global epidemic of obesity: an overview. Epidemiol Rev 2007, 29: 1-5.
3. Yang W, Kelly T, He J. Genetic epidemiology of obesity. Epidemiol Rev 2007, 29: 49-61.
4. Fantuzzi G. Adipose tissue, adipokines, and inflammation. J Allergy Clin Immunol 2005, 115: 911-9.
5. Contaldo F, Pasanisi F, Finelli C, de Simone G. Obesity, heart failure and sudden death. Nutr Metab Cardiovasc Dis 2002, 12: 190-7.
6. WHO Consultation. Definition, diagnosis and classification of diabetes mellitus and its complications. Geneva: World Health Organization. 1999, p. 31-3.

7. Grundy SM, Cleeman JI, Daniels SR, et al. Diagnosis and management of the metabolic syndrome: an American Heart Association/National Heart, Lung, and Blood Institute Scientific Statement. Circulation 2005, 112: 2735-52.
8. Inoue M, Yano M, Yamakado M, Maehata E, Suzuki S. Relationship between the adiponectin-leptin ratio and parameters of insulin resistance in subjects without hyperglycemia. Metabolism 2006, 55: 1248-54.
9. Norata GD, Raselli S, Grigore L, et al. Leptin:adiponectin ratio is an independent predictor of intima media thickness of the common carotid artery. Stroke 2007, 38: 2844-6.
10. Marchesini G, Bugianesi E, Forlani G, et al. Nonalcoholic fatty liver, steatohepatitis, and the metabolic syndrome. Hepatology 2003, 37: 917-23.
11. Yan E, Durazo F, Tong M, Hong K. Nonalcoholic fatty liver disease: pathogenesis, identification, progression, and management. Nutr Rev 2007, 65: 376-84.
12. Colicchio P, Tarantino G, del Genio F, et al. Non-alcoholic fatty liver disease in young adult severely obese non-diabetic patients in South Italy. Ann Nutr Metab 2005, 49: 289-95.
13. Baranova A, Gowder SJ, Schlauch K, et al. Gene expression of leptin, resistin, and adiponectin in the white adipose tissue of obese patients with non-alcoholic fatty liver disease and insulin resistance. Obes Surg 2006,16: 1118-25.
14. Mozo J, Emre Y, Bouillaud F, Ricquier D, Criscuolo F. Thermoregulation: what role for UCPs in mammals and birds? Biosci Rep 2005, 25: 227-49.
15. Kontani Y, Wang Y, Kimura K, et al. UCP1 deficiency increases susceptibility to diet-induced obesity with age. Aging Cell 2005, 4: 147-55.
16. Del Mar Gonzalez-Barroso M, Ricquier D, Cassard-Doulcier A-M. The human uncoupling protein-1 gene (UCP1): present status and perspectives in obesity research. Obes Rev 2000, 1: 61-72.
17. Bellentani S, Saccoccio G, Masutti F, et al. Prevalence of and risk factors for hepatic steatosis in Northern Italy. Ann Intern Med 2000, 132: 112-7.
18. Saverymuttu SH, Joseph AEA, Maxwell JD. Ultrasound scanning in the detection of hepatic fibrosis and steatosis. Br Med J 1986, 292: 13-5.
19. Ricci C, Longo R, Gioulis E, et al. Noninvasive in vivo quantitative assessment of fat content in human liver. J Hepatol 1997, 27: 108-13.
20. Osawa H, Mori Y. Sonographic diagnosis of fatty liver using a histogram technique that compares liver and renal cortical echo amplitudes. J Clin Ultrasound 1996, 24: 25-9.
21. Marchesini G, Melchionda N, Apolone G, et al; QUOVADIS Study Group. The metabolic syndrome in treatment-seeking obese persons. Metabolism 2004, 53: 435-40.
22. Eckel RH, Grundy SM, Zimmet PZ. The metabolic syndrome (Review). Lancet 2005, 365: 1415-28.
23. Willner IR, Waters B, Patil SR, Reuben A, Morelli J, Riely CA. Ninety patients with nonalcoholic steatohepatitis: insulin resistance, familial tendency, and severity of disease. Am J Gastroenterol 2001, 96: 2957-61.
24. Moller DE, Kaufman KD. Metabolic syndrome: a clinical and molecular perspective. Annu Rev Med 2005, 56: 45-62.
25. Angulo P. Nonalcoholic fatty liver disease. N Engl J Med 2002, 346: 1221-31.
26. Dixon JB, Bhathal PS, O'Brien PE. Nonalcoholic fatty liver disease: predictors of nonalcoholic steatohepatitis and liver fibrosis in the severely obese. Gastroenterology 2001, 121: 91-100
27. Scheen AJ, Luyckx FH. Obesity and liver disease. Best Pract Res Clin Endocrinol Metab 2002, 16: 703-16.
28. Aygun C, Senturk O, Hulagu S, et al. Serum levels of hepatoprotective peptide adiponectin in non-alcoholic fatty liver disease. Eur J Gastroenterol Hepatol 2006, 18: 175-80.
29. Pagano C, Soardo G, Esposito W, et al. Plasma adiponectin is decreased in nonalcoholic fatty liver disease. Eur J Endocrinol 2005, 152: 113-8.
30. Yoon D, Lee SH, Park HS, et al. Hypoadiponectinemia and insulin resistance are associated with nonalcoholic fatty liver disease. J Korean Med Sci 2005, 20: 421-6.
31. Ikejima K, Okumura K, Kon K, Takei Y, Sato N. Role of adipocytokines in hepatic fibrogenesis. J Gastroenterol Hepatol 2007, 22 (Suppl 1): S87-92.
32. Forga L, Corbalán M, Marti A, Fuentes C, Martinez-Gonzalez MA, Martinez A. Influence of the polymorphism -3826 A --> G in the UCP1 gene on the components of metabolic syndrome. An Sist Sanit Navar 2003, 26: 231-6.
33. Heilbronn LK, Kind KL, Pancewicz E, Morris AM, Noakes M, Clifton PM. Association of -3826 G variant in uncoupling protein-1 with increased BMI in overweight Australian women. Diabetologia 2000, 43: 242-4.
34. Kiec-Wilk B, Wybranska I, Malczewska-Malec M, et al. Correlation of the -3826A >G polymorphism in the promoter of the uncoupling protein 1 gene with obesity and metabolic disorders in obese families from southern Poland. J Physiol Pharmacol 2002, 53: 477-90.
35. Ramis JM, González-Sánchez JL, Proenza AM, et al. The Arg64 allele of the beta 3-adrenoceptor gene but not the -3826G allele of the uncoupling protein 1 gene is associated with increased leptin levels in the Spanish population. Metabolism 2004, 53: 1411-6.
36. Urhammer SA, Hansen T, Borch-Johnsen K, Pedersen O. Studies of the synergistic effect of the Trp/Arg64 polymorphism of the beta3-adrenergic receptor gene and the -3826 A-->G variant of the uncoupling protein-1 gene on features of obesity and insulin resistance in a population-based sample of 379 young Danish subjects. J Clin Endocrinol Metab 2000, 85: 3151-4.
37. Evans D, Minouchehr S, Hagemann G, et al. Frequency of and interaction between polymorphisms in the beta3-adrenergic receptor and in uncoupling proteins 1 and 2 and obesity in Germans. Int J Obes Relat Metab Disord 2000, 24: 1239-45.
38. Oh HH, Kim KS, Choi SM, Yang HS, Yoon Y. The effects of uncoupling protein-1 genotype on lipoprotein cholesterol level in Korean obese subjects. Metabolism 2004, 53: 1054-9.
39. Nakano T, Shinka T, Sei M, et al. A/G heterozygote of the A-3826G polymorphism in the UCP-1 gene has higher BMI than A/A and G/G homozygote in young Japanese males. J Med Invest 2006, 53: 218-22.
40. Kotani K, Sakane N, Saiga K, et al. Relationship between A-3826G Polymorphism in the Promoter of the Uncoupling protein-1 Gene and High-density Lipoprotein Cholesterol in Japanese Individuals: A Cross-sectional Study. Arch Med Res 2008, 39: 142-6.
41. Ishigaki Y, Katagiri H, Yamada T, et al. Dissipating excess energy stored in the liver is a potential treatment strategy for diabetes associated with obesity. Diabetes 2005, 54: 322-32.
42. Cinti S. The role of brown adipose tissue in human obesity. Nutr Metab Cardiovasc Dis 2006, 16: 569-74.

High Leptin/Adiponectin Ratio and Serum Triglycerides Are Associated With an "At-Risk" Phenotype in Young Severely Obese Patients

Giuseppe Labruna[1], Fabrizio Pasanisi[2], Carmela Nardelli[3], Rosanna Caso[4], Dino F. Vitale[5], Franco Contaldo[2] and Lucia Sacchetti[3]

"At-risk" severely obese subjects are characterized by insulin resistance, and higher visceral fat and plasma lipid levels compared with metabolically healthy obese (MHO) subjects, although both groups have a high BMI and fat mass. The aim of this study was to measure several serum adipokines and gastrointestinal hormones in a young severely obese population from Southern Italy to identify biochemical markers of the "at-risk" insulin-resistant obese profile. We studied 160 unrelated white young adults (mean age = 25.2 years, mean BMI = 44.9 kg/m^2, 65% women) affected by obesity for at least 5 years. Serum concentrations of glucagon, ghrelin, gastric inhibitory peptide, glucagon like peptide-1, interleukin-6, tumor necrosis factor α, leptin, adiponectin, adipsin, and visfatin were measured. The leptin/adiponectin (L/A) ratio and fatty liver index (FLI) were calculated. We found a prevalence of 21.3% of MHO patients in our young severely obese patients. At univariate analysis, the "at-risk" group had higher mean levels of BMI ($P < 0.0001$), leptin ($P = 0.039$, men) and the L/A ratio ($P = 0.003$), and lower mean levels of visfatin ($P = 0.026$) than the MHO group. The L/A ratio, serum triglycerides, and male sex were significantly associated with "at-risk" obesity and accounted for 19.5% of insulin resistance at multivariate analysis. In conclusion, we demonstrate that a high serum L/A ratio and high levels of serum triglycerides may be markers of "at-risk" obesity, independent of waist circumference (WC) and BMI, in young severely obese population.

Obesity (2010) doi:10.1038/oby.2010.309

INTRODUCTION

The obese phenotype is widely heterogeneous: it includes an "at-risk" phenotype and a so-called "metabolically healthy phenotype" (MHO) that is present in 10% to over 30% of the obese population (1). "At-risk" obese subjects are characterized by insulin resistance and by higher visceral fat and plasma lipid levels compared with MHO subjects, although both groups have a high BMI and fat mass (2). Low visceral fat (2) and early obesity onset (<20 year of age) (3) accounted for 22% and 13% respectively of the insulin sensitivity observed in MHO patients, but 65% of the phenotype remained unexplained (2). The MHO phenotype has been well described in mild obesity (4,5), in postmenopausal obesity (3,6), and in a randomly selected population (7), but not in young severely obese people (8).

In the attempt to identify biochemical markers of the MHO and "at-risk" obese profiles, we measured several serum adipose and gastrointestinal hormones in a young severely obese population from Southern Italy. The identification of an "at-risk" profile, particularly in young subjects, could have important implications in their clinical management. In fact, "at-risk" obese subjects need aggressive treatment to prevent or delay obese-associated metabolic complications, whereas attempts to loose weight might be potentially harmful, or not effective in MHO individuals (9,10).

METHODS AND PROCEDURES

Study population

We studied 160 unrelated white young adults (mean age ± s.d. = 25.2 ± 9.6 years; mean BMI [95% confidence interval (CI)] = 44.9 [43.6–46.3] kg/m^2; 65% women) from Southern Italy who had suffered from obesity for at least 5 years. The population was recruited at the Obesity Outpatient Clinic of the Department of Internal Medicine, Federico II University Hospital, Naples, Italy. Clinical, functional, and biochemical data were obtained from each patient at the baseline. Secondary causes of obesity were excluded, and no patient was an alcohol abuser or under pharmacological treatment for any disease. We measured: BMI (weight/height^2; kg/m^2), waist circumference (WC; cm), blood pressure (systolic blood pressure and diastolic blood pressure; mm Hg) and heart rate (beats/min) in each individual after they had been sitting for 5 min; we also recorded smoking habits and body composition (fat mass and

[1]Fondazione IRCCS SDN–Istituto di Ricerca Diagnostica e Nucleare, Napoli, Italy; [2]Centro Interuniversitario di Studi e Ricerche nell'Obesità e Disturbi del Comportamento Alimentare and Dipartimento di Medicina Clinica e Sperimentale, Università di Napoli Federico II, Napoli, Italy; [3]CEINGE Biotecnologie Avanzate S.C. a R.L. and Dipartimento di Biochimica e Biotecnologie Mediche, Università di Napoli Federico II, Napoli, Italy; [4]Dipartimento Assistenziale di Medicina di Laboratorio AOU Federico II, Napoli, Italy; [5]Fondazione Salvatore Maugeri, Istituto IRCCS, Telese Terme, Benevento, Italy. Correspondence: Lucia Sacchetti (sacchett@unina.it)

Received 29 June 2010; accepted 15 November 2010; advance online publication 23 December 2010. doi:10.1038/oby.2010.309

Table 1 Physical and biochemical characteristics (mean and 95% CI) in MHO and "at-risk" severely obese young patients from Southern Italy

	MHO (*n* = 34)		M vs. F	"At risk" (*n* = 126)		M vs. F	MHO vs. "at risk"
Characteristics[a]	Mean	95% CI	*P* value[c]	Mean	95% CI	*P* value[c]	*P* value[c]
Age (years)[b]	22.6	19.7–25.5	Ns	25.8	24.1–27.6	Ns	Ns
BMI (kg/m^2)[b]	41.1	38.9–43.3	Ns	46.1	44.5–47.7	Ns	0.003
WC (cm)[b]	122.5	118.0–127.0	Ns	(M) 140.8 (F) 128.6	135.2–146.5 124.8–132.3	<0.0001	Ns
RQ	0.9	0.82–0.89	Ns	0.9	0.85–0.88	Ns	Ns
FFM (%)	(M) 56.3 (F) 50.0	50.4–62.2 47.9–52.1	0.010	(M) 53.9 (F) 50.2	52.2–55.6 48.9–51.3	0.001	Ns
FM (%)[b]	(M) 43.6 (F) 49.9	37.7–49.6 47.9–52.1	0.010	(M) 46.1 (F) 50.1	44.4–47.8 48.9–51.3	<0.0001	Ns
SBP (mm Hg)[b]	119.4	117.7–121.1	Ns	122.1	120.5–123.7	Ns	Ns
DBP (mm Hg)	77.4	75.7–79.1	Ns	78.7	77.6–79.8	Ns	Ns
Heart rate (beats/min)	76.8	74.4–79.2	Ns	78.6	77.5–79.8	Ns	Ns
Glucose (mmol/l)	4.1	3.9–4.3	Ns	4.7	4.5–4.9	Ns	<0.0001
Total cholesterol (mmol/l)	4.3	3.9–4.7	Ns	(M) 4.4 (F) 4.6	4.1–4.7 4.4–4.8	0.041	Ns
HDL cholesterol (mmol/l)	(M) 1.0 (F) 1.2	0.8–1.2 1.1–1.3	0.032	(M) 1.0 (F) 1.2	0.9–1.1 1.1–1.3	0.007	Ns
Triglycerides (mmol/l)[b]	1.0	0.8–1.2	Ns	1.5	1.4–1.7	Ns	<0.0001
AST (U/l)	(M) 25.9 (F) 18.6	20.6–31.2 17.2–19.9	0.002	(M) 35.1 (F) 23.8	25.4–44.9 20.8–26.8	<0.0001	(F) 0.029
ALT (U/l)	(M) 39.3 (F) 20.9	28.7–49.9 18.0–23.9	<0.0001	(M) 52.2 (F) 30.7	41.1–63.2 26.3–35.1	<0.0001	Ns
GGT (U/l)[b]	(M) 29.4 (F) 15.1	20.2–38.7 13.2–17.0	<0.0001	(M) 34.5 (F) 29.3	24.4–44.6 21.4–37.2	0.002	(F) 0.001
FLI[b]	86.7	81.4–92.1	Ns	94.4	92.7–96.1	Ns	<0.0001
Fibrinogen (μmol/l)	11.2	10.5–12.0	Ns	12.0	11.6–12.5	Ns	Ns
Creatinine (μmol/l)	(M) 79.5 (F) 61.8	70.7–88.4 53.0–62.0	<0.0001	(M) 70.7 (F) 61.8	61.8–79.5 53.0–62.0	<0.0001	(M) 0.042
Urea (mmol/l)[b]	4.6	4.2–5.0	Ns	5.1	4.9–5.3	Ns	0.039
C-peptide (ng/ml)	2.4	2.1–2.7	Ns	(M) 4.4 (F) 4.0	4.0–4.7 3.7–4.4	0.046	<0.0001
Insulin (mIU/l)	8.7	7.8–9.7	Ns	23.9	21.8–26.0	Ns	<0.0001
HOMA	1.5	1.4–1.7	Ns	(M) 4.5 (F) 3.8	4.0–4.9 3.5–4.1	0.009	<0.0001
Glucagon (ng/ml)	0.96	0.91–1.02	Ns	0.94	0.91–0.97	Ns	Ns
Ghrelin (pg/ml)	122.0	104.4–139.7	Ns	116.5	105.8–127.3	Ns	Ns
GIP (pg/ml)	61.2	50.8–71.5	Ns	55.1	50.5–59.8	Ns	Ns
GLP-1 (ng/ml)	1.1	0.8–1.3	Ns	0.9	0.8–1.1	Ns	Ns
IL-6 (pg/ml)	14.1	11.4–16.8	Ns	12.5	11.2–13.7	Ns	Ns
TNFα (pg/ml)	39.7	30.5–48.8	Ns	36.7	32.3–41.0	Ns	Ns
Leptin (ng/ml)	(M) 4.3 (F) 6.9	2.1–6.4 5.6–8.3	0.010	(M) 6.9 (F) 8.2	5.8–7.9 7.3–9.0	Ns	(M) 0.023
Adiponectin (μg/ml)	28.0	24.7–31.3	Ns	24.1	22.3–25.8	Ns	Ns
L/A ratio[b]	0.25	0.19–0.31	Ns	0.37	0.32–0.41	Ns	0.003
Adipsin (ng/ml)	592.2	507.9–676.4	Ns	503.3	460.7–545.9	Ns	Ns
Visfatin (ng/ml)[b]	7.6	6.0–9.2	Ns	5.8	5.1–6.5	Ns	0.026

ALT, alanine aminotransferase; AST, aspartate aminotransferase; DBP, diastolic blood pressure; F, females; FLI, fatty liver index; FFM, fat free mass; FM, fat mass; GIP, gastric inhibitory peptide; GGT, γ-glutamyl transferase; GLP-1, glucagon-like peptide-1; HOMA, homeostasis model assessment; IL-6, interleukin-6; L/A, leptin/adiponectin ratio; M, males; MHO, metabolically healthy obese subjects; Ns, not significant; RQ, respiratory quotient; SBP, systolic blood pressure; TNFα, tumor necrosis factor-α; WC, waist circumference.

[a]Reported as mean and 95% confidence interval (CI). [b]Variables used in the logistic model to assess their association with the "at-risk" characteristic in our obese population. [c]At Mann–Whitney or Student's t-test, as appropriate.

fat free mass using the bioelectrical impedance technique). The physical and biochemical characteristics of the population are reported in **Supplementary Table S1** online. A venous blood sample was collected from each patient at 8.00 AM after an overnight fast. The families of all subjects had lived in Southern Italy for at least three generations and all subjects gave their informed consent to the study. The research was approved by the Ethics Committee of the Faculty of Medicine, University of Naples Federico II, and was carried out according to the Helsinki II Declaration.

Laboratory investigations

Serum glucose, total cholesterol, high-density lipoprotein cholesterol, triglycerides, aspartate aminotransferase, alanine aminotransferase, γ-glutamyl transferase (GGT), fibrinogen, creatinine, urea, C-peptide and insulin were measured by routine laboratory methods. Insulin resistance was estimated according to the homeostasis model assessment and the formula: fasting insulin (mIU/l) × fasting glucose (mmol/l)/22.5. We calculated the fatty liver index (FLI) according to the formula $FLI = (e^{0.953 \times \ln(\text{triglycerides}) + 0.139 \times \text{BMI} + 0.718 \times \ln(\text{GGT}) + 0.053 \times \text{waist circumference} - 15.745})/(1 + e^{0.953 \times \ln(\text{triglycerides}) + 0.139 \times \text{BMI} + 0.718 \times \ln(\text{GGT}) + 0.053 \times \text{waist circumference} - 15.745}) \times 100$ as a measure of hepatic steatosis (11).

Serum glucagon, ghrelin, gastric inhibitory peptide, glucagon-like peptide-1, interleukin-6, tumor necrosis factor-α (TNFα), leptin, adiponectin, adipsin, and visfatin were measured by Luminex xMAP Technology on a BioRad Multiplex Suspension Array System (BioRad, Hemel Hempstead, Herts), according to the manufacturer's instructions. We also calculated the leptin/adiponectin (L/A) ratio.

The study population was divided into two groups: MHO individuals, i.e., subjects who were "insulin sensitive" and had no more than one risk factor (hypertension or dyslipidemia); and "at-risk" individuals, i.e., subjects who were "insulin-resistant" with or without other risk factors, namely, hypertension, dyslipidemia, and hyperglycemia. A homeostasis model assessment index (HI) lower or greater than 1.95 defined insulin sensitivity or resistance, respectively (6,12).

Statistics

Data are reported as mean ± s.d. or the 95% CI. Angular transformation (arcsin of the square root) of the L/A ratio was applied before statistical analyses. The unpaired Student's *t*-test, the Mann–Whitney test or the χ^2-test were used for between-group comparisons, as appropriate. Differences were considered statistically significant at a P level <0.05. Binomial logistic regression analysis was used to investigate the association between the biochemical and clinical characteristics and the "at-risk" condition, as previously defined. The odds ratio relative to clinically meaningful differences for the continuous variables are reported. To explore the possibility of missing a potential association due to the loss of information consequent to the introduction of the binary categorization of the HI in the logistic analysis, a multiple linear regression analysis was performed using the continuous HI as dependent variable for the same set of independent variables used in the logistic regression analysis. Both forward and backward procedures were used for model selection and gave concordant results. Statistical analyses were carried out with the SPSS package for Windows (ver. 17; SPSS, Chicago, IL).

RESULTS

A family history of obesity was recorded in 31.5% individuals, of concomitant obesity + hypertension + diabetes in 53% and hypertension alone in 6.2%. Thirty-four individuals (21.3%) were classified "MHO". There were no significant differences between "at-risk" and MHO individuals regarding sex, smoking habit, and family history of obesity. Only 6.3% of insulin-resistant "at-risk" individuals were also hyperglycemic. Mild hypertransaminasemia was also present in 52/160 (32.3%) of the study population: 37.3% of the "at-risk" group and 11.8% of the MHO group ($P = 0.004$). Hypertension (mean systolic blood pressure/diastolic blood pressure >133/89 mm Hg) was present in 11% of our "at-risk" patients; moreover, these patients also had a higher mean L/A ratio and HI values (hypertensive vs. normotensive patients, L/A ratio: 0.46 vs. 0.35, $P = 0.038$; HI: 5.3 vs. 3.9, $P = 0.002$). However, all our hypertensive obese patients belonged to the "at-risk" group.

Levels of GGT (women, $P = 0.001$) and of urea ($P = 0.027$) were higher in the "at-risk" than in the MHO group. The FLI was higher in the "at-risk" group (94.4), as expected, given the liver involvement, than in the MHO group (86.7) ($P < 0.0001$). Table 1 shows the mean serum levels of adipokines and hormones measured in MHO and "at-risk" individuals together with the other physical and biochemical parameters measured in this study. The "at-risk" individuals had, at univariate analysis, higher mean levels of BMI ($P < 0.0001$), leptin ($P = 0.039$, men) and L/A ratio ($P = 0.003$), and lower mean levels of visfatin ($P = 0.026$) than the MHO group.

The variables used in the logistic model to assess their association with the "at-risk" phenotype in our obese population are indicated in Table 1 (variables "[b]" labelled). The final model showed a Nagelkerke $R^2 = 0.19$, and only two variables were retained as significant: the L/A ratio (odds ratio/95% CI = 1.44/1.07–1.94), and the serum concentration of triglycerides (odds ratio/95% CI = 1.87/1.19–2.94). The final multiple linear regression model resulted in the addition of gender to the other significant factors, i.e., the L/A ratio and serum triglycerides. The overall adjusted R^2 was equal to 0.195, indicating that both the logistic and the multiple linear models are, in practice, equivalent.

DISCUSSION

The characterization of several serum adipokines and gastrointestinal hormones in the young severely obese population reported herein suggests that the serum L/A ratio, serum triglycerides, male sex, and the HI could be useful markers for the diagnosis of "at-risk" obese patients. Based on an almost complete absence of traditional risk factors for cardiovascular and metabolic diseases (1,2,6,13), a variable proportion (between 10% and 30%) of obese subjects is classified "MHO". Using an HI <1.95 as classification criterion (3), we found a prevalence of 21.3% of MHO patients in our young severely obese patients. This prevalence was similar to or lower (from 24.4% to 31.7%) than those obtained in mild and/or severe older obese subjects in other European and non-European populations (3,4,7,8,14). Besides the use of different criteria to classify MHO, these differences could be explained by the different age, female/male ratio, and classes of obesity investigated. In fact, the prevalence of uncomplicated obesity was reported to be higher in a very young (16–29 years) obese population than in other age groups, independent of BMI category (8). Our patients had been obese for at least 5 years, but the MHO group was 3 years younger than the "at-risk" group. This finding suggests that juvenile onset obesity rapidly progresses toward a more severe phenotype as observed in older obese populations (4,5,7,8,14).

Levels of the two inflammatory markers interleukin-6 and TNFα did not differ between the MHO and the "at-risk" groups in our obese population. This finding is in agreement with some reports (15,16) but not with others (6,7,17). It is possible that the discrepancy stems from the young age of the population we studied.

The young age of our patients might also explain the relatively low percentage of hypertensive subjects in our population. In a previous study of a nonobese male population of our geographical area, hypertension was associated with decreased insulin sensitivity (18). However, the L/A ratio remained significantly higher in the "at-risk" group than in the MHO group, also when hypertensive patients were excluded from the statistical analysis (0.35 vs. 0.25, $P = 0.008$). This suggests that factors other than hypertension are at play during the onset of insulin resistance in young obese subjects. Furthermore, the low high-density lipoprotein cholesterol levels in our MHO and "at-risk" subjects probably reflects the similar sedentary lifestyle of our subjects.

In agreement with a lower hepatic insulin resistance and a lower liver fat content in MHO patients observed in postmenopausal women (19), in the general population (11) and by us in a middle-aged obese population (20), the levels of FLI, an index of liver steatosis, were higher in "at-risk" individuals than in the MHO group ($P < 0.0001$). This could be due to the fact that trapping of free fatty acids is impaired in "at-risk" individuals (19). Furthermore, in overweight patients, the L/A ratio was reported to be higher in nonalcoholic steatohepatitis than in simple steatosis, irrespective of insulin resistance (21). In our study, the L/A ratio was not correlated with FLI, although the latter was significantly higher in "at-risk" than in MHO patients. This observation could be due to the lower sensitivity of FLI compared to liver biopsy, which is not routinely performed in severe obesity, in diagnosing liver steatosis (21).

In our study, the serum L/A ratio, serum triglycerides, and male sex were the most significant parameters associated with "at-risk" obesity; indeed they accounted for 19.5% of the insulin-resistant phenotype. The L/A ratio was reported to be negatively correlated with insulin sensitivity indexes in a large population of nonobese and nondiabetic individuals (22), and we previously demonstrated that this ratio contributed to the metabolic syndrome in severe obesity (20).

Brochu *et al*. found that visceral adipose tissue plays a relevant role in insulin resistance insurgence (3). We are unable to evaluate the relative effect of this tissue or of the L/A ratio on insulin resistance because we did not measure visceral adipose tissue in our population. However, the lack of a significant association between WC, a rough index of visceral adiposity, and the BMI, an index of total adiposity, with the HI in both the logistic and the multiple regression models probably indicates that, in this selected population with severe obesity, the L/A ratio is a better marker of "at-risk" obesity than either WC or BMI. This observation is supported by the fact that the association of WC and BMI with HI becomes statistically significant ($P = 0.031$ and $P = 0.042$, respectively) when the adipokines are not included in the model. Consequently, the L/A ratio-HI association that we observed is independent of both WC and BMI. The apparent discrepancy between our findings and those of Brochu *et al*. is probably due to the differences between the two examined populations, namely mean age (MHO vs. "at risk", Brochu *et al*: 58.0 vs. 58.6 years; our data: 22.6 vs. 25.8 years), gender composition, (Brochu *et al*. 100% females, in our population 65% females) and underlying physiopathologic conditions (severity of obesity and postmenopausal condition) and to different methodological aspects.

In conclusion, we demonstrate that a high serum L/A ratio and high levels of serum triglycerides may be markers of "at-risk" obesity, independent of WC and BMI, in young severely obese population.

SUPPLEMENTARY MATERIAL

Supplementary material is linked to the online version of the paper at http://www.nature.com/oby

ACKNOWLEDGMENTS

We thank Jean Ann Gilder (Scientific Communication) for text revision and editing. This work was supported by grants Conv. CEINGE-Regione Campania (DGRC 1901/2009), Regione Campania LR n5/2005 and MIUR PRIN 2008. Progetto di Ricerca Finalizzata RF-SDN-2007-635809 (Ministero del Lavoro, della Salute e delle Politiche Sociali).

DISCLOSURE

The authors declared no conflict of interest.

REFERENCES

1. Blüher M. The distinction of metabolically 'healthy' from 'unhealthy' obese individuals. *Curr Opin Lipidol* 2010;21:38–43.
2. Karelis AD, St-Pierre DH, Conus F, Rabasa-Lhoret R, Poehlman ET. Metabolic and body composition factors in subgroups of obesity: what do we know? *J Clin Endocrinol Metab* 2004;89:2569–2575.
3. Brochu M, Tchernof A, Dionne IJ *et al*. What are the physical characteristics associated with a normal metabolic profile despite a high level of obesity in postmenopausal women? *J Clin Endocrinol Metab* 2001;86:1020–1025.
4. Stefan N, Kantartzis K, Machann J *et al*. Identification and characterization of metabolically benign obesity in humans. *Arch Intern Med* 2008;168:1609–1616.
5. Succurro E, Marini MA, Frontoni S *et al*. Insulin secretion in metabolically obese, but normal weight, and in metabolically healthy but obese individuals. *Obesity (Silver Spring)* 2008;16:1881–1886.
6. Messier V, Karelis AD, Prud'homme D *et al*. Identifying metabolically healthy but obese individuals in sedentary postmenopausal women. *Obesity (Silver Spring)* 2010;18:911–917.
7. Wildman RP, Muntner P, Reynolds K *et al*. The obese without cardiometabolic risk factor clustering and the normal weight with cardiometabolic risk factor clustering: prevalence and correlates of 2 phenotypes among the US population (NHANES 1999-2004). *Arch Intern Med* 2008;168:1617–1624.
8. Iacobellis G, Ribaudo MC, Zappaterreno A, Iannucci CV, Leonetti F. Prevalence of uncomplicated obesity in an Italian obese population. *Obes Res* 2005;13:1116–1122.
9. Karelis AD, Messier V, Brochu M, Rabasa-Lhoret R. Metabolically healthy but obese women: effect of an energy-restricted diet. *Diabetologia* 2008;51:1752–1754.
10. Brochu M, Malita MF, Messier V *et al*. Resistance training does not contribute to improving the metabolic profile after a 6-month weight loss program in overweight and obese postmenopausal women. *J Clin Endocrinol Metab* 2009;94:3226–3233.
11. Bedogni G, Bellentani S, Miglioli L *et al*. The Fatty Liver Index: a simple and accurate predictor of hepatic steatosis in the general population. *BMC Gastroenterol* 2006;6:33.
12. Bonora E, Kiechl S, Willeit J *et al*. Prevalence of insulin resistance in metabolic disorders: the Bruneck Study. *Diabetes* 1998;47:1643–1649.

13. Wildman RP. Healthy obesity. *Curr Opin Clin Nutr Metab Care* 2009;12: 438–443.
14. Aguilar-Salinas CA, García EG, Robles L *et al*. High adiponectin concentrations are associated with the metabolically healthy obese phenotype. *J Clin Endocrinol Metab* 2008;93:4075–4079.
15. Solá E, Jover A, López-Ruiz A *et al*. Parameters of inflammation in morbid obesity: lack of effect of moderate weight loss. *Obes Surg* 2009;19: 571–576.
16. Barbarroja N, López-Pedrera R, Mayas MD *et al*. The obese healthy paradox: is inflammation the answer? *Biochem J* 2010;430:141–149.
17. Klöting N, Fasshauer M, Dietrich A *et al*. Insulin-sensitive obesity. *Am J Physiol Endocrinol Metab* 2010;299:E506–E515.
18. Galletti F, D'Elia L, Barba G *et al*. High-circulating leptin levels are associated with greater risk of hypertension in men independently of body mass and insulin resistance: results of an eight-year follow-up study. *J Clin Endocrinol Metab* 2008;93:3922–3926.
19. Messier V, Karelis AD, Robillard ME *et al*. Metabolically healthy but obese individuals: relationship with hepatic enzymes. *Metabolism* 2010;59:20–24.
20. Labruna G, Pasanisi F, Nardelli C *et al*. UCP1 -3826 AG+GG genotypes, adiponectin, and leptin/adiponectin ratio in severe obesity. *J Endocrinol Invest* 2009;32:525–529.
21. Lemoine M, Ratziu V, Kim M *et al*. Serum adipokine levels predictive of liver injury in nonalcoholic fatty liver disease. *Liver Int* 2009;29:1431–1438.
22. Finucane FM, Luan J, Wareham NJ *et al*.; European Group for the Study of Insulin Resistance: Relationship between Insulin Sensitivity and Cardiovascular Disease Risk Study Group). Correlation of the leptin:adiponectin ratio with measures of insulin resistance in nondiabetic individuals. *Diabetologia* 2009;52:2345–2349.

Hindawi Publishing Corporation
Journal of Obesity
Volume 2011, Article ID 269043, 4 pages
doi:10.1155/2011/269043

Research Article

Sequence Analysis of the *UCP1* Gene in a Severe Obese Population from Southern Italy

Giuseppe Labruna,[1] Fabrizio Pasanisi,[2] Giuliana Fortunato,[3,4] Carmela Nardelli,[3,4] Carmine Finelli,[5] Eduardo Farinaro,[6] Franco Contaldo,[2] and Lucia Sacchetti[3,4]

[1] *Fondazione IRCCS SDN, Istituto di Ricerca Diagnostica e Nucleare, Via Gianturco 113, 80143 Naples, Italy*
[2] *Centro Interuniversitario di Studi e Ricerche sull'Obesità e Dipartimento di Medicina Clinica e Sperimentale, Università degli Studi di Napoli Federico II, Via Pansini 5, 80131 Naples, Italy*
[3] *CEINGE Biotecnologie Avanzate S.C. a R.L., Via Gaetano Salvatore 486, 80145, Naples, Italy*
[4] *Dipartimento di Biochimica e Biotecnologie Mediche, Università degli Studi di Napoli Federico II, Via Pansini 5, Via Pansini 5, 80131 Naples, Italy*
[5] *Fondazione Stella Maris Mediterraneo, Centro Disturbi del Comportamento Alimentare e del Peso "G. Gioia", Chiaromonte, C/da S. Lucia, 85100, Chiaromonte, Potenza, Italy*
[6] *Dipartimento di Scienze Mediche Preventive, Università degli Studi di Napoli Federico II, Via Pansini 5, 80131 Naples, Italy*

Correspondence should be addressed to Lucia Sacchetti, sacchett@unina.it

Received 1 December 2010; Accepted 8 April 2011

Academic Editor: Francesco Saverio Papadia

Brown adipose tissue, where Uncoupling Protein 1 (UCP1) activity uncouples mitochondrial respiration, is an important site of facultative energy expenditure. This tissue may normally function to prevent obesity. Our aim was to investigate by sequence analysis the presence of *UCP1* gene variations that may be associated with obesity. We studied 100 severe obese adults (BMI $> 40\,kg/m^2$) and 100 normal-weight control subjects (BMI range = 19–24.9 kg/m^2). We identified 7 variations in the promoter region, 4 in the intronic region and 4 in the exonic region. Globally, 72% of obese patients bore *UCP1* polymorphisms. Among *UCP1* variants, g.IVS4−208T>G SNP was associated with obesity (OR: 1.77; 95% CI = 1.26–2.50; $P = .001$). Further, obese patients bearing the g.−451C>T (CT+TT) or the g.940G>A (GA+AA) genotypes showed a higher BMI than not polymorphic obese patients ($P = .008$ and $P = .043$, resp.). In conclusion, *UCP1* SNPs could represent "thrifty" factors that promote energy storage in prone subjects.

1. Introduction

Brown adipose tissue (BAT) plays an important role in energy expenditure [1]. Its thermogenic activity requires not only the presence of a dense vascularisation and sympathetic innervation, but also the expression of Uncoupling Protein 1 (UCP1) [2, 3]. UCP1 is localized on the inner mitochondrial membrane where it uncouples oxidative metabolism from ATP synthesis, resulting in the dissipation of energy through the release of heat [4]. In humans, BAT exerts its function especially during the first years of life and decreases with age [5]. However, several metabolic active depots of BAT have been recently demonstrated also in adult humans [6–8]. It has been calculated that BAT malfunction could lead to a weight gain of 1-2 kg/yr [9]. These data suggest that BAT specific proteins, such as UCP1, could be involved in obesity onset so representing a possible target of pharmaceutical interventions in this field [10, 11]. In the last years, *UCP1* loss has been associated with obesity susceptibility in $UCP1^{-/-}$ mice, particularly during aging and a high-fat diet [12, 13]. We previously described the association between the variation −3826A>G in the *UCP1* promoter and a severe fatty liver steatosis during obesity [14]. The aim of this study was to search for further gene alterations associated with obese phenotype in the *UCP1* gene (ENSG00000109424) by sequence analysis.

Table 1: General and biochemical characteristics of obese patients and control subjects.

	Obese patients ($n = 100$)	Control subjects ($n = 100$)
Females (%)	60	64
Age (years)	32.1 ± 10.9	33.3 ± 8.1
BMI* (kg/m^2)	47.9 ± 6.9	22.8 ± 2.1
Adiponectin* (μg/mL)	31.6 ± 30.0	53.8 ± 38.6
Leptin* (ng/mL)	119.6 ± 72.4	21.9 ± 18.7
Resistin (ng/mL)	12.2 ± 8.4	12.7 ± 7.9
Glucose* (mmol/L)	4.9 ± 0.8	4.5 ± 0.4
Total cholesterol (mmol/L)	4.7 ± 1.1	5.0 ± 0.7
Triacylglycerols* (mmol/L)	1.5 ± 0.6	0.9 ± 0.3
AST* (U/L)	26.5 ± 16.7	19.8 ± 5.6
ALT* (U/L)	39.8 ± 35.0	22.5 ± 12.9
GGT* (U/L)	35.3 ± 26.0	17.4 ± 10.4
Creatinine (mg/dL)	0.9 ± 0.2	0.7 ± 0.1

* Statistically significant difference between obese and control subjects, $P < .001$ at Mann-Whitney test. Biochemical parameters were measured by routine laboratory methods. Adipokines concentrations were measured by ELISA assay (LINCO Research, Mo, USA). Values are expressed as mean ± SD.

2. Materials and Methods

We studied 200 age-matched unrelated Caucasian subjects from Southern Italy: 100 adult severe obese patients (60% female, mean ± SD: BMI = 47.9 ± 6.9 kg/m^2; age = 32.1 ± 10.9 years) and 100 unrelated adult normal-weight subjects (64% female, mean ± SD: BMI = 22.8 ± 2.1 kg/m^2; age = 33.3 ± 8.1 years). The patients were recruited at the obesity outpatient clinic of the Department of Clinical and Experimental Medicine, University of Naples Federico II, Italy, from 2007 to 2008, whereas control subjects were recruited at the Department of Preventive Medical Science of the Federico II University Hospital. Clinical and biochemical data were obtained from each patient on their first admission. The general and biochemical characteristics of the studied populations are reported in Table 1. All patients and controls gave their informed consent to the study, which was carried out according to the Helsinki II Declaration. The research was also approved by the Ethics Committee of the School of Medicine, University of Naples Federico II.

Genomic DNA was extracted from whole blood (Nucleon BACC-II; Amersham Science Europe). *UCP1* 5′ flanking region, exons and intron-exon junction regions were amplified by ten sets of primers (primers ID: RSA000984680, RSA000984677, RSA000984675, RSA000984673, RSA000984666, RSA000990288, RSA000990284, RSA000990283, RSA000990281, and RSA000990278 http://www.ncbi.nlm.nih.gov/sites/entrez). PCR products were sequenced on ABI Prism 3130 Genetic Analyzer (Applied Biosystems, Foster City, CA). PCR conditions were 96°C for 5 min; than 94°C for 30 sec, 60°C for 45 sec and 72°C for 45 sec, for 40 cycles; final extension at 72°C for 10 min; final soak at 25°C.

The mean value and the standard deviation (SD) were calculated for each investigated parameter. The Mann-Whitney test and/or χ^2, when necessary, were used for between-group comparisons. Differences were considered significant at P level <.05. Linkage analysis was performed by using Haploview 4.0 software [15]. Binomial logistic regression analysis was used to investigate the association between the biochemical and genetic characteristics (i.e., glucose, total cholesterol and triacylglycerols concentrations and AST activity; g.−451C>T, g.940G>A, g.IVS4−208, and g.6537A>T polymorphisms) and the condition of being obese, after adjustment for age and sex.

Statistical analyses were carried out with the PASW package for Windows (Ver.18; SPSS Inc. Headquarters, Chicago, Ill).

3. Results and Discussion

Adiponectin and leptin concentrations were statistically different ($P < .001$) between obese and control subjects (mean level ± SD respectively: adiponectin 31.6 ± 30.0 μg/mL versus 53.8 ± 38.6 μg/mL; leptin 119.6 ± 72.4 versus 21.9 ± 18.7 ng/mL). Higher concentrations or activities of glucose, triacylglycerols, AST, ALT and GGT were measured in obese patients than in controls ($P < .001$) (Table 1).

We identified 15 sequence variations in *UCP1* gene (Table 2): 7 in the promoter region (3/7 described for the first time), 4 in the intronic regions (1/4 described for the first time) and 4 in the exonic regions (2 in the 5′ UTR; 2 in the translated region). Globally, 72% of obese patients bore one or more *UCP1* polymorphisms.

There were no differences in genotype frequencies between obese and control subjects at level of the detected SNPs, except for g.IVS4−208T>G polymorphism more frequent in obese than in control subjects ($P = .002$). After a permutation test with 100000 permutations, the association of the polymorphic allele with the obese phenotype remained statistically significant ($P = .017$). Subjects bearing this polymorphism (TG or GG) were at high risk for obesity (OR: 1.774; 95% CI = 1.26–2.50, $P = .001$). At binomial logistic regression analysis, the g.IVS4−208 (TG+GG) genotype was confirmed to be statistically associated in our patients with obesity independently of sex and age (OR: 22.0; 95% CI = 5.6–87.1). This SNP did not alter the splicing site nor the branch site [16, http://www.umd.be/HSF/], and the polymorphic allele did not change the ΔG of the predicted mRNA secondary structure by mfold analysis (http://mfold.bioinfo.rpi.edu), suggesting that the stability of the polymorphic mRNA is the same as the wild-type. The G allele may be a marker linked to other gene variants promoting energy storage as well as fat accumulation in prone subjects.

The novel *UCP1* variants g.−637T>C, g.−206C>A, and g.IVS2+174T>A, each of them present in a single obese patient, were not associated with differences in clinical and/or biochemical parameters measured in the obese and control populations. Among them, only the g.−206C>A occurred in a conserved region indentified by cisRED algorithm (http://www.cisred.org/) as a *cis*-regulatory element

Table 2: *UCP1* sequence variations and their frequencies in obese and control subjects.

Polymorphisms		Obese patients $n = 100$			Control subjects $n = 100$		
Position	rs#	wt	HE	HO	wt	HE	HO
g.−637T>C[1]		99	1	0	100	0	0
g.−451C>T	rs36207410	82	16	2	86	14	0
g.−412A>C	rs3811787	57	36	7	49	43	8
g.−372A>C	rs1800660	97	3	0	97	3	0
g.−206C>A[1]		99	1	0	100	0	0
g.−56C>T	rs3749539	91	9	0	90	10	0
g.−17C>G[1]		94	6	0	94	6	0
g.12A>C	rs10011540	91	9	0	90	10	0
g.21G>A	rs1800661	86	13	1	79	21	0
g.940G>A (p.A64T)	rs45539933	92	8	0	91	9	0
g.IVS2+138C>T	rs7688743	80	15	5	70	27	3
g.IVS2+174T>A[1]		99	1	0	100	0	0
g.IVS2+201T>G	rs2071416	79	21	0	77	22	1
g.IVS4−208T>G[2]	rs1494808	45	44	11	69	23	8
g.6537A>T (p.M229L)	rs2270565	89	11	0	87	13	0

[1] New variants; [2] More frequent polymorphism in obese patients ($P = .002$) than in controls. wt: wild-type homozygous subjects; HE: heterozygous and HO: homozygous subjects at level of the detected variant.

(craHsap157022), and we could hypothesize to alter the interaction with transcriptional factors.

Regarding the previously described *UCP1* polymorphisms, a higher mean BMI was observed in our obese patients bearing the g.−451C>T (CT+TT) than in not polymorphic obese patients (resp., $52.6 \pm 7.4\,kg/m^2$ versus $47.0 \pm 6.6\,kg/m^2$, $P = .008$).

The amino acidic substitution p.M229L (g.6537A>T) in the fifth helix of the protein is due to an A>T transversion in the 5th exon of the *UCP1* gene [17]. Mori and colleagues [18] found a higher frequency of the *Leu* allele of the p.M229L (g.6537A>T) polymorphism in a Japanese obese population with Type II diabetes, indicating this gene variation as a diabetes-associated SNP, while other studies failed to demonstrate such association [9, 19, 20]. In our study we found that patients carrying the polymorphic allele for the p.M229L polymorphism showed a slightly higher mean BMI than the wild-type patients ($50.6\,kg/m^2$ versus $47.6\,kg/m^2$, resp.) while no difference were found at level of glucose and insulin concentration or regarding the homeostatic model assessment (HOMA) index (a measure of insulin sensitivity) (data not shown). This difference could be due to the lower mean age of our studied subjects (32.1 years in our patients versus 58.6 years in Mori et al. [18]), since Type II diabetes is more frequent in middle aged than in young adult patients.

Further, the haplotype investigation by Haploview software showed a significant linkage disequilibrium among the three SNPs g.−56C>T (a), g.12A>C (b) and g.940G>A (c) (a-b: log likelihood ratio, LOD = 27.5; $r^2 = 1$; b-c and a-c: LOD = 22.6; $r^2 = 0.9$); however no statistically significant association was observed between obesity and this haplotype, the frequency of this latter being the same in obese and control subjects (8.0% versus 9.0%, resp.).

The g.12A>C polymorphism is located in the insulin response sequence (IRS). In *in vitro* experiments, the DNA mutated C allele was demonstrated to reduce the transcription of *UCP1* by 40% respect to the wild-type allele. This variation was hypothesized to impair the affinity of the transcription factors for the consensus motif of IRS [18]. Further, this SNP was previously indicated as contributing to hepatic lipid accumulation and altering insulin sensitivity in Japanese individuals with Type II diabetes mellitus (NIDDM) [18]. In our population, the lack of association of this SNP with any obesity-related phenotype could be due to the younger mean age of our patients respect to those investigated by Fukuyama et al. [21] (32.1 years versus 56.6 years, resp.) and to different ethnic background of the studied groups.

The amino acidic substitution p.A64T (g.940G>A) in the first matrix loop of the protein is due to a G>A transition in the 2nd exon of the *UCP1* gene [17].

Cha et al. [22] reported in a Korean female population an association between the mutated allele and a higher blood pressure. In our population, polymorphic patients compared to wild-type patients showed a higher mean BMI ($52.0 \pm 6.4\,kg/m^2$ versus $47.5 \pm 6.9\,kg/m^2$, $P = .043$) but only a trend toward a higher mean systolic blood pressure (130.0 mmHg versus 124.4 mmHg, resp.). This difference does not raise the statistically significant level probably due to the lower number of patients in our examined casistic.

4. Conclusions

Functional activity of BAT has been recently demonstrated in adult humans [6–8] and its amount is inversely related to body fat percentage [23]. We do not have any information

in our patients about BAT amount. However, variations in the BAT marker *UCP1* gene were present in most of our obese patients. These variations could represent common factors contributing to the development of obesity, particularly, g.−451C>T, g.940G>A, and g.IVS4−208T>G could represent "thrifty" factors that promote energy storage. The precise role in obesity of these variants should be investigated in a larger casistic.

Acknowledgments

The authors thank Jean Ann Gilder (Scientific Communication srl) for text revision and editing. The work supported by grants Conv. CEINGE-Regione Campania (DGRC 1901/2009), Regione Campania LR n5/2005 and MIUR PRIN 2008, and Progetto di Ricerca Finalizzata RF-SDN-2007-635809 (Ministero del Lavoro, della Salute e delle Politiche Sociali).

References

[1] S. R. Farmer, "Molecular determinants of brown adipocyte formation and function," *Genes and Development*, vol. 22, no. 10, pp. 1269–1275, 2008.

[2] M. C. Zingaretti, F. Crosta, A. Vitali et al., "The presence of UCP1 demonstrates that metabolically active adipose tissue in the neck of adult humans truly represents brown adipose tissue," *The FASEB Journal*, vol. 23, no. 9, pp. 3113–3120, 2009.

[3] M. Rosenbaum and R. L. Leibel, "Adaptive thermogenesis in humans," *International Journal of Obesity*, vol. 34, pp. S47–S55, 2010.

[4] B. Cannon and J. Nedergaard, "Metabolic consequences of the presence or absence of the thermogenic capacity of brown adipose tissue in mice (and probably in humans)," *International Journal of Obesity*, vol. 34, pp. S7–S16, 2010.

[5] A. Frontini and S. Cinti, "Distribution and development of brown adipocytes in the murine and human adipose organ," *Cell Metabolism*, vol. 11, no. 4, pp. 253–256, 2010.

[6] S. Enerbäck, "Brown adipose tissue in humans," *International Journal of Obesity*, vol. 34, pp. S43–S46, 2010.

[7] K. A. Virtanen, M. E. Lidell, J. Orava et al., "Functional brown adipose tissue in healthy adults," *The New England Journal of Medicine*, vol. 360, no. 15, pp. 1518–1525, 2009.

[8] A. M. Cypess, S. Lehman, G. Williams et al., "Identification and importance of brown adipose tissue in adult humans," *The New England Journal of Medicine*, vol. 360, no. 15, pp. 1509–1517, 2009.

[9] S. A. Urhammer, M. Fridberg, T. I. Sørensen et al., "Studies of genetic variability of the uncoupling protein 1 gene in Caucasian subjects with juvenile-onset obesity," *Journal of Clinical Endocrinology and Metabolism*, vol. 82, no. 12, pp. 4069–4074, 1997.

[10] S. Costford, A. Gowing, and M. E. Harper, "Mitochondrial uncoupling as a target in the treatment of obesity," *Current Opinion in Clinical Nutrition and Metabolic Care*, vol. 10, no. 6, pp. 671–678, 2007.

[11] J. Nedergaard and B. Cannon, "The changed metabolic world with human brown adipose tissue: therapeutic visions," *Cell Metabolism*, vol. 11, no. 4, pp. 268–272, 2010.

[12] Y. Kontani, Y. Wang, K. Kimura et al., "UCP1 deficiency increases susceptibility to diet-induced obesity with age," *Aging Cell*, vol. 4, no. 3, pp. 147–155, 2005.

[13] H. M. Feldmann, V. Golozoubova, B. Cannon, and J. Nedergaard, "UCP1 ablation induces obesity and abolishes diet-induced thermogenesis in mice exempt from thermal stress by living at thermoneutrality," *Cell Metabolism*, vol. 9, no. 2, pp. 203–209, 2009.

[14] G. Labruna, F. Pasanisi, C. Nardelli et al., "UCP1 -3826 AG+GG genotypes, adiponectin, and leptin/adiponectin ratio in severe obesity," *Journal of Endocrinological Investigation*, vol. 32, no. 6, pp. 525–529, 2009.

[15] J. C. Barrett, B. Fry, J. Maller, and M. J. Daly, "Haploview: analysis and visualization of LD and haplotype maps," *Bioinformatics*, vol. 21, no. 2, pp. 263–265, 2005.

[16] F. O. Desmet, D. Hamroun, M. Lalande, G. Collod-Béroud, M. Claustres, and C. Béroud, "Human splicing finder: an online bioinformatics tool to predict splicing signals," *Nucleic Acids Research*, vol. 37, no. 9, article e67, 2009.

[17] J. Jiménez-Jiménez, R. Zardoya, A. Ledesma et al., "Evolutionarily distinct residues in the uncoupling protein UCP1 are essential for its characteristic basal proton conductance," *Journal of Molecular Biology*, vol. 359, no. 4, pp. 1010–1022, 2006.

[18] H. Mori, H. Okazawa, K. Iwamoto, E. Maeda, M. Hashiramoto, and M. Kasuga, "A polymorphism in the 5' untranslated region and a Met229−− >Leu variant in exon 5 of the human UCP1 gene are associated with susceptibility to type II diabetes mellitus," *Diabetologia*, vol. 44, no. 3, pp. 373–376, 2001.

[19] A. Hamann, J. Tafel, B. Büsing, H. Münzberg, A. Hinney, H. Mayer et al., "Analysis of the uncoupling protein-1 (UCP1) gene in obese and lean subjects: identification of four amino acid variants," *International Journal of Obesity*, vol. 22, no. 9, pp. 939–941, 1998.

[20] K. S. Vimaleswaran, V. Radha, R. Deepa, and V. Mohan, "Absence of association of metabolic syndrome with PPARGC1A, PPARG and UCP1 gene polymorphisms in Asian Indians," *Metabolic Syndrome and Related Disorders*, vol. 5, no. 2, pp. 153–162, 2007.

[21] K. Fukuyama, T. Ohara, Y. Hirota et al., "Association of the -112A>C polymorphism of the uncoupling protein 1 gene with insulin resistance in Japanese individuals with type 2 diabetes," *Biochemical and Biophysical Research Communications*, vol. 339, no. 4, pp. 1212–1216, 2006.

[22] M. H. Cha, B. K. Kang, D. Suh, K. S. Kim, Y. Yang, and Y. Yoon, "Association of UCP1 genetic polymorphisms with blood pressure among Korean female subjects," *Journal of Korean Medical Science*, vol. 23, no. 5, pp. 776–780, 2008.

[23] W. D. van Marken Lichtenbelt, J. W. Vanhommerig, N. M. Smulders et al., "Cold-activated brown adipose tissue in healthy men," *The New England Journal of Medicine*, vol. 360, no. 15, pp. 1500–1508, 2009.

Open

International Journal of Obesity (2011) 1–11

0307-0565/11
www.nature.com/ijo

ORIGINAL ARTICLE

Four novel *UCP3* gene variants associated with childhood obesity: effect on fatty acid oxidation and on prevention of triglyceride storage

CV Musa[1,2], A Mancini[3], A Alfieri[1,4], G Labruna[1,3], G Valerio[4], A Franzese[5], F Pasanisi[6], MR Licenziati[7], L Sacchetti[1] and P Buono[1,3,4]

[1]*Dipartimento di Biochimica e Biotecnologie Mediche, Università degli Studi di Napoli 'Federico II', Naples, Italy;* [2]*CEINGE Biotecnologie Avanzate s.c.a.r.l., Naples, Italy;* [3]*Fondazione SDN-IRCCS, Naples, Italy;* [4]*Dipartimento di Studi delle Istituzioni e dei Sistemi Territoriali, Università degli Studi di Napoli 'Parthenope', Naples, Italy;* [5]*Dipartimento di Pediatria, Università degli Studi di Napoli 'Federico II', Naples, Italy;* [6]*Dipartimento di Medicina Clinica e Sperimentale-CISRO, Università degli Studi di Napoli 'Federico II', Naples, Italy and* [7]*UOS Auxoendocrinologia dell'età evolutiva, AORN A. Cardarelli, Naples, Italy*

Objective: The objective of the study was to look for uncoupling protein 3 (*UCP3*) gene variants in early-onset severe childhood obesity and to determine their effect on long-chain fatty acid oxidation and triglyceride storage.
Methods and results*:* We identified four novel mutations in the *UCP3* gene (V56M, A111V, V192I and Q252X) in 200 children with severe, early-onset obesity (body mass index-standard deviation score >2.5; onset: <4 years) living in Southern Italy. We evaluated the role of wild-type (wt*)* and mutant UCP3 proteins in palmitate oxidation and in triglyceride storage in human embryonic kidney cells (HEK293). Palmitate oxidation was $\sim$60% lower ($P<0.05$; $P<0.01$) and triglyceride storage was higher in HEK293 cells expressing the four UCP3 mutants than in cells expressing wt UCP3. Moreover, mutants V56M and Q252X exerted a dominant-negative effect on wt protein activity ($P<0.01$ and $P<0.05$, respectively). Telmisartan, an angiotensin II receptor antagonist used in the management of hypertension, significantly ($P<0.05$) increased palmitate oxidation in HEK293 cells expressing wt and mutant proteins ($P<0.05$; $P<0.01$), including the dominant-negative mutants.
Conclusions: These data indicate that protein UCP3 affects long-chain fatty acid metabolism and can prevent cytosolic triglyceride storage. Our results also suggest that telmisartan, which increases fatty acid oxidation in rat skeletal muscle, also improves UCP3 wt and mutant protein activity, including the dominant-negative UCP3 mutants.
International Journal of Obesity advance online publication, 19 April 2011; doi:10.1038/ijo.2011.81

Keywords: *UCP3* variants; childhood obesity; palmitate oxidation; telmisartan; Oil Red O; dominant negative

Context: Human uncoupling protein 3 (UCP3) is the muscle-specific mitochondrial transmembrane carrier that uncouples oxidative adenosine-5′-triphosphate (ATP) phosphorylation.

Introduction

Human uncoupling protein 3 (UCP3) is a member of a family of mitochondrial inner membrane anion carrier proteins that uncouples the oxidative phosphorylation from adenosine-5′-triphosphate synthesis.[1,2] The *UCP3* gene consists of seven exons, six of which encode a transmembrane region. It encodes two forms of transcripts: a full-length messenger (UCP3L) and a short isoform (UCP3S) that lacks the sixth transmembrane domain; the two messengers are equally expressed in skeletal muscle.[3] The UCP3 protein is more abundant in glycolytic, type 2 human muscle fibers than in oxidative, type 1 human muscle fibers. It is also expressed, although at lower levels, in cardiac muscle and white adipose tissue.[4,5] Several lines of evidence suggest that UCP3 is related to cellular fatty acid metabolism rather than to mitochondrial uncoupling of oxidative phosphorylation. In fact, UCP3 messenger expression in skeletal muscle is rapidly upregulated during fasting, acute exercise and high dietary intake of fat,[6–9] and declines in situations in which fat oxidative capacity is improved, such as after endurance training or weight reduction, and in type 1 muscle fibers that are characterized by a high rate of fat oxidation.[10,11] The

Correspondence: Professor P Buono, Dipartimento di Studi delle Istituzioni e dei Sistemi Territoriali, Università degli Studi di Napoli 'Parthenope', Via Medina 40, Naples 80133, Italy.
E-mail: buono@uniparthenope.it
Received 22 September 2010; revised 8 February 2011; accepted 27 February 2011

UCP3 gene has recently been proposed as a candidate gene for obesity.[12]

In the present study, we looked for *UCP3* variants in a cohort of severe obese children (body mass index-standard deviation score >2.5) with early-onset obesity (mean age 4 years) living in Southern Italy. We found four novel mutations in the *UCP3* gene, all in the heterozygous state. We conducted a functional analysis of wild-type (wt) and mutant UCP3 proteins to assess their role in long-chain fatty acid β-oxidation and triglyceride storage.

We also investigated the association between the −55C/T polymorphism in the *UCP3* gene promoter and BMI in our cohort, because only recent studies found an association between the *UCP3* −55 C/T polymorphism and BMI in some populations.

Telmisartan and valsartan are two angiotensin II receptor blockers frequently used to ameliorate hypertension in patients who are prone to visceral obesity, metabolic syndrome and diabetes.[13] Recently, telmisartan, but not valsartan, was found to improve long-chain fatty acid oxidation in rat skeletal muscle[14] and to reduce lipid accumulation in liver.[13] It also ameliorates hypertension, improves glucose and lipid metabolism and protects against visceral fat accumulation. In this paper, we also tested the effects of telmisartan treatment on UCP3 wt and mutant protein activity in HEK293 cells.

Subject and methods

Subjects

Between 2003 and 2005, 200 obese children (107 girls (53.5%) and 93 boys (46.5%); 1.5–10 years of age) were recruited by the outpatient clinic of the Department of Pediatrics, 'Federico II' University of Naples and by the Department of Pediatrics, A. Cardarelli Hospital, Naples, Italy. All children were Caucasian and lived in the Campania region (Southern Italy). Inclusion criteria were obesity classified as BMI (weight/height^2) >95th centile, obesity onset <10 years of age and absence of any syndromic or endocrine form of obesity. As controls, 100 (54 males and 46 females) normal-weight healthy individuals (BMI <25 kg m^{-2}; aged 24.2 ± 3.4 years), previously enrolled by us,[15] underwent genetic testing for obesity.

Written informed consent was obtained from participants and/or their parents. The study was approved by the ethics committee of the School of Medicine, University of Naples 'Federico II' and was conducted in accordance with the principles of the Helsinki II Declaration.

Physical measurements

A trained dietitian measured the height, weight and waist circumference (recorded to the nearest 0.1 cm, 0.1 kg and 0.1 cm, respectively) of the enrolled children. Waist was measured with a flexible steel tape measure while children were in the standing position after gentle expiration. BMI percentiles for age and BMI-standard deviation scores were determined based on the Center for Disease Control normative curves.[16] Blood pressure was measured with an aneroid sphygmomanometer on the left arm with the subject supine after 5 min of rest, with an appropriately sized cuff.[17] Systolic (Korotkoff phase I) and diastolic blood pressure (Korotkoff phase V) were measured three times and the average was used for analysis.

Laboratory measurements

After a 12-h overnight fast, plasma glucose and insulin, and serum triglycerides, total cholesterol and high-density lipoprotein cholesterol were measured in enrolled children. Insulin resistance was calculated with the homeostasis model assessment of insulin resistance (HOMA-IR) index (fasting insulin × fasting glucose/22.5), as described by Matthews *et al.*[18] HOMA-IR ⩾2.5 was considered an index of impaired insulin sensitivity. The general characteristics of the obese children are reported in Table 1.

Body composition was evaluated with bioimpedance analysis (STA/BIA; Akern, Florence, Italy) in children carrying a *UCP3* mutation and in their matched controls.

DNA amplification and genotyping

Genomic DNA was obtained from whole blood of obese and non-obese subjects using Nucleon BACC-2 (GE Healthcare Europe–Amersham, Little Chalfont, UK). The *UCP3* gene was amplified in a final volume of 50 μl containing 50 ng of genomic DNA; 1 U of Taq DNA polymerase (Invitrogen S.r.l.,

Table 1 Clinical and biochemical characteristics of the severely obese children ($n = 200$) genotyped

Parameters	*Mean values ± s.d.*	*Normal value range*
Age (years)	5.5 ± 3.2	
BMI (kg m^{-2})	26.4 ± 3.7	
BMI-SDS	3 ± 0.75	(<2)
Waist-to-hip ratio	0.97 ± 0.06	(<0.88)
Hip circumference	79.8 ± 9.2	(<57.1 cm)
SBP	94.5 ± 13.7	(<111 mm Hg)
DBP	61.5 ± 7.1	(<71 mm Hg)
Triglycerides	82.5 ± 41.8	(<103 mg dl^{-1})
Cholesterol	160.6 ± 31.9	(<180 mg dl^{-1})
LDL cholesterol	95.9 ± 30.0	(<130 mg dl^{-1})
HDL cholesterol	46.9 ± 11.1	(> 36 mg dl^{-1})
AST	27.8 ± 5.4	(10–40 U l^{-1})
ALT	24.8 ± 10.2	(<40 U l^{-1})
TSH	2.7 ± 1.2	(0.54–4.53 μU ml^{-1})
FT3	4.4 ± 0.5	(3.0–9.1 pmol l^{-1})
FT4	1.2 ± 0.2	(0.85–1.75 ng dl^{-1})
HOMA	2.2 ± 1.4	(<2.5)
Insulin	10.82 ± 41.8	(<28 μU ml^{-1})

Abbreviations: ALT, alanine aminotransferase; AST, aspartate aminotransferase; BMI-SDS, body mass index-standard deviation score; DBP, diastolic blood pressure; FT3, free triiodothyronine; FT4, free thyroxine; HDL, high-density lipoprotein; HOMA, homeostasis model assessment; LDL, low-density lipoprotein; SBP, systolic blood pressure; TSH, thyroid-stimulating hormone. Values are means ± s.d.; numbers in parenthesis indicate the normal range corrected for the sample mean age (5.5 ± 3.2 years).

Milan, Italy); 200 μM of each deoxynucleotide triphosphate, 50 mM KCl, 10 mM Tris-HCl (pH 8.8), 2.5 mM $MgCl_2$, 0.2 mg ml^{-1} bovine serum albumin (BSA) and 200 nM of the specific primers. The primers used for *UCP3* gene sequencing are here reported:

Promoter-Fw	5′-GCGTCCACAGCTTAAAGGAG-3′
Promoter-Rev	5′-GAACAAGGAGAAGGGAGAGG-3′
UCP3-F2	5′-ATCACTCCATCAGCCTTCTC-3′
UCP3-F2	5′-TCTTTGTCAGGGTTCTGAGG-3′
UCP3-F3	5′-CAGCATGGTTGTTCTCAGGC-3′
UCP3-F3	5′-TGCCTCTGAGTCTAGACTTC-3′
UCP3-F4	5′-AGGAGGTCTGAGTGGACATC-3′
UCP3-F4	5′-GTCAGTGAAGTATCTTTGGTTGTG-3′
UCP3-F5	5′-CATTTCTCCCATTTCCCATTCC-3′
UCP3-F5	5′-TCCTTCTAAAACCCAGTTGCC-3′
UCP3-F6	5′-TTGGGGACAAACAGTGCATAC-3′
UCP3-F6	5′-GTACTCTTCACCGCTACATC-3′
UCP3-F7	5′-GAGAGCACACGCATCTGTTG-3′
UCP3-F7	5′-TCTGTGTCCATGTGTGCGTG-3′

PCR fragments were separated by electrophoresis on a 1.5% agarose gel and purified. The two strands were sequenced (BigDye Terminator v3.1 cycle sequencing method on an ABI-Prism 3100 Genetic Analyzer; Applied Biosystems, Foster City, CA, USA).

Cloning of human wt and mutant UCP3 complementary (c)DNAs in a eukaryotic expression vector

Total mRNA from a human osteosarcoma cell line (Saos-2) expressing UCP3 protein was reverse transcribed using oligo (dT). UCP3L and UCP3S cDNAs were amplified in PCR reactions using the same 5′-primer (CTTCCAGGACTATGGTGG) but different 3′-primers: GTTCAAAACGGTGATTCCCG for UCP3L and GAAAGAAGCCCCTGTTCTCTG for UCP3S, respectively.[19] UCP3L and UCP3S cDNAs were inserted into the mammalian expression vector p3xFLAG-CMV-7.1 (Sigma-Aldrich S.r.l., Milan, Italy) downstream from the N-terminal 3× FLAG epitope and then sequenced in both directions. QuickChange site-directed mutagenesis kit (Stratagene Inc., La Jolla, CA, USA) was used to generate the four mutants (V56M, A111V, V192I and Q252X) from the cloned wt UCP3L cDNA according to the manufacturer's protocol. Recombinant constructs were purified using a Qiagen column (Qiagen S.p.A., Milan, Italy) and sequenced on both strands.

Cell culture and UCP3 protein expression

HEK293 cells were grown in Dulbecco's modified Eagle's medium supplemented with 10% fetal bovine serum, 100 units ml^{-1} penicillin and 100 μg ml^{-1} streptomycin (Invitrogen S.r.l.) at 37 °C with 5% CO_2. The plasmids expressing the wt or the mutated UCP3 proteins were transiently transfected in HEK293 cells using Lipofectamine 2000 reagent (Invitrogen S.r.l.) according to the manufacturer's instructions. The pRL CMV vector (Promega Italia S.r.l., Milan, Italy) expressing the *Renilla* luciferase cDNA (Rluc) reporter gene was co-transfected (0.1 μg) and used as internal control reporter to verify transfection efficiency.

All the experiments were performed at 24 h post-transfection: at this time, we verified that the wt and mutants UCP3 proteins were expressed in appreciable amounts and correctly localized in the mitochondria. We also performed a cell-viability test, using Trypan blue (Sigma-Aldrich S.r.l.) according to the manufacturer's protocol and we observed 100% cell viability at 24 h post-transfection.

Preparation of mitochondrial and submitochondrial extracts and western blot

HEK293 cells were transiently transfected with plasmids that express wt or mutant UCP3 proteins. At 24 h after transfection, cells were washed in phosphate-buffered saline (PBS) pH 6.9 (Sigma-Aldrich S.r.l.), harvested and mitochondrial protein extracts were prepared using the Qproteome Mitochondria Isolation Kit (Qiagen S.p.A.) according to the manufacturer's instructions. Submitochondrial protein extracts were prepared from mitochondria freshly isolated as described above. Briefly, mitochondria were resuspended in a hypotonic medium (10 mM KCl, 2 mM HEPES, pH 7.2) and incubated for 20 min on ice to swell mitochondria and break the outer mitochondrial membrane, thereby releasing proteins from the intermembrane space. The swollen mitochondria were subsequently centrifuged at 11 200 r.p.m. and the supernatant (containing the soluble intermembrane space proteins) and the pellet (containing proteins on or associated with the inner mitochondrial membrane and matrix) were collected. Protein concentration was determined using the Bio-Rad protein assay kit (Bio-Rad Laboratories S.r.l., Segrate, Milan, Italy).

For western blot analysis, 40 μg of mitochondrial and submitochondrial protein fractions were run on a 12% sodium dodecyl sulfate-polyacrylamide gel electrophoresis gel and transferred to a nitrocellulose membrane (GE Healthcare Europe–Amersham). Membranes were incubated for 1 h and 30 min at room temperature with specific antibodies and then incubated for 1 h with antibody–horseradish peroxidase-conjugated anti-mouse Ig (1:3000 Sigma-Aldrich). Immunoreactive bands were visualized with the enhanced chemiluminescence reagents kit (ECL; GE Healthcare Europe–Amersham) according to the manufacturer's instructions. We used antitumor necrosis factor type 1 associated protein, TRAP-1 antibody (1:1000; Santa Cruz Biotechnology Inc., Santa Cruz, CA, USA), anti-COX-IV mouse monoclonal antibody (1:1000; Santa Cruz Biotechnology Inc.), anti-FLAG antibody (1:5000) and anti-tubulin antibody (1:500; Sigma-Aldrich S.r.l.).[20,21]

Palmitate oxidation and telmisartan treatment

Wt and mutant UCP3 proteins were expressed in HEK293 cells to evaluate the role of UCP3 in long-chain fatty acid

oxidation. HEK293 cells were seeded into 24-well plates and transiently transfected with either wt or mutant UCP3-expressing constructs alone or with wt and mutant UCP3-expressing constructs in equal amounts (1:1 ratio), such that the amount of DNA transfected each time was the same (namely, 0.8 μg). The pRL CMV vector was also co-transfected. Palmitate oxidation was measured as reported elsewhere.[22] Briefly, 24 h after transfection, cells were washed with PBS and incubated with 500 μl of preincubation medium (Krebs Ringer Bicarbonate Medium; Sigma-Aldrich S.r.l.) containing 0.5 g l^{-1} BSA (fatty acid free; Sigma-Aldrich S.r.l.) for 1 h. After preincubation, the medium was removed and 200 μl of incubation medium (110 μmol l^{-1} palmitate, 16.7 Ci ml^{-1} [^{3}H] palmitate and 0.5 g l^{-1} BSA in PBS) were added to each well, which were incubated at 37 °C for 2 h. The incubation medium was transferred to columns containing ~3 ml of Dowex-1 ion-exchange resin (Sigma-Aldrich S.r.l.) previously charged with 1.0 mol l^{-1} NaOH and washed with MilliQ water until the eluate had the same pH as the water. Then, each well was washed once with 300 μl of PBS that was collected and applied to the columns. The columns were finally washed with 2 ml of water. The resin binds the nonmetabolized palmitate and allows the tritiated water produced by β-oxidation to pass through. The eluate (2.5 ml) was collected in a scintillation vial. Then, 6 ml of scintillation cocktail (Picofluor 40; Packard Instruments Co Inc., Downers Grove, IL, USA) was added to each vial and the vials were counted in a liquid scintillation counter Tri-CARB 1500 (Packard Instrument Co Inc.). For each sample, counts per min (c.p.m.) were normalized to the luciferase activity determined by the Dual-Luciferase Reporter Assay System (Promega Italia S.r.l.), according to the manufacturer's instructions. The background signal was determined on untransfected control cells.

To evaluate the effects of the angiotensin II antagonist telmisartan on long-chain fatty acid β-oxidation in the presence of wt and mutated UCP3 proteins, HEK293 cells were transfected with wt UCP3L-expressing construct alone or co-transfected with wt and mutant UCP3-expressing constructs in equal amounts (1:1 ratio). At 24 h after transfection, cells were incubated first with 500 μl of preincubation medium for 1 h at 37 °C and then with 200 μl of a medium containing 110 μmol l^{-1} palmitate and 0.5 g l^{-1} BSA in PBS for 3 h. After the first 30 min, telmisartan (Sigma-Aldrich S.r.l.) was added to the medium at a final concentration of 10 μM,[14] and the incubation was continued for an additional 1 h and 30 min. During the last 1 h of incubation, [^{3}H] palmitate (16.7 Ci ml^{-1}) was added to the cells. Lastly, palmitate oxidation was measured in the medium, as reported above.

Oil Red O staining

Intracellular triglyceride accumulation was determined by Oil Red O staining. Briefly, HEK293 cells were seeded in poly-D-lysine eight-well culture slides (VWR International S.r.l., Milan, Italy), and transiently transfected with either wt or mutant UCP3-expressing plasmids alone or with wt and mutant UCP3 constructs in a 1:1 ratio, such that the amount of DNA transfected each time was the same (namely, 0.4 μg). At 24 h after transfection, cells were treated with 500 μM and 1 mM palmitate (Sigma-Aldrich, S.r.l.) complexed with BSA for 24 h. Then, cells were washed twice with PBS, fixed in a 10% formalin-containing PBS solution for 15 min and stained with Oil Red O working solution (5 mg Oil Red O ml^{-1} isopropanol) for 15 min at room temperature. Cells were counterstained with hematoxylin and then covered with a coverslip. The stained lipids were viewed and photographed using a phase-contrast microscope (Leica Microsystems S.r.l., Milan, Italy) at ×40 magnification. The number of Oil Red O-stained lipid droplets/number of cells were counted. At least five randomly chosen fields were counted for each sample.

Statistical analysis

Allele frequencies were calculated by allele counting, and the deviation from Hardy–Weinberg equilibrium was evaluated by χ^2 analysis. The difference between metabolic and anthropometric variables in the two groups, wt and heterozygous mutation carriers, was evaluated by one-way analysis of variance. The statistical analysis was performed with SPSS software, version 10 (IBM, Chicago, IL, USA). The data relative to functional analysis are shown as mean ± s.d. and were analyzed with the Student's *t*-test. Differences were considered statistically significant at a *P*-value of <0.05.

Results

Clinical, biochemical and genetic features of study participants

All clinical and biochemical parameters were within reference intervals for the mean age of the sample (Table 1). The 200 obese children had only high BMI-standard deviation score (mean 3) and waist-to-hip ratio (mean 0.97) values as expected in a sample with an average age of 5.5 years and early-onset obesity <4 years. Clinical (BMI, diastolic and systolic blood pressure) and biochemical characteristics (serum total cholesterol, triglycerides, glucose, aspartate aminotransferase and alanine aminotransferase) of the control normal-weight young subjects were in the reference range for the mean age of the sample (24.2 years).[15]

To determine whether *UCP3* gene variants contribute to the early-onset of obesity, we genotyped the cohort of severely obese children and 100 normal-weight non-diabetic subjects living in Southern Italy. We found three novel missense (V56M, A111V and V192I), one non-sense (Q252X, which generates a truncated protein) and two silent (S101S and A122A) mutations in the obese children and one polymorphism (V9V) in two normal-weight and two obese children. We also found a nucleotide change (10 372 C/T) in intron 4 in one obese child (Table 2). All mutations are in the heterozygous state; mutations A111V, V192I and Q252X

Table 2 Mutations and polymorphisms detected in the *UCP3* gene in severely obese children ($n=200$) and non-obese controls ($n=100$) living in Southern Italy

Region	*Nucleotide change*	*Amino-acid change*	*Obese,* n *(%)*	*Control group,* n *(%)*
UCP3 variants				
5′-UTR	−55 C/C; C/T; T/T	—	143 (75.6); 44 (23.3); 2 (1)	65 (73.6); 22 (25.3); 1 (1.1)
Exon 2	8990 G/A	V9V	2 (1)	2 (2)
Exon 3	9666 G/A	V56M	3 (1.5)	—
Exon 3	9832 C/T	A111V	1 (0.5)	—
Exon 3	9576 C/T	S101S	1 (0.5)	—
Exon 4	10 099 C/T	A122A	1 (0.5)	—
Exon 5	11 449 G/A	V192I	1 (0.5)	—
Exon 6	12 105 C/T	Q252X	1 (0.5)	—
Intron 4	10 372 C/T	—	1 (0.5)	—

Abbreviations: UCP3, uncoupling protein 3; UTR, untranslated region.

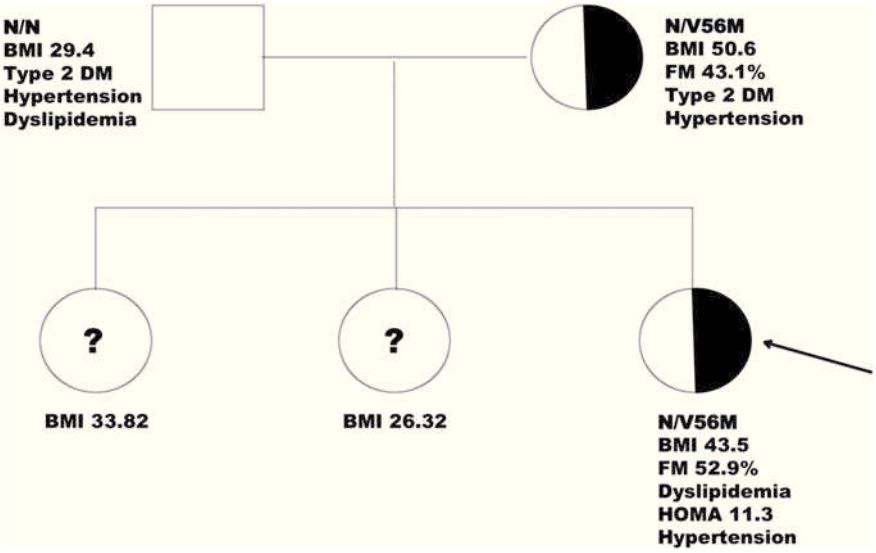

Figure 1 Pedigree of the family with the V56M mutation. The arrow indicates the female proband carrying the V56M mutation. Status for BMI (kg m^{-2}), % fat mass (% FM), type 2 diabetes mellitus (type 2 DM), blood pressure, dyslipidemia and HOMA are indicated.

were found in three unrelated probands; mutation V56M was found in two male siblings and in an unrelated girl (Table 2). We also analyzed the −55C/T polymorphism in the promoter region of the *UCP3* gene in the obese and control groups. The genotype distribution for *UCP3* −55C/T (CC, CT, TT) was in Hardy–Weinberg equilibrium. Genotype and allele frequencies did not differ between obese and non-obese subjects (Table 2).

To exclude the involvement of other obesity gene variants in the increased fat mass in our obese subjects, we genotyped them for POMC, MC4R and UCP1 variants, but found no mutations.

The parents of the 200 obese children were invited to undergo genotyping to determine the mode of transmission of mutations in families, but only the parents of the girl carrying mutation V56M consented to genotyping. As shown in Figure 1, the mother, who was severely obese (BMI 50.6), carried mutation V56M in the heterozygous state, similar to her daughter. Furthermore, she had waist circumference of 114 cm (normal 80 cm) and was affected by type 2 diabetes and hypertension. Mutation V56M was absent from the father, who was overweight (BMI 29.4) and also affected by type 2 diabetes, hypertension and dyslipidemia. Their daughter was severely obese (BMI 43.5); of her two sisters, one was overweight (BMI 26.3) and the other was obese (BMI 33.8), but they were not available for genotyping. Interestingly, the three children carrying mutation V56M had a much higher percentage of fat mass ($\sim$50.0%) than the children carrying other UCP3 gene mutations (between 36 and 45%). Furthermore, the girl carrying mutation V56M (see Figure 1) had elevated systolic blood pressure (130 mm Hg), low levels of high-density lipoprotein cholesterol (39 mg dl^{-1}), high levels of low-density lipoprotein cholesterol (113.4 mg dl^{-1}) and a high HOMA index (11.3). Hence, this girl had three components of the metabolic syndrome, as did her parents, plus insulin -resistance.

Involvement of UCP3 wt and mutant proteins in long-chain fatty acid metabolism

We investigated the effects of wt UCP3 proteins and V56M, A111V, V192I and Q252X mutant proteins on long-chain fatty acid oxidation and triglyceride storage in HEK293 cells. HEK293 cells are, at present, the most widely used cell line for *in vitro* studies in which expression plasmids are transfected in order to produce proteins (also channel proteins) and to study their activity. Wild-type long and short UCP3 isoforms and mutant proteins were expressed in HEK293 cells that lacked endogenous UCP3 protein in the mitochondria. First, we evaluated the correct targeting of wt and mutant proteins in the inner membrane and matrix (IMM) using mitochondrial and sub-mitochondrial protein fractions from HEK293-expressing wt or mutated UCP3 proteins. Both wt UCP3L and UCP3S isoforms were correctly localized in the IMM, and were absent in the intermembrane space (Figure 2a, lanes 2–4 and 17–19, respectively). Similarly, all UCP3 mutant proteins were correctly localized in IMM, and were absent in the intermembrane space (Figure 2a, lanes 7, 10, 13, 16 and lanes 6, 9, 12, 15, respectively).

We next evaluated the β-oxidation capacity of palmitate, a long-chain fatty acid, in HEK293 cells expressing wt or mutant UCP3 proteins and treated with ^{3}H-labeled palmitate. Palmitate β-oxidation capacity was evaluated by measuring tritiated water produced by cells and it was expressed as a percentage of UCP3L activity, taken as 100%. The UCP3S isoform retained 55% of UCP3L activity (Figure 2b); moreover, palmitate oxidation was significantly reduced in HEK293 cells expressing the mutated proteins. In particular, V56M and Q252X mutants retained only 40 and 35% of UCP3L activity, respectively. A111V and V192I retained ~45% of UCP3L activity (Figure 2b).

Because all mutations were found in the heterozygous state, we tested the possibility that mutated proteins can

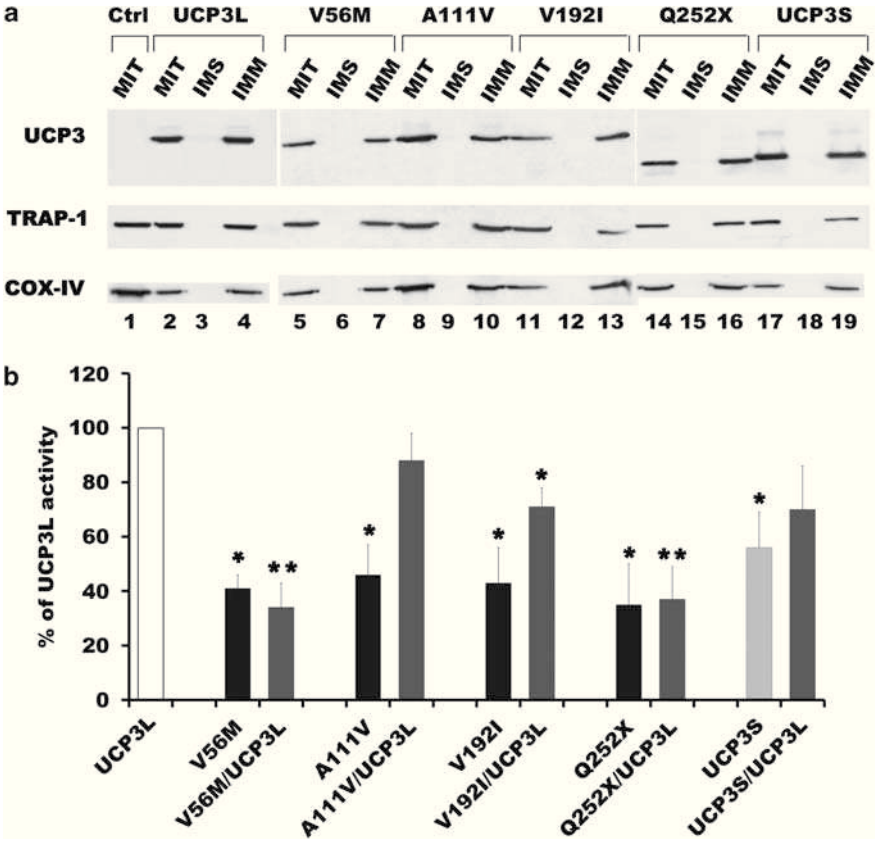

Figure 2 Sublocalization (**a**) and activity (**b**) of wt and mutant UCP3 proteins. (**a**) Western blot of mitochondrial (MIT) and submitochondrial (intermembrane space (IMS) and IMM) protein extracts (40 μg) obtained from untransfected HEK293 cells (lane 1, Ctrl) and from HEK293 cells expressing wt UCP3L (lanes 2–4) and V56M (lanes 5–7), A111V (lanes 8–10), V192I (lanes 11–13) and Q252X (lanes 14–16) mutant proteins. Protein extracts from cells expressing wt UCP3S (lanes 17–19) are also shown. A specific anti-FLAG monoclonal antibody was used to reveal wt and mutant UCP3 proteins. Anti-Trap-1 and anti-COX-IV antibodies were used as control for IMM localization. (**b**) Activity of wt and mutant UCP3 proteins calculated as percentage of ^{3}H-labeled palmitate oxidation. Percentage of palmitate oxidation capacity of wt UCP3 isoforms (UCP3L, white bar and UCP3S, light gray bar) and of V56M, A111V, V192I and Q252X mutant proteins (black bars) in HEK293 cells. We assigned an arbitrary value of 100% to UCP3L isoform activity. Palmitate β-oxidation capacity was also assayed in HEK293 cells coexpressing UCP3L isoform and mutant proteins in equal amounts (V56M/UCP3L, A111V/UCP3L, V192I/UCP3L, Q252X/UCP3L and UCP3S/UCP3L, gray bars). Data represent the means ± s.d. of four different experiments. *$P<0.05$ and **$P<0.01$ represent statistical differences vs UCP3L.

exert a dominant-negative effect on wt UCP3L activity. We choose to refer all successive analyses to long isoform of UCP3 (UCP3L) activity in that the UCP3L protein is the only isoform detectable in the human skeletal muscle also using such large amounts of protein mitochondrial extracts as 15 mg.[5] To this aim, we co-transfected equal amounts of UCP3L-expressing construct with constructs expressing V56M, A111V, V192I or Q252X in HEK293 cells, and evaluated the dominant-negative effect of mutated proteins on UCP3L activity by determining palmitate β-oxidation capacity. V56M and Q252X mutants exerted a dominant-negative effect on UCP3L activity, whereas A111V and V192I activity were rescued by UCP3L co-transfection (Figure 2b). Also, the UCP3S isoform activity was only partially rescued in co-transfected cells mimicking a slight dominant-negative effect on UCP3L activity (Figure 2b).

Interestingly, the V56M mutant protein was associated with higher BMI, percentage of fat mass and HOMA and insulin values in obese children carrying UCP3 mutations. To evaluate the role of long and short wt UCP3 isoforms in the prevention of triglyceride storage, we treated HEK293 cells expressing wt UCP3 isoforms (long and short) or mutant proteins with 500 μM or 1 mM palmitate and evaluated triglyceride storage by Oil Red O staining. Similar results were obtained with either palmitate concentration. The number of Oil Red O-positive spots was significantly lower in cells expressing the UCP3L isoform than in untransfected cells (Control (Ctrl); Figures 3a and b, compare UCP3L with Ctrl). As expected, neither the UCP3S isoform nor the four mutant proteins prevented triglyceride storage (Figures 3a and b), although at different extent, as shown by the higher number of Oil Red O-positive spots compared with UCP3L-expressing cells. Again, as expected, UCP3L co-transfection partially rescued the activity of the A111V and V192I mutant proteins as well as UCP3S isoform but did not affect the activity of the V56M and Q252X dominant-negative mutant proteins (Figure 3b). Interestingly, subjects carrying V56M or Q252X dominant-negative mutations had the highest plasma non-esterified fatty acid values, mild liver steatosis and higher fat mass and lower free fat mass values (data not shown).

Telmisartan improved palmitate oxidation capacity in HEK293 cells coexpressing UCP3L and mutant proteins

Telmisartan, 10 μM, increases fatty acid oxidation in skeletal muscle by activating the peroxisome proliferator-activated receptor-γ pathway.[14] Therefore, we evaluated whether telmisartan improves palmitate β-oxidation capacity in cells coexpressing the UCP3L isoform and mutated UCP3 proteins. HEK293 cells were transiently transfected with UCP3L-expressing construct alone or co-transfected with constructs expressing the UCP3L and V56M, A111V, A192I and Q252X mutant proteins in equal amounts in order to mimic the heterozygous state of probands. Telmisartan, 10 μM, was added to the culture for 3 h and long-chain fatty acid β-oxidation capacity was evaluated in the presence of tritiated palmitate. Palmitate oxidation capacity was calculated as percentage with respect to UCP3L-expressing cells in the absence of telmisartan taken as 100% (Figure 4, UCP3L). We found that 10 μM telmisartan increased β-oxidation capacity in cells expressing UCP3L, by ∼40% with respect to untreated cells. β-Oxidation capacity was also significantly higher in telmisartan-treated cells coexpressing UCP3L and all mutant proteins than in the untreated counterpart cells (Figure 4, compare gray with black bars). Interestingly, telmisartan increased β-oxidation capacity by approximately two- to three-fold in cells coexpressing UCP3L and the dominant-negative mutants Q252X and V56M.

Discussion

Different functional roles have been postulated for UCP3: UCP3 has been implicated in fatty acid metabolism in conditions of excess mitochondrial fatty acid supply;[23,24] UCP3 is involved in body energy balance. In fact, mice overexpressing human UCP3 have a lower body weight than wt mice.[25–28] Furthermore, observational studies in humans showed that UCP3 protein expression was reduced by 40% after weight loss in type 2 diabetic patients,[11] and UCP3 protein expression was negatively correlated with BMI in non-diabetic obese subjects.[29]

In humans, UCP3 expression is restricted to skeletal muscle. Because skeletal muscle is responsible for most of the daily energy expenditure, and a reduction in energy expenditure is a risk factor for the development of obesity,[30] UCP3 has been indicated as an obese susceptibility gene. Furthermore, the *UCP3* gene was mapped on chromosome 11q13, in a region that has been linked to obesity and hyperinsulinemia.[31]

Several *UCP3* gene variants have been implicated in obesity in humans.[32–34] The most extensively studied *UCP3* variant is the −55C/T polymorphism in the promoter region. The association of this polymorphism with overweight is controversial. In fact, it was associated with elevated UCP3 mRNA expression in male non-diabetic Pima Indians,[35] with an increased BMI in a French population,[36] with an increased hip-to-waist ratio in women of Asian origin[37] and with BMI and diabetes mellitus in a German population.[38] Conversely, the −55C/T polymorphism was associated with a lower BMI in a UK population[39] and in US Caucasian and Spanish populations,[40,41] whereas no association was found between −55C/T and BMI or percentage of body fat in Danish obese and control subjects.[42,43] In our cohort, we found no association between −55C/T and BMI, which is in agreement with Dalgaard and Berentzen.[42,43]

Only few studies have been reported so far on the positive association between UCP3 mutations and obese phenotype, but no functional analyses were performed in eukaryotic cells.[32–34] Hence, the functional analysis of the wt and

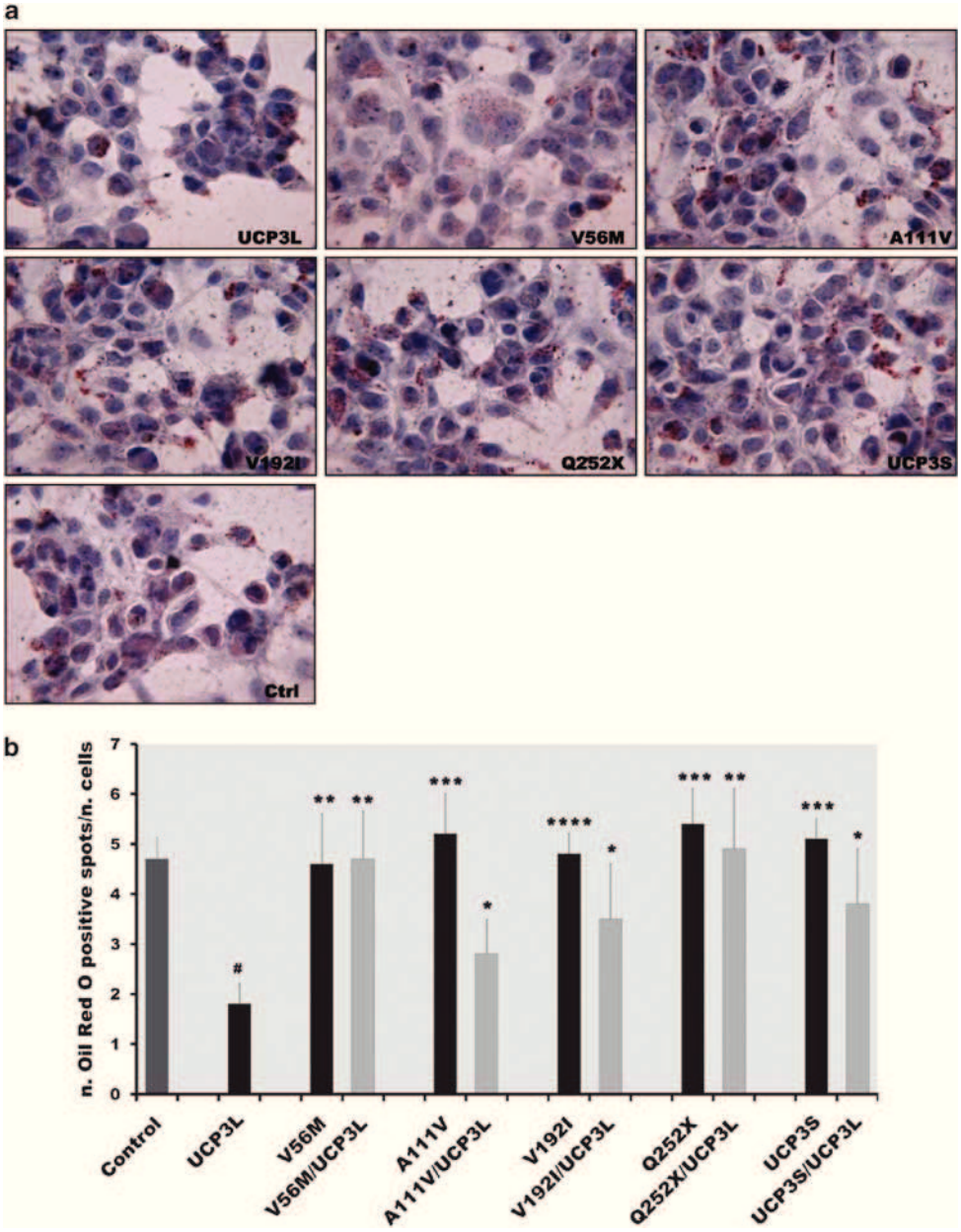

Figure 3 Triglyceride storage of wt and mutant UCP3 proteins. (**a**) Oil Red O staining of HEK293 cells expressing wt UCP3L and UCP3S isoforms and mutant V56M, A111V, V192I and Q252X UCP3 proteins treated with 1 mM palmitate. Red points indicate triglyceride depots; ×40 magnification. Ctrl indicates HEK293 cells not expressing UCP3 protein. (**b**) The number of Oil Red O-positive spots/number of cells is reported. Control (heavy gray bar) represents number of Oil Red O-spots/number of cells in HEK293 not expressing UCP3 protein. Black bars represent Oil Red O-spots/number of cells in HEK293 expressing wt UCP3L or UCP3S isoforms or V56M, A111V, V192I and Q252X mutant proteins; light gray bars represent Oil Red O-spots/number of cells in HEK293 coexpressing UCP3L isoform and UCP3S isoform or mutant proteins in equal amounts (UCP3S/UCP3L, V56M/UCP3L, A111V/UCP3L, V192I/UCP3L and Q252X/UCP3L). Data represent the means ± s.d. of five different fields. $^{\#}P<0.001$ vs Control; $^{*}P<0.05$, $^{**}P<0.01$, $^{***}P<0.005$, $^{****}P<0.001$ vs UCP3L-expressing cells.

mutant UCP3 proteins identified in our severely obese children is the first attempt made in eukaryotic cells to unravel the role of UCP3 in handling long-chain fatty acids.

In our experimental system, the UCP3 short isoform is localized in the IMM and shows a slight dominant-negative effect on UCP3 long isoform activity. Further experiments are required to validate the functional activity of the short isoform of UCP3, also in muscle cells. Similarly, it will be necessary to define *in vivo* the expression and the localization of the Q252X mutant protein, which lacks the sixth transmembrane domain.

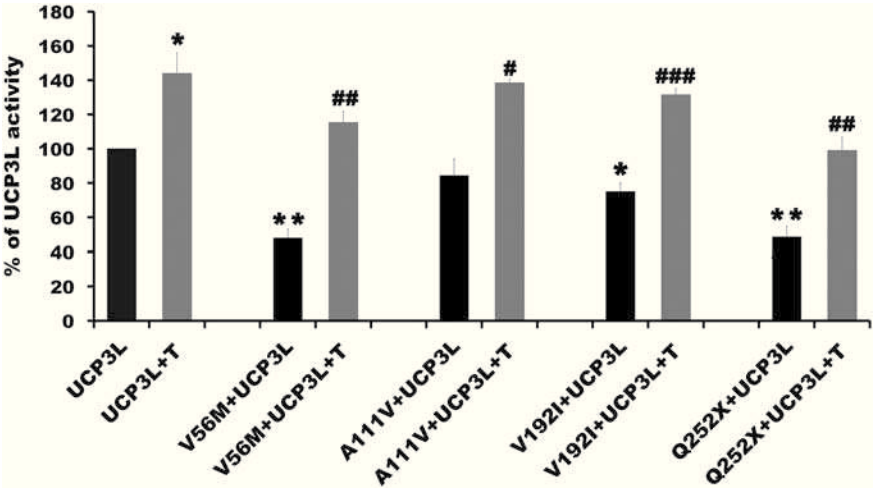

Figure 4 Effects of telmisartan treatment on palmitate oxidation activity of wt and mutant UCP3 proteins. Oxidation of ^{3}H-labeled palmitate in HEK293 cells expressing either UCP3L isoform or UCP3L and mutant UCP3 proteins in equal amounts (V56M/UCP3L, A111V/UCP3L, V192I/UCP3L and Q252X/UCP3L), in the absence (black bars) or presence (gray bars; +T) of telmisartan treatment. Data represent the means ± s.d. of four different experiments reported as a percentage of the value obtained for UCP3L-expressing cells in the absence of telmisartan treatment (UCP3L black bar) to which we assigned an arbitrary value of 100%. *$P<0.05$ and **$P<0.005$ vs UCP3L; $^{\#}P<0.05$, $^{\#\#}P<0.005$ and $^{\#\#\#}P<0.001$ vs corresponding black bar (–T).

The crystallographic structure of the UCP3 protein is not available, and hence we are not able to correlate the mutations identified with the UCP3 protein structure. Regarding the structure, we can only speculate on the type of amino acid substitution and/or on UCP3 domains in which the changed amino acids are located. All the data reported in our paper regarding the domains and the transmembrane structures of the UCP3 protein were obtained from the UniProT database. V56M is a mutation that consists of a substitution of a non-polar amino acid in an amino acid that is also non-polar. V56 amino acid, highly conserved in eukaryotes, falls in a domain (Ith solute carrier = solcar repeat) involved in transporting fatty acid anions from the mitochondrial matrix into the intermembrane space. V192I is a substitution of a non-polar amino acid in a hydrophobic amino acid. V192 amino acid, highly conserved in eukaryotes, falls in the fourth transmembrane domain included in the II solcar repeat. Despite the fact that these two variants are located in important regions involved in the transport of anions of fatty acids, they affect differently the activity of UCP3L.

Similarly, we do not know if the Q252X variant is essentially the same as making cells homozygous for UCP3S. What we know is that in our experimental system, both the Q252X mutant and the UCP3 short isoform are localized in the mitochondria associated with the inner membrane (IMM), but they show a different effect on UCP3L isoform activity. In particular, the UCP3S isoform retained 55% of UCP3L activity, whereas the Q252X mutant retained only 35% of UCP3L activity. However, as we mentioned previously,
in vivo, we never detected the UCP3S isoform in mitochondrial extracts from skeletal muscle biopsies. Moreover, we have no data *in vivo* regarding the expression of the Q252X mutated protein because muscle biopsies of the subject carrying the Q252X mutation are not available.

UCP3 expression increases glucose metabolism and protects against hyperglycemia.[25,44] Moreover, UCP3 messenger and protein expression was found to be decreased in muscle tissue of pre-diabetic and diabetic subjects.[45,13] Because of the early onset of obesity in our cohort (mean age 4 years), we found no correlation between the HOMA index and the activity of mutated UCP3 protein. However, the HOMA index was elevated in two subjects carrying mutation V56M (11.24 and 3.05, respectively, compared with the mean value of 2.2 in our obese cohort), as were insulin plasma concentrations (53.9 and 14.7, respectively, vs 10.82). We re-examined the female proband carrying mutation V56M 10 years after the first observation when she was 17 years old. She was still obese (BMI 47.6) and reported diet-resistant weight gain. These data suggest a link between V56M and severe human obesity, and extend our knowledge about the role of UCP3 in fatty acid oxidation and in the prevention of triglyceride storage. Interestingly, the highest percentage of fat mass was found among obese subjects carrying the V56M and Q252X dominant- negative mutants.

Telmisartan is both a selective peroxisome proliferator-activated receptor modulator and an angiotensin II receptor blocker.[13,14,46–49] Recently, it was found to be effective in the treatment of hypertension, to improve glucose and lipid metabolism and to protect against diet-induced weight gain and visceral fat accumulation. Telmisartan also increased fatty acid metabolism in murine muscle myotubes by decreasing acetyl CoA carboxylase 2 expression, thereby resulting in inhibition of fatty acid synthesis and stimulation of fatty acid oxidation.[49] Finally, studies conducted in

humans showed that telmisartan positively affected HbA1c, total and low-density lipoprotein cholesterol and hypertension in type 2 diabetes patients.[50–52] Consequently, telmisartan could be used to treat obese, type 2 diabetes with hypertension and hence reduce the risk of cardiovascular diseases.

In conclusion, our data support the notion that protein UCP3 is involved in long-chain fatty acid metabolism in mitochondria and in the prevention of cytosolic triglyceride storage. We also provide evidence that telmisartan improves palmitate oxidation in cells expressing the dominant-negative UCP3 mutant proteins V56M and Q252X. Further experiments are needed in order to test if telmisartan may be useful in subjects in whom fatty acid metabolism is severely impaired.

Our future aim is also to enlarge our cohort study and to investigate if the activity of mutant-negative UCP3 proteins is correlated with dietary fat intake and/or with the degree of daily physical activity.

Conflict of interest

The authors declare no conflict of interest.

Acknowledgements

We are indebted to Jean Ann Gilder for text editing. We also thank Dr Nicola Ferrara for kind suggestions. This work was supported by grants from Ministero Salute, Co-funding the Istituto di Ricovero e Cura a carattere scientifico, IRCCS, Fondazione SDN, Naples, Italy (RF2007-635809) and from CEINGE-Biotecnologie Avanzate s.ca.r.l., Naples, Italy.

References

1 Cannon B, Nedergaard J. Brown adipose tissue: function and physiological significance. *Physiol Rev* 2004; **84**: 277–359.
2 Nedergaard J, Golozoubova V, Matthias A, Asadi A, Jacobsson A, Cannon B. UCP1: the only protein able to mediate adaptive non-shivering thermogenesis and metabolic inefficiency. *Biochim Biophys Acta* 2001; **1504**: 82–106.
3 Solanes G, Vidal-Puig A, Grujic D, Flier JS, Lowell BB. The human uncoupling protein-3 gene. Genomic structure, chromosomal localization, and genetic basis for short and long form transcripts. *J Biol Chem* 1997; **272**: 25433–25436.
4 Vidal-Puig A, Solanes G, Grujic D, Flier JS, Lowell BB. UCP3: an uncoupling protein homologue expressed preferentially and abundantly in skeletal muscle and brown adipose tissue. *Biochem Biophys Res Commun* 1997; **235**: 79–82.
5 Hesselink MK, Keizer HA, Borghouts LB, Schaart G, Kornips CF, Slieker LJ *et al*. Protein expression of UCP3 differs between human type 1, type 2a, and type 2b fibers. *FASEB J* 2001; **15**: 1071–1073.
6 Weigle DS, Selfridge LE, Schwartz MW, Seeley RJ, Cummings DE, Havel PJ *et al*. Elevated free fatty acids induce uncoupling protein 3 expression in muscle: a potential explanation for the effect of fasting. *Diabetes* 1998; **47**: 298–302.
7 Tsuboyama-Kasaoka N, Tsunoda N, Maruyama K, Takahashi M, Kim H, Ikemoto S *et al*. Up-regulation of uncoupling protein 3 (UCP3) mRNA by exercise training and down-regulation of UCP3 by denervation in skeletal muscles. *Biochem Biophys Res Commun* 1998; **247**: 498–503.
8 Schrauwen P, Hesselink MK, Vaartjes I, Kornips E, Saris WH, Giacobino JP *et al*. Effect of acute exercise on uncoupling protein 3 is a fat metabolism-mediated effect. *Am J Physiol Endocrinol Metab* 2002; **282**: E11–E17.
9 Schrauwen P, Hoppeler H, Billeter R, Bakker AH, Pendergast DR. Fiber type dependent upregulation of human skeletal muscle UCP2 and UCP3 mRNA expression by high-fat diet. *Int J Obes Relat Metab Disord* 2001; **25**: 449–456.
10 Boss O, Samec S, Desplanches D, Mayet MH, Seydoux J, Muzzin P *et al*. Effect of endurance training on mRNA expression of uncoupling proteins 1, 2, and 3 in the rat. *FASEB J* 1998; **12**: 335–339.
11 Schrauwen P, Schaart G, Saris WH, Slieker LJ, Glatz JF, Vidal H *et al*. The effect of weight reduction on skeletal muscle UCP2 and UCP3 mRNA expression and UCP3 protein content in Type II diabetic subjects. *Diabetologia* 2000; **43**: 1408–1416.
12 Boss O, Muzzin P, Giacobino JP. The uncoupling proteins, a review. *Eur J Endocrinol* 1998; **139**: 1–9.
13 Sugimoto K, Qi NR, Kazdová L, Pravenec M, Ogihara T, Kurtz TW. Telmisartan but not valsartan increases caloric expenditure and protects against weight gain and hepatic steatosis. *Hypertension* 2006; **47**: 1003–1009.
14 Sugimoto K, Kazdová L, Qi NR, Hyakukoku M, Kren V, Simáková M *et al*. Telmisartan increases fatty acid oxidation in skeletal muscle through a peroxisome proliferator-activated receptor-gamma dependent pathway. *J Hypertens* 2008; **26**: 1209–1215.
15 Fortunato G, Fattoruso O, De Caterina M, Mancini A, Di Fiore R, Alfieri A *et al*. RAS and MTHFR gene polymorphisms in a healthy exercise-trained population: association with the MTHFR (TT) genotype and a lower hemoglobin level. *Int J Sports Med* 2007; **28**: 172–177.
16 Kuczmarski RJ, Ogden CL, Guo SS, Grummer-Strawn LM, Flegal KM, Mei Z *et al*. 2000 CDC Growth Charts for the United States: methods and development. *Vital Health Stat* 2002; **246**: 1–190.
17 National High Blood Pressure Education Program Working Group on Hypertension Control in Children Adolescents. Update on the 1987 Task Force Report on High Blood Pressure in Children and adolescents: the Third National Health and Nutrition Examination Survey. *Pediatrics* 1996; **98**: 649–658.
18 Matthews DR, Hosker JP, Rudenski AS, Naylor BA, Treacher DF, Turner RC. Homeostasis model assessment: insulin resistance and beta-cell function from fasting plasma glucose and insulin concentrations in man. *Diabetologia* 1985; **28**: 412–419.
19 Renold A, Koehler CM, Murphy MP. Mitochondrial import of the long and short isoforms of human uncoupling protein 3. *FEBS Lett* 2000; **465**: 135–140.
20 Felts SJ, Owen BA, Nguyen P, Trepel J, Donner DB, Toft DO. The hsp-90-related protein TRAP1 is a mitochondrial protein with distinct functional properties. *J Biol Chem* 2000; **275**: 3305–3312.
21 Kang BH, Plescia J, Dohi T, Rosa J, Doxsey SJ, Altieri DC. Regulation of tumor cell mitochondrial homeostasis by an organelle-specific Hsp90 chaperone network. *Cell* 2007; **131**: 257–270.
22 Narayan SB, Boriack RL, Messmer B, Bennett MJ. Establishing a reference interval for measurement of flux through the mitochondrial fatty acid oxidation pathway in cultured skin fibroblasts. *Clin Chem* 2005; **51**: 644–646.
23 Schrauwen P, Saris WH, Hesselink MK. An alternative function for human uncoupling protein 3: protection of mitochondria against accumulation of nonesterified fatty acids inside the mitochondrial matrix. *FASEB J* 2001; **15**: 2497–2502.
24 Himms-Hagen J, Harper ME. Physiological role of UCP3 may be export of fatty acids from mitochondria when fatty acid oxidation predominates: an hypothesis. *Exp Biol Med* 2001; **226**: 78–84.

25 Clapham JC, Arch JR, Chapman H, Haynes A, Lister C, Moore GB *et al*. Mice overexpressing human uncoupling protein-3 in skeletal muscle are hyperphagic and lean. *Nature* 2000; **406**: 415–418.
26 Costford SR, Chaudhry SN, Salkhordeh M, Harper M. Effects of the presence, absence, and overexpression of uncoupling protein-3 on adiposity and fuel metabolism in congenic mice. *Am J Physiol Endocrinol Metab* 2006; **290**: E1304–E1312.
27 Son C, Hosoda K, Ishihara K, Bevilacqua L, Masuzaki H, Fushiki T *et al*. Reduction of diet-induced obesity in transgenic mice overexpressing uncoupling protein 3 in skeletal muscle. *Diabetologia* 2004; **47**: 47–54.
28 Bezaire V, Spriet LL, Campbell S, Sabet N, Gerrits M, Bonen A *et al*. Constitutive UCP3 overexpression at physiological levels increases mouse skeletal muscle capacity for fatty acid transport and oxidation. *FASEB J* 2005; **19**: 977–979.
29 Mingrone G, Rosa G, Greco AV, Manco M, Vega N, Hesselink MK *et al*. Decreased uncoupling protein expression and intramyocytic triglyceride depletion in formerly obese subjects. *Obes Res* 2003; **11**: 632–640.
30 Ravussin E, Lillioja S, Knowler WC, Christin L, Freymond D, Abbott WG *et al*. Reduced rate of energy expenditure as a risk factor for body-weight gain. *N Engl J Med* 1988; **318**: 467–472.
31 Fleury C, Neverova M, Collins S, Raimbault S, Champigny O, Levi-Meyrueis C *et al*. Uncoupling protein-2: a novel gene linked to obesity and hyperinsulinemia. *Nat Genet* 1997; **15**: 223–224.
32 Argyropoulos G, Brown AM, Willi SM, Zhu J, He Y, Reitman M *et al*. Effects of mutations in the human uncoupling protein 3 gene on the respiratory quotient and fat oxidation in severe obesity and type 2 diabetes. *J Clin Invest* 1998; **102**: 1345–1351.
33 Urhammer SA, Dalgaard LT, Sørensen TI, Tybjaerg-Hansen A, Echwaldm SM, Andersen T *et al*. Organisation of the coding exons and mutational screening of the uncoupling protein 3 gene in subjects with juvenile-onset obesity. *Diabetologia* 1998; **41**: 241–244.
34 Brown AM, Willi SM, Argyropoulos G, Garvey WT. A novel missense mutation, R70W, in the human uncoupling protein 3 gene in a family with type 2 diabetes. *Hum Mutat* 1999; **13**: 508.
35 Schrauwen P, Xia J, Walder K, Snitker S, Ravussin E. A novel polymorphism in the proximal UCP3 promoter region: effect on skeletal muscle UCP3 mRNA expression and obesity in male non-diabetic Pima Indians. *Int J Obes Relat Metab Disord* 1999; **23**: 1242–1245.
36 Otabe S, Clement K, Dubois S, Lepretre F, Pelloux V, Leibel R *et al*. Mutation screening and association studies of the human uncoupling protein 3 gene in normoglycemic and diabetic morbidly obese patients. *Diabetes* 1999; **48**: 206–208.
37 Cassell PG, Saker PJ, Huxtable SJ, Kousta E, Jackson AE, Hattersley AT *et al*. Evidence that single nucleotide polymorphism in the uncoupling protein 3 (UCP3) gene influences fat distribution in women of European and Asian origin. *Diabetologia* 2000; **43**: 1558–1564.
38 Herrmann SM, Wang JG, Staessen JA, Kertmen E, Schmidt-Petersen K, Zidek W *et al*. Uncoupling protein 1 and 3 polymorphisms are associated with waist-to-hip ratio. *J Mol Med* 2003; **81**: 327–332.
39 Halsall DJ, Luan J, Saker P, Huxtable S, Farooqi IS, Keogh J *et al*. Uncoupling protein 3 genetic variants in human obesity: the c-55t promoter polymorphism is negatively correlated with body mass index in a UK Caucasian population. *Int J Obes Relat Metab Disord* 2001; **25**: 472–477.
40 Liu YJ, Liu PY, Long J, Lu Y, Elze L, Recker RR *et al*. Linkage and association analyses of the UCP3 gene with obesity phenotypes in Caucasian families. *Physiol Genomics* 2005; **22**: 197–203.
41 Alonso A, Marti A, Corbalan MS, Martinez-Gonzalez MA, Forga L, Martinez JA. Association of UCP3 gene −55C/T polymorphism and obesity in a Spanish population. *Ann Nutr Metab* 2005; **49**: 183–188.
42 Dalgaard LT, Hansen T, Urhammer SA, Drivsholm T, Borch-Johnsen K, Pedersen O. The uncoupling protein 3−55 C/T variant is not associated with type II diabetes mellitus in Danish subjects. *Diabetologia* 2001; **44**: 1065–1067.
43 Berentzen T, Dalgaard LT, Petersen L, Pedersen O, Sorensen TI. Interactions between physical activity and variants of the genes encoding uncoupling proteins -2 and -3 in relation to body weight changes during a 10-y follow-up. *Int J Obes* 2005; **29**: 93–99.
44 Vincent AM, Olzmann JA, Brownlee M, Sivitz WI, Russell JW. Uncoupling proteins prevent glucose-induced neuronal oxidative stress and programmed cell death. *Diabetes* 2004; **53**: 726–734.
45 Patti ME, Butte AJ, Crunkhorn S, Cusi K, Berria R, Kashyap S *et al*. Coordinated reduction of genes of oxidative metabolism in humans with insulin resistance and diabetes: potential role of PGC1 and NRF1. *Proc Natl Acad Sci USA* 2003; **100**: 8466–8471.
46 Pershadsingh HA. Treating the metabolic syndrome using angiotensin receptor antagonists that selectively modulate peroxisome proliferator-activated receptor-gamma. *Int J Biochem Cell Biol* 2006; **38**: 766–781.
47 Schupp M, Janke J, Clasen R, Unger T, Kintscher U. Angiotensin type 1 receptor blockers induce peroxisome proliferator-activated receptor-gamma activity. *Circulation* 2004; **109**: 2054–2057.
48 Benson SC, Pershadsingh HA, Ho CI, Chittiboyina A, Desa P, Pravenec M *et al*. Identification of telmisartan as a unique angiotensin II receptor antagonist with selective PPAR-modulating activity. *Hypertension* 2004; **43**: 993–1002.
49 Fujimoto M, Masuzaki H, Tanaka T, Yasue S, Tomita T, Okazawa K *et al*. An angiotensin II AT1 receptor antagonist, telmisartan augments glucose uptake and GLUT4 protein expression in 3T3-L1 adipocytes. *FEBS Lett* 2004; **576**: 492–497.
50 Derosa G, Ragonesi PD, Mugellini A, Ciccarelli L, Fogari R. Effects of telmisartan compared with eprosartan on blood pressure control, glucose metabolism and lipid profile in hypertensive, type 2 diabetic patients: a randomized, double-blind, placebo-controlled 12-month study. *Hypertens Res* 2004; **27**: 457–464.
51 Honjo S, Nichi Y, Wada Y, Hamamoto Y, Koshiyama H. Possible beneficial effect of telmisartan on glycemic control in diabetic subjects. *Diabetes Care* 2005; **28**: 498.
52 Miura Y, Yamamoto N, Tsunekawa S, Taguchi S, Eguch Y, Ozaki N *et al*. Replacement of valsartan and candesartan by telmisartan in hypertensive patients with type 2 diabetes: metabolic and antiatherogenic consequences. *Diabetes Care* 2005; **28**: 757–758.

J. Endocrinol. Invest. 35: 2-4, 2012

RAPID COMMUNICATION

The absence of polymorphisms in ADRB3, UCP1, PPARγ, and ADIPOQ genes protects morbid obese patients toward insulin resistance

R. Bracale[1], G. Labruna[2,3], C. Finelli[4], A. Daniele[5], L. Sacchetti[2,3], G. Oriani[1,2], F. Contaldo[4], and F. Pasanisi[4]

[1]Dipartimento di Scienze per la Salute, Università del Molise, Campobasso; [2]CEINGE Biotecnologie Avanzate S.C. a R.L.; [3]Dipartimento di Biochimica e Biotecnologie Mediche; [4]Centro Interuniversitario di Studi e Ricerche sull'Obesità e Dipartimento di Medicina Clinica e Sperimentale, Università degli Studi di Napoli Federico II, Napoli; [5]Dipartimento di Scienze Ambientali, Seconda Università di Napoli, Caserta, Italy

ABSTRACT. ***Background and aims:*** **The insulin resistance (IR) is a major metabolic impairment in severe obesity, a multifactorial disease in which the importance of the effect of single nucleotide polymorphisms (SNP) associations in different rather than individual genes was established. The aim of this study was to test the predictive value of presence/absence of polymorphisms/variants in β3-adrenergic receptor (ADRB3), uncoupling protein 1 (UCP1), peroxisome proliferator-activated receptor γ (PPARγ), and adiponectin (ADIPOQ) genes in diagnosing the IR in obesity.** ***Subjects and methods:*** **We studied 112 (40 males, 72 females) severely obese (body mass index: 48.5±7.5 kg/m²) subjects recruited from the outpatient obesity clinic of Federico II University Hospital in Naples. Genomic DNA was extracted from peripheral leukocytes with a commercial kit. The gene polymorphisms Trp64Arg in ADRB3, -3826 A>G in UCP1, Pro12Ala in PPARγ, and c.268G>A, c.331T>C, and c.334C>T in ADIPOQ were characterized by TaqMan assay or by direct sequencing (ADIPOQ).** ***Results and conclusion:*** **Our results demonstrate that -3826A>G UCP1 polymorphism is associated with IR in morbid obesity. Further, the lack of any polymorphisms, Trp64Arg in ADRB3 and/or -3826 A>G in UCP1 and/or Pro12Ala in PPARγ and/or c.268G>A, c.331T>C and c.334C>T in ADIPOQ, appears a useful prognostic factor (NPV=100%) toward the IR onset in these obese patients representing a further parameter for an earlier and appropriate therapy.**

(J. Endocrinol. Invest. 35: 2-4, 2012)

INTRODUCTION

During the last decades, an alarming increase in the prevalence of obesity ("globesity") has been observed worldwide among both children and adults (1). Obesity is associated with increased risk for several morbidities including diabetes mellitus, dyslipidemia, cardiovascular diseases, and some cancers (2). Weight gain due to increased fat mass is the consequence of a long-standing imbalance between energy intake and energy expenditure, influenced by multiple and complex interactions between genes and environment (3). High-calorie diet and sedentary lifestyle are considered to be the main environmental factors leading to weight gain (1). On the other hand, genetic factors affecting appetite, energy expenditure, and adipocyte metabolism may predispose individuals to develop obesity (4). Epigenetic interactions have also been described as predisposing factors for abdominal obesity and related diseases (5). Among the most common obesity-related complications, the metabolic syndrome (MS) has a high prevalence in severe obesity representing a cluster of metabolic alterations, such as altered levels of adipokines, hyperglycemia, dyslipidemia and/or hypertension (6, 7).

Some genes directly interact with glucose and lipid metabolism and can therefore determine a greater prevalence of metabolic alterations (8). Polymorphisms/variants in genes encoding molecules known to be involved in energy expenditure, fat metabolism, and insulin sensitivity such as β3-adrenergic receptor (ADRB3) and uncoupling protein 1 (UCP1) or other genes related to adipocytes differentiation and anti-inflammatory mechanisms, like peroxisome proliferator-activated receptor γ (PPARγ), and adiponectin (ADIPOQ), have been extensively studied (4, 8).

Single nucleotide polymorphisms (SNP) in the abovementioned genes have been reported in healthy and unhealthy subjects (4, 9, 10). Particularly, our group showed the Trp64Arg ADRB3 polymorphism to be related to insulin resistance (IR) in severe obesity (11), whereas UCP1 -3826 A>G polymorphism and several SNP in ADIPOQ predisposed to MS (12, 13).

Since the importance of the SNP associations in different genes related to complex diseases, rather than individual genes, in this study, our aim was to evaluate the global influence of polymorphisms Trp64Arg in ADRB3 gene, Pro12Ala in PPARγ gene, -3826 A>G in UCP1 gene, and 3 SNP previously described in association with IR (c.268G>A,

Key-words: ADIPOQ, ADRB3, insulin resistance, PPARγ, severe obesity, UCP1.

Correspondence: G. Labruna, Dipartimento di Biochimica e Biotecnologie Mediche, Università degli Studi di Napoli Federico II, Via Pansini 5, 80131 Napoli, Italy.

E-mail: labruna@dbbm.unina.it

Accepted December 14, 2011.

c.331T>C and c.334C>T) in ADIPOQ gene, on the IR in a morbid obese population from Southern Italy.

SUBJECTS AND METHODS

Subjects

The study population consisted of 112 (40 males, 72 females) severely obese non-diabetic subjects recruited from the outpatient obesity clinic of the Department of Medicine, Federico II University Hospital in Naples. All subjects had normal liver, kidney and thyroid function, and none had a history of excessive alcohol intake. None was taking anti-hypertensive drugs or substances known to affect resting metabolic rate, or glucose or lipid metabolism.

Anthropometric and metabolic measurements

Weight and height were measured in standardized conditions and the body mass index (BMI) was calculated. Systolic and diastolic blood pressures were measured after the subject had rested for 5 min in a sitting position. After a 10-h overnight fast, blood was collected and centrifuged. Plasma glucose was measured by the hexokinase method adapted for an autoanalyzer. Total cholesterol, triglycerides, and HDL cholesterol were determined by standard enzymatic methods. MS was diagnosed considering the combination of 3 out of 5 risk factors according to American Heart Association (AHA) criteria (6). Serum insulin was measured by the chemiluminescence method (Immulight 2000; Italy). IR was estimated according to the homeostasis model assessment (HOMA-IR) method from fasting glucose and insulin concentrations, according to the formula: insulin (mU/ml) × glucose (mmol/l)/22.5. We used to classify as IR the threshold of 4.65, previously indicated for obese subjects (14).

Genotyping

Genomic DNA was extracted from peripheral leukocytes with a widely used procedure (Nucleon BAAC-2, Amersham, UK).

We identified Trp64Arg for ADRB3, -3826 A>G for UCP1 and various SNP (mutations) for ADIPOQ, respectively as described elsewhere (11-13).

The PPARγ Pro12Ala polymorphism was identified by the real-time TaqMan method (Applied Biosystems, USA) and two fluorescent probes. We used the Primer Express program to design the PCR primers forward 5'-TGACTCATGGGTGTATTCACAA-3', reverse 5'-CAAACACAACCTGGAAGACAAA-3'; MGB TaqMan probes VIC-TCCTATTGACCCAGAAAGCGA-Q-MGB and FAM-TCCTATTGACGCAGAAAGCGA-Q-MGB where MGB is the minor groove binder, a molecule that stabilizes the duplex DNA probe thereby increasing the ability of the hybridization probe to discriminate the single-nucleotide polymorphism. The protocol was the same as previously described (11).

Statistics

Allele frequencies were calculated by allele counting and the departure from Hardy-Weinberg expectation was evaluated by the χ^2 test using the Haploview 3.2 software with default p value cut-off (15). The χ^2 test was also used to test any difference in allele SNP frequency between obese patients and controls. Multiple comparisons were corrected by using the Bonferroni test. Binomial logistic regression analysis was used to investigate the association between the genetic and clinical characteristics and the presence of IR. To explore the possibility of missing a potential association due to the loss of information introduced by the binary categorization of the HOMA in the logistic analysis (HOMA > or <4.65), a multiple linear regression analysis was performed using the continuous HOMA as dependent variable for the same set of independent variables used in the logistic. Both forward and backward procedures were used for model selection and gave concordant results. Differences were considered statistically significant with a *p*-value <0.05. Statistical analyses were carried out with the PASW package for Windows (Ver.18; SPSS Inc. Headquarters, Chicago, Ill).

RESULTS AND CONCLUSION

The mean age of obese patients in the study was 32.7±10.5 yr and mean BMI was 48.5±7.5 kg/m^2. According to the used threshold of HOMA=4.65, 50/112 (45%) of obese subjects were IR (+). Table 1 reports the frequen-

Table 1 - *Genotype frequencies of the studied polymorphisms according to the presence/absence of insulin resistance in 112 severe obese patients.*

Gene	Genotype	Total obese population no. (%)	Insulin resistance		χ^2 test *p*
			IR (-) no. (%)	IR (+) no. (%)	
ADRB3	WT	102 (91.1)	57 (50.9)	45 (40.1)	ns[b]
	Pol[a] - Trp64Arg	10 (8.9)	5 (4.5)	5 (4.5)	
UCP1	WT	29 (25.9)	23 (20.5)	6 (5.4)	0.003
	Pol[a] - -3826 A>G	83 (74.1)	39 (34.8)	44 (39.3)	
PPARγ	WT	86 (76.8)	47 (42.0)	39 (34.8)	ns[b]
	Pol[a] - Pro12Ala	26 (23.2)	15 (13.4)	11 (9.8)	
ADIPOQ	WT	105 (93.8)	58 (51.8)	47 (42.0)	ns[b]
	Pol[a] - c.268G>A, c.331T>C, and c.334C>T	7 (6.3)	4 (3.6)	3 (2.6)	
4 genes[c]	WT	11 (9.8)	11 (9.8)	0 (0)	0.001
	Pol[a]	101 (90.2)	51 (45.5)	50 (44.7)	

[a]Polymorphic (heterozygous + homozygous) genotype; [b]not statistically significant difference of genotypes distribution between insulin resistance yes/no; [c]subjects were considered polymorphic if bearing at least 1 studied single nucleotide polymorphism in the investigated genes.

Table 2 - *Results of multiple linear regression analysis with homeostasis model assessment index as dependent variable.*

Models	p	R^2	Partial R^2	B coefficient	95% CI
1[a]	<0.0001	0.121	0.121	2.3	1.2-3.5
2[b]	0.007	0.169	0.048	1.8	0.5-3.1
3[c]	0.015	0.201	0.032	2.0	0.8-3.9

Predictors: [a]male sex; [b]male sex + UCP1 polymorphism; [c]male sex + UCP1 polymorphism + ADRB3 polymorphism. CI: confidence interval.

cies of the genotypes observed, at level of the investigated genes, in the total obese population and in the two groups IR (+) and IR (-) obese patients. The -3826A>G UCP1 polymorphic genotypes were more present among the IR (+) (88%) than in IR (-) (63%) obese patients [p=0.003; odds ratio (OR): 4.3, 95% confidence Interval (CI): 1.6-11.7]. All IR (+) obese patients were polymorphic in one or more genes (p=0.001) (Table 1); in addition, the absence of any assessed polymorphism had an high negative predictive value (NPV=100%) for IR.

The binomial logistic regression analysis [dependent variable: IR (+)/IR (-); independent variables: presence/absence of polymorphisms in the studied genes, biochemical variables (triglycerides, total and HDL cholesterol, aspartate aminotransferase, alanine aminotransferase, and γ-glutamyl transferase)], showed, after correction for confounding variables (BMI, age, sex), a significant positive association between the IR (+) with male sex (p<0.0001; OR/95% CI: 10.3/3.0-35.2), UCP1 polymorphic genotype (p=0.001; OR/95% CI: 17.8/3.4-92.7) and triglycerides (p=0.004; OR/95% CI 1.01/1.00-1.02). By multiple linear regression analysis, the final model resulted in the addition of ADRB3 polymorphism to male sex and UCP1 as further significant factor, being the overall adjusted R square equal to 0.201 (p=0.015) (Table 2).

The studies on obesity and its association with metabolic alterations are complicated by the highly heterogeneous genetic basis; in fact, several genes are involved and contribute to the pathogenesis of this complex disease, but while each single gene has only a small effect, a combined effect of all genes results in pathologic phenotypes.

In conclusion, our results demonstrate that -3826A>G UCP1 polymorphism, that we previously demonstrated to be associated with MS (12), is also associated with IR (+) in morbid obesity. Further, the lack of polymorphisms at level of the Trp64Arg in ADRB3 and/or the -3826 A>G in UCP1 and/or the Pro12Ala in PPARγ and/or the c.268G>A, c.331T>C and c.334C>T in ADIPOQ, appears an useful prognostic factor (NPV=100%) toward the IR onset in these obese patients. Hence, our findings could suggest additional criteria to characterize the clinical background in morbid obesity in order to design targeted therapies based on specific metabolic alterations of the single subjects. This preliminary observation requires further investigation in larger population studies.

ACKNOWLEDGMENTS

Research supported by grants from CEINGE-Regione Campania DGRC 1901/2009 and MIUR PRIN 2008 E61J10000020001.

REFERENCES

1. Azagury DE, Lautz DB. Obesity overview: epidemiology, health and financial impact, and guidelines for qualification for surgical therapy. Gastrointest Endosc Clin N Am 2011, 21: 189-201.
2. Kopelman PG. Obesity as a medical problem. Nature 2000, 404: 635-43.
3. Bouchard C. Gene-environment interactions in the etiology of obesity: defining the fundamentals. Obesity (Silver Spring) 2008, 16 (Suppl 3): S5-10.
4. Walley AJ, Asher JE, Froguel P. The genetic contribution to non-syndromic human obesity. Nat Rev Genet 2009, 10: 431-42.
5. Martinelli R, Nardelli C, Pilone V, et al. miR-519d overexpression is associated with human obesity. Obesity (Silver Spring) 2010, 18: 2170-6.
6. Grundy SM, Cleeman JI, Daniels SR, et al; American Heart Association; National Heart, Lung, and Blood Institute. Diagnosis and management of the metabolic syndrome: an American heart association/national heart, lung, and blood institute scientific statement. Circulation 2005, 25: 2735-52.
7. Labruna G, Pasanisi F, Nardelli C, et al. High leptin/adiponectin ratio and serum triglycerides are associated with an "at-risk" phenotype in young severely obese patients. Obesity (Silver Spring) 2011, 19: 1492-6.
8. Ramachandrappa S, Farooqi IS. Genetic approaches to understanding human obesity. J Clin Invest 2011, 121: 2080-6.
9. Macias-Gonzalez M, Moreno-Santos I, García-Almeida JM, Tinahones FJ, Garcia-Fuentes E. PPARgamma2 protects against obesity by means of a mechanism that mediates insulin resistance. Eur J Clin Invest 2009, 39: 972-9.
10. Bell CG, Walley AJ, Froguel P. The genetics of human obesity. Nat Rev Genet 2005, 6: 221-34.
11. Bracale R, Pasanisi F, Labruna G, et al. Metabolic syndrome and ADRB3 gene polymorphism in severely obese patients from South Italy. Eur J Clin Nutr 2007, 61: 1213-9.
12. Labruna G, Pasanisi F, Nardelli C, et al. UCP1 -3826 AG+GG genotypes, adiponectin, and leptin/adiponectin ratio in severe obesity. J Endocrinol Invest 2009, 32: 525-9.
13. Daniele A, Cammarata R, Pasanisi F, et al. Molecular analysis of the adiponectin gene in severely obese patients from Southern Italy. Ann Nutr Metab 2008, 53: 155-61.
14. Stern SE, Williams K, Ferrannini E, DeFronzo RA, Bogardus C, Stern MP. Identification of individuals with insulin resistance using routine clinical measurements. Diabetes 2005, 54: 333-9.
15. Gabriel SB, Schaffner SF, Nguyen H, et al. The structure of haplotype blocks in the human genome. Science 2002, 296: 2225-9.

High Aminopeptidase N/CD13 Levels Characterize Human Amniotic Mesenchymal Stem Cells and Drive Their Increased Adipogenic Potential in Obese Women

Running Title

Increased expression of CD13 in obese hA-MSCs

Laura Iaffaldano,[1,2*] Carmela Nardelli,[1,2*] Maddalena Raia,[1] Elisabetta Mariotti,[1] Maddalena Ferrigno,[1] Filomena Quaglia,[3] Giuseppe Labruna,[4] Valentina Capobianco,[1,2] Angela Capone,[3] Giuseppe Maria Maruotti,[3] Lucio Pastore,[1,2] Rosa Di Noto,[1,2] Pasquale Martinelli,[3] Lucia Sacchetti,[1,2†] Luigi Del Vecchio.[1,2]

[1]CEINGE-Biotecnologie Avanzate S.C.a R.L., Naples, Italy.

[2]Dipartimento di Medicina Molecolare e Biotecnologie Mediche, Università degli Studi di Napoli Federico II, Naples, Italy.

[3]Dipartimento di Neuroscienze e Scienze Riproduttive ed Odontostomatologiche, Naples, Italy.

[4]Fondazione IRCCS SDN–Istituto di Ricerca Diagnostica e Nucleare, Naples, Italy.

*****These two authors contributed equally to this work.

[†]**Corresponding author:** Lucia Sacchetti, CEINGE-Biotecnologie Avanzate S.C.a R.L.

Via G. Salvatore 486 - 80145 Naples, Italy.

Fax 0039-081-7462404

Tel. 0039-081-7463541

e-mail: sacchett@unina.it

Abstract

Maternal obesity is associated to increased fetal risk of obesity and other metabolic diseases. Human amniotic mesenchymal stem cells (hA-MSC) have not been characterized in obese women. The aim of this study was to isolate and compare hA-MSC immunophenotypes from obese (Ob-) and normal weight control (Co-) women to identify alterations possibly predisposing the fetus to obesity. We enrolled 16 Ob- and 7 Co-women at delivery (mean/SEM pre-pregnancy BMI: 40.3/1.8 kg/m^2 and 22.4/1.0 kg/m^2, respectively) and 32 not pregnant women. hA-MSCs were phenotyped by flow cytometry; several maternal and newborn clinical and biochemical parameters were also measured. The expression of membrane antigen CD13 was higher on Ob-hA-MSCs than on Co-hA-MSCs (P=0.0043). Also serum levels of CD13 at delivery were higher in Ob- versus Co-pregnant women and correlated with CD13 antigen expression on Ob-hA-MSCs (r^2=0.84, P<0.0001). Adipogenesis induction experiments revealed that Ob-hA-MSCs had a higher adipogenic potential than Co-hA-MSCs as witnessed by higher PPARγ and aP2 mRNA levels (P=0.02 and P=0.03, respectively) at post-induction day 14 associated with increased CD13 mRNA levels from baseline to day 4 post-induction (P<0.05). Adipogenesis was similar in the two sets of hA-MSCs after CD13 silencing, whereas it was increased in Co-hA-MSCs after CD13 overexpression. CD13 expression was high also in Ob-h-MSCs from umbilical cords or visceral adipose tissue of not pregnant women. In conclusion, antigen CD13, by influencing the adipogenic potential of hA-MSCs could be an *in-utero* risk factor for obesity. Our data strengthen the hypothesis that high levels of serum and MSC CD13 are obesity markers.

Introduction

The increase in the incidence of obesity in pregnant women in the last two decades has paralleled that observed in the general population [1-3]. Although maternal fat stores increase in all pregnant women, irrespective of pre-pregnancy weight [4], the storage capacity of subcutaneous adipose tissue (SAT) is impaired, and fat predominantly accumulates in visceral adipose tissue (VAT) [5]. VAT is an important risk factor for metabolic imbalance in human subjects, also during pregnancy [6-8]. In fact, maternal obesity is related to offspring obesity [9], and there is an increased risk of adverse outcomes for both mother and child [10-13]. Moreover, the risk of childhood obesity was quadrupled if the mother was obese before pregnancy [14], which suggests that the *in utero* environment is obesogenic. In mammals, the placenta is the main interface between fetus and mother; it regulates intrauterine development and modulates adaptive responses to suboptimal *in utero* conditions [15,16].

Placenta is also an important source of stem/progenitor cells [17-19]. In particular, human amniotic mesenchymal stem cells (hA-MSCs) have been shown to differentiate into cell types of mesenchymal origin such as chondrocytes, adipocytes and osteocytes [20-22]. The phenotype of hA-MSCs from normal pregnant women has been characterized and found to differ in terms of cytokine expression from that of pregnant women affected by preeclampsia [23]. Thus far, little is known about hA-MSCs from obese women.

The aim of this study was to characterize hA-MSCs from term placenta of obese (Ob-) women and to test their adipogenic potential with respect to that of normal weight control (Co-) women. We also measured several maternal and newborn clinical and biochemical parameters, and looked for correlations between these parameters with the hA-MSC immunophenotype. We found that the Ob-hA-MSC immunophenotype was characterized by increased expression levels of the CD13 surface antigen that correlated with maternal CD13 serum levels. Adipogenesis was higher in Ob-hA-MSCs than in Co-hA-MSCs, and returned to the control value after CD13 silencing. On the other hand, CD13

overexpression increased the adipogenic potential of Co-hA-MSCs. Our findings suggest that CD13 could contribute to obesity programming in the fetus and indicates that maternal serum CD13 is an obesity risk marker.

Materials and methods

Patients and controls

Sixteen Ob- (age range: 26–39 years) and seven Co-pregnant women, (age range: 26–38 years), pre-pregnancy BMI (mean/SEM) 40.3/1.8 kg/m^2 and 22.4/1.0 kg/m^2, respectively and thirty-two not pregnant women (16 obese and 16 normal weight, BMI >30 kg/m^2 and <25 kg/m^2, respectively) were recruited at the Dipartimento di Neuroscienze e Scienze Riproduttive ed Odontostomatologiche, University of Naples "Federico II". The clinical, personal and family history of the 23 women was recorded during a medical interview conducted by an expert upon hospitalization. Data relative to each pregnancy follow-up and delivery were also recorded. The general characteristics of the newborn and clinical data (birth weight, length, head circumference, Apgar score) were recorded at birth.

Sample collection

Two fasting peripheral blood samples were collected in the morning from not pregnant women and from Ob- and Co-pregnant women, immediately before delivery. One sample was used for DNA extraction, whereas the other was centrifuged at 2,500 rpm for 15 min and serum was stored at -80°C until further processing. At delivery, placentas were collected by C-section from each enrolled women and immediately processed. Bioptic samples of visceral adipose tissue (VAT) were also collected from not pregnant obese and control women during obstetric surgery (ovarian cysts). All patients and controls gave their informed consent to the study and both parents gave consent for their newborns.

The study was performed according to the Helsinki II Declaration and was approved by the Ethics Committee of our Faculty.

Biochemical evaluations

The main serum biochemical parameters were evaluated by routine assays. Leptin and adiponectin were measured in maternal serum with Luminex xMAP Technology on a BioRad Multiplex Suspension Array System (Bio-Rad, Hemel Hempstead, Herts., UK), according to the manufacturer's instructions. The ratio leptin/adiponectin (L/A) was also calculated.

Aminopeptidase N/CD13 ELISA assay

Aminopeptidase N (APN)/CD13 serum levels were measured by ELISA (Life Science, Houston). Briefly, the microtiter plate was pre-coated with a specific anti-CD13 antibody. Standards or samples were then added to the appropriate microtiter plate wells with a biotin-conjugated polyclonal antibody preparation specific for CD13. Next, avidin conjugated to horseradish peroxidase was added to each microplate well and incubated for 15 min at room temperature. A TMB substrate solution (3,3′,5,5′-tetramethylbenzidine) was then added to each well. The enzyme-substrate reaction was terminated by the addition of a sulphuric acid solution and the color change was measured spectrophotometrically at a wavelength of 450 nm. The amount of CD13 in each sample was determined by comparing the absorbance of the sample to a standard curve.

Cell isolation from placenta tissue

Placentas were collected and immediately processed, according to Parolini et al. [24]. After removal of the maternal decidua, the amnion was manually separated from the chorion and extensively washed 5 times in 40 mL of phosphate-buffered saline (PBS) containing 100 U/mL penicillin, 100 µg/mL

streptomycin and 250 µg/mL amphotericin B (all from Sigma-Aldrich, Missouri) after which it was mechanically minced into small pieces [24]. Amnion fragments were digested overnight at 4°C in ACCUMAX® reagent (Innovative Cell Technology, San Diego), a combination of DNase, protease and collagenolytic enzymes [25], containing 100 U/mL penicillin, 100 µg/mL streptomycin and 250 µg/mL amphotericin B. The next day, digestion enzymes were inactivated with complete culture medium constituted by low glucose D-MEM (Sigma-Aldrich) supplemented with 10% of heat-inactivated bovine serum (FBS), 1% of non-essential amino acids and 2% of Ultraglutamine (all from Lonza, Basel, Switzerland). After centrifugation at 300g for 10 min, cell pellets and digested tissue fragments were seeded in a cell culture dish (BD Falcon, New York) in complete culture medium and incubated at 37°C in 5% CO_2. One week later, digested tissue pieces were removed from the dish and discarded, and isolated cells formed distinct fibroblast colony-forming units. When the colonies reached 70% confluence, they were washed with PBS and detached with trypsin/EDTA (Sigma-Aldrich), counted and reseeded in complete medium for expansion at a concentration of about 5,000/cm^2 [24].

Cell preparation

hA-MSCs were expanded for several passages. Absence of mycoplasma contamination was assessed as described previously [26]. The population-doubling level was calculated for each subcultivation with the following equation: population doubling= $[\log_{10}(N_H) - \log_{10}(N_I)]/\log_{10}(2)$, where N_I is the cell inoculum number and N_H is cell harvest number [27]. The increase in population doubling was added to the population doubling levels of the previous passages to yield the cumulative population doubling level. When 70%-80% confluent cultures reached about 4 population doublings they were detached with trypsin/EDTA, resuspended in PBS with 10% FBS, and processed for flow cytometry, DNA and RNA extraction. Cellular viability was assessed by both Trypan blue dye exclusion and the analysis of light scatter proprieties in flow cytometry, and it was never lower than 90%.

Using the above cell isolation and preparation procedures, h-MSCs were also isolated from umbilical cord (hUC-MSCs) of one obese and one control pregnant woman.

Isolation of visceral adipose tissue mesenchymal stem cells (hVAT-MSCs)

Briefly, VAT bioptic samples were washed with phosphate buffered saline (PBS) containing 100 U/mL penicillin, 100 µg/mL streptomycin and 250 µg/mL amphotericin B (all from Sigma-Aldrich), minced into small pieces and digested with 1.5 mg/ml collagenase type I (GIBCO, USA) at 37C°. The digestion enzymes were inactivated with FBS. After centrifugation at 1500*g* for 5 min, cell pellets and digested tissue fragments were washed and seeded in a cell culture dish (BD Falcon, New York) in complete culture medium and incubated at 37°C in 5% CO_2. When the colonies reached 60-70% confluence, they were washed with PBS and detached with trypsin/EDTA (Sigma-Aldrich), counted and reseeded in complete medium for expansion at a concentration of about 5,000/cm^2 [28].

DNA typing

The fetal origin of both amnion and hA-MSCs was verified by DNA typing. Genomic DNA was extracted from the mother's peripheral blood, from amnion samples and from hA-MSCs using the Nucleon BACC2 extraction kit (Illustra DNA Extraction Kit BACC2, GE Healthcare, Calfont St. Giles, Bucks., UK). DNA concentration was evaluated using the NanoDrop® ND-1000 UV-Vis spectrophotometer (NanoDrop Technologies, Wilmington, DE). Genomic DNA (1 ng) was amplified in a final volume of 25 µL using the AmpFlSTR® Identifiler™ PCR Amplification Kit (Applied Biosystems, Foster City). The AmpFlSTR® Identifiler™ PCR Amplification Kit is a short tandem repeat (STR) multiplex assay that amplifies 15 repeat loci and the Amelogenin gender determining marker in a single PCR amplification using a primer set labeled with four fluorescent molecules. The amplification was performed with the GeneAmp PCR System 9700 (Applied Biosystems) instrument.

PCR products were then analyzed by capillary electrophoresis on the ABI Prism 3130 Genetic Analyzer (Applied Biosystems) together with an allelic ladder that contained all the most common alleles for the analyzed loci that were present in Caucasian populations and both a negative- and a positive-quality control sample. Typically, 1μL of each sample was diluted in 18.7μL of deionized formamide; each sample was supplemented with 0.3μL of an internal size standard (LIZ 500 Applied Biosystems) labeled with an additional fluorophore. The samples were denatured at 95 °C for 4 min and then placed in the auto sampler tray (maximum of 96 samples) on the ABI Prism 3130 for automatic injection in the capillaries. The data were analyzed by Gene Mapper Software (Applied Biosystems).

Immunophenotyping of h-MSCs by flow cytometry

We analyzed the expression of 38 hematopoietic, mesenchymal, endothelial, epithelial and no-lineage membrane antigens on the surface of hA-MSCs, hUC-MSCs and hVAT-MSCs by four-color flow cytometry (Table 1). The antibody cocktails contained in each tube are detailed in Supplementary Table 1. All monoclonal antibodies (MoAbs) were from Becton Dickinson (San Jose) except anti-CD338-APC, which was from R&D (Minneapolis), anti-CD-133-PE and anti-CD271-APC MoAbs, which were from Milenyi Biotec (Bergisch Gladbach, Germany). For all antibody staining experiments, at least $1x10^5$ hA-MSCs isolated from each placenta sample were incubated at 4°C for 20 min with the appropriate amount of MoAbs, washed twice with PBS and finally analyzed with an unmodified Becton-Dickinson FACSCanto II flow cytometer (Becton-Dickinson, San Jose), that was set up according to published guidelines [29]. For each sample the respective control was prepared in order to determine the level of background cellular autofluorescence without antibody staining.

CaliBRITE beads (Becton-Dickinson, catalog no. 340486) were used as quality controls across the study as described elsewhere [30, 31], according to the manufacturer's instructions. Daily control of

CaliBRITE intensity showed no change in instrument sensitivity throughout the study. The relative voltage range for each detector was assessed *una tantum* using the "eight-peak" technology (Rainbow Calibration Particles, Becton-Dickinson, catalog no. 559123) at the beginning of the study.

Compensation was set in the FACS-DiVa (Becton-Dickinson) software, and compensated samples were analyzed. Samples were acquired immediately after staining using the FACSCanto II instrument, and at least 10,000 events were recorded for each monoclonal combination. Levels of CD antigen expression were displayed as median fluorescence intensity (MFI). The FACS-DiVa software (Becton-Dickinson) was used for cytometric analysis.

Differentiation potential towards the adipogenic lineage

hA-MSCs and hVAT-MSCs were cultured in low glucose D-MEM (Sigma-Aldrich) supplemented with 10% of FBS, 2% of ultraglutamine and 1% of non-essential amino acids at 37°C in 5% CO_2 (all from Lonza, Basel, Switzerland). The cells were passaged twice before the addition of differentiation medium composed of DMEM with the addition of 10% FBS, 1 µM dexamethasone, 0.5 mM 3-isobutyl-1-methylxhantine, 200 µM indomethacin and 10 µg/mL insulin. Media were changed every two days and cells were either stained or collected for RNA extraction.

CD13 RNA interference and overexpression

hA-MSCs plated at a density of 5,000 cells/cm^2 were transfected using 20 µL Lipofectamine 2000 according to the manufacturer's instructions (Invitrogen, Paisley, UK) with 8 µg short hairpin RNAs (shRNAs)-expressing plasmids (Open Biosystem, Huntsville) or with 8 µg pCMV-Sport 6 Vector (Invitrogen, Paisley, UK), to silence or to overexpress CD13 mRNA, respectively. Transfected cells were induced to differentiate towards the adipogenic lineage up to 4 days.

Effect of IFN-γ on the expression of CD13 on the surface of h-MSCs

The expression of CD13 on the surface of Co- and of Ob-h-MSCs isolated from amnion, umbilical cord and VAT was measured after exposure of cells to 0.8 and 12.5 ng/mL IFN-γ at 37° C for 24 h, using untreated Co- and Ob-h-MSCs as controls. At the end of incubation, the cells were harvested by trypsin, washed in PBS, counted, and adjusted to the same concentrations of $1x10^5$ h-MSCs. Subsequently, their immunophenotype was examined by flow cytometry.

Adipocyte staining

After 14 days of differentiation, the adipocyte cultures were stained for lipid droplets, which are an index of differentiation. The cells were washed in PBS and fixed in 10% formalin for 1 h. Then they were washed in PBS and the lipids were stained for 15 min with Oil-red-O prepared by mixing vigorously three parts of stock solution (0.5% Oil-red-O in 98% isopropanol) with two parts of water and then eliminating undissolved particles with a 0.4-μm filter. Cells were then washed with water and the number of adipocytes was evaluated with a microscope. Relative lipid levels were assessed by redissolving the Oil-Red-O present in stained cells in 98% isopropanol and then determining absorbance at 550 nm.

RNA isolation

Total RNA was purified from hA-MSCs isolated from term placentas of Co- and of Ob-pregnant women using the mirVana™ miRNA isolation kit (Ambion, Austin) and its concentration was evaluated with the NanoDrop® ND-1000 UV-Vis spectrophotometer (NanoDrop Technologies, Wilmington).

Quantitative real-time polymerase chain reaction (qRT-PCR) of mRNAs

Real-time quantitative PCR was carried out on the Applied Biosystems 7900HT Sequence Detection system (Applied Biosystems). cDNAs were synthesized from 2 μg of total RNA using hexamer random primers and M-MuLV Reverse Transcriptase (New England BioLabs, Beverly). The PCR reaction was performed in a 20 μL final volume containing cDNA, 1X SYBR Green PCR mix, 10 μM of each specific primer. Supplementary Table 2 lists the oligonucleotide primers used for PCR of selected genes: peroxisome proliferator-activated receptor gamma (PPARγ), CD13, protein homologous to myelin P2 (aP2), and glyceraldehyde-3-phosphate dehydrogenase (GAPDH). The PCR conditions for reverse transcription were: stage 1: 50°C, 2 min; stage 2: 95°C, 10 min; stage 3: 95°C, 15 s; 60°C, 1 min/40 cycles; and stage 4: 95°C, 15 s; 60°C, 1 min. Levels of target genes were quantified using specific oligonucleotide primers and normalized for GAPDH expression.

Statistical analysis

The parameters investigated were expressed as mean and standard error of the mean (SEM) (parametric distributions) or as median value and 25^{th} and 75^{th} percentiles (non parametric distributions). Student's "t" and Mann-Whitney tests were used to compare parametric and nonparametric data, respectively. P values <0.05 were considered statistically significant. Correlation analysis was performed with the SPSS package for Windows (ver. 18; SPSS Inc., Headquarters, Chicago).

Results

The clinical and biochemical characteristics of the mothers and their newborns are reported in Table 2 (A and B, respectively). Weight gain was lower (P=0.025) and diastolic blood pressure was higher (P=0.039) in Ob- than in Co-pregnant women. Both leptin concentration (P<0.0001) and the L/A ratio (P<0.0001) were higher in Ob- than in Co-pregnant women at delivery. Biometric characteristics did not differ significantly between Ob- and Co-newborns.

Isolation of hA-MSCs

We isolated hA-MSCs from the mesenchymal layer of amniotic membranes obtained from our Ob- and Co-pregnant women at delivery. The fetal origin of all isolated hA-MSCs was confirmed by STR typing of DNA of the mother and of the hA-MSCs. Mycoplasma contamination of cultures was checked and excluded (data not shown). All isolated hA-MSCs were characterized by a high proliferation potential and collected after 4 population doublings. Morphologically, cultured Ob- and Co-hA-MSCs showed a similar fibroblastic-like morphology after 4 population doublings (Supplementary Fig. 1).

Immunophenotyping of h-MSCs

The antigenic mosaic displayed by Ob- and Co-hA-MSCs is shown in Table 3. Seventeen of the 38 antigens investigated were not expressed on the surface of hA-MSCs (hematopoietic antigens: CD14, CD15, CD16, CD19, CD28, CD33, CD34, CD45 and CD117; the endothelial marker PECAM-1/CD31; and no-lineage markers: thrombospondin receptor/CD36, Bp50/CD40, Prominin-1/CD133, MDR-1/CD243, NGFR/CD271, ABCG-2/CD338 and HLA-DR). Both Ob- and Co-hA-MSCs were positive for the following mesenchymal markers: CD9, CD10, CD13, CD26, CD29, CD44, CD47, CD49d, CD54, CD56, CD58, CD71, CD81, CD90, CD99, CD105, CD151, CD166, CD200 and HLA-ABC. A

very weak positivity for the epithelial antigen E-cadherin/CD324 was also observed. Interestingly, CD13 expression was significantly higher in Ob-hA-MSCs than in Co-hA-MSCs, i.e., MFI: 9,802.0 and 3,950.0, respectively (P=0.0043) (Table 3 and Fig. 1A). The immunophenotype characterization confirmed the mesenchymal origin and the higher CD13 expression in hVAT-MSCs and hUC-MSCs from Ob- than from Co-women (hVAT-MSCs - MFI: 8,200.0 *vs* 1,100.0 and hUC-MSCs - MFI: 4,965.0 *vs* 3,155.0, respectively).

APN/CD13 serum levels

We first measured baseline serum levels of CD13 in a small group of not pregnant obese and normal weight women and found significantly higher values in the obese subset (medians: 6.00 U/L and 1.00 U/L, P=0.02, respectively) (Fig. 1B). The serum levels of CD13 were also significantly higher in Ob- than in Co-pregnant women at delivery (medians: 24.00 U/L and 7 U/L, P=0.002, respectively), (Fig. 1B). CD13 levels were significantly higher in Ob- and Co-pregnant women than in not pregnant Ob- and Co-women: 4 (P=0.0003) and 7 times (P=0.003), respectively. Furthermore, in Ob-pregnant women, serum CD13 levels were significantly correlated to the levels of CD13 on the surface of hA-MSCs (r^2=0.84; P<0.0001) (Fig. 1C).

CD13 h-MSC expression and adipogenic differentiation

To investigate whether CD13 is involved in adipogenesis, we cultured Ob- and Co-hA-MSCs for 14 days in adipogenic induction medium. At the end of incubation, the adipogenic potential, as measured by PPARγ and aP2 mRNA levels, was higher in Ob- than in Co-hA-MSCs. In fact, as shown in Fig. 2A and 2B, the mean RQs at day 14 were 0.04 and 0.02, respectively for PPARγ (P=0.02), and 0.02 and 0.01, respectively for aP2 (P=0.03). The same results were obtained with Oil-Red staining; in fact, staining was more intense in Ob- than in Co-hA-MSCs at day 14 of differentiation [Abs (550 nm) = 0.6

and 0.4, P=0.02, respectively] (Fig. 2C). During adipogenesis, CD13 mRNA levels remained higher in Ob- than in Co-hA-MSCs. CD13 silencing by shRNA in Ob-hA-MSCs resulted in a switch-off of CD13 mRNA expression, as evaluated by RT-PCR (Fig. 3A), and, at the same time, the adipogenic potential of these cells did not differ from that observed in Co-hA-MSCs, as shown by similar PPARγ mRNA levels measured in silenced Ob-hA-MSCs and in Co-hA-MSCs (P=0.71) (Fig. 3B). In agreement to CD13 involvement in adipogenesis, we overexpressed CD13 in Co-hA-MSCs (mRNA CD13 mean RQ=7.23) and observed at day 4 of differentiation that PPARγ mRNA levels were higher in treated (mean RQ=0.015) than in untreated (mean RQ=0.001) Co-hA-MSCs. The adipogenic potential at day 14 was also higher in Ob- than in Co-hVAT-MSCs isolated from not pregnant women [aP2: RQs were 0.050 and 0.036; Oil-red-O Abs (550 nm): 0.559 and 0.437, respectively].

Upregulation of CD13 h-MSC expression by IFN-γ

We next evaluated if CD13 expression could be upregulated in h-MSCs by IFN-γ as occurs in murine cellular models [32]. To this aim, we treated the Co- and Ob-hA-MSCs with 0.8 ng/mL or 12.5 ng/mL IFN-γ for 24 h. We found that CD13 expression was significantly higher on membranes of Co-hA-MSCs treated with 12.5 ng/mL IFN-γ (P=0.04) than in untreated cells, whereas there was a slight, not significant, increase in treated Ob-hA-MSCs (Supplementary Fig. 2) versus the untreated counterpart cells. In addition, IFN-γ treatment (12.5 ng/mL at 37° C for 24 h) induced the increase of CD13 membrane expression in hVAT-MSCs (Ob- and Co-MSCs: 39% and 8%, respectively) and in Co-hUC-MSCs (4%) versus the untreated counterpart cells, but not in Ob-hUC-MSCs. Our results suggest that high levels of INF-γ drive the up-regulation of CD13 expression in Co-h-MSCs, irrespective of their source and of pregnancy, whereas its effect on Ob-h-MSCs CD13 expression during obesity is ambiguous.

Discussion

Human amniotic membrane is a readily available source of abundant fetal MSCs that are free from ethical concerns [33]. hA-MSCs isolated from normal weight healthy women at delivery have been characterized [24, 34, 35], but, to our knowledge, the features of hA-MSCs from obese women are largely unknown. In this study, we used flow cytometry to characterize hA-MSCs isolated at delivery from two groups of women: pre-pregnancy normal weight and pre-pregnancy severely obese women. The immunophenotypic characterization confirmed the mesenchymal origin of the isolated cells [36]. In particular, the distribution of CD56 was in agreement with the placental origin of the isolated hA-MSCs. In fact, this marker is absent from bone marrow [34] and from adipose tissue-derived mesenchymal stem cells [37]. Similarly, the endothelial marker PECAM-1/CD31, and the hematopoietic antigens CD14, CD15, CD16, CD19, CD28, CD33, CD34, CD45 and CD117 were absent from isolated Ob- and Co-hA-MSCs. Staining for the E-cadherin/CD324 epithelial antigen was very weak in our Ob- and Co-hA-MSC preparations; the co-expression of epithelial, albeit at a low intensity, and mesenchymal markers on our h-AMSCs was in agreement with previous findings [38, 39]. Overall, our results are similar to those reported by Parolini et al. [24] and/or Roubelakis [35] regarding the expressed (CD49d, CD90, HLA-ABC, CD13, CD56, CD105, CD166, CD10, CD29, CD44 and CD54) and not expressed (PECAM-1/CD31, HLA-DR, CD14, Prominin-1/CD133, NGFR/CD271, CD34 and CD45) membrane-bound antigens in hA-MSCs. We found that the Ob-hA-MSC immunophenotype is characterized by a significantly higher expression of the APN/CD13 antigen with respect to the Co-hA-MSC phenotype. Besides amnion, CD13 was overexpressed in h-MSCs isolated from umbilical cord in obese womenand in those isolated from VAT in not pregnant women.

Type II metalloprotease APN/CD13 (EC. 3.4.11.2) is a heavily glycosylated membrane-bound protein (~ 960aa, ~ 150 kDA) that is encoded by the human ANPEP gene located on chromosome 15 (q25-q26) [40]. This protein exists also in a soluble form. APN/CD13 is a ubiquitous enzyme present in

a wide variety of human organs, tissues and cell types including placenta, human umbilical vein endothelial cells, monocytes, lymphocytes T, hypothalamus, and epithelial intestinal cells [41]. It has various mechanisms of action: enzymatic cleavage of peptides, endocytosis and signal transduction [42]. APN/CD13 is involved in inflammation, cellular differentiation and proliferation, apoptosis, cell adhesion and motility [42]. Dysregulated expression of membrane and/or soluble forms of APN/CD13 has been observed in many diseases [43], but until now it has never been associated with obesity. Here, we provide the first demonstration that the CD13 antigen is increased on hA-MSCs during obesity and could play a role in adipogenesis. In fact, we first detected a higher adipogenic potential in Ob- than in Co-hA-MSCs after 14 days of adipogenic differentiation and then observed that the adipogenic potential of Ob-hA-MSCs was comparable to that of Co-hA-MSCs after CD13 silencing. Conversely, the adipogenic potential increased in Co-hA-MSCs after CD13 overexpression. Furthermore, we provide evidence that INFγ upregulated CD13 expression in Co-hA-MSCs.

Intriguingly, in Ob-pregnant women APN/CD13 serum levels at delivery were higher than in Co-pregnant women and correlated with CD13 surface Ob-hA-MSC expression (r^2=0.89, P<0.0001), which support the hypothesis that the placenta is the major source of the high CD13 levels measured in maternal serum [44]. We also found that leptin concentration and the L/A ratio were increased in Ob-maternal serum at delivery. This finding confirms the concept that these two parameters are obesity risk markers [45, 46].

In conclusion, this characterization of Ob-hA-MSCs shows that antigen CD13, by influencing the adipogenic potential of these cells, could be an *in-utero* risk factor for obesity. Our data strengthen the hypothesis that high serum CD13 and mesenchymal stem cell CD13 are markers of obesity.

Acknowledgments

The present work was supported by grants from CEINGE Regione Campania (DGRC 1901/2009) and by MIUR-PRIN 2008. We thank Jean Ann Gilder (Scientific Communication srl, Naples, Italy) for revising and editing the manuscript.

Author Disclosure Statement

The authors declare no financial conflicts of interest.

References

1. Guelinckx I, Devlieger R, Beckers K, Vansant G. (2008). Maternal obesity: pregnancy complications, gestational weight gain and nutrition. Obes Rev 9:140-50.
2. Heslehurst N, Ells LJ, Simpson H, Batterham A, Wilkinson J, Summerbell CD. (2007). Trends in maternal obesity incidence rates, demographic predictors, and health inequalities in 36,821 women over a 15-year period. BJOG 114:187-94.
3. Kim SY, Dietz PM, England L, Morrow B, Callaghan WM. (2007). Trends in pre-pregnancy obesity in nine states, 1993-2003. Obesity (Silver Spring) 15:986-93.
4. Pipe NG, Smith T, Halliday D, Edmonds CJ, Williams C, Coltart TM. (1979). Changes in fat, fat-free mass and body water in human normal pregnancy. Br J Obstet Gynaecol 86:929-40.
5. Ehrenberg HM, Huston-Presley L, Catalano PM. (2003). The influence of obesity and gestational diabetes mellitus on accretion and the distribution of adipose tissue in pregnancy. Am J Obstet Gynecol 189:944-8.
6. Capobianco V, Nardelli C, Ferrigno M, Iaffaldano L, Pilone V, Forestieri P, Zambrano N, Sacchetti L. (2012). miRNA and Protein Expression Profiles of Visceral Adipose Tissue Reveal miR-141/YWHAG and miR-520e/RAB11A as Two Potential miRNA/Protein Target Pairs Associated with Severe Obesity. J Proteome Res. 11:3358−3369.
7. Drolet R, Richard C, Sniderman AD, Mailloux J, Fortier M, Huot C, Rhéaume C, Tchernof A. (2008). Hypertrophy and hyperplasia of abdominal adipose tissues in women. Int J Obes (Lond) 32:283-91.
8. Bartha JL, Marín-Segura P, González-González NL, Wagner F, Aguilar-Diosdado M, Hervias-Vivancos B. (2007). Ultrasound evaluation of visceral fat and metabolic risk factors during early pregnancy. Obesity (Silver Spring) 15:2233-9.

9. Harvey NC, Poole JR, Javaid MK, Dennison EM, Robinson S, Inskip HM, Godfrey KM, Cooper C, Sayer AA; SWS Study Group. (2007). Parental determinants of neonatal body composition. J Clin Endocrinol Metab 92:523-6.
10. Chu SY, Callaghan WM, Kim SY, Schmid CH, Lau J, England LJ, Dietz PM. (2007). Maternal obesity and risk of gestational diabetes mellitus. Diabetes Care 30:2070-6.
11. O'Brien TE, Ray JG, Chan WS. (2003). Maternal body mass index and the risk of preeclampsia: a systematic overview. Epidemiology 14:368-74.
12. Metwally M, Ong KJ, Ledger WL, Li TC. (2008). Does high body mass index increase the risk of miscarriage after spontaneous and assisted conception? A meta-analysis of the evidence. Fertil Steril 90:714-26.
13. Sattar N, Clark P, Holmes A, Lean ME, Walker I, Greer IA. (2001). Antenatal waist circumference and hypertension risk. Obstet Gynecol 97:268-71.
14. Li C, Kaur H, Choi WS, Huang TT, Lee RE, Ahluwalia JS. (2005). Additive interactions of maternal prepregnancy BMI and breast-feeding on childhood overweight. Obes Res 13:362-71.
15. Fowden AL, Forhead AJ. (2004). Endocrine mechanisms of intrauterine programming. Reproduction 127:515-26.
16. Fowden AL, Forhead AJ, Coan PM, Burton GJ. (2008). The placenta and intrauterine programming. J Neuroendocrinol 20:439-50.
17. Okawa H, Okuda O, Arai H, Sakuragawa N, Sato K. (2001). Amniotic epithelial cells transform into neuron-like cells in the ischemic brain. Neuroreport 12:4003-7.
18. Zeigler BM, Sugiyama D, Chen M, Guo Y, Downs KM, Speck NA. (2006). The allantois and chorion, when isolated before circulation or chorio-allantoic fusion, have hematopoietic potential. Development 133:4183-92.

19. Fukuchi Y, Nakajima H, Sugiyama D, Hirose I, Kitamura T, Tsuji K. (2004). Human placenta-derived cells have mesenchymal stem/progenitor cell potential. Stem Cells 22:649-58.
20. Pittenger MF, Mackay AM, Beck SC, Jaiswal RK, Douglas R, Mosca JD, Moorman MA, Simonetti DW, Craig S, Marshak DR. (1999). Multilineage potential of adult human mesenchymal stem cells. Science 284:143–7.
21. In 't Anker PS, Scherjon SA, Kleijburg-van der Keur C, de Groot-Swings GM, Claas FH, Fibbe WE, Kanhai HH. (2004). Isolation of mesenchymal stem cells of fetal or maternal origin from human placenta. Stem Cells 22:1338–45.
22. Katz AJ, Tholpady A, Tholpady SS, Shang H, Ogle RC. (2005). Cell surface and transcriptional characterization of human adipose-derived adherent stromal (hADAS) cells. Stem Cells 23:412–23.
23. Hwang JH, Lee MJ, Seok OS, Paek YC, Cho GJ, Seol HJ, Lee JK, Oh MJ. (2010). Cytokine expression in placenta-derived mesenchymal stem cells in patients with pre-eclampsia and normal pregnancies. Cytokine 49:95-101.
24. Parolini O, Alviano F, Bagnara GP, Bilic G, Bühring HJ, Evangelista M, Hennerbichler S, Liu B, Magatti M, Mao N, Miki T, Marongiu F, Nakajima H, Nikaido T, Portmann-Lanz CB, Sankar V, Soncini M, Stadler G, Surbek D, Takahashi TA, Redl H, Sakuragawa N, Wolbank S, Zeisberger S, Zisch A, Strom SC. (2008). Concise review: isolation and characterization of cells from human term placenta: outcome of the first international Workshop on Placenta Derived Stem Cells. Stem Cells 26:300-11.
25. Grant A, Palzer S, Hartnett C, Bailey T, Tsang M, Kalyuzhny AE. (2005). A cell-detachment solution can reduce background staining in the ELISPOT assay. Methods Mol Biol 302:87-94.
26. Mariotti E, Mirabelli P, Di Noto R, Fortunato G, Salvatore F. (2008). Rapid detection of mycoplasma in continuous cell lines using a selective biochemical test. Leuk Res 32:323-6.

27. Bieback K, Kern S, Klüter H, Eichler H. (2004). Critical parameters for the isolation of mesenchymal stem cells from umbilical cord blood. Stem Cells 22:625-34.

28. Schäffler A, Büchler C. (2007). Concise review: adipose tissue-derived stromal cells--basic and clinical implications for novel cell-based therapies. Stem Cells. 25:818-27.

29. Perfetto SP, Ambrozak D, Nguyen R, Chattopadhyay P, Roederer M. (2006). Quality assurance for polychromatic flow cytometry. Nat Protocols 1:1522–1530.

30. Lamoreaux L, Roederer M, Koup R. (2006). Intracellular cytokine optimization and standard operating procedure. Nat Protocols 1:1507–1516.

31. Maeker HT, Trotter J. (2006). Flow cytometry controls, instrument setup, and the determination of positivity. Cytometry Part A 69A:1037–1042.

32. Gabrilovac J, Cupić B, Zivković E, Horvat L, Majhen D. (2011). Expression, regulation and functional activities of aminopeptidase N (EC 3.4.11.2; APN; CD13) on murine macrophage J774 cell line. Immunobiology 216:132-44.

33. Miki T, Lehmann T, Cai H, Stolz DB and Stromk SC. (2005). Stem cell characteristics of amniotic epithelial cells. Stem Cells 23:1549-1559.

34. Mariotti E, Mirabelli P, Abate G, Schiattarella M, Martinelli P, Fortunato G, Di Noto R, Del Vecchio L. (2008). Comparative characteristics of mesenchymal stem cells from human bone marrow and placenta: CD10, CD49d, and CD56 make a difference. Stem Cells Dev 17:1039-41.

35. Roubelakis MG, Trohatou O, Anagnou NP. (2012) Amniotic fluid and amniotic membrane stem cells: marker discovery. Stem Cells Int 2012:107836.

36. Delorme B, Ringe J, Gallay N, Le Vern Y, Kerboeuf D, Jorgensen C, Rosset P, Sensebé L, Layrolle P, Häupl T, Charbord P. (2008). Specific plasma membrane protein phenotype of culture-amplified and native human bone marrow mesenchymal stem cells. Blood 111:2631-5.

37. Gronthos S, Franklin DM, Leddy HA, Robey PG, Storms RW, Gimble JM. (2001). Surface protein characterization of human adipose tissue-derived stromal cells. J Cell Physiol 189:54-63.

38. Sakuragawa N, Kakinuma K, Kikuchi A, Okano H, Uchida S, Kamo I, Kobayashi M, Yokoyama Y. (2004). Human amnion mesenchyme cells express phenotypes of neuroglial progenitor cells. J Neurosci Res 78:208-14.

39. Soncini M, Vertua E, Gibelli L, Zorzi F, Denegri M, Albertini A, Wengler GS, Parolini O. (2007). Isolation and characterization of mesenchymal cells from human fetal membranes. J Tissue Eng Regen Med 1:296-305.

40. Watt, V.M. and Willard, H.F. (1990). The human aminopeptidase N gene: isolation, chromosome localization, and DNA polymorphism analysis. Hum Genet 85:651–654.

41. Lai A, Ghaffari A, Ghahary A. (2010). Inhibitory effect of anti-aminopeptidase N/CD13 antibodies on fibroblast migration. Mol Cell Biochem 343:191-9.

42. Paola Mina-Osorio. (2008). The moonlighting enzyme CD13: old and new functions to target. Trends in Molecular Medicine 14:361-371.

43. Luan Y, Xu W. (2007). The structure and main functions of aminopeptidase N. Curr Med Chem 14:639-47.

44. Kawai M, Araragi K, Shimizu Y, Hara Y. (2009). Identification of placental leucine aminopeptidase and triton-slowed aminopeptidase N in serum of pregnant women. Clin Chim Acta 400:37-41.

45. Labruna G, Pasanisi F, Nardelli C, Tarantino G, Vitale DF, Bracale R, Finelli C, Genua MP, Contaldo F, Sacchetti L. (2009). UCP1 -3826 AG+GG genotypes, adiponectin, and leptin/adiponectin ratio in severe obesity. J Endocrinol Invest 32:525-9.

46. Labruna G, Pasanisi F, Nardelli C, Caso R, Vitale DF, Contaldo F, Sacchetti L. (2011). High leptin/adiponectin ratio and serum triglycerides are associated with an "at-risk" phenotype in young severely obese patients. Obesity (Silver Spring) 19:1492-6.

Legends

FIG. 1. Expression of CD13 antigen in control (Co-) and obese (Ob-) pregnant women. A: Ob-hA-MSCs expressed significantly higher amounts (at Mann-Whitney test) of CD13 surface antigen compared with Co-hA-MSCs (P=0.0043); **B**: serum levels of CD13 were significantly higher both in Ob- than in Co-not pregnant women (P=0.02) and in Ob- than in Co-women at delivery (P=0.002); **C**: Serum CD13 levels were correlated with CD13 surface expression levels in Ob-pregnant women (r^2=0,84; P<0.0001). The box plots provide a vertical view of the data expressed as median, 25th percentile, 75th percentile and extreme values.

FIG. 2. Adipogenic potential in Ob-hA-MSCs and in Co-hA-MSCs. The statistically significant higher mRNA expression levels of PPARγ (P=0.02) (**A**) and of aP2 (P=0.03) (**B**) measured 14 days after the adipogenic induction, indicated increased adipogenesis in Ob- versus Co-hA-MSCs. (**C**) The higher adipogenesis in Ob- than in Co-hA-MSCs was also confirmed by Oil-Red staining [Abs (550 nm) = 0.6 and 0.4, P=0.02, respectively].

FIG. 3. Role of CD13 in adipogenesis. (**A**) mRNA expression levels of CD13 were significantly higher in Ob- than in Co-hA-MSCs at day 0 (P=0.02), day 2 (P=0.02) and day 4 (P=0.04) when cultured with adipogenic medium. CD13 mRNA expression was switched-off in Ob-hA-MSCs after CD13 silencing with shRNA. (**B**) At day 4 of adipogenic induction, PPARγ mRNA expression levels that were significantly higher in Ob-hA-MSCs than in Co-hA-MSCs (P=0.01), decreased to the levels detected in Co-hA-MSCs after CD13 silencing (P=0.71), which indicates that CD13 enhances adipogenesis in hA-MSCs. n.s.: not statistically significant difference.

Table 1. Surface immunophenotypic profile investigated in hA-MSCs by flow cytometry

Fluorochrome	CD Antigen	Other Names	Molecular Weight (kDa)	Cell expression	Function
FITC	**CD9**	Tspan-29	24-26	Platelets, pre-B cells, activated T cells	Adhesion, migration, platelet activation
APC	**CD10**	CALLA	100	B/T precursors, stromal cells	Endopeptidase
PE	**CD13**	APN	150	Granulocytes, monocytes and their precursors, endothelial cells, epithelial cells, mesenchymal stem cells	Metalloproteinase
PE	**CD14**	LPS-R	53-55	Monocytes, macrophages	Receptor for LPS/LPB complex
APC	**CD15**	Lewis X	_	Granulocyte, monocyte, epithelial cells	Cell adhesion
PE	**CD16**	FCγRIIIa	50-65	Neutrophils, NK, macrophages	Low affinity with FCγ receptor, mediates phagocytosis
APC	**CD19**	Bgp95	95	B cells, not on plasma cells	Signal transduction
FITC	**CD26**	DPP IV	110	Mature thymocytes, T, B, NK cells	Exoprotease, co-stimulation
APC	**CD28**	Tp44	44	Most T cells, thymocytes, NKs and plasma cells	Co-stimulation
APC	**CD29**	VLA β1-chain	130	T, B, granulocytes, monocytes, fibroblasts, endothelial cells, NKs , platelet	Adhesion activation, embryogenesis and development
FITC	**CD31**	PECAM-1	130-140	Monocytes, platelets, granulocytes and endothelial cells	Cell adhesion
APC	**CD33**	My9	67	Monocytes, granulocytes, mastocytes and myeloid progenitors	Cell adhesion
APC	**CD34**	My10	105-120	Hematopoietic stem cells and progenitors, endothelial cells	Cell adhesion
APC	**CD36**	Platelet GPIV	85	Platelets, monocytes, macrophages, endothelial cells, erythroid precursors	Adhesion and phagocytosis
FITC	**CD40**	Bp50	48	Monocytes, macrophages, B cells, endothelial cells, fibroblasts, keratinocytes	Co-stimulation to B cells, growth, differentiation and isotype switching
APC	**CD44**	H-CAM	90	Leukocytes, erythrocytes and epithelial cells	Rolling, homing and aggregation
Per Cp	**CD45**	LCA	180-220	Hematopoietic cells, except erythrocytes and platelets	Critical for T and B cell receptor mediated activation
FITC	**CD47**	IAP I	50-55	Hematopoietic, epithelial, endothelial and brain mesenchymal cells	Adhesion
FITC	**CD49d**	VLA-4	150	B cells, T cells, monocytes, eosinophils, basophils, NKs, dendritic cells	Adhesion, migration, homing, activation
APC	**CD54**	ICAM-1	80-114	Epithelial and endothelial cells monocyte. Low on resting lymphocytes, upregulate on activated	T cell activation
PE	**CD56**	NCAM	175-220	Neural, tumors, embryonic tissue, NK	Homophilic and heterophilic adhesion
PE	**CD58**	LFA-3	40-70	Leucocytes, erythrocytes, epithelial endothelial cells and fibroblasts	Costimulation
FITC	**CD71**	Transferrin recepor	95	Reticulocytes, erythroid precursor	Controls iron intake during cell proliferation
APC	**CD81**	TAPA-1	26	B and T cells, monocytes, endothelial cells	Signal transduction
FITC	**CD90**	Thy-1	25-35	Hematopoietic stem cells, neurons, mesenchymal stem cells	Inhibition of hematopoietic stem cells and neuron differentiation
PE	**CD99**	MIC2	32	Leucocyte, NK, monocytes, endothelial and epithelial cells	Leucocyte migration, T cell activation, cell adhesion
PE	**CD105**	Endoglin	90	Endothelial and mesenchymal stem cells, erythroid precursors, monocytes	Angiogenesis, modulates cellular response to TGFβ1
PE	**CD117**	c-kit	145	Hematopoietic stem cells and progenitors	Crucial for hematopoietic stem cells
PE	**CD133**	Prominin-1	120	Hematopoietic stem cell, endothelial, epithelial and neural precursors	Unknown function, stem cell marker
PE	**CD151**	PETA-3	32	Endothelial and epithelial cells, megakaryocytes, platelets	Adhesion
PE	**CD166**	ALCAM	100-105	Neurons, activated T cells, epithelial cells, mesenchymal stem cells	Adhesion, T cell activation
PE	**CD200**	OX-2	33	B cells, activated T cells, thymocytes, neurons endothelium	Down-regulatory signal for myeloid cell functions
FITC	**CD243**	MDR-1	170	Stem cells, multi drug resistant tumors	Influences the up-take, distribution, elimination of drugs
APC	**CD271**	NGFR	75	Neurons, stromal and dendritic follicular cells	Low affinity for NGF receptor
APC	**CD324**	E-cadherin	120	Epithelial, keratinocytes, platelet	Adhesion, growth, differentiation
APC	**CD338**	ABCG-2	72	Hematopoietic stem cells, liver, kidney, intestine, side population of stem cells	Absorption and excretion of xenobiotics
FITC	**HLA-ABC**	Class I MHC	46	All nucleated cells and platelets	Antigen presentation
FITC	**HLA-DR**	Class II MHC	30	B cells, monocytes, myeloid progenitors, activated T and dendritic cells	Antigen presentation

Table 2. Clinical and biochemical characteristics of obese (Ob-) and normal weight control (Co-) pregnant women at delivery and their newborns.

A		
Mother's parameters	**Ob-pregnant women (n=16)**	**Co-pregnant women (n=7)**
Age (years)	32.6 (0.9)	30.7 (1.5)
Weight (kg) [a]	110.1 (5.4)	65.2 (3.6)
Height (m)	163.3(1.6)	169.0 (1.7)
BMI pre-pregnancy (kg/m^2) [a]	40.3 (1.8)	22.4 (1.0)
Weight gain in pregnancy [b]	8.4 (1.3)	14.3 (1.8)
Systolic blood pressure (mmHg)	124.3 (2.7)	117.1 (5.1)
Diastolic blood pressure (mmHg) [c]	82.5 (2.2)	74.2 (2.0)
Frequency cardiac	79.6 (1.7)	79.0 (3.7)
Gestational age	38.4 (0.3)	38.7 (0.2)
Glucose (mmol/L)	4.3 (0.1)	4.0 (0.3)
Total cholesterol (mmol/L)	6.9 (0.4)	7.3 (0.1)
Triglycerides (mmol/L)	2.8 (0.2)	2.3 (0.3)
AST (U/L)	15 [d] (12.2-26.5[d])	14.8 (0.7)
ALT (U/L)	13 [d] (9.2-17.7[d])	12.1 (1.1)
ALP (U/L)	124.2 (11.1)	115.0 (12.6)
GGT (U/L)	11.0 (1.7)	8.8 (1.5)
Leptin (L) (ng/ml) [a]	38.5 (2.2)	15.2 (3.3)
Adiponectin (A) (μg/ml)	6.0 (0.7)	7.5 (1.4)
L/A [a]	7.7 (0.6)	2.6 (0.5)
B		
Newborn features	**Ob-newborns (n=16)**	**Co-newborns (n=7)**
Birth weight (kg)	3162 (0.1)	3401 (0.1)
Length (cm)	49.6 (0.7)	50.8 (0.7)
Head circumference (cm)	34.0 (0.4)	34.8 (0.3)
Apgar 1'	7.0 [d] (7.0-8.0 [d])	7.8 (0.2)
Apgar 5'	9.0 [d] (8.5-9.0 [d])	8.7 (0.1)

Data are expressed as mean (SEM) (parametric distributions).
Statistically significant difference at Student *t* test: [a] P<0.0001, [b] P =0.025 and [c] P=0.039.
[d] median value and 25th–75th percentiles (non parametric distributions).

Table 3. Immunophenotyping of hA-MSCs isolated from obese (Ob-) and control (Co-) pregnant women

		Ob-hA-MSCs		Co-hA-MSCs		
Not expressed antigens						
Fluorochrome	**Antigen**	**MFI**	**25th-75th Percentiles**	**MFI**	**25th-75th Percentiles**	**p Value**
FITC	**CD31**	364.0	278.3-511.3	306.5	286.8-368.0	0.3254
	CD40	444.0	336.5-568.3	388.0	357.0-457.8	0.4824
	CD243	363.0	292.3-528.3	307.5	274.0-378.3	0.2061
	HLA-DR	355.0	283.8-530.0	297.0	272.5-374.8	0.2415
	NC	325.0	250.0-516.3	279.0	218.8-418.8	0.4260
PE	**CD14**	166.5	125.5-197.8	134.5	124.5-157.8	0.2815
	CD16	36.0	11.5-71.7	65.5	50.5-72.0	0.2407
	CD117	142.5	109.5-189.3	121.0	116.0-176.8	0.6065
	CD133	95.5	80.5-112.8	87.5	76.50-110.5	0.5423
	NC	115.5	91.75-181.5	102.5	93.25-135.0	0.5427
APC	**CD15**	122.0	91.0-283.5	122.5	80.0-162.5	0.6065
	CD36	241.5	194.0-388.5	200.5	145.5-267.3	0.2417
	CD271	208.0	127.0-296.5	170.0	127.5-233.3	0.6065
	CD338	200.5	106.5-373.0	107.5	101.8-146.8	0.1223
	CD19	192.0	154.0-241.3	144.0	120.3-182.2	0,1012
	CD28	91.0	5.2-228.5	85.5	0-122.0	0.1722
	CD33	147.5	10.0-189.5	105.5	90.0-132.3	0.6734
	CD34	186.5	105.0-241.5	133.0	17.5-206.0	0.4250
	NC	169.0	99.5-244.8	92.0	64.0-204.0	0.2061
Per Cp	**CD45**	215.5	133.8-251.3	167.0	146.0-208.0	0.6734
	NC	305.0	252.0-483.3	288.5	261.3-348.8	0.7431
Expressed antigens						
Fluorochrome	**Antigen**	**MFI**	**25th-75th Percentiles**	**MFI**	**25th-75th Percentiles**	**p Value**
FITC	**CD9**	3,538.0	2,172.0-6,871.0	2,156.0	1,743.0-3,495.0	0.2417
	CD26	1,287.0	651.8-3,235.0	1,308.0	742.3-1,920.0	0.9626
	CD47	1,339.0	980.3-2,312.0	1,287.0	1,106.0-1,344.0	0.4824
	CD49d	1,185.0	946.8-1,393.0	941.0	708.3-1,140.0	0.2061
	CD71	1,271.0	796.5-2,147.0	1,093.0	897.0-1,538.0	0.7431
	CD90	37,140.0	22,740.0-52,690.0	36,210.0	21,640.0-50,260.0	0.8149
	CD324	517.0	463.0-551.0	436.0	375.0-545.0	0.3027
	HLA-ABC	9,363.0	4,033.0-14,180.0	5,424.0	3,987.0-6,539.0	0.1223
	NC	325.0	250.0-516.3	279.0	218.8-418.8	0.4260
PE	**CD13**	9,802.0	6,786.0-17,130.0	3,950.0	3,634.0-4,961.0	0.0043 [a]
	CD56	496.0	293.8-711.0	528.0	151.0-1,048.0	0.9626
	CD58	2,432.0	1,723.0-2,792.0	2,009.0	1,798.0-2,459.0	0.5427
	CD99	405.0	296.5-586.3	467.5	360.5-651.0	0.3736
	CD105	652.0	507.0-1,329.0	790.0	746.0-847.8	0.6734
	CD151	16,010.0	10,970.0-21,430.0	19,410.0	11,090.0-23,690.0	0.4260
	CD166	5,215.0	3,551.0-7,382.0	4,634.0	3,962.0-5,608.0	0.6734
	CD200	722.5	205.8-1,699.0	1,137.0	631.5-1,444.0	0.3736
	NC	115.5	91.7-181.5	102.5	93.2-135.0	0.5427
APC	**CD10**	1,247.0	999.3-2,319.0	1,890.0	1,122.0-3,031.0	0.3736
	CD29	45,150.0	25,130.0-54,610.0	24,240.0	17,660.0-40,000.0	0.0832
	CD44	11,440.0	8,186.0-16,290.0	7,259.0	6,613.0-9,753.0	0.0678
	CD54	9,910.0	5,404.0-14,260.0	10,660.0	9,486.0-24,670.0	0.3736

	CD81	31,240.0	19,110.0-55,050.0	38,890.0	24,500.0-44,640.0	0.8149
	NC	169.0	99.5-244.8	92.0	64.0-204.0	0.2061

MFI, Median fluorescence intensity; [a] significant P value at Mann-Whitney test.

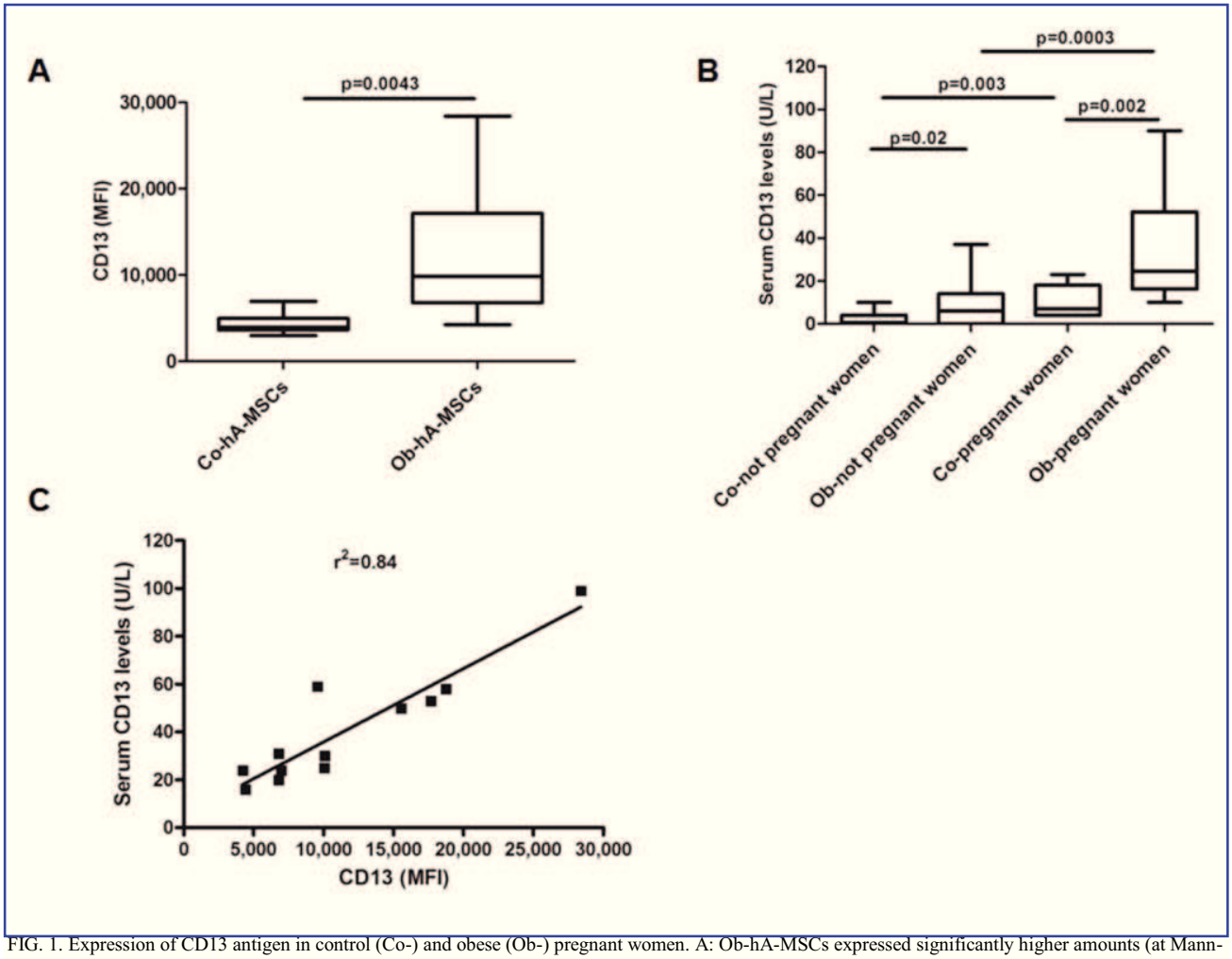

FIG. 1. Expression of CD13 antigen in control (Co-) and obese (Ob-) pregnant women. A: Ob-hA-MSCs expressed significantly higher amounts (at Mann-Whitney test) of CD13 surface antigen compared with Co-hA-MSCs (P=0.0043); B: serum levels of CD13 were significantly higher both in Ob- than in Co-not pregnant women (P=0.02) and in Ob- than in Co-women at delivery (P=0.002); C: Serum CD13 levels were correlated with CD13 surface expression levels in Ob-pregnant women (r²=0,84; P<0.0001). The box plots provide a vertical view of the data expressed as median, 25th percentile, 75th percentile and extreme values.

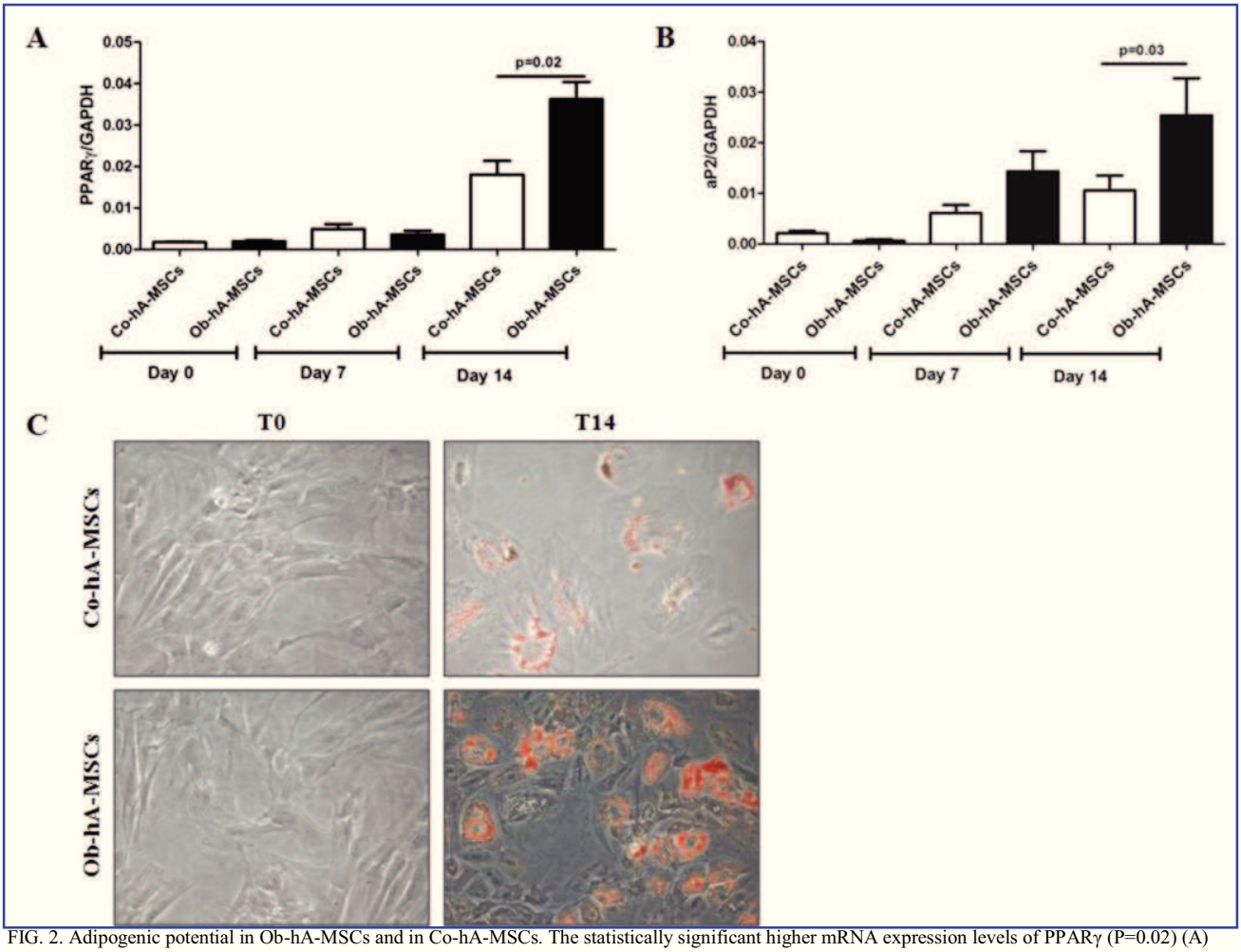

FIG. 2. Adipogenic potential in Ob-hA-MSCs and in Co-hA-MSCs. The statistically significant higher mRNA expression levels of PPARγ (P=0.02) (A) and of aP2 (P=0.03) (B) measured 14 days after the adipogenic induction, indicated increased adipogenesis in Ob- versus Co-hA-MSCs. (C) The higher adipogenesis in Ob- than in Co-hA-MSCs was also confirmed by Oil-Red staining [Abs (550 nm) = 0.6 and 0.4, P=0.02, respectively].

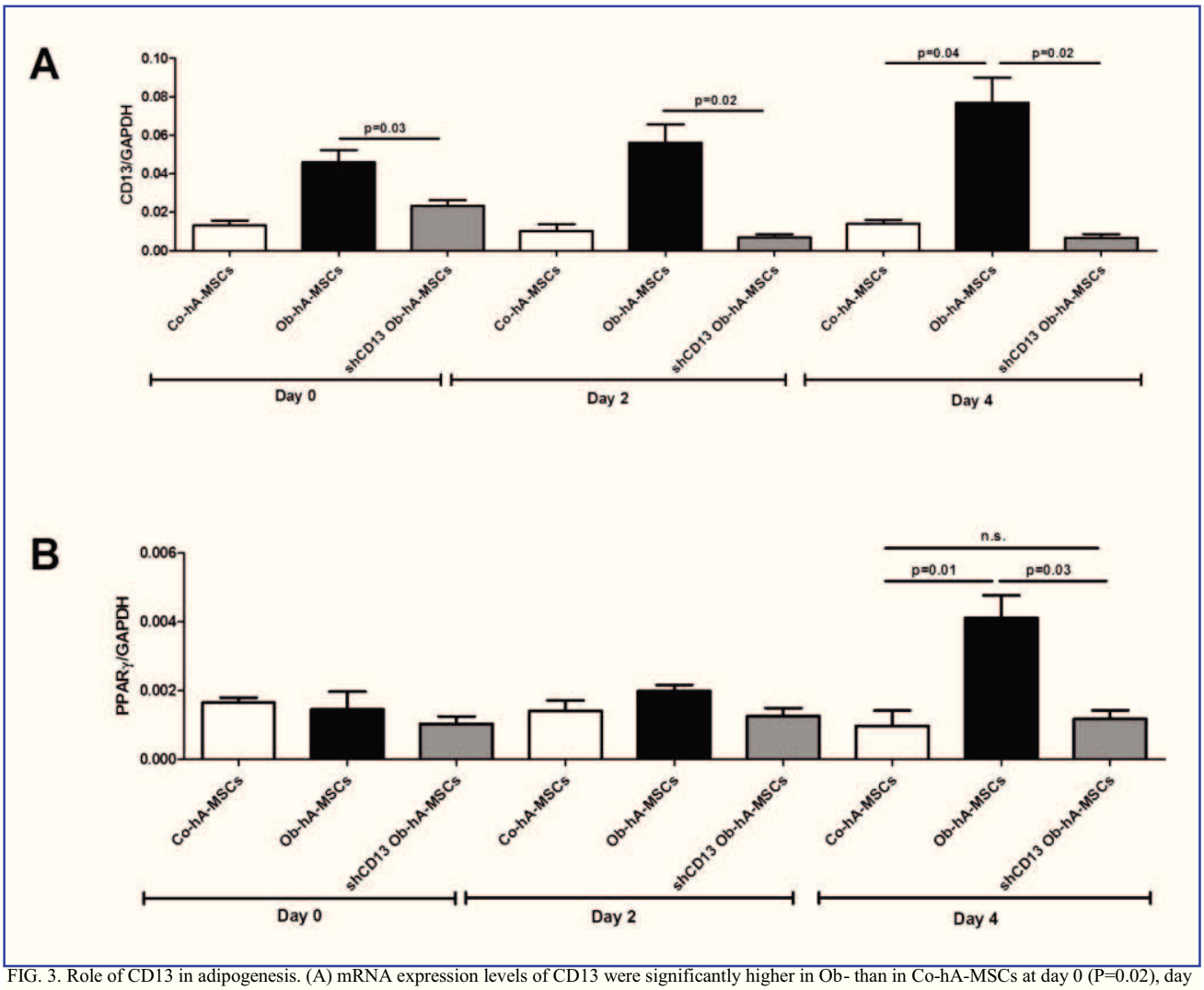

FIG. 3. Role of CD13 in adipogenesis. (A) mRNA expression levels of CD13 were significantly higher in Ob- than in Co-hA-MSCs at day 0 (P=0.02), day 2 (P=0.02) and day 4 (P=0.04) when cultured with adipogenic medium. CD13 mRNA expression was switched-off in Ob-hA-MSCs after CD13 silencing with shRNA. (B) At day 4 of adipogenic induction, PPARγmRNA expression levels that were significantly higher in Ob-hA-MSCs than in Co-hA-MSCs (P=0.01), decreased to the levels detected in Co-hA-MSCs after CD13 silencing (P=0.71), which indicates that CD13 enhances adipogenesis in hA-MSCs. n.s.: not statistically significant difference.

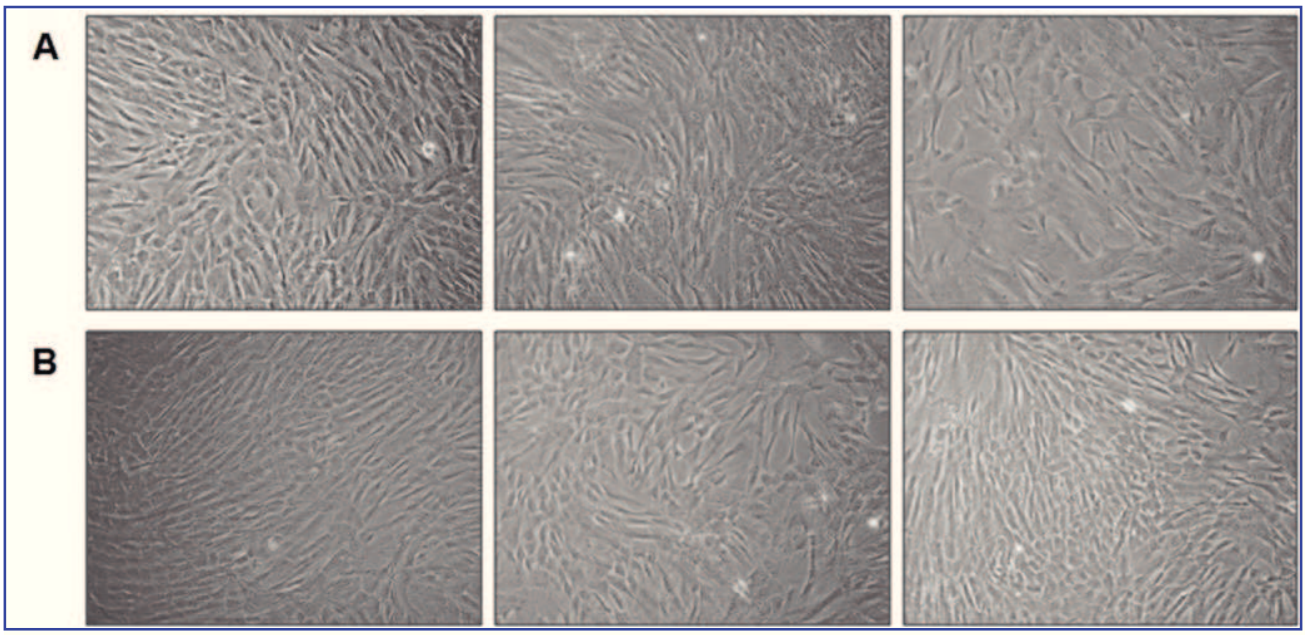

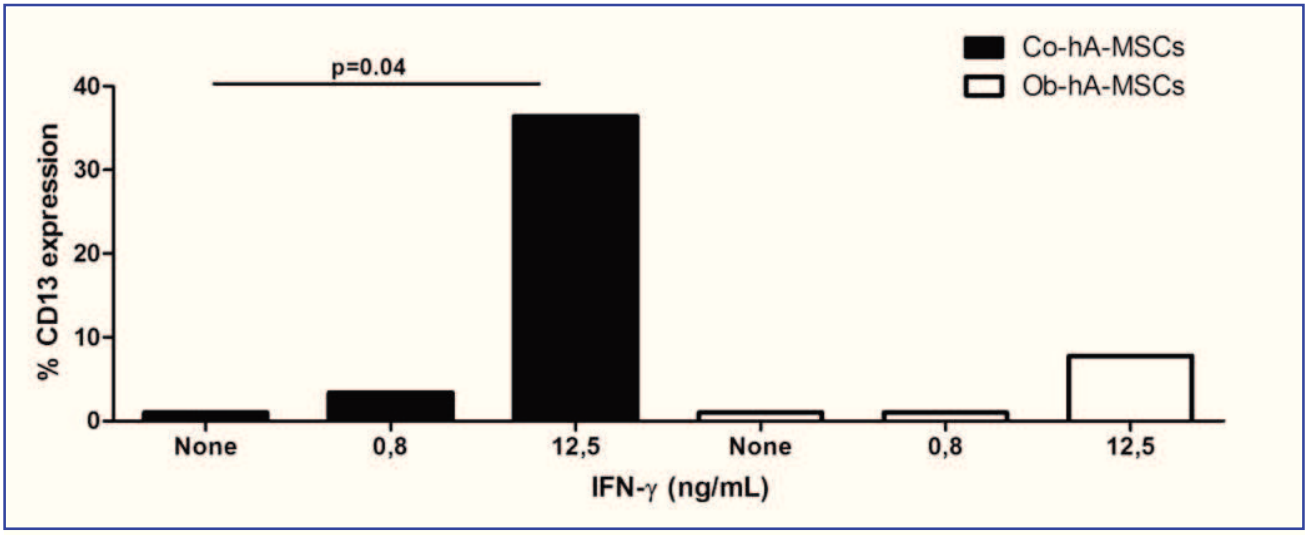

Supplementary Figures legend

Supplementary Figure 1: Morphology of hA-MSCs isolated from pregnant women. A similar fibroblastic-like shape was observed in three Ob- **(A)** and three Co- **(B)** hA-MSCs after 4 population doublings by phase contrast light microscopy (magnification 10x).

Supplementary Figure 2: CD13 expression on Co- and Ob-hA-MSCs treated with 0.8 ng/mL or 12.5 ng/mL IFN-γ for 24 h. CD13 expression significantly increased on membranes of Co-hA-MSCs treated with 12.5 ng/mL IFN-γ (P=0.04) versus untreated counterpart cells, whereas there was a slight, not significant increase, in treated Ob-hA-MSCs versus untreated cells.

Supplementary Table 1: Antibody cocktails contained in each tube for hA-MSCs immunophenotyping by flow cytometry.

Tube	CD Antigens
1	Anti-CD90-FITC (clone 5E10)/anti-CD13-PE (clone L138)/anti-CD45-PerCP (clone 2D1)/anti-CD34-APC (clone 8G12)
2	Anti-HLA-DR-FITC (clone l243)/anti-CD14-PE (clone MΦP9)/anti-CD45-PerCP (clone 2D1)/anti-CD29-APC (clone MAR4)
3	Anti-CD243-FITC (clone17F9)/anti-CD56-PE (clone MY31)/anti-CD45-PerCP (clone 2D1)/anti-CD44-APC (clone g44-26)
4	Anti-CD324-FITC (clone 36)/anti-CD105-PE (clone 266)/anti-CD45-PerCP (clone 2D1)/anti-CD338-APC (clone 5D3)
5	Anti-CD71-FITC (clone L01.1)/anti-CD56-PE (clone MY31)/anti-CD45-PerCP (clone 2D1)/anti-CD28-APC (clone CD28.2)
6	Anti-CD90-FITC (clone 5E10)/anti-CD200-PE (clone MRC OX-104)/anti- CD45-PerCP (clone 2D1)/anti-CD33-APC (clone p67.6)
7	Anti-HLA-A,B,C-FITC (clone G46-2.6)/anti-CD16-PE (clone B73.1)/anti-CD45-PerCP (clone 2D1)/anti-CD36-APC (clone CB38 NL07)
8	Anti-CD90-FITC (clone 5E10)/anti-CD200-PE (clone MRC OX-104)/anti-CD45-PerCP (clone 2D1)/anti-CD34-APC (clone 8G12)
9	Anti-CD9-FITC (clone ML-13)/anti-CD133-PE (clone ACC133/1)/anti-CD45-PerCP (clone 2D1)/anti-CD10-APC (clone HI10A)
10	Anti-49d-FITC (clone R1-2)/anti-CD58-PE (clone L306.4)/anti-CD45-PerCP (clone 2D1)/anti-CD271-APC (clone ME20.4-1.H4)
11	Anti-CD31-FITC (clone WM59)/anti-CD117-PE (clone 104D2)/anti-CD45-PerCP (clone 2D1)/anti-CD81-APC (clone JS-81)
12	Anti-CD26-FITC (clone L272)/anti-CD99-PE (clone TU12)/anti-CD45-PerCP (clone 2D1)/anti-CD19-APC (clone SJ25C1)
13	Anti-CD40-FITC (clone 53C)/anti-CD151-PE (clone 14A.H1)/anti-CD45-PerCP (clone 2D1)/anti-CD54-APC (clone HA58)
14	Anti-CD47-FITC (clone B6H12)/anti-CD166-PE (clone 3A6)/anti-CD45-PerCP (clone 2D1)/anti-CD15-APC (clone HI98)

FITC: fluorescein isothiocyanat; PE: R-Phycoerythrin; PerCP: peridinin-chlorophyll-protein complex; APC: allophycocyanin

Supplementary Table 2: PCR oligonucleotide primers.

CD13 Forward	GGACAGCGAGTTCGAGGGGGA
CD13 Reverse	AGTGGCCACCACCTTTCTGACA
PPARγ Forward	CATACATAAAGTCCTTCCCGCTG
PPARγ Reverse	CGAATGGTGATTTGTCTGTTGTCT
aP2 Forward	GGTGGTGGAATGCGTCATG
aP2 Reverse	CAACGTCCCTTGGCTTATGC
GAPDH Forward	GTCGGAGTCAACGGATTTGG
GAPDH Reverse	AAAAGCAGCCCTGGTGACC

A PEGylated helper-dependent adenoviral vector expressing human apo A-I reduces atherosclerosis in LDLR deficient mice

E. Leggiero,[1, 2] D. Astone,[1, 2] V. Cerullo,[1, 2, 3] P. Wonganan,[3] C. Mazzaccara,[2] G. Labruna,[2] L. Sacchetti,[1, 2] F. Salvatore,[1, 2] M. Croyle[3, 4] and L. Pastore[1, 2]

[1]CEINGE-Biotecnologie Avanzate, Napoli, Italia; [2]Dipartimento di Biochimica e Biotecnologie Mediche, Università di Napoli "Federico II", Napoli, Italia; [3]Division of Pharmaceutics, College of Pharmacy, The University of Texas at Austin, Austin, USA; [4]Institute of Cellular and Molecular Biology, The University of Texas at Austin, Austin, USA.

[#]Actual address:
Division of Biopharmaceutics and Pharmacokinetics
Faculty of Pharmacy University of Helsinki, Helsinki Finland
Viikinkaari 5 E (P.O. Box 56)
00014, University of Helsinki

Correspondence should be addressed to L.P. (lucio.pastore@unina.it)
CEINGE-Biotecnologie Avanzate,
Via G. Salvatore 486, 80145, Napoli, Italia
Ph. +39-081-3737885
Fax: +39-081-3737808
Email: lucio.pastore@unina.it

Running title: PEGylatd HD-Ad vector for atherosclerosis gene therapy

Abstract

Helper-dependent adenoviral (HD-Ad) vectors have tremendous potential for gene therapy applications: however, their administration induces an acute toxicity that impairs safe clinical applications. We have previously observed that PEGylation of HD-Ad vectors strongly reduces acute response in murine and primate models. To evaluate whether PEGylated HD-Ad vectors can combine reduced toxicity with pathological phenotype correction, we administered an HD-Ad vector expressing the human apolipoprotein A-I (hApoA-I) to LDL receptor-deficient mice, a model for familial hypercholesterolemia under a regimen of high cholesterol diet. Mice were treated with high doses of either HD-Ad expressing apo A-I or the PEGylated version of the same vector. After 12 weeks, mice treated with either vector showed reduction of LDL-C and elevation of HDL-C levels compared to untreated mice. After terminal sacrifice, mice treated with either vector showed significantly smaller areas of atherosclerotic plaques compared to control animals. In addition, mice treated with PEGylated vector had an mild increase in pro-inflammatory cytokines with an improved toxicity profile. This data indicates, for the first time, that the reduction of toxicity due to HD-Ad vectors PEGylation does not impair correction of pathological phenotypes and support the possibility for the clinical application of these vectors.

Introduction

Atherosclerosis is a complex multifactorial disorder ultimately leading to coronary artery disease (CAD). Atherosclerosis is characterized by the accumulation of inflammatory cells, lipoproteins and fibrous tissue in the wall of large arteries [1].The etiology of this disorder is highly heterogeneous with numerous known and unknown genetic and environmental factors influencing both lipoprotein metabolism and inflammation [2]. One of the major predisposing factor is hypercholesterolemia; in fact, elevated low density lipoprotein cholesterol (LDL-C), due to environmental as well as genetic factors, is frequently associated with the development of atherosclerosis and higher frequency of CAD. Mutations in the LDL receptor gene cause familial hypercholesterolemia (FH), an inherited metabolic disorder characterized by increase of LDL-C plasma levels and a consequent increased risk of premature atherosclerosis and CAD [3].

Reduced levels of high density lipoprotein cholesterol (HDL-C) are also associated with higher incidence of CAD. In addition, there are some human disorders in which premature atherosclerosis is associated with extreme reduction of HDL-C (e.g. Tangier disease and mutations in the human ApoA-I gene) [4-5]. HDL particles transport excess cholesterol from periphery to the liver with a mechanism known as reverse cholesterol transport that mediates their atheroprotective role [6]: in fact cardiovascular risk can also be reduced rising HDL-cholesterol levels [7] . HDL and its components (expecially antioxidant enzymes) can reduce oxidized lipid species in LDL particles, reducing their atherogenic potential [8]. Apolipoprotein A-I (ApoA-I) constitutes approximately 70% of the

apolipoprotein content of HDL particles, and there is a strong correlation between plasma ApoA-I and HDL-C levels [9]. In addition, ApoA-I is reported to have intrinsic anti-oxidant and anti-inflammatory properties, which have led to the development of ApoA-I mimetic peptides, comprising investigational drugs that are currently being tested for their potential to reduce atherosclerosis [10].

Overexpression of anti-atherogenic proteins has been attempted using a variety of viral vectors[11]. First generation adenoviral (FG-Ad) vectors are capable to induce high levels of apoA-I [12]; however, duration of transgene expression is extremely short with these vectors making them unsuitable for clinical applications[13]. Adeno-associated vectors (AAV) have also been used for ApoA-I expression; even though these vectors present a more favourable toxicity profile, levels of expression were not sufficient to induce effects on aortic atherosclerosis[14]. Helper-dependent adenoviral (HD-Ad) vectors are, on the other hand, capable of inducing prolonged high levels of transgene expression with a more favourable toxicity profile [13, 15-18]. We have previously overexpressed human apoA-I in two different mouse models using HD-Ad vectors obtaining long-term corrective levels of human ApoA-I (hApoA-I) with a consequent reduction of aortic atherosclerosis [13, 17]. HD-Ad vectors reduce long-term toxicity due to accumulation of viral proteins [19]; however, innate immunity with consequent cytokine secretion is still present and is due to the interaction of Ad particles with Toll-like receptors (TLRs) at the level of the plasma membrane [20] and at the endosome level where TLR9 interacts with the vector genome [21]. In order to overcome innate immunity several pre-treatment including

corticosteroid administration and TNF-alpha blockade have been suggested [22]. We have focused our attention on HD-Ad vector particles modification: in particular we have chemically modified HD-Ad vectors by PEGylation [19]. PEGylated HD-Ad vectors show an improved toxicity profile in both mice [19] and non-human primates [23]. PEGylation does not significantly influence transduction efficiency in hepatocytes and increases the vector half-life in the systemic circulation [19, 24]. This modification significantly reduces vector-mediated production of inflammatory cytokines immediately after administration and protects vectors from inactivation by complement and neutralizing antibodies [19]. However, at the moment, proof-of concept for the in vivo efficacy of PEGylated HD-Ad vectors for therapeutic purposes has not been obtained. Therefore, we decided to evaluate these vectors for gene transfer in the mouse model of familial hypercholesterolemia, the LDL receptor-deficient mice previously generated by homologous recombination [25]. These mice develop only a modest hypercholesterolemia where fed with a normal diet; however, on a high-fat diet they develop extensive atherosclerotic lesions throughout the aorta [26].This model has been previously demonstrated to be responsive to HD-Ad-mediated increase in ApoA-I levels, showing a significant reduction of aortic atherosclerosis [17]. We decided to evaluate whether we were able to reduce aortic atherosclerosis development in this model in absence of innate host response against the vector; we have therefore chemically modified a HD-Ad vector containing the entire human ApoA-I gene by PEGylation and administered it to LDLR-deficient mice fed on a high-fat diet. We then evaluated efficacy on both lipoprotein

profile and development of aortic atherosclerosis and compared these parameters and toxicity profiles to mice treated with the naïve vectors. Overall, our results support the possibility the clinical application of PEGylated HD-Ad vectors for correction of genetic diseases.

Results

PEG-HD-Ad vectors allow high levels long-term expression of ApoA-I

In order to determine whether the PEGylated HD-Ad vector containing the entire hApoA-I gene was able to transduce cells in culture, we infected 293 and W20-17 cells with the naive (HD-Ad-AI) and the PEGylated (PEG-HD-Ad-AI) vectors and determined ApoA-I levels in the medium. Both 293 and W20-17 cells constitutively secrete a small amount of ApoA-I (17 ± 3.5ng/ml and 13 ± 0.3 ng/ml in untransfected media, respectively). Infection with HD-Ad-AI led to a four-fold increase of Apo A-I in 293 (77 ± 28 ng/ml) and two-fold increase in W20-17 (27 ± 6 ng/ml) cells; in the same cells, a three-fold (54 ± 8 ng/ml) and a two-fold increases (32 ± 6 ng/ml) were observed when they were infected with the PEGylated version (Figure 1A, B). The lower levels of ApoA-I observed in W20-17 cells may be due to either a reduced ability of these cells to be infected with Ad5 or to a lower expression of the transgene driven by the endogenous ApoA-I promoter. Most importantly, there were no significant differences in the secretion of ApoA-I after infection with either PEGylated or naive vectors. This data confirms the efficiency of both vectors *in vitro* and that PEGylation does not significantly influence vector transduction efficiency and transgene expression. In order to assess whether PEG-HD-Ad-AI administration would

lead to a long-term expression of hApoA-I *in vivo*, we administered the 1x10E13 vp/kg of either PEG-HD-Ad-AI or HD-Ad-AI to 2 groups of LDLR-deficient mice fed on a high-fat diet; a third group was treated with PBS as control. Administration of either PEG-HD-Ad-AI or HD-Ad-AI vectors led to a prolonged expression of human ApoA-I for the entire duration of the experiment (12 weeks, Figure 1C). One week after treatment, we observed the highest levels of hApo A-I in both groups (250±3 mg/dL and 210±2 mg/dL). We observed a slow decrease of hApoA-I levels in all treated animals; however, levels of expression remained in the therapeutic range for the entire duration of the experiment in both groups of mice.

PEGylated vectors induce an extremely low toxicity in presence of high levels of transgene expression

To evaluate host response due to vector administration, we assessed cytokine activation profiles in LDLR-deficient mice treated with HD-Ad-AI, PEG-HD-Ad-AI or PBS. Eight weeks old LDLR-deficient mice (n=5) were fed on high cholesterol diet for 4 weeks and then treated with 1x10E13 vp/kg of either HD-Ad-AI or PEG-HD-Ad-AI; control animals (n=5) were treated with an equal volume of PBS. Six hours after administration, blood samples were collected to determine interleukin 6 (IL-6), one of the main markers of inflammation, interleukin 12p40 (IL-12p40), interleukin 12p70 (IL-12p70), tumor necrosis factor (TNF-alpha), monocyte chemotactic protein-1 (MCP-1) and keratinocyte-derived cytokine (KC) levels. IL-12p40, IL-12p70 and TNF-α are markers commonly associated to the activation of the innate immune response against recombinant adenoviral vectors. Moreover, numerous studies have indicated that adenoviral vectors injection induce not only

cytokines but also chemokines (MCP-1 and KC) secretion, the latter being dependent upon activation of Kupffer cells [20]. We determined cytokines levels 6 hours after vector administration since prior data showed that at this time point we can observe the highest activation of cytokine response that usually return to baseline within 24 hours.

We did not observe any differences among groups prior to the administration as expected (Figure 2). Mice treated with HD-Ad-AI showed a larger increase in serum levels of IL-6 compared to animals receiving PEG-HD-AI (1300 ± 300 pg/ml and 400 ± 61 pg/ml, respectively, Figure 2A, panel C). We observed significant differences between PEGylated and naïve vectors for all the cytokines determined except IL-12p40. PEGylated vectors also seems to induce a very mild inflammatory response compared to PBS controls; however, levels of all the cytokines are significantly lower compared to what observed in mice treated with unmodified vectors. Taken together these data further confirm that PEGylation of HD-Ad vectors reduces the innate host response in presence of high levels of transgene expression.

Over-expression of hApo A-I after PEGylated vector administration modifies lipid profile and reduces aortic atherosclerosis

To evaluate the effects of overexpression of hApoA-I on the cholesterol metabolism, the same group of mice previously described (treated with 1x10E13 vp/kg of either HD-Ad-AI or PEG-HD-Ad-AI or with an equal volume of PBS) were fed on an atherogenic diet for 12 weeks. We determined triglycerides, total cholesterol (TC), LDL-cholesterol (LDL-C) and HDL-cholesterol (HDL-C) at different time-points (0, 1, 2, 4, 8 and 12 weeks) after

treatment. Basal plasma triglycerides were 85 ± 5 mg/dL in control mice, 89.5 ± 2mg/dL in HD-Ad-AI treated mice and 84.6 ± 1 mg/dL in mice receiving PEG-HD-Ad-AI (see Figure 3A). These levels were not significantly modified by hApoA-I expression; indeed, no differences were observed among the different groups compared to baseline triglycerides value. On the other hand, basal levels of TC were 549.4 ± 1 mg/dL, 569.06 ± 1 mg/dL, 554 ± 1 mg/dL in PBS, HD-AD-AI and PEG-HD-Ad-AI injected mice, respectively (Figure 3 B). After administration of either HD-Ad-AI or PEG-HD-Ad-AI, we observed a decrease in total cholesterol. The decrease was already evident 1 week after administration, showing significant differences compared to control mice: in fact, mice treated with PBS showed 565.46±1 mg/dL of TC, whereas HD-Ad-AI and PEG-HD-Ad-AI levels were 500.78±1 and 512.94±1 mg/dL, respectively.

To evaluate the influence of hApoA-I on reverse transport of cholesterol, we also analyzed serum levels of LDL-C and HDL-C. The basal LDL-C level was comparable among the 3 groups (420±2, 436 ±2 and 423.5±1 mg/dL in PBS, HD-Ad-AI and PEG-HD-Ad-AI groups, respectively; Figure 3D). In HD-Ad-AI and PEG-HD-Ad-AI treated mice, LDL-C showed an evident decline that started the first week after vector administration and lasted for the entire duration of experiment. Also for HDL-C, the basal levels were similar in the 3 groups (112.2±1, 115.2±1 and 113.6±2 mg/dL in PBS, HD-Ad-AI and PEG-HD-Ad-AI groups, respectively see Figure 3C), but, starting from the first week after administration, HDL-C values increased in mice treated with either HD-Ad-AI or PEG-HD-Ad-AI. In those two groups of animals, HDL-C was significantly higher than that in control mice for the entire

duration of the experiment. Taken together these data suggest that treatment with the PEG-HD-Ad-AI vector induces long-term modifications of lipid metabolism in presence of an extremely reduced toxicity.

We finally evaluated whether changes in lipid metabolism had an effect on atherosclerotic lesions development. We sacrificed the experimental animals 12 weeks after treatment and dissected aortas, from heart to iliac branching. At a macroscopic analysis, we observed fat deposits, as expected, in the intimal layer of brachiocephalic trunk, left common carotid artery and left subclavian artery, the branches gives off aortic arch (Figure 4A). Moreover, other lesions were present throughout the abdominal aorta, upstream kidney arteries bifurcation. A thorough analysis showed more consistent fat deposits in mice treated with PBS compared to mice treated with either HD-Ad-AI or PEG-HD-Ad-AI. Indeed, PBS-treated animals had a greater amount of fats at the level of both aortic arch and abdominal aorta compared to the other groups of mice. In mice treated with PBS, it was possible to observe an occlusion of the aorta, associated with a dilatation of the vessel in the points with highest fat deposition. This obstruction was not observed in mice receiving either HD-Ad-AI or PEG-HD-Ad-AI vector.

In order to quantify atherosclerotic lesions, directly correlated with fat deposits, we performed an O-Red-Oil staining on the aortas *en-face*, after the removal of external fat and residual tissues. The area of fat deposits was quantified in the experimental animals as ultimate determination of the efficacy of vector treatment. In mice treated with PBS, stained areas were 4.22 ± 0.53 mm^2; in mice treated with either HD-Ad-AI or PEG-HD-Ad-

AI we observed an extremely significant ($p<0.01$) reduction of lesion areas (1.09 ± 0.48mm^2 and 1.74 ± 0.67mm^2, respectively, see Figure 4). Altogether these data strongly suggest that PEGylated HD-Ad-induced over-expression of hApo A-I leads to a long-term transgene expression and modification of cholesterol metabolism that ultimately reduce aortic atherosclerosis development.

Discussion

Adenovirus-mediated gene therapy holds significant potential for applications requiring high levels and long-term transgene expression. Nevertheless, clinical translation of adenoviral gene replacement therapy for genetic disease is lagged by vector-associated toxicity. Advances in vector development have led to the HD-Ads that are characterized by the absence of all viral coding genes. HD-Ad vectors show significantly reduced chronic toxicity that, on the contrary, is strongly induced by systemic administration of early generation adenoviral vectors in both small and large animal models [19, 23]. However, even with HD-Ad vectors, innate immune response to adenoviral capsid proteins persists as well as the adaptive immune response to transgene [27]. Together, these two host responses lead to a decrease in the effectiveness of therapeutic index for any particular treatment, so far. Several studies have been carried out in order to reduce the innate immune response to HD-Ad vectors using different approaches such as hydrodynamic injection in mice [28], balloon occlusion catheter-based method in non-human primates [29] and PEGylation of vectors, whose administration has been performed in mice, in association or not with immunosuppressive drugs [19, 30]

Previous studies on toxicity of PEG-HD-Ad vectors have been carried out on C57BL/6 mice [19] and in primates [23], in order to determinate the effect of vector administration on host response. In these studies the LacZ transgene has been often used at aim of determining vector distribution after systemic administration; it is therefore relevant to investigate whether different transgenes may affect host response or their expression may be influenced by PEGylation.

In this study, we have decided to evaluate whether PEG-HD-Ad vectors can be used for correction of a disease in an animal model. At this aim, we chose the mouse model for FH (LDLR-deficient mice) that has been extensively studied and is known to develop high basal levels of LDL-C and extensive atherosclerotic lesions under a regimen of high cholesterol diet [17]. In addition, in a previous work on the same model, we have observed a reduction of its pathological phenotype after the administration of HD-Ad-AI vector expressing hApoAI [17]. In the above-mentioned study, the delay in atherosclerosis progression and remodeling of the lesions was due to the overexpression of hApoA-I and a consequent increase in HDL and, therefore, in reverse transport of cholesterol. In the present study, we treated LDLR-deficient mice with high doses of the some HD-Ad vector expressing hApo-AI and its PEGylated version and followed, for 12 weeks changes in cholesterol metabolism and in particular, TC, LDL-C and HDL-C. Together with the evaluation of treatment efficacy we determined host response to the vector. We observed that the PEGylated HD-Ad vector expressing hApoAI induce a lower increase in pro-inflammatory cytokines compared to its naïve version. The possibility to mitigate host

response associated with adenoviral vectors administration was largely investigate especially after the death of a patient in a clinical trial after treatment with a high dose of a recombinant adenoviral vector containing a functional gene for ornithine trascarbamylase [31]. However, the viral capsid responsible for triggering the acute inflammatory response in a dose-dependent manner is identical for both FG-Ad and HD-Ad vectors [32-33]; in addition, a large body of data points out that FG-Ad vectors are unsuitable for atherosclerosis gene therapy because of limited duration of expression and severe host response [34]. Therefore PEGylation of HD-Ad can be considered a relevant strategy that may increase the ability of effectively use these vectors to treat inborn errors of metabolism.

In mice treated either with HD-Ad-AI or PEG-HD-Ad-AI, concentration of TC, LDL-C and HDL-C showed significant changes compared to mice treated with PBS. This observation is mirrored by the analysis of fat deposits accumulation at level of aortic arch and abdominal aorta. In fact, PBS-treated mice showed more consistent deposits in comparison to the groups injected with either HD-Ad AI or PEG-HD-Ad-AI. This data also indicates, for the first time, that vector PEGylation reduce host response independently from the transgene used and does not affect its expression and its efficacy.

Our data clearly confirm that PEG-HD-Ad vectors are able to reduce innate immune response and are nonetheless effective for hepatocytes transduction after a systemic administration. Moreover, we were able to demonstrate the efficacy of PEG-HD-Ad-ApoA-I to inducing long-term expression of hApoA-I both in vitro and in vivo and its ability to

reduce atherosclerosis in LDLR-deficient mice. Given these results we believe that PEG-HD-Ad-mediated gene therapy may become a valid therapeutic alternative especially in subgroups of FH patients where other therapies are poorly effective; one treatment may lead to a long-lasting effect on lipid metabolism and it is likely to be less expensive than life-long oral medication with an increase in patients compliance.

Materials and methods

Production of Helper-dependent adenoviral vectors

The HD-Ad adenoviral vector (HD-Ad-AI), used in this study, contains 10 kb of the hApo A-I gene, including the promoter region [17]. Rescue and amplification of the vector were performed using the HV-Ad-NG163R-2 helper virus as described. Briefly, a 60-mm dish of 116 cells at 80% confluency were transfected with 20 μg of *PmeI*-digested parental plasmid. Next day, the cells were infected with AdNG163R-2 at an m.o.i. of 1,000 vp/cell. The vector was amplified by serial coinfections of 60-mm dishes of 116 cells at 90% confluency with 10% of the crude lysate from the previous passage and AdNG163R-2 at an m.o.i. of 200 vp/cell. After 3 infections in 60 mm dish (P1, P2, P3), for P4 one 150-mm dish of 116 cells at 90% confluency was coinfected with 10% of the crude serial passage 2 lysate and Ad-NG163R-2 at an m.o.i. of 200 vp/cell. Large-scale HD-Ad production was performed in 3 liters of 116 cells (3–4x10E5 cells/ml) coinfected with 100% of the crude lysate from the 150-mm dish of serial passage 3 and Ad-NG163R-2 48 hours later, coinfected cells were harvested and resuspended in TM solution (10 mM Tris-HCl pH 8.0 and 2mM $MgCl_2$).

The harvested cells were lysed by three freeze-thaw cycles and were incubated with 2M $MgCl_2$ and DNaseI for 1 hour at 37°C. After incubation the cellular debris was spinned down and the lysate was subjected to ultracentrifugation as described elsewhere [35]. Vector concentration was measured in particle number and determined by absorbance at 260 nm. Helper virus contamination and vector characterization were obtained as described previously [36].

PEGylation of HD-Ad vectors

Aliquots of vectors were desalted on Econo-Pac 10DG disposable chromatography columns (Bio-Rad, Hercules, CA) and equilibrated with 0.2 *M* sodium phosphate (pH 7.2) buffer for optimal conjugation. Viral concentrations were determined by absorbance at 260 nm. The protein content of each viral preparation was determined with Bio-Rad DC Protein assay reagents using bovine serum albumin as standard. 10 mg of monomethoxypoly (ethylene) glycol activated by succinimidyl succinate (SSPEG, mw 5000) were added for each microgram of proteins present in each preparation. Conjugation reactions were performed at 25°C with gentle agitation for 2 hours. Reactions were stopped by addition of a 10 fold excess of L-lysine with respect to the amount of PEG added. Unreacted PEG, excess lysine, and reaction products were eliminated by buffer exchange over a second Econo-Pac 10DG disposable chromatography column, equilibrated with 100 mM KPBS (pH 7.4). A separate aliquot of virus was treated and processed in the same manner as the conjugated virus in absence of SSPEG and served as

unPEGylated control. PEGylated and unPEGylated adenoviral vectors were characterized by capillary zone electrophoresis as previously described [19].

Immunoturbidimetric assay

hApo A-I levels were determined by immunoturbidimetric analysis. 293 and W20-17 cells were infected with 200 vp/cell of HD-Ad-AI and PEG-HD-Ad-AI. Uninfected cells were used as negative controls. Forty-eight hours after infection, medium was collected and a detergent solution was added at 37°C for 2 min.

Absorbance at 610 nm was read (Abs1) and goat serum containing anti-human Apo A-I was added. The absorbance at 610 nm was read again (Abs2) and the concentration of human Apo A-I was calculated as ΔAbs=Abs2-Abs1 on the calibration curve. Human serum with high and low concentration of hApoA-I was used as controls.

Animals studies

All experimental procedures were conducted in accordance with institutional guidelines for animal care and use. Food and water were provided *ad libitum*. The mice used in the toxicity experiment were 8-week old female LDL receptor-deficient (LDLR-/-) mice, on a C57BL/6 background. Mice were fed on a diet supplemented with 0.2% (wt/wt) cholesterol and 10% coconut oil (vol/wt) for 4 weeks. HD-Ad was diluted in sterile PBS, prewarmed at 37°C, and injected into tail vein as described [13]. Injections were performed in a total volume of 200 µl.

Mice were anesthetized with Avertine before collecting blood from the retroorbital plexus. For cytokines analyses, blood was collected 6 hours after injection. For

triglycerides, total cholesterol, LDL-C and HDL-C analysis blood was collected at 0, 1, 2, 4, 8 and 12 weeks after vector administration from 12 hours fasting mice. Serum was frozen immediately and stored at −20°C until further processing. Mice were, terminally sacrificed 12 weeks after treatment and aortas were taken for assessment of atherosclerotic lesions,

Evaluation of acute toxicity.

Mouse IL-6, IL-12p40, IL-12p70, TNF-alpha and MCP-1 and KC was determined using the BioRad Bio-plex cytokine multiplex and analyzed using a Bioplex instrument, according to manufacturer's instructions (Biorad,[37]). Samples were run at Bio-Plex Readers and the data were analysed by Bioplex Software. Briefly, beads coated with antibodies against the selected cytokines were mixed to 10 µl of serum and incubated at room temperature for 1 hour. Afrer incubation with streptavidin-PE detection reagent for 30 minutes and subsequent beads resuspension, the plate was read on the Bioplex instruments.

Quantification of atherosclerotic lesions

After sacrifice, aortas were dissected from heart to iliac branching, with particular attention at external fat in order to stain exclusively subintimal aortic fat. Aortas staining were performed as previously described [17]. Images were acquired using Nikon Coolscope (Nikon), and the fat amount was quantified with NIS elements program (Nikon). Results were statistically analyzed using GraphPad Prism (GraphPad Software). $p<0.05$ was considered statistically significant.

Acknowledgments

The work was supported by the Telethon grant GTF08013 and from MIUR, project PRIN protocol number 2004069479_004.

References

1. Fitzgerald, ML, Mujawar, Z, and Tamehiro, N (2010). ABC transporters, atherosclerosis and inflammation. *Atherosclerosis* 211: 361-370.

2. Yusuf, S*, et al.* (2004). Effect of potentially modifiable risk factors associated with myocardial infarction in 52 countries (the INTERHEART study): case-control study. *Lancet* 364: 937-952.

3. Civeira, F (2004). Guidelines for the diagnosis and management of heterozygous familial hypercholesterolemia. *Atherosclerosis* 173: 55-68.

4. Rashid, S, Marcil, M, Ruel, I, and Genest, J (2009). Identification of a novel human cellular HDL biosynthesis defect. *Eur Heart J* 30: 2204-2212.

5. Oram, JF, and Vaughan, AM (2006). ATP-Binding cassette cholesterol transporters and cardiovascular disease. *Circ Res* 99: 1031-1043.

6. Lewis, GF, and Rader, DJ (2005). New insights into the regulation of HDL metabolism and reverse cholesterol transport. *Circ Res* 96: 1221-1232.

7. Robinson, JG, Bakris, G, Torner, J, Stone, NJ, and Wallace, R (2007). Is it time for a cardiovascular primary prevention trial in the elderly? *Stroke* 38: 441-450.

8. Assmann, G, and Gotto, AM, Jr. (2004). HDL cholesterol and protective factors in atherosclerosis. *Circulation* 109: III8-14.

9. Van Craeyveld, E, Gordts, S, Jacobs, F, and De Geest, B (2010). Gene therapy to improve high-density lipoprotein metabolism and function. *Curr Pharm Des* 16: 1531-1544.

10. Van Lenten, BJ*, et al.* (2009). Apolipoprotein A-I mimetic peptides. *Curr Atheroscler Rep* 11: 52-57.

11. Harris, JD, Evans, V, and Owen, JS (2006). ApoE gene therapy to treat hyperlipidemia and atherosclerosis. *Curr Opin Mol Ther* 8: 275-287.

12. De Geest, B, Van Linthout, S, and Collen, D (2001). Sustained expression of human apo A-I following adenoviral gene transfer in mice. *Gene Ther* 8: 121-127.

13. Pastore, L*, et al.* (2004). Helper-dependent adenoviral vector-mediated long-term expression of human apolipoprotein A-I reduces atherosclerosis in apo E-deficient mice. *Gene* 327: 153-160.

14. Kassim, SH, Wilson, JM, and Rader, DJ (2010). Gene therapy for dyslipidemia: a review of gene replacement and gene inhibition strategies. *Clin Lipidol* 5: 793-809.

15. Toietta, G*, et al.* (2005). Lifelong elimination of hyperbilirubinemia in the Gunn rat with a single injection of helper-dependent adenoviral vector. *Proc Natl Acad Sci U S A* 102: 3930-3935.

16. Oka, K*, et al.* (2001). Long-term stable correction of low-density lipoprotein receptor-deficient mice with a helper-dependent adenoviral vector expressing the very low-density lipoprotein receptor. *Circulation* 103: 1274-1281.

17. Belalcazar, LM*, et al.* (2003). Long-term stable expression of human apolipoprotein A-I mediated by helper-dependent adenovirus gene transfer inhibits atherosclerosis progression and remodels atherosclerotic plaques in a mouse model of familial hypercholesterolemia. *Circulation* 107: 2726-2732.

18. Cerreto, M*, et al.* (2012). Reversal of metabolic and neurological symptoms of phenylketonuric mice treated with a PAH containing helper-dependent adenoviral vector. *Curr Gene Ther* 12: 48-56.

19. Croyle, MA*, et al.* (2005). PEGylated helper-dependent adenoviral vectors: highly efficient vectors with an enhanced safety profile. *Gene Ther* 12: 579-587.

20. Appledorn, DM*, et al.* (2008). Adenovirus vector-induced innate inflammatory mediators, MAPK signaling, as well as adaptive immune responses are dependent upon both TLR2 and TLR9 in vivo. *J Immunol* 181: 2134-2144.

21. Cerullo, V*, et al.* (2007). Toll-like receptor 9 triggers an innate immune response to helper-dependent adenoviral vectors. *Mol Ther* 15: 378-385.

22. Mane, VP*, et al.* (2006). Modulation of TNFalpha, a determinant of acute toxicity associated with systemic delivery of first-generation and helper-dependent adenoviral vectors. *Gene Ther* 13: 1272-1280.

23. Wonganan, P, Clemens, CC, Brasky, K, Pastore, L, and Croyle, MA (2011). Species differences in the pharmacology and toxicology of PEGylated helper-dependent adenovirus. *Mol Pharm* 8: 78-92.

24. Alemany, R, Suzuki, K, and Curiel, DT (2000). Blood clearance rates of adenovirus type 5 in mice. *J Gen Virol* 81: 2605-2609.

25. Ishibashi, S, Brown, MS, Goldstein, JL, Gerard, RD, Hammer, RE, and Herz, J (1993). Hypercholesterolemia in low density lipoprotein receptor knockout mice and its reversal by adenovirus-mediated gene delivery. *J Clin Invest* 92: 883-893.

26. Tangirala, RK, Rubin, EM, and Palinski, W (1995). Quantitation of atherosclerosis in murine models: correlation between lesions in the aortic origin and in the entire aorta, and differences in the extent of lesions between sexes in LDL receptor-deficient and apolipoprotein E-deficient mice. *J Lipid Res* 36: 2320-2328.

27. Brunetti-Pierri, N, and Ng, P (2009). Progress towards liver and lung-directed gene therapy with helper-dependent adenoviral vectors. *Curr Gene Ther* 9: 329-340.

28. Brunetti-Pierri, N*, et al.* (2005). Sustained phenotypic correction of canine hemophilia B after systemic administration of helper-dependent adenoviral vector. *Hum Gene Ther* 16: 811-820.

29. Brunetti-Pierri, N*, et al.* (2007). Pseudo-hydrodynamic delivery of helper-dependent adenoviral vectors into non-human primates for liver-directed gene therapy. *Mol Ther* 15: 732-740.

30. De Geest, B, Snoeys, J, Van Linthout, S, Lievens, J, and Collen, D (2005). Elimination of innate immune responses and liver inflammation by PEGylation of adenoviral vectors and methylprednisolone. *Hum Gene Ther* 16: 1439-1451.

31. Raper, SE*, et al.* (2003). Fatal systemic inflammatory response syndrome in a ornithine transcarbamylase deficient patient following adenoviral gene transfer. *Mol Genet Metab* 80: 148-158.

32. Brunetti-Pierri, N, Palmer, DJ, Beaudet, AL, Carey, KD, Finegold, M, and Ng, P (2004). Acute toxicity after high-dose systemic injection of helper-dependent adenoviral vectors into nonhuman primates. *Hum Gene Ther* 15: 35-46.

33. Muruve, DA (2004). The innate immune response to adenovirus vectors. *Hum Gene Ther* 15: 1157-1166.

34. Flynn, R, Buckler, JM, Tang, C, Kim, F, and Dichek, DA (2010). Helper-dependent adenoviral vectors are superior in vitro to first-generation vectors for endothelial cell-targeted gene therapy. *Mol Ther* 18: 2121-2129.

35. Palmer, D, and Ng, P (2003). Improved system for helper-dependent adenoviral vector production. *Mol Ther* 8: 846-852.

36. Toietta, G, Pastore, L, Cerullo, V, Finegold, M, Beaudet, AL, and Lee, B (2002). Generation of helper-dependent adenoviral vectors by homologous recombination. *Mol Ther* 5: 204-210.

37. Heinze, DM, Wikel, SK, Thangamani, S, and Alarcon-Chaidez, FJ (2012). Transcriptional profiling of the murine cutaneous response during initial and subsequent infestations with Ixodes scapularis nymphs. *Parasit Vectors* 5: 26.

Figure legends

Figure 1. PEG-HD-Ad-AI and HD-Ad-AI vector treatment induce Apo A-I expression in vitro and in vivo.

293 (panel A) and W20-17 (panel B) cells have been infected with HD-Ad-AI and PEG-HD-Ad-AI and human Apo A-I secreted in the medium was determined. Uninfected 293 and W20-17 cells were used as negative controls. Infection with both vectors led to a significant increase in human Apo A-I levels in the medium in both cells lines. LDLR-deficient mice were treated systemically with 1x10E13 vp/kg of either HD-Ad-AI (■) or PEG-HD-Ad-AI (▲); a third group of mice was treated with the same volume of PBS as control (●). Human Apo A-I levels were determined from blood samples 1, 2, 4, 8 and 12 weeks after treatment (panel C). Mice treated with either HD-Ad-AI or PEG-HD-Ad-AI showed long-term high levels of human Apo A-I expression that lasted for the entire duration of the experiment.

Figure 2. Administration of PEG-HD-Ad-AI in LDLR$^{-/-}$ mice is associated to a lower toxicity compared to unmodified vector.

LDLR-deficient mice were treated systemically with 1x10E13 vp/kg of either PEG-HD-Ad-AI or HD-Ad-AI; a third group of mice was treated with the same volume of PBS as negative control. Six hours after the administration blood samples were collected and cytokines level were determined. Levels of IL12p70 (panel A), IL12p40 (panel B), IL-6 (panel C), KC (panel D), MCP1 (panel E) and TNF-alpha (panel F) were compared between different

groups to evaluate vectors toxicity. Statistically significant differences were expressed as *p<0.05 and **p<0.01

Figure 3. Administration of PEG-HD-Ad-AI increases Apo A-I levels and modify cholesterol metabolism in LDLR$^{-/-}$ mice.

LDLR-deficient mice were treated systemically with 1x10E13 vp/kg of either HD-Ad-AI (■) or PEG-HD-Ad-AI (▲). A group of mice was treated with the same volume of PBS as control (●). Samples were collected prior to treatment and 1, 2, 4, 8 and 12 weeks after administration. Levels of triglycerides (panel A; HD-Ad-AI vs. control, p<0.05), total cholesterol (TC, panel B; PEG-HD-AI vs. control, p<0.01), LDL cholesterol (LDL-C, panel C; PEG-HD-Ad-AI vs. control, p<0.01), HDL cholesterol (HDL-C, panel D; HD-Ad-AI vs. control, p<0.01, PEG-HD-Ad-AI vs. control, p<0.05), and human Apo A-I (panel E; HD-Ad-AI vs. control, p<0.01, PEG-HD-Ad-AI vs. control, p<0.01) were determined and differences compared to control group were determined.

Figure 4. PEG-HD-Ad-A-I treatment reduces aortic atherosclerosis development

LDLR-deficient mice were treated systemically with 1x10E13 vp/kg of either HD-Ad-AI or PEG-HD-Ad-AI; a third group of mice was treated with the same volume of PBS as control. Twelve weeks after administration mice were sacrificed and aortas were dissected. Fat deposits in aortic arch and abdominal aorta were visibly reduced in mice treated with PEG-HD-Ad Apo AI and HD-Ad Apo AI compared to the control group (panel A). Aortas were then stained with O-Red-Oil to identify fat deposits in LDLR-deficient mice treated with 1x10E13 vp/kg of either HD-Ad-AI (■) or PEG-HD-Ad-AI (▲) and compared to the

control group that received PBS (●). Stained areas were measured and compared to the area of the entire aorta as index of atherosclerotic lesions; statistically significant differences were expressed as *$p<0.05$ and **$p<0.01$.

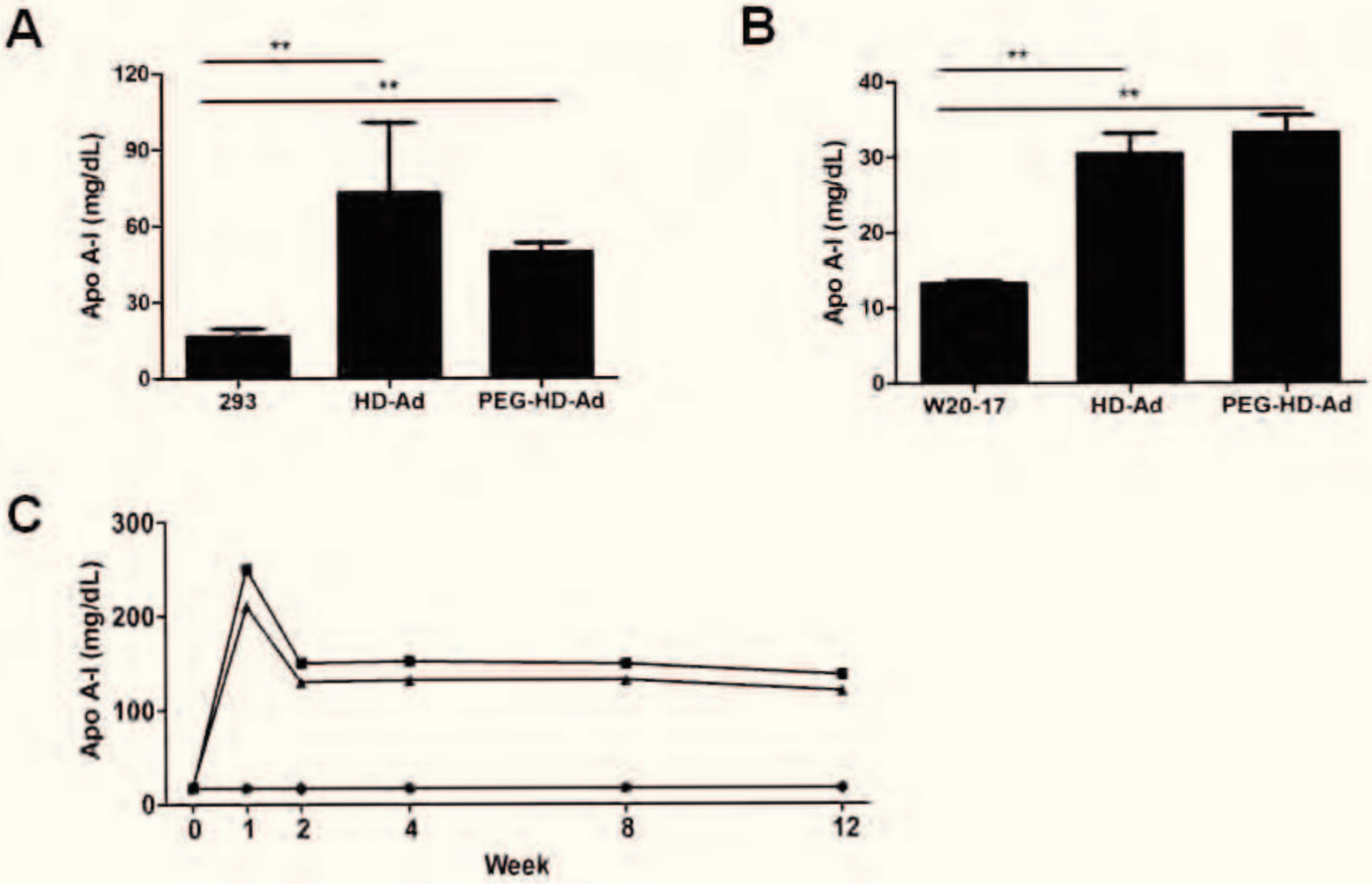
A
**
**
120
90
60
30
0
Apo A-I (mg/dL)
293
HD-Ad
PEG-HD-Ad
B
**
**
40
30
20
10
0
Apo A-I (mg/dL)
W20-17
HD-Ad
PEG-HD-Ad
C
300
200
100
0
Apo A-I (mg/dL)
0
1
2
4
8
12
Week

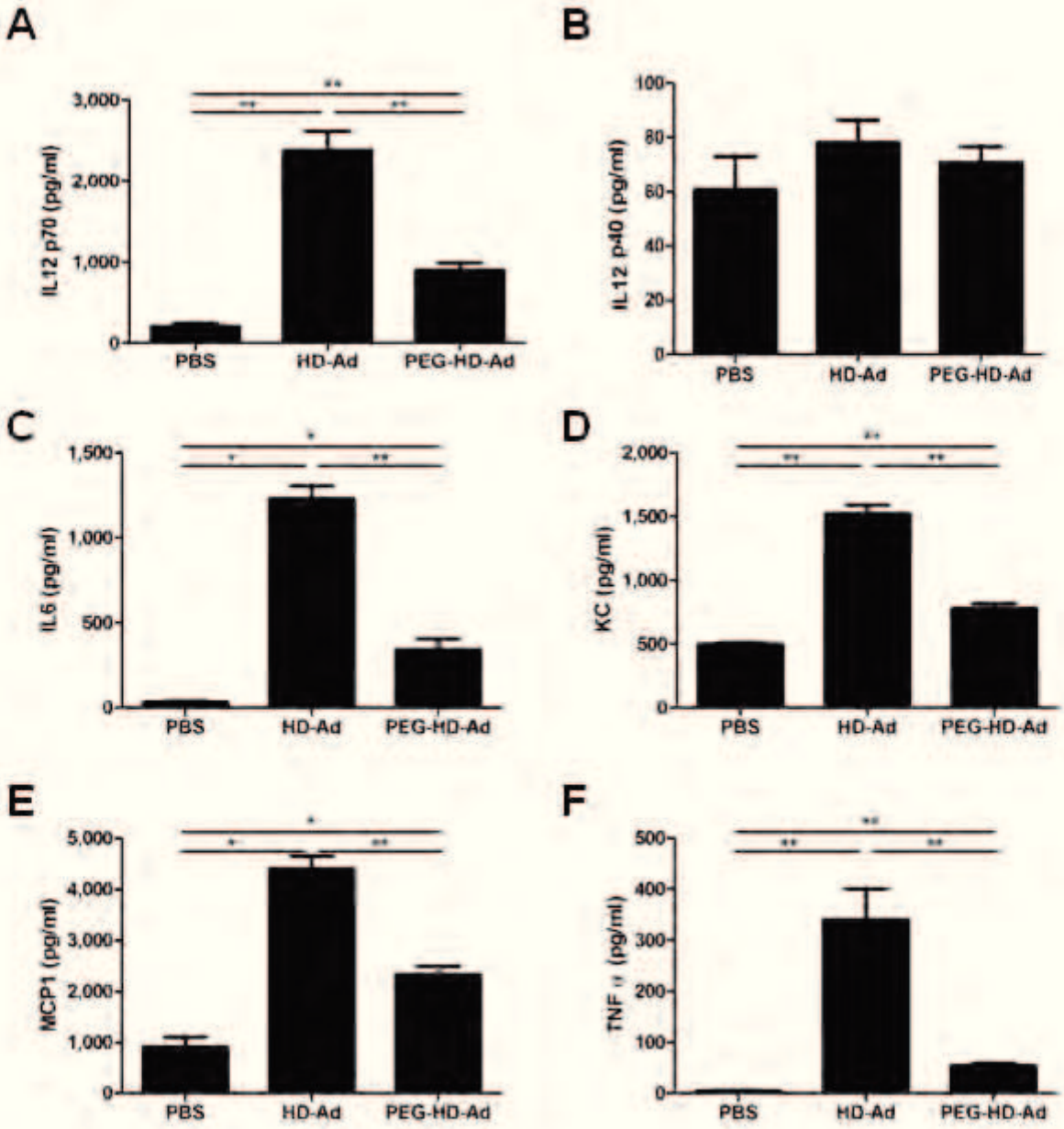
A
IL12 p70 (pg/ml)
3,000
2,000
1,000
0
PBS
HD-Ad
PEG-HD-Ad
B
IL12 p40 (pg/ml)
100
80
60
40
20
0
PBS
HD-Ad
PEG-HD-Ad
C
IL6 (pg/ml)
1,500
1,000
500
0
PBS
HD-Ad
PEG-HD-Ad
D
KC (pg/ml)
2,000
1,500
1,000
500
0
PBS
HD-Ad
PEG-HD-Ad
E
MCP1 (pg/ml)
5,000
4,000
3,000
2,000
1,000
0
PBS
HD-Ad
PEG-HD-Ad
F
TNF (pg/ml)
500
400
300
200
100
0
PBS
HD-Ad
PEG-HD-Ad

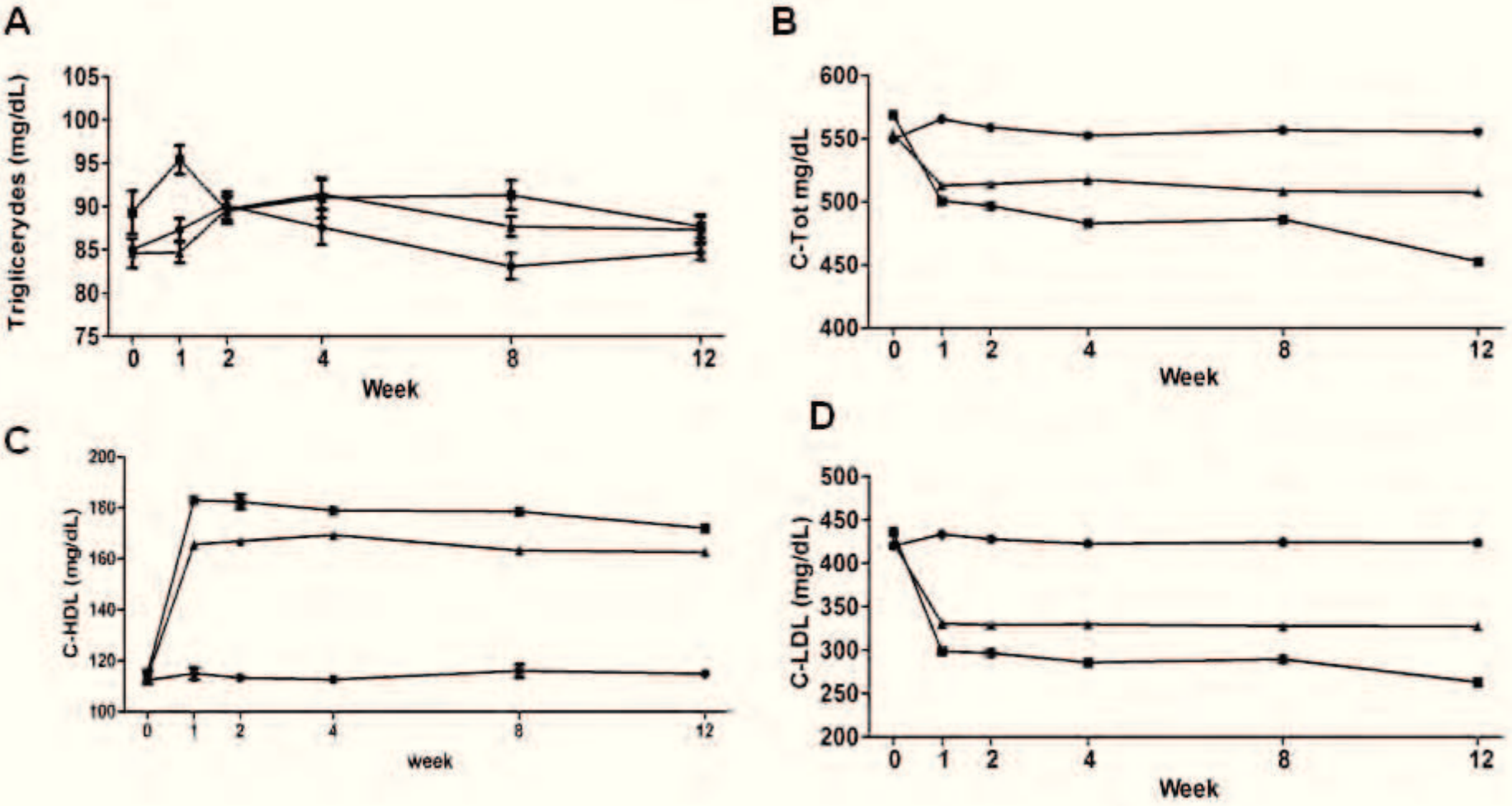
A
Triglicerydes (mg/dL)
105
100
95
90
85
80
75
0
1
2
4
8
12
Week
B
C-Tot mg/dL
600
550
500
450
400
0
1
2
4
8
12
Week
C
C-HDL (mg/dL)
200
180
160
140
120
100
0
1
2
4
8
12
week
D
C-LDL (mg/dL)
500
450
400
350
300
250
200
0
1
2
4
8
12
Week

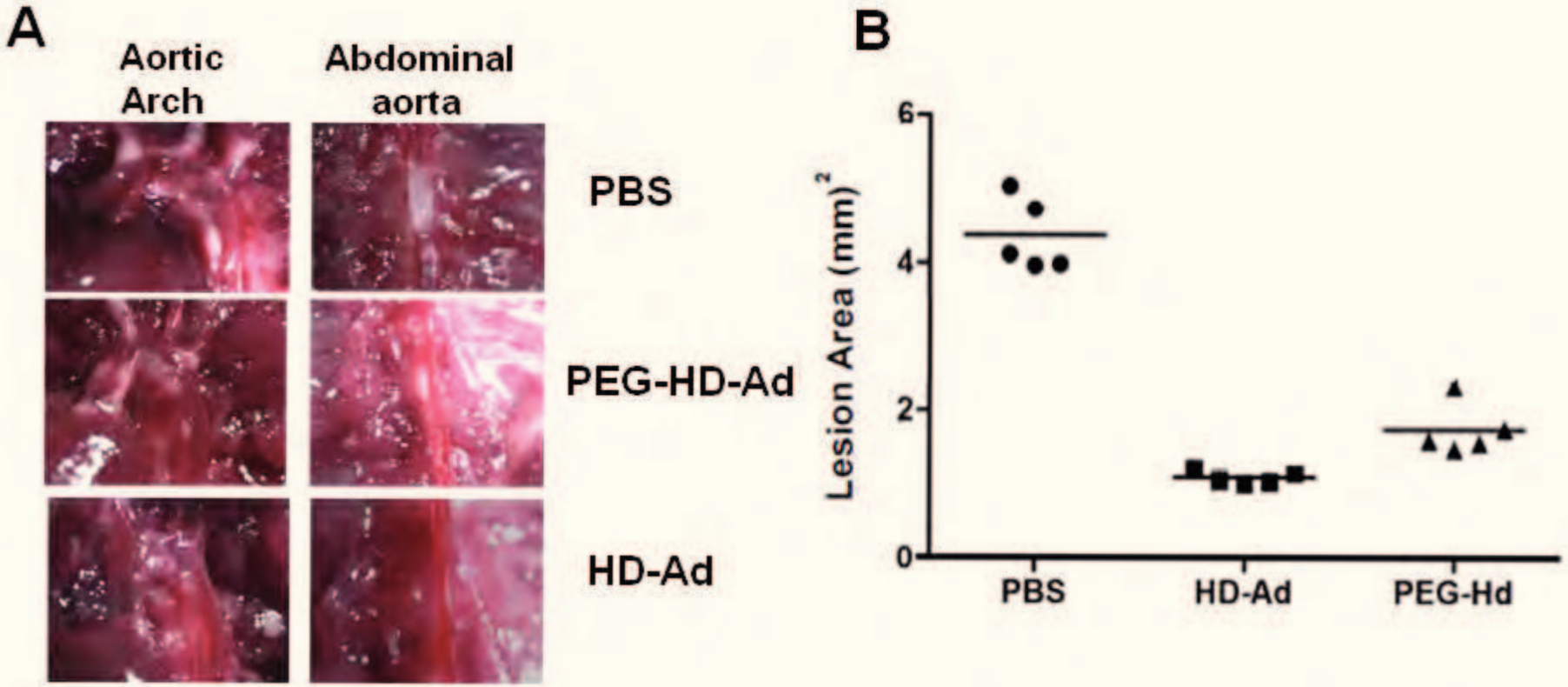
A
Aortic Arch
Abdominal aorta
PBS
PEG-HD-Ad
HD-Ad
B
Lesion Area (mm)²
6
4
2
0
PBS
HD-Ad
PEG-Hd

MC4R, SIRT1 and FTO gene polymorphisms and metabolic syndrome in morbidly obese subjects from southern Italy

Fabrizio Pasanisi[1]*, Rosario Liguori[2, 3]*, Giuseppe Labruna[4], Andreina Alfieri[2, 5], Domenico Martone[2,5], Eduardo Farinaro[6], Franco Contaldo[1], Lucia Sacchetti[2, 3], Pasqualina Buono[4, 5, #].

[1]Centro Interuniversitario di Studi e Ricerche sull'Obesità e Dipartimento di Medicina Clinica e Chirurgia, Università degli Studi di Napoli Federico II, Naples, Italy; [2]CEINGE Biotecnologie Avanzate S.C. a R.L., Naples, Italy; [3]Dipartimento di Medicina Molecolare e Biotecnologie Mediche, Università degli Studi di Napoli Federico II, Naples, Italy; [4]Fondazione IRCCS SDN, Istituto di Ricerca Diagnostica e Nucleare, Naples, Italy; [5]Dipartimento di Studi delle Istituzioni e dei Sistemi Territoriali, Università degli Studi di Napoli "Parthenope", Naples, Italy; [6]Dipartimento di Sanità Pubblica, Università degli Studi di Napoli Federico II, Naples, Italy

*These authors contributed equally to the study.

[#]Correspondence: P. Buono, Dipartimento di Studi delle Istituzioni e dei Sistemi Territoriali, Università degli Studi di Napoli "Parthenope" Via Medina 40, 80133 Naples, Italy; Phone:+39 081 7463146; Fax: +39 081 7464359. E-mail: buono@uniparthenope.it.

Running title: FTO polymorphisms and MS in morbid obesity

Abstract

Objective: *MC4R*, *SIRT1* and *FTO* variants are associated with severe obesity and metabolic impairment in various populations. We investigated the association of common *MC4R*, *SIRT1* and *FTO* variants with obesity and metabolic syndrome (MS) in a large group of severely obese young adults from southern Italy.

Subjects and Methods: 1000 morbidly obese subjects (62% women, mean body mass index [BMI] 46.5 kg/m2, mean age 32.6y) and 100 normal weight healthy controls whose families had lived in southern Italy for at least 2 generations were recruited. Single-nucleotide polymorphisms (SNPs) rs12970134, rs477181, rs502933 (*MC4R* locus), rs3818292, rs7069102, rs730821, rs2273773, rs12413112 (*SIRT1* locus) and rs1421085, rs9939609, 9930506, 1121980 (*FTO* locus) were genotyped by Taqman assay; blood parameters were assayed by routine methods; fat mass, free fat mass, respiratory quotient, basal metabolic rate (BMR) and waist circumference were also determined.

Results: The frequency of 5 SNP genotypes differed significantly between obese and control subjects: rs12413112 ($p=0.037$) in the *SIRT1* gene, rs1421085 ($p=0.003$), rs9939609 ($p<0.0001$), rs9930506 ($p<0.0001$) and rs1121980 ($p=0.007$) in the *FTO* gene. Binomial logistic regression confirmed the association of rs9939609 (*FTO*) with obesity. In fact, the AA mutated homozygous genotype conferred an odds ratio (OR) of 3.79 (1.91-7.50) for obesity. Binomial logistic regression analysis showed that the *TA* heterozygous genotype of the rs9939609 SNP in the *FTO* gene was associated with the presence of MS in our patients (OR/95% CI: 2.53/1.16-5.55).

Conclusions: The FTO rs9939609 SNP and male gender accounted for 11.6% of obese phenotype whereas FTO rs9939609 SNP, total cholesterol, BMR and age accounted for 21.3% with the MS phenotype. Our results enlarge the knowledge on genotype susceptibility for obesity and for MS in relation to a specific geographical area of residence.

Key words: Morbid obesity; SNPs; FTO, MC4R, SIRT1, metabolic syndrome.

INTRODUCTION

Obesity is a condition in which the imbalance between energy intake and expenditure causes excessive fat accumulation and predisposes to a high risk of metabolic diseases and premature death.[1] Human obesity is due to a complex interaction among environmental, behavioral, developmental and genetic factors. The latter account for 40-70% of the obese phenotype.[2]

Rare monogenic forms of obesity are mainly caused by impairment of the leptin-melanocortin hypothalamic circuit due to mutations in genes involved in food intake, particularly leptin and its receptor (*LEPR*), proopiomelanocortin (*POMC*) and melanocortin receptor 4 (*MC4R*).[3]

Genomewide association studies have shown that polymorphisms in the latter and in other genes are involved in common obesity or in obese-associated diseases. Globally, at least 50 genetic loci, each exerting a small effect, appear to contribute to common obesity insurgence.[4] Among the polymorphisms identified by genome-wide association studies, those in the *MC4R*, in the Fat Mass and Obesity (*FTO*) and in the Sirtuin1 (*SIRT1*) genes regulate energy metabolism and/or insulin sensitivity and/or adipogenesis[5-7].

In this study we investigated the association of three common variants in the *MC4R* locus (rs12970134, rs477181, rs502933), five common variants in the *SIRT1* gene (rs3818292, rs7069102, rs730821, rs2273773, rs12413112) and four in the *FTO* gene (rs1421085, rs9939609, rs9930506, rs1121980) with several parameters associated to obesity and the metabolic syndrome (MS), in a large population of morbidly obese young adults whose families have lived in southern Italy for at least 2 generations.

PATIENTS AND METHODS

Subjects

Control subjects (n=100, 33% women, mean/SEM body mass index [BMI] 23.2/0.28 kg/m2, mean/SEM age 29.9/1.03 y) and morbidly obese patients (n=1000, 62% women, mean/SEM BMI 46.5/0.23 kg/m2, mean/SEM age 32.6/0.36 y) respectively were recruited at the Department of

Preventive Medical Science and at the Obesity Outpatient Clinic of the Department of Clinical and Experimental Medicine, University of Naples Federico II (Italy), from 2007 to 2008. The families of all subjects had lived in the same region of south Italy for at least two generations. All patients and controls gave their informed consent to the study, which was carried out according to the Helsinki II Declaration. The research was approved by the Ethics Committee of the School of Medicine, University of Naples Federico II.

Two blood samples (one for biochemical analysis and one for DNA extraction) were obtained from each enrolled subject after an overnight fast. Biochemical parameters were measured enzymatically with routine methods on an automated analyzer (Hitachi 747; Boehringer Mannheim, Germany). The HDL-cholesterol concentration was determined enzymatically by measuring cholesterol in the supernatant after precipitation with phosphotungstate. Insulin resistance was estimated in obese subjects according to the homeostasis model assessment (HOMA) and the formula: fasting insulin (mU/L) X fasting glucose (mmol/L)/22.5. We also calculated the fatty liver index (FLI) according to the formula FLI = (e0.953 × ln (triglycerides) + 0.139 × BMI + 0.718 × ln (GGT) + 0.053 × waist circumference−15.745)/ (1 + e0.953 × ln (triglycerides) + 0.139 × BMI + 0.718 × ln (GGT) + 0.053 × waist circumference−15.745) X100 as a measure of hepatic steatosis.[8]

The clinical and anamnestic data of each obese subject were collected and the main metabolic parameters were evaluated. In particular, fat mass (FM) and fat free mass (FFM) measurements were obtained by bioimpedentiometric analysis (Sta/BIA Akern, Firenze, Italy), and respiratory quotient (RQ) and basal metabolic rate (BMR) by indirect calorimetry (Sensor Medics Vmax29, Anaheim, USA). The BMI was calculated as ratio weight (kg)/height (m^2). Systolic and diastolic blood pressure and cardiac frequency (beats/min) were collected by standard procedures.

The presence of MS, a cluster of metabolic risk factors, namely, abdominal obesity, dyslipidemia (hypertriglyceridemia and low HDL-cholesterol concentrations), elevated blood pressure and hyperglycemia, as defined by the American Heart Association criteria, was diagnosed if 3 out of 5 criteria were present.[9]

DNA extraction and real time Taqman assay

Genomic DNA was extracted from peripheral blood samples with the Nucleon BACC2 kit (Amersham Life Science, Little Chalfont, Bucks, UK) and all the SNPs (*MC4R* locus: rs12970134, rs477181, rs502933; *SIRT1* gene: rs3818292, rs7069102, rs730821, rs2273773, rs12413112; *FTO* gene: rs1421085, rs9939609, rs9930506, rs1121980) were assayed, in duplicate, by the real time Taqman assay (Applied Biosystems, Foster City, CA, USA). Briefly, two probes are used in a biallelic system; one probe is specific for the wild type allele and the other is complementary to the mutant allele. The alleles are distinguished with fluorogenic probes, which consist of an oligonucleotide with a fluorescent reporter dye (VIC or FAM) a non-fluorescent quencher and a minor groove binder (MGB). The latter molecule forms a hyperstabilized duplex with complementary DNA thereby increasing the capacity of the hybridization probe to discriminate the SNP. The Primer Express program (Applied Biosystems) was used to design the PCR primers and the MGB TaqMan probes. Reaction mixtures were assembled in a 384-well plate using a Biomek 2000 Workstation (Beckman Instruments Inc., Fullerton, CA, USA). Together with samples from obese and control subjects, we tested negative (i.e., no DNA sample) and positive (i.e., homozygotes and a heterozygote, for the SNP) controls. The positive controls had been previously typed by sequence analysis on an ABI 3100 Genetic Analyzer (Applied Biosystems). Real-time PCR was performed on an ABI Prism 7900- HT instrument with the Sequence Detection System (SDS 2.1) and the SDS Enterprise Database (Applied Biosystems).

Statistical analysis

Genotype frequencies were calculated by allele counting, and departure from Hardy-Weinberg expectation was evaluated by χ^2 analysis. The mean value and the standard error of the mean (SEM) were calculated for each investigated parameter. The Student *t* test and/or χ^2, where appropriate, were used for between-group comparisons. Differences were considered statistically

significant at a $p<0.05$ level. Multiple comparisons were corrected by using the Bonferroni test. Binomial logistic regression analysis was used to investigate the association between the biochemical, clinical and genetic characteristics and the obese phenotype or the presence of MS, as described above. Linkage analysis was performed with Haploview software (version 4.2). Statistical analyses were carried out with the PASW package for Windows (Ver.18; SPSS Inc. Headquarters, Chicago, Ill, USA).

Results

The clinical and biochemical characteristics of the obese subjects (62% women) are reported in Table 1. Metabolic syndrome was present in 37.2 % of our obese subjects, and was significantly more frequent in men than in women (43% versus 34%; $p=0.006$). The genotype frequencies of the investigated SNPs in the *MC4R*, *SIRT1* and *FTO* genes were in Hardy-Weinberg equilibrium ($0.11< p <0.9$) and are reported in Table 2. To verify that our control group, albeit small, could be considered representative of the Caucasian population, we compared the genotype frequencies of each SNP in our controls to those reported in the National Center for Biotechnology Information database (www.ncbi.nlm.nih.gov, accessed October 2012) and found no statistically significant differences (Supplemental Table 1), which suggests that our control group is indeed representative of the Caucasian population.

The χ^2 test revealed that the genotype frequency of 5 polymorphisms differed significantly between obese and control subjects: rs12413112 ($p=0.037$) in the *SIRT1* gene, rs1421085 ($p=0.003$), rs9939609 ($p<0.0001$), rs9930506 ($p<0.0001$) and rs1121980 ($p=0.007$) in the *FTO* gene (Table 2). These associations remained statistically significant also after a permutation test with 100,000 permutations ($0.0006<p<0.03$). In particular, the recessive allele, G, of rs12413112 in *SIRT1* was negatively associated with the obese phenotype, suggesting that this allele plays a protective role in obesity insurgence. Haplotyping with the Haploview software showed a significant linkage disequilibrium between rs12413112 and rs7069102 in *SIRT1*, and rs2273773 and

rs3818292 also in *SIRT1;* a significant linkage disequilibrium was also found among the three tested SNPs in *MC4R* (Figure 1). The *AC* haplotype of the first two SNPs in *SIRT1* was negatively associated with the obese phenotype (p=0.01; p=0.04 after 100,000 permutations), whereas only a weak association was found between the *GTA* haplotype in *MC4R* and obesity (p=0.04, not confirmed after the permutation test).

Binomial logistic regression analysis, after correction for age and sex, confirmed that rs9939609 (*FTO*), the heterozygous and mutated homozygous genotypes, and male sex were associated with obesity (Table 3A). In particular, patients bearing the *TA* heterozygous genotype had an OR equal to 2.51 (95% CI: 1.43-4.46), whereas patients bearing the *AA* mutated homozygous genotype had an OR of 3.79 (1.91-7.50). Our results demonstrate that the FTO rs9939609 SNP and male gender accounted for 11.6% of the obese phenotype (according to the Nagelkerke model). Binomial logistic regression analysis showed that the *TA* heterozygous genotype of the rs9939609 SNP in the *FTO* gene was associated with the presence of MS in our patients (OR/95% CI: 2.53/1.16-5.55), whereas only weak associations were found for total cholesterol, BMR and age (Table 3B). The final model showed a Nagelkerke $R^2 = 0.213$, which indicates that the tested clinical, biochemical and genetic variables accounted for 21.3% of the MS phenotype.

Discussion

We evaluated 12 common obesity-related variants in the *SIRT1*, *FTO* and *MC4R* genes in a large population of morbidly obese young adults from southern Italy to identify variants specifically correlated to the obese phenotype or to obesity-associated metabolic complications such as MS. The prevalence of MS in our obese subjects (37.2 %) was comparable to those reported in a multicenter study carried out in Italy (38%)[10] and in European and US Caucasian populations of a similar age range.[11] This suggests that obesity and MS could result from a similar unhealthy lifestyle in these populations.

Among the investigated polymorphisms in *SIRT 1*, rs2272773 was associated with BMR in a Finnish population[12] and with BMI in a Dutch population;[13] rs7069102 was associated with obesity in a Belgian population;[14] and in the same Belgian study, rs3818292 was associated to visceral fat only in obese males.[14] Finally, 4 of the 5 *SIRT1* variants that we analyzed were found to be associated with a metabolic and lifestyle intervention program in a cross-sectional study.[15] In our obese subjects the rs3818292, rs7069102, rs730821, rs2273773, rs12413112 polymorphisms were not correlated with BMI, BMR, abdominal adiposity or lifestyle at multivariate regression analysis. This discrepancy could be due to differences in the populations investigated. In fact, the patients in the Finnish, Dutch and Belgian studies differed from our obese subjects in terms of age and BMI. Differently, our data coincide with those of Clark et al.[16] who found a positive association between the recessive allele, G, of rs12413112 in *SIRT1* and the non-obese phenotype, which indicates that this allele plays a protective role also in our study population.

Mutations in the *MC4R* gene account for about 4-5% of monogenic forms of human obesity,[17] and for 2.5% in our population.[18,19] The three common variants in the *MC4R* locus, rs12970134, rs477181, rs502933, that we investigated, were recently reported to be associated with BMI, waist circumference and insulin resistance in a Indian-Asian population,[20] and with obesity in a Scottish population.[21] In our study, there was a significant linkage disequilibrium among the three tested *MCR4R* SNPs; haplotype *GTA* was only weakly associated with morbid obesity, but we found no association with MS. Again, a different genetic background and different clinical characteristics could explain our discordant data concerning the relevance of these polymorphisms in glycemic control.

Based on genome-wide association studies conducted in various populations, *FTO* appears to be the gene most often related to obesity development.[22] In particular, SNP rs9939609, located within the first intron of the *FTO* gene, has been reported to be closely associated with BMI in obese children and adults in Europe.[22-24] Moreover, a positive association was recently reported between the rs9939609 *FTO* genetic variant and risk for obesity and type 2 diabetes in East and

South Asians.[25] In addition, SNP rs9939609 was reported to be associated with increased cardiovascular risk and diabetes in the Finnish Diabetes Prevention Study.[26], Furthermore, in all previous studies the FTO rs9939609 SNP association with obesity and metabolic impairment was affected by age, gender, or ethnic background, as well as by physical activity and educational level.[23, 27-35]

In our study, all the 4 *FTO* polymorphisms investigated were significantly associated with the obese phenotype ($0.0001<p<0.003$). In particular, the homozygous genotype variants of all FTO SNPs were at least 1.5-fold higher in the obese subjects than in the control group. The presence of the *AA* genotype in the rs9939609 *FTO* SNP conferred the highest risk for obesity (OR=3.79 - 95% CI: 1.91-7.50), followed by male gender (OR =3.46- 95%CI: 2.07-5.79). Interestingly, the rs9939609 *FTO* SNP was a strong risk factor for MS in our population (OR=2.53- 95% CI: 1.16-5.55); in fact, the *TA* heterozygous genotype, together with total cholesterol, BMR and age accounted for 21.3% of this syndrome. Our data are in agreement with the recently reported associations between rs9939609 and MS in European and in other ethnic groups.[36-38]

In conclusion, we identified a strong association between the *A* allele in the *FTO* rs9939609 SNP and MS in a population of morbidly obese subjects living in southern Italy. This confirms that the *A* allele conferred a greater susceptibility to develop MS also in our study population. Our data also revealed that the FTO rs9939609 SNP and male gender accounted for 11.6% of obese phenotype whereas FTO rs9939609 SNP, total cholesterol, BMR and age accounted for 21.3% with the MS phenotype. Our results enlarge the knowledge on genotype susceptibility for obesity and for MS in relation to specific geographical area of residence.

Acknowledgements: This work was supported by grants from MIUR, PRIN 2008, Italy and from CEINGE-biotecnologie avanzate s.ca.r.l. Naples, Italy. We are indebted to Jean Ann Gilder (Scientific Communication srl, Naples, Italy) for text editing.

Conflict of interest: The authors declare no conflict of interest.

References

1 Guh DP, Zhang W, Bansback N, Amarsi Z, Birmingham CL, Anis AH. The incidence of comorbidities related to obesity and overweight: a systematic review and meta-analysis. *BMC Public Health.* 2009;**9**:88

2 Marti A, Martinez-González MA, Martinez JA. Interaction between genes and lifestyle factors on obesity. *Proc Nutr Soc.* 2008; **67**: 1-8.

3 Ramachandrappa S, Farooqi IS. Genetic approaches to understanding human obesity. *J Clin Invest* 2011;**121**:2080-2086.

4 Day FR, Loos RJ. Developments in obesity genetics in the era of genome-wide association studies. *J Nutrigenet Nutrigenomics* 2011;**4**:222-238.

5 Chambers JC, Elliott P, Zabaneh D, Zhang W, Li Y, Froguel P *et al*. Common genetic variation near MC4R is associated with waist circumference and insulin resistance. *Nat Genet* 2008; **40**: 716-718.

6 Peng S, Zhu Y, Xu F, Ren X, Li X, Lai M. FTO gene polymorphisms and obesity risk: a metaanalysis. *BMC Med* 2011;**9**:71.

7 Wang Y, Xu C, Liang Y, Vanhoutte PM. SIRT1 in metabolic syndrome: Where to target matters. *Pharmacol Ther* 2012;**136**:305-318.

8 Bedogni G, Bellentani S, Miglioli L, Masutti F, Passalacqua M, Castiglione A *et al*. The Fatty Liver Index: a simple and accurate predictor of hepatic steatosis in the general population. *BMC Gastroenterol* 2006; **6**: 33.

9 Grundy SM, Cleeman JI, Daniels SR, Donato KA, Eckel RH, Franklin BA *et al*. American Heart Association; National Heart, Lung, and Blood Institute. Diagnosis and management of the metabolic syndrome: an American Heart Association/National Heart, Lung, and Blood Institute Scientific Statement. *Circulation* 2005, **112**: 2735-2752.

10 Marchesini G, Melchionda N, Apolone G, Cuzzolaro M, Mannucci E, Corica F *et al.* QUOVADIS Study Group. The metabolic syndrome in treatment-seeking obese persons.

Metabolism 2004, **53**: 435-440.

11 Eckel RH, Grundy SM, Zimmet PZ. The metabolic syndrome. *Lancet* 2005, **365**: 1415-1428.

12 Lagouge M, Argmann C, Gerhart-Hines Z *et al*. Resveratrol improves mitochondrial function and protects against metabolic disease by activating SIRT1 and PGC-1alpha. *Cell* 2006;**127**:1109–1122.

13 van den Berg SW, Dollé ME, Imholz S *et al*. Genetic variations in regulatory pathways of fatty acid and glucose metabolism are associated with obesity phenotypes: a population-based cohort study. *Int J Obes (Lond)* 2009; **33**:1143–1152.

14 Peeters AV, Beckers S, Verrijken A, Mertens I, Roevens P, Peeters PJ, Van Hul W, Van Gaal LF. Association of SIRT1 gene variation with visceral obesity. Hum Genet 2008; **124**:431-436.

15 Weyrich P, Machicao F, Reinhardt J, Machann J, Schick F, Tschritter O *et al*. SIRT1 genetic variants associate with the metabolic response of Caucasians to a controlled lifestyle intervention--the TULIP Study. *BMC Med Genet* 2008; **12**:100-107.

16 Clark SJ, Falchi M, Olsson B, Jacobson P, Cauchi S, Balkau B *et al*. Association of sirtuin 1 (SIRT1) gene SNPs and transcript expression levels with severe obesity. *Obesity* 2012; **20**:178-185.

17 Farooqi IS. Monogenic human obesity. *Front Horm Res* 2008; **36**: 1-11.

18 Buono P, Pasanisi F, Nardelli C, Ieno L, Capone S, Liguori R *et al.* Six novel mutations in the proopiomelanocortin and melanocortin receptor 4 genes in severely obese adults living in southern Italy. *Clin Chem* 2005 ; **51**: 1358-1364.

19 Alfieri A, Pasanisi F, Salzano S, Esposito L, Martone D, Tafuri D *et al.* Functional analysis of melanocortin-4-receptor mutants identified in severely obese subjects living in Southern Italy. *Gene* 2010; **457**: 35-41.

20 Chambers JC, Elliott P, Zabaneh D, Zhang W, Li Y, Froguel P, Balding D *et al.* Common genetic variation near MC4R is associated with waist circumference and insulin resistance. *Nat Genet* 2008; **40**: 716-718.

21 Tenesa A, Campbell H, Theodoratou E, Dunlop L, Cetnarskyj R, Farrington SM *et al*. Common genetic variants at the MC4R locus are associated with obesity, but not with dietary energy intake or colorectal cancer in the Scottish population. *Int J Obes (Lond)* 2009; **33**: 284-288.

22 Scuteri A, Sanna S, Chen W, Uda M, Albai G, Strait J *et al*. Genome-wide association scan shows genetic variants in the FTO gene are associated with obesity-related traits. *PLoS Genet* 2007; **3**: e115.

23 Frayling TM, Timpson NJ, Weedon MN, Zeggini E, Freathy RM, Lindgren CM *et al*. A common variant in the FTO gene is associated with body mass index and predisposes to childhood and adult obesity. *Science* 2007; **316** :889.

24 González-Sánchez JL, Zabena C, Martínez-Larrad MT, Martínez-Calatrava MJ, Pérez-Barba M and Serrano-Ríos M. Variant rs9939609 in the FTO gene is associated with obesity in an adult population from Spain. *Clinical Endocrinology* 2009; **70**: 390–393.

25 Li H, Kilpeläinen YO, Liu C, Zhu J, Liu Y, Hu C *et al.* Association of genetic variation in FTO with risk of obesity and type 2 diabetes with data from 96,551 East and South Asians. *Diabetologia* 2012; **55**: 981–995.

26 Lappalainen T, Kolehmainen M, Schwab US, Tolppanen AM, Stancakova A, Lindström J *et al*. Association of the FTO gene variant (rs9939609) with cardiovascular disease in men with abnormal glucose metabolism -The Finnish Diabetes Prevention Study. *Nutr Metab Cardiovasc Dis* 2011; **21**: 691-698.

27 Jacobsson JA, Risérus U, Axelsson T, Lannfelt L, Schiöth HB, Fredriksson R. The common FTO variant rs9939609 is not associated with BMI in a longitudinal study on a cohort of Swedish men born 1920-1924. *BMC Med Genet* 2009; **10**: 131.

28 Hennig BJ, Fulford AJ, Sirugo G, Rayco-Solon P, Hattersley AT, Frayling TM *et al.* FTO gene variation and measures of body mass in an African population. *BMC Med Genet* 2009; **10**:21.

29 Ohashi J, Naka I, Kimura R, Natsuhara K, Yamauchi T, Furusawa T *et al.* FTO polymorphisms in oceanic populations. *J Hum Genet* 2007; **52**:1031-1035.

30 Hardy R, Wills AK, Wong A, Elks CE, Wareham NJ, Loos RJ *et al*. Life course variations in the associations between FTO and MC4R gene variants and body size. *Hum Mol Genet* 2010; **19**: 545-552.

31 Tan JT, Dorajoo R, Seielstad M, Sim XL, Ong RT, Chia KS *et al.* FTO variants are associated with obesity in the Chinese and Malay populations in Singapore. *Diabetes* 2008; **57**: 2851-2857.

32 Xi B, Shen Y, Zhang M, Liu X, Zhao X, Wu L *et al.* The common rs9939609 variant of the fat mass and obesity-associated gene is associated with obesity risk in children and adolescents of Beijing, China. *BMC Med Genet* 2010; **11**: 107.

33 Rampersaud E, Mitchell BD, Pollin TI, Fu M, Shen H, O'Connell JR *et al.* Physical activity and the association of common FTO gene variants with body mass index and obesity. *Arch Int Med* 2008; **168**: 1791–1797.

34 Ruiz JR, Labayen I, Ortega FB, Legry V, Moreno LA, Dallongeville J *et al*. Attenuation of the effect of the FTO rs9939609 polymorphism on total and central body fat by physical activity in adolescents: the HELENA study. *Arch Pediatr Adolesc Med* 2010; **164**: 328-333.

35 Corella D, Carrasco P, Sorlì JV, Coltell O, Ortega-Azorìn C, Guillen M *et al*. Education modulates the association of the FTO rs9939609 polymorphism with body mass index and obesity risk in the Mediterranean population *Nutr Metab Cardiovasc Dis* 2012; **22**: 651-658.

36 Wang H, Dong S, Xu H, Qian J, Yang J. Genetic variants in FTO associated with metabolic syndrome: a meta- and gene-based analysis. *Mol Biol Rep* 2012; **39**: 5691-5698.

37 Freathy RM, Timpson NJ, Lawlor DA , Pouta A, Ben-Shlomo Y, Ruokonen A *et al*. Common variation in the FTO gene alters diabetes-related metabolic traits to the extent expected given its effect on BMI. *Diabetes* 2008; **57**: 1419–1426.

38 Al-Attar SA, Pollex RL, Ban MR, Young TK, Bjerregaard P, Anand SS et al. Association between the FTO rs9939609 polymorphism and the metabolic syndrome in a non-Caucasian multi-ethnic sample. *Cardiovasc Diabetol* 2008; **7**:5.

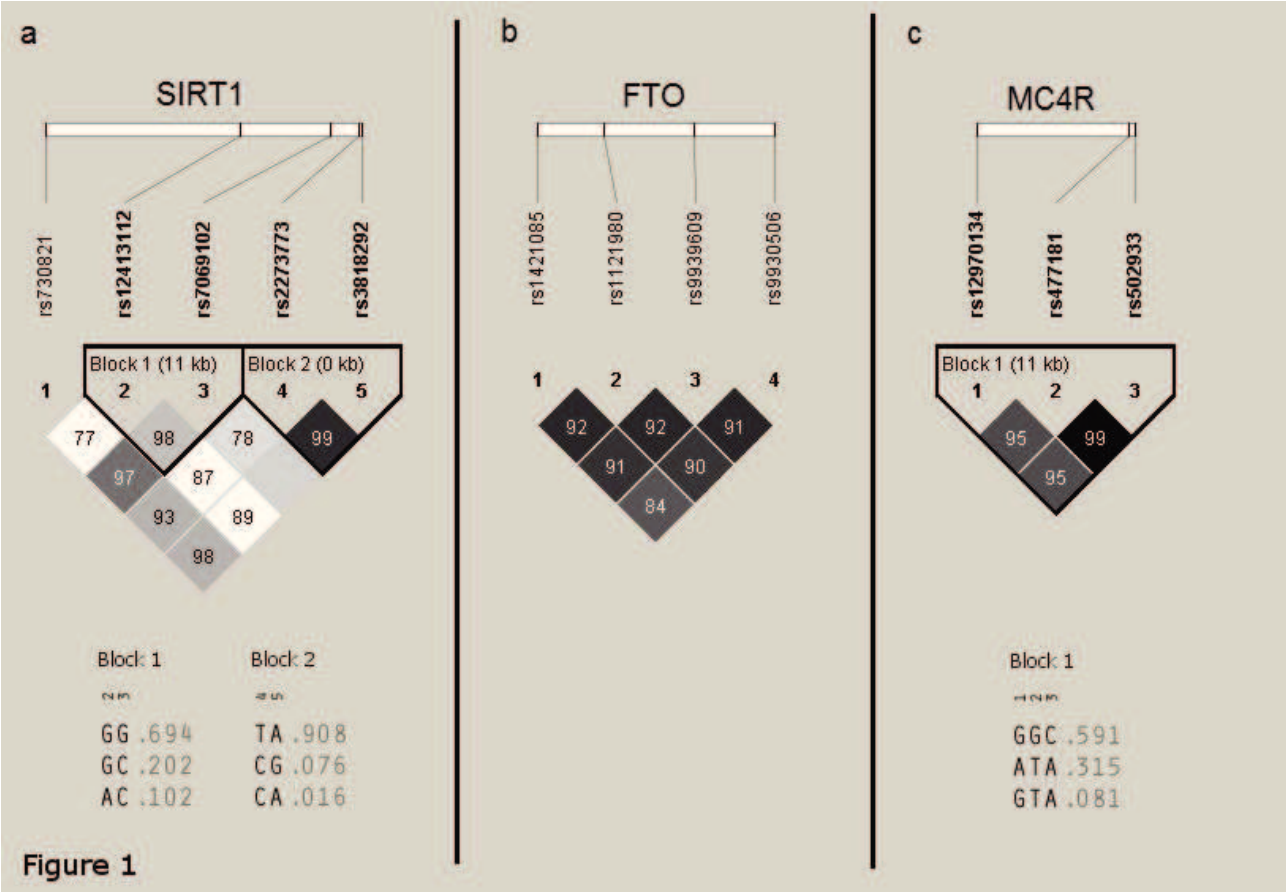

Figure 1. Linkage disequilibrium (D') plot of SIRT1 (panel a), FTO (panel b) and MC4R (panel c) polymorphisms. The numbers in the squares are the D' values expressed as percentage; shades of grey represent r^2 (white: $r^2=0$; black: $r^2=1$).

Table 1. General and biochemical characteristics of studied obese patients (n=1000).

	Mean	SEM
Age (years)	32.62	0.36
Height (m)	1.67	0.00
Weight (kg)	129.14	0.71
BMI (kg/m2)	46.50	0.23
WC (cm)	131.81	0.68
Hips circumference (cm)	135.30	1.36
W/H ratio	0.98	0.01
RQ	0.86	0.00
BMR (kcal)	2386.86	18.94
FFM (%)	52.09	0.24
FM (%)	47.89	0.24
SBP (mmHg)	124.86	0.40
DBP (mmHg)	79.83	0.27
Cardiac Frequency (beats/min)	78.44	0.26
Glucose (mmol/L)	5.13	0.04
Total Cholesterol (mmol/L)	4.74	0.03
HDL-Cholesterol (mmol/L)	1.18	0.01
Triglycerides (mmol/L)	1.51	0.03
AST (U/L)	25.80	0.42
ALT (U/L)	37.68	0.86
GGT (U/L)	32.69	1.02
CHE (U/mL)	10065.10	68.07
Total Bilirubin (µmol/L)	9.92	0.17
Uric Acid (mmol/L)	0.35	0.01
Albumin (g/dL)	4.37	0.01
Total Protein (g/dL)	7.55	0.01
Creatinin (µmol/L)	71.6	0.88
Urea (mmol/L)	5.26	0.04
ALP (U/L)	100.72	7.47
Cortisol (µg/L)	122.45	1.62
C-Peptide (ng/mL)	4.16	0.05
Insulin (mU/L)	21.61	0.43
HOMA	5.07	0.13
FLI	94.79	0.57

SEM: standard error of the mean; BMI: Body Mass Index; WC: Waist Circumference; W/H: waist/hip; RQ: respiratory quotient; BMR: basal metabolic rate; FFM: fat free mass; FM: fat mass; SBP: systolic blood pressure; DBP: diastolic blood pressure; AST: aspartate transaminase; ALT: alanine transaminase; GGT: γ-glutamyl transferase; CHE: cholinesterase; ALP: alkaline phosphatase; HOMA: homeostatic model assessment; FLI: fatty liver index.

Table 2. Genotype frequencies of the tested SNPs in obese and control subjects.

			WT	Het	Hom	*p*
SIRT1	rs3818292	C	81.0%	19.0%	0.0%	
		O	85.6%	14.1%	0.3%	
	rs7069102	C	40.0%	52.0%	8.0%	
		O	46.9%	45.8%	7.3%	
	rs730821	C	59.0%	39.0%	2.0%	
		O	64.4%	33.2%	2.5%	
	rs2273773	C	84.0%	16.0%	0.0%	
		O	81.6%	18.4%	0.0%	
	rs12413112	C	71.0%	27.0%	2.0%	0.037
		O	81.3%	17.6%	1.1%	
FTO	rs1421085	C	29.0%	47.0%	24.0%	0.003
		O	16.0%	45.9%	38.1%	
	rs9939609	C	36.0%	46.0%	18.0%	<0.0001
		O	16.3%	48.3%	35.4%	
	rs9930506	C	35.0%	46.0%	19.0%	<0.0001
		O	18.0%	50.4%	31.6%	
	rs1121980	C	29.0%	48.0%	23.0%	0.007
		O	16.7%	47.3%	35.9%	
MC4R	rs12970134	C	54.0%	32.0%	14.0%	
		O	46.3%	41.7%	12.0%	
	rs477181	C	36.0%	46.0%	18.0%	
		O	36.7%	47.0%	16.3%	
	rs502933	C	37.0%	46.0%	17.0%	
		O	36.8%	47.3%	15.9%	

C: controls; O: obese subjects; WT: wild type; Het: heterozygous; Hom: homozygous for the variant; OR (95% CI): Odd ratio (95% Confidence Interval). $p<0.05$ indicates statistically significant difference at χ^2 test

Table 3. Association of the tested SNPs with the obese phenotype (A) and with the presence of metabolic syndrome (B) at binomial logistic regression analysis.

		Genotype	b	p	OR(95%CI)	Nagelkerke R^2
A	Male gender		1.24	<0.0001	3.46(2.07-5.79)	0.116
	rs9939609 (FTO)	TA	0.93	0.001	2.51(1.43-4.46)	
		AA	1.33	<0.0001	3.79(1.91-7.50)	
B	Total Cholesterol		0.01	0.001	1.01(1.00-1.02)	0.213
	BMR		0.01	0.003	1.01(1.00-1.01)	
	rs9939609 (FTO)	TA	0.93	0.02	2.53(1.16-5.55)	
	Age		0.03	0.03	1.03(1.01-1.06)	

Tested variables: Model A: rs3818292, rs730821, rs12413112, rs1421085, rs9939609, rs9930506, rs1121980, rs12970134, sex and age; Model B: rs3818292, rs730821, rs12413112, rs1421085, rs9939609, rs9930506, rs1121980, rs12970134, sex, age, BMR, FFM, FM, RQ, total cholesterol, AST, ALT, GGT, total protein, urea and uric acid.

Supplemental Table 1. Minor allele frequencies of the tested SNPs found in our population compared with those reported into the National Center for Biotechnology Information (NCBI) database.

	SNP	Minor Allele	MAF	NCBI MAF
SIRT1	rs3818292	G	0.09	0.08
	rs7069102	C	0.34	0.32
	rs730821	C	0.22	0.18
	rs2273773	C	0.08	0.08
	rs12413112	A	0.16	0.14
FTO	rs1421085	C	0.48	0.46
	rs9939609	A	0.42	0.45
	rs9930506	G	0.42	0.48
	rs1121980	A	0.47	0.48
MC4R	rs12970134	A	0.29	0.28
	rs477181	T	0.41	0.35
	rs502933	A	0.41	0.35

MAF: minor allele frequency.